Histone H1 phosphorylation during mitosis

A dissertation presented in partial fulfilment of the

requirements for the degree of

Doctor of Philosophy

in

Biochemistry

at Massey University, Manawatū,

New Zealand

Sarah D Bond

2016

Abstract

Histone H1 phosphorylation is important for the regulation of high order chromosome organisation during mitosis. One of these phosphorylation sites in the linker histone subtype H1.4 is shown here to be phosphorylated by Aurora B kinase, a master regulator of mitosis. Altered phosphorylation of H1.4 on this phosphorylation site at serine 27 illustrated the significance of the timing of this phosphorylation. When serine 27 of H1.4 is mutated to prevent this phosphorylation chromosome congression to the equatorial plate during metaphase is hindered. In contrast, in the presence of the constitutive H1.4 serine 27 phosphorylation mimic, bridging and lagging chromosomes occurred, leading to a corresponding increase in the proportion of cells with a micronucleus. These phenotypes could be brought about through disruption of the Heterochromatin protein 1 family members bound to the adjacent methylated lysine. Such aberrations during mitosis can lead to genetic instability and ultimately aneuploidy, a hallmark of cancer. With the frequently reported over-expression of Aurora B in cancer this shows another mechanism in which this kinase, via histone H1.4 phosphorylation, can push a cell toward malignancy.

Another important mitotic kinase, Cyclin dependent kinase 1 together with cyclin B, is responsible for the hyperphosphorylation of histone H1.4 during mitosis; which is required for condensing the cells genetic information into highly compact metaphase chromosomes. This vital mitotic event ensures the faithful transmission of the duplicated DNA into the dividing daughter cells. The mechanisms through which histone H1 hyperphosphorylation contribute to chromosome condensation are poorly understood. One mechanism through which this may occur is via the recruitment of condensation factors such as the condensins or Topoisomerase II. Here the interaction between the Condensin I subunit, CAPD2, and histone H1.4 is explored. CAPD2 interacts with the two most prominent linker histone subtypes, H1.4 and H1.2, through their C-terminal tails. H1.4 and CAPD2 can interact *in vitro* whilst each is phosphorylated by cyclin dependent kinase as they are during mitosis, in a manner dependent on RNA.

Overall, these results indicate that histone H1.4 is a vital component of higher order chromatin and its phosphorylation is essential for the normal progression through mitosis.

Acknowledgements

First and foremost, I would like to thank my supervisor Dr Tracy Hale. I am immensely grateful for her guidance, support and encouragement throughout my doctoral studies. Tracy has been there for me through challenging times and is an inspiration, and I will be forever grateful for all she has taught me. Our regular meetings have led to many helpful discussions and I appreciate this time Tracy has generously spent with me. I wish Tracy all the best in her future endeavours.

My co-supervisors Dr Helen Fitzsimons and Professor Kathryn Stowell have provided helpful advice and support. I am thankful for this and their guidance and constructive discussions. I am also grateful to Helen for her generosity in sharing her lab space and equipment with our group. Kathryn kindly allowed our group to join in with shared lab meetings which has been platform for friendly discussions, advice and constructive criticism.

I have really enjoyed working in the laboratory thanks to the supportive environment created by colleagues. Both present and past lab members of the Chromatin Research Group and the Molecular Neurogenetics Group have assisted me through their advice and sharing of lab reagents, equipment and protocols, thank you to you all.

There are many colleagues within the Institute of Fundamental Sciences that have generously given their time for training me to use specialised equipment and kindly shared reagents; I appreciate all of this assistance. Thank you to those of you who maintain equipment, assist in getting the reagents to the right place and for the friendly environment within the institute.

I would also like to thank the staff within the Manawatu Microscopy and Imaging Centre for providing training, advice and assistance with microscopy.

In the wider university campus colleagues have allowed me to visit their institute and have assisted using equipment, thank you to Dr Fran Wolber for her flow cytometry expertise, and to Dr Matthew Perrott and his staff, for allowing me to use their immunohistochemistry facilities. I would also like to thank pathologists Dr Bruce

Lockett from Medlab Central, and Assistant Professor Alejandro Contreras from The MD Anderson Cancer centre, for their assistance analysing tumour samples.

I have been fortunate to receive financial support for my doctoral studies, thank you to Massey providing support through the Vice Chancellors Doctoral Scholarship. I am immensely grateful to the Institute of Fundamental Sciences for their support and for funding me for an additional six months to allow me to complete my studies. Thank you to the Graduate Women Manawatu Trust and Zonta for the Zonta Manawatu Women in Science Award which allowed me to travel to Boston, Massachusetts for the Gordon Research Conference on Chromatin Structure and Function in 2014.

Last, but not least I would like to thank family and friends for their support and for always being there for me.

Table of Contents

List of Figures and Tables

Abbreviations

2N	Diploid
4N	Tetraploid
A	Adenine
ATP	Adenosine triphosphate
BCA	Bicinchoninic acid
BD	Becton Dickinson
bp	Base pairs
BSA	Bovine serum albumin
C	Cytosine
C-terminus	Carboxyl-terminus
CAPD2	Condensin complex subunit 1
CAPSO	3-(Cyclohexylamino)-2-hydroxy-1-propanesulfonic acid
CDK	Cyclin dependent kinase
cDNA	Complementary DNA
CENPA	Centromere protein A
CRG	Chromatin Research Group
CTD	C-terminal domain of CAPD2 (final 113 amino acids)
DAB+	3,3′-Diaminobenzidine
DAPI	4′,6-Diamidino-2-phenylindole
DMEM	Dulbecco's Modified Eagle Medium
DMSO	Dimethyl sulfoxide
DNA	Deoxyribonucleic acid
Dox	Doxycycline
DTT	Dithiothreitol
ECL	Enhanced chemiluminescence
EDTA	Ethylenediaminetetraacetic acid
EGTA	Ethylene glycol tetraacetic acid
EZH2	Enhancer of zeste homolog 2
FBS	Fetal bovine serum
FFPE	Formalin fixed paraffin embedded
FRAP	Fluorescence recovery after photobleaching
g	Grams
G	Guanine
G_1 phase	Gap 1 phase
G_2 phase	Gap 2 phase
GFP	Green fluorescent protein
GST	Glutathione S-transferase
GST-CAPD2	Wild-type CAPD2 with an N-terminal GST-tag
GST-CTD	CTD of CAPD2 with an N-terminal GST-tag
GST-HP1β	HP1β with an N-terminal GST-tag

H1	Histone H1
H1.4-FLAG	Wild-type histone H1.4 with a C-terminal FLAG-tag
H1.4K26	Histone H1.4 lysine 26
H1.4K26A	H1.4-FLAG where lysine at position 26 was substituted with alanine to prevent K26 methylation
H1.4K26me3	Histone H1.4 trimethylated on lysine 26
H1.4S27	Histone H1.4 serine 27
H1.4S27A	H1.4-FLAG where serine at position 27 was substituted with alanine to prevent S27 phosphorylation
H1.4S27E	H1.4-FLAG where serine at position 27 was substituted with glutamic acid to mimic constitutive phosphorylation
H1.4S27p	H1.4 phosphorylated on serine 27
H3	Histone H3
H3K9	Histone H3 lysine 9
H3K9me3	Histone H3 trimethylated on lysine 9
H3S10	Histone H3 serine 10
H3S10A	H3 where serine at position 10 was substituted with alanine to prevent S10 phosphorylation
H3S10E	H3 where serine at position 10 was substituted with glutamic acid to mimic constitutive S10 phosphorylation
H3S10p	H3 phosphorylated on serine 10
HAT	Histone acetyltransferase
HEPES	2-[4-(2-Hydroxyethyl)piperazin-1-yl]ethanesulfonic acid
HMT	Histone methyltransferase
HP1	Heterochromatin protein 1
HRP	Horseradish peroxidase
IDT	Integrated DNA Technologies
IF	Immunofluorescence
IgG	Immunoglobulin G
IHC	Immunohistochemistry
IP	Immunoprecipitation
IPTG	Isopropyl β-D-1-thiogalactopyranoside
K9	Lysine 9
K26	Lysine 26
Kb	Kilobase
KCM buffer	Potassium chromosome medium buffer
K_d	Dissociation constant
kDa	Kilodalton
L	Litre
LB	Lysogeny broth
M phase	Mitotic phase
Min	Minutes

MGS	Massey Genome Service
MMIC	Massey Microscopy and Imaging Centre
MNase	Micrococcal nuclease
MSK1	Mitogen- and stress-activated kinase 1
N-terminus	Amino-terminus
NEB	New England BioLabs
NFM	Non-fat milk
PBS	Phosphate buffered saline
PCR	Polymerase chain reaction
PFA	Paraformaldehyde
PI	Propidium iodide
PP1	Protein phosphatase 1
PP2A	Protein phosphatase 2A
PRC2	Polycomb repressive complex 2
PTM	Post-translational modification
RIPA	Radioimmunoprecipitation assay buffer
RNA	Ribonucleic acid
RNase A	Ribonuclease A
rpm	Revolutions per minute
RT	Room temperature
S phase	Synthesis phase
S10	Serine 10
S27	Serine 27
SDM	Site-directed mutagenesis
SDS	Sodium dodecyl sulphate
SDS-PAGE	SDS-polyacrylamide gel electrophoresis
SMC	Structural maintenance of chromosomes
S.O.C	Super optimal broth with catabolite repression
Supplemented DMEM	DMEM supplemented with 10% FBS and 1% penicillin/ streptomycin
SUV39H1	Suppressor of variegation 3-9 homolog 1
SWI/SNF	Switch/Sucrose non-fermentable
T	Thymine
TAE	Tris-acetate-EDTA
TBS	Tris-buffered saline
TBST	TBS with 0.1% Tween 20
TCA	Trichloroacetic acid
TGS	Tris-glycine-SDS
U	Unit
UV	Ultraviolet
WB	Western blotting

Chapter One
Introduction

1.1 The cell cycle

The process of cell division is fundamental to all living organisms and one of its primary functions is to facilitate the faithful replication of DNA, so that each daughter cell inherits an identical copy (Belmont, 2006; Maresca & Heald, 2006; Norbury & Nurse, 1992). Work in the yeast *Saccharomyces cerevisiae* and other model organisms revealed the stages of the cell cycle and the proteins essential for its regulation (Evans *et al.*, 1983; Hartwell, 1971; Hartwell *et al.*, 1970; Norbury & Nurse, 1992; Nurse *et al.*, 1976). The cell cycle is a highly organised process divided into interphase, mitosis, and cytokinesis (Vermeulen *et al.*, 2003). Interphase consists of the phases G_1 (first gap), S (synthesis), and G_2 (second gap), and spans around 90% of the cell cycle duration (Norbury & Nurse, 1992). During G_1 the cell grows and prepares for S phase, where the DNA is replicated (Vermeulen *et al.*, 2003). Once DNA synthesis is complete the cell enters G_2 where growth is continued until the cell is ready to divide (Vermeulen *et al.*, 2003). At this time the highly coordinated process of mitosis occurs, where the duplicated sister chromatids are separated ready to be distributed into two individual cells (Vermeulen *et al.*, 2003).

Mitosis occurs as a continuous process that takes approximately one hour in most human cell lines, which can be divided into distinct phases (Belmont, 2006; Vermeulen *et al.*, 2003). Initially, during prophase, the duplicated chromosomes undergo compaction and the mitotic spindle begins to form from the centrosomes at the poles of the cell (Kops *et al.*, 2005). Next, in prometaphase, the nuclear envelope disintegrates and the spindle attaches to the sister chromatids at the newly formed kinetochore on the centromere (Kops *et al.*, 2005). In metaphase, the attached sister chromatids align on the equatorial plate due to the opposing tensions on the chromosome (Kops *et al.*, 2005). During anaphase the duplicated sister chromatids are pulled to the opposing poles of the cell, ultimately resulting in two genetically identical nuclei (Kops *et al.*, 2005). In the final stage of mitosis, telophase, the nuclear membrane reforms around the two distinct nuclei and the chromosomes begin to decondense and return to the interphase state (Kops *et al.*, 2005). To complete cell division the contractile ring forms

and pinches along the central axis during cytokinesis forming individual daughter cells (Schroeder, 1973).

Faithful passage through mitosis is necessary to prevent the loss of the genetic information of the cell (Kops *et al.*, 2005; Maresca *et al.*, 2005). For mitosis to occur with fidelity, choreographed changes in compaction of the DNA must take place (Belmont, 2006; Maresca & Heald, 2006). This occurs through the organisation of the DNA around histone proteins, and RNA, forming chromatin (Kornberg, 1974).

1.2 Organisation of the genome

Eukaryotic DNA is constrained by the nucleus, and its organisation into chromatin ensures that DNA of over two metres in length is compacted within the nucleus that is 10 μm in diameter (Maresca & Heald, 2006). While chromatin is a stable structure, its organisation and compaction is dynamic (Misteli, 2001). This facilitates DNA replication, repair and access of proteins to the DNA to enable regulation of gene expression in a temporal and spatial manner (Kouzarides, 2007).

During the cell cycle chromatin undergoes massive changes in compaction (Belmont, 2006). In interphase, genes that are actively expressed remain within an open euchromatic structure to allow access of the transcription machinery to the DNA (Kouzarides, 2007). Whereas DNA that is not undergoing active processes is folded into denser heterochromatic structures that are transcriptionally silent (Kouzarides, 2007). Higher orders of chromatin compaction are facilitated by folding into loops, until the most compact state is reached during mitosis (Mora-Bermudez *et al.*, 2007; Woodcock & Dimitrov, 2001).

1.3 The hierarchy of chromatin folding

The chromatin fibre undergoes several layers of folding to reach the compact states that occur during the cell cycle (Woodcock & Dimitrov, 2001). This begins with the wrapping of DNA around nucleosomes forming the 11 nm fibre, and then the folding of nucleosomal arrays into higher order domains (Figure 1.1; Kornberg, 1977).

1.3.1 The nucleosome

The basic repeating unit of chromatin is the nucleosome, which consists of 147 bp of DNA wrapped around an octamer of core histones (Eickbush & Moudrianakis, 1978; Kornberg, 1974, 1977; Luger *et al.*, 1997). There are four core histones, H2A, H2B, H3, and H4, and the octamer contains an H3-H4 tetramer and a pair of H2A-H2B dimers (Eickbush & Moudrianakis, 1978; Luger *et al.*, 1997). These four core histones are highly conserved basic proteins with ancient origins (Arents & Moudrianakis, 1995; Thatcher & Gorovsky, 1994). They each possess a long unstructured amino (N)-terminal tail, with a globular domain that forms the histone fold, followed by a short carboxyl (C)-terminal tail (Arents & Moudrianakis, 1995). Within the nucleosome the core histones interact through their histone fold, which consists of three α-helices (Arents & Moudrianakis, 1995). In contrast, the N-terminal tail that is enriched in basic amino acids protrudes from the nucleosome structure (Luger *et al.*, 1997). These protruding tails are post-translationally modified, which alters their charge and controls access of regulatory proteins to the DNA (Kouzarides, 2007). The structure of the nucleosome was solved to 2.8 Å resolution in 1997 by Luger *et al.* (1997) as shown in Figure 1.2.

An array of nucleosomes and the adjoining linker DNA form the 11 nm fibre, which has a 'beads on a string' appearance (Figure 1.1; Finch & Klug, 1976; Olins & Olins, 1974). The nucleosome acts as a spool, of which 1.65 turns of the DNA is organised around (Luger *et al.*, 1997; Lutter, 1978), with linker DNA joining adjacent nucleosomes (Kornberg, 1974, 1977). Together, the DNA wound around the nucleosome, and linker DNA give a nucleosome repeat length near 200 bp (Noll & Kornberg, 1977). However,

the linker DNA can vary in length in different organisms, and even across tissues types (Woodcock *et al.*, 2006). A higher degree of chromatin compaction is achieved with the addition of the linker histone, H1, in a structure known as the chromatosome (Simpson, 1978).

1.3.2 The chromatosome

The H1 class of linker histones sit at the entry-exit site of the DNA wrapped around the nucleosome, to form the chromatosome (Figure 1.3; Bednar *et al.*, 1998; Thoma *et al.*, 1979). A molecule of H1 bridges the DNA, with its N- and C-terminal tails thought to neutralise the charge of the linker DNA, thus organising the DNA so that it enters and exits the nucleosome on the same side (Thoma *et al.*, 1979). This arrangement of the linker DNA into a stem motif by linker histones contributes to both the order and stability of condensed chromatin fibres enabling higher packing ratios (Bednar *et al.*, 2016). Histone H1 directly interacts with 20 bp of linker DNA, sealing the nucleosomes with two full turns of DNA (167 bp; Thoma *et al.*, 1979). The stoichiometry of H1 is often considered to be one molecule per nucleosome (Bates & Thomas, 1981; Woodcock *et al.*, 2006). However, the actual H1 occupancy can differ, with the number of H1 molecules per nucleosome in mice varying from 0.5 in embryonic stem cells to near 0.8 in the liver and thymus (Fan *et al.*, 2003; Fan *et al.*, 2005; Woodcock *et al.*, 2006). This range in H1 occupancy affects the nucleosome repeat length, with a robust linear relationship seen (Woodcock *et al.*, 2006). Increasing amounts of H1 allow for longer linker DNA, presumably through charge neutralisation (Woodcock *et al.*, 2006). Thus the chromatosome contains the required components for the organisation of chromatin into higher order structures (Simpson, 1978).

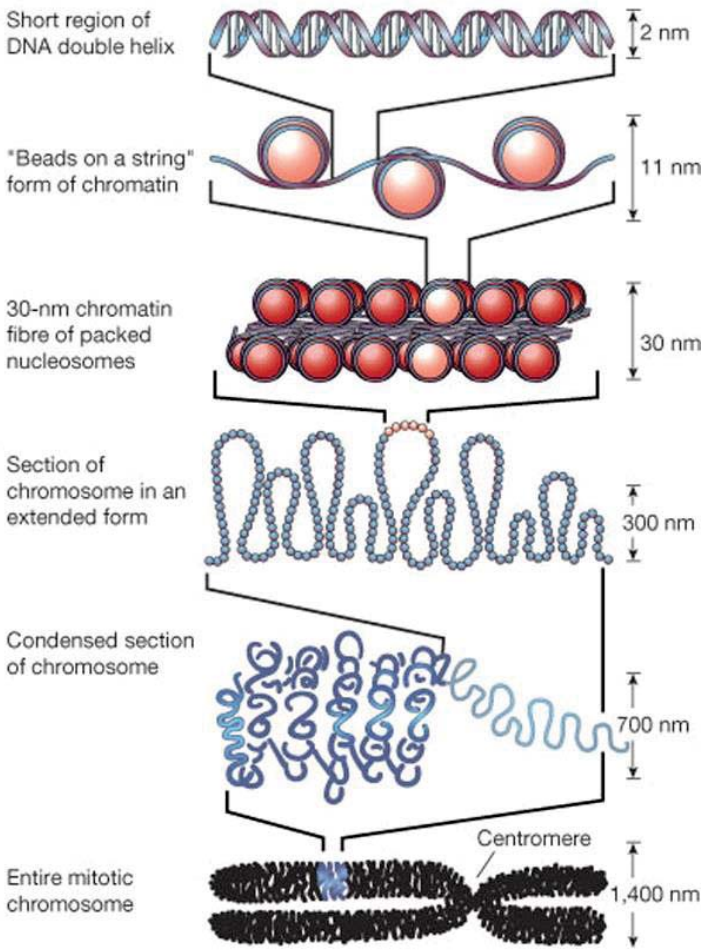

Figure 1.1. The hierarchy of chromatin folding.
Illustration of the way DNA is organised and condensed within chromatin. The DNA is wound around an octamer of core histones forming the 11 nm fibre, which progressively folds into the proposed 30 nm fibre. This 30 nm fibre forms loops that compact forming the classic X-shaped mitotic chromosomes. Figure from Felsenfeld and Groudine (2003).

Figure 1.2. The structure of the nucleosome core.
Atomic model of the nucleosome at 2.8 Å resolution, where 147 bp of DNA (green and brown) is wound around the core histone octamer, that contains an H3-H4 tetramer (blue and green), and two H2A-H2B dimers (yellow and red). Partial N- and C-terminal tails are shown that protrude from the nucleosome and are able to be post-translationally modified. Figure from Luger *et al.* (1997).

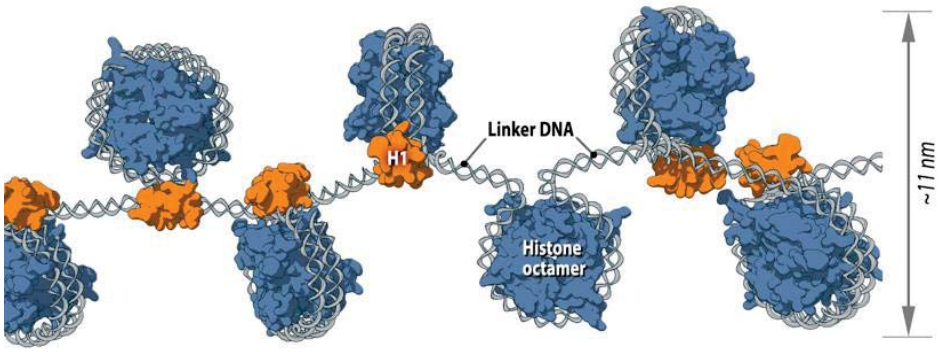

Figure 1.3. The chromatosome.
Depiction of the position of the linker histone H1 (orange) on the 11 nm fibre. DNA is wound around the core histone octamer (blue), to form the nucleosome. Histone H1 then binds the entry-exit site of the DNA on the nucleosome forming the chromatosome, with the linker DNA connecting adjoining chromatosomes. Figure retrieved from https://mbi-figure.storage.googleapis.com/figure/1389942837319.jpg.

1.3.3 The 30 nm fibre

The next level of higher order chromatin is the 30 nm fibre proposed by Finch and Klug (1976), however, its existence *in vivo* has become increasingly controversial in recent years (Maeshima *et al.*, 2010). While the structure of the nucleosome is well understood, the topology and folding beyond the chromatosome remains elusive (Maeshima *et al.*, 2010). Structures with a 30 nm diameter were regularly observed when H1 was present in chromatin isolated from cells under low ionic strength (Finch & Klug, 1976). Solenoid and zig-zag models for the nucleosome organisation of the 30 nm fibre have been proposed (Finch & Klug, 1976; Thoma *et al.*, 1979; Woodcock *et al.*, 1984), with the zig-zag model gaining favour (Schalch *et al.*, 2005; Woodcock & Dimitrov, 2001). These models differ in the arrangement of nucleosomes, with the solenoid model having adjacent spiralling nucleosomes (Finch & Klug, 1976; Widom & Klug, 1985), and the latter showing alternation of adjacent nucleosomes in a zig-zag arrangement (Thoma *et al.*, 1979). Both models hypothesize that the linker DNA and histone H1 are in the interior of the 30 nm fibre (Dimitrov *et al.*, 1987; Graziano *et al.*, 1994; Song *et al.*, 2014).

In recent advances, *in vitro* results using electron microscopy with reconstituted arrays and computer modelling reveal that the 30 nm fibre is predominantly in a zig-zag confirmation (Grigoryev *et al.*, 2009). However, there is a small proportion of the fibre in a solenoid configuration, which differs depending on the presence of divalent cations, giving a heteromorphic structure (Grigoryev *et al.*, 2009). The predominance of zig-zag structures is also supported by cryo-electron microscopy of reconstituted arrays, where H1 bound to nucleosomes in an asymmetric manner (Song *et al.*, 2014). Yet other groups aiming to capture mitotic chromosomes in their native state with this technique failed to observe structures containing a 30 nm diameter (Dubochet *et al.*, 1988; Eltsov *et al.*, 2008). Consequently, it is still to be determined if this structure exists *in vivo*. Given the lack of *in vivo* evidence for the 30 nm fibre in both interphase and mitosis, it has been proposed that a highly disordered interdigitated 'polymer melt' of the 11 nm fibre alone can account for the necessary levels of folding (Eltsov *et al.*, 2008; Maeshima *et al.*, 2010). Chromosome capture experiments and other recent

technologies will be invaluable in exploring the *in vivo* structure, and how H1 is positioned to facilitate the stability and regulation of these high order fibres.

1.3.4 Chromosome structure during mitosis

Much greater compaction of the interphase chromosomes is required to achieve the condensed mitotic state (Maresca *et al.*, 2005). This compaction allows accurate segregation of the replicated sister chromatids into the genetically identical daughter nuclei without tangling or breaking the DNA, minimising the loss of genetic material (Belmont, 2006). Compact chromosomes also require structural integrity so they can withstand the mechanical forces imposed on them when they are pulled apart during anaphase (Hagstrom *et al.*, 2002). As for the 30 nm fibre, the higher order chromosome structures observed during mitosis are yet to be structurally defined (Belmont, 2006). Classical models of mitotic chromosomes proposed radial looping, where the 30 nm fibre is anchored in loops around a central scaffold (Earnshaw & Laemmli, 1983; Marsden & Laemmli, 1979; Paulson & Laemmli, 1977). Alternatively, models of hierarchical folding into thicker fibres arranged in a defined and complex architecture (Belmont *et al.*, 1987), or through successive folding of the 30 nm fibre into larger sequential helical coils have been proposed (Bak *et al.*, 1979).

New advances in techniques deviate from these classic hierarchical models as *in vivo* evidence of the 30 nm fibre is limited (Horowitz-Scherer & Woodcock, 2006). As proposed for the 30 nm fibre during interphase, there is potential for disordered arrays in mitotic chromosomes (Maeshima *et al.*, 2010; Naumova *et al.*, 2013). Combined data from polymer physics simulations, microscopic analysis and Hi-C chromosome capture experiments have shown that metaphase chromosomes form variable compressed consecutive linear loops with a cylindrical geometry, which form an irregular 'melt' of uniform density (Naumova *et al.*, 2013). Both the 11 nm and 30 nm fibres were able to exist within this model, as was the possibility of a central scaffold (Naumova *et al.*, 2013; Paulson & Laemmli, 1977). Protein complexes such as topoisomerase II and the condensins may form a scaffold aiding in the formation of

condensed metaphase chromosomes (Earnshaw *et al.*, 1985; Lewis & Laemmli, 1982), alternatively, chromosome 'self-assembly' may occur through the post-translational modification of histones, including the linker histone, H1 (Kouzarides, 2007; Roque *et al.*, 2008).

1.4 Histone H1, the linker histone

Particularly vital for the regulation of higher order chromatin structures is the linker histone, H1, whose major function is the formation and stabilisation of these chromatin structures (Thoma *et al.*, 1979). There are several subtypes of linker histone within one species, and the conservation between species is much less than that of the core histones (Cole, 1984; Kasinsky *et al.*, 2001; Thatcher & Gorovsky, 1994). These subtypes give varying compaction properties to the chromatin fibre (Clausell *et al.*, 2009; Th'ng *et al.*, 2005). Much of what is known about the role of H1 comes from *in vitro* analysis of chromatin in the presence or absence of H1 (Finch & Klug, 1976; Thoma *et al.*, 1979). Chromatin lacking H1 can condense to some degree in the presence of divalent cations, although the packing density is greater in chromatin containing H1 (Thoma *et al.*, 1979). Chromatin depleted of histone H1 that was condensed using increasing salt concentrations lacked structural order, and didn't elegantly repeat as it does in the presence of the linker histone H1 (Thoma *et al.*, 1979). In addition, the entry and exit sites of linker DNA from the nucleosome were random, and not on the same side, as is seen in native chromatin (Thoma *et al.*, 1979). In the presence of histone H1, nucleosomes formed at salt concentrations where they wouldn't otherwise form, thus histone H1 stabilises nucleosomes and guides higher order folding (Thoma *et al.*, 1979), which is necessary for the cell to perform highly regulated chromatin based processes (Kouzarides, 2007).

1.4.1 The structure of histone H1

Mammalian histone H1 has a tripartite structure that is enriched in basic amino acids, particularly lysine (Hartman *et al.*, 1977). This structure consists of a central globular domain, a short N-terminal tail, and a longer C-terminal tail (Hartman *et al.*, 1977). The globular proportion of histone H1 folds into a winged helix motif, which is common in transcription factors and other DNA binding proteins (Ramakrishnan *et al.*, 1993). This domain is unrelated to the histone fold present in the core histones (Arents & Moudrianakis, 1995; Kasinsky *et al.*, 2001), which histone H1 does not possess. Both tails of H1 are unstructured in solution (Hartman *et al.*, 1977); although they can attain a particular structure upon DNA binding (Roque *et al.*, 2005; Vila *et al.*, 2001). The short N-terminal tail of histone H1 has little impact on binding to chromatin (Allan *et al.*, 1986; Hendzel *et al.*, 2004), whereas the C-terminus is critical for chromatin binding (Allan *et al.*, 1986; De *et al.*, 2002; Hendzel *et al.*, 2004; Lever *et al.*, 2000; Th'ng *et al.*, 2005). The globular domain of H1 is conserved across subtypes, while the N- and C-terminal tails of H1 are more variable across subtypes and between species (Izzo *et al.*, 2008).

Unlike the core histones which evolved in archaea, histone H1 is of bacterial origin (Kasinsky *et al.*, 2001), thus the relationship between the core and linker histones, although both key components of chromatin, is divergent (Kasinsky *et al.*, 2001). Linker histones are more lysine rich than the core histones (Hartman *et al.*, 1977; Johns, 1964), and while the histone fold domain present in the core histones is thought to have its origins in a DNA binding protein from archaea, there are no genes that resemble histone H1 in archaea (Kasinsky *et al.*, 2001). The winged helix motif in the globular domain of H1 can instead be traced back to bacteria (Kasinsky *et al.*, 2001). Taken together, these data suggest that these groups of histones evolved independently, and then came together to act in concert in eukaryotes (Kasinsky *et al.*, 2001). Bacteria and the protist *Tetrahymena thermophila* have proteins that resemble the C-terminus of histone H1 (Hackstadt *et al.*, 1991; Hayashi *et al.*, 1987). Whereas *Saccharomyces cerevisiae* has a protein similar to mammalian histone H1 called Hho1p, which has a tripartite structure with an additional globular domain at its C-terminus (Landsman, 1996).

1.4.2 Histone H1 subtypes

While the core histones are highly conserved in evolution (Arents & Moudrianakis, 1995; Thatcher & Gorovsky, 1994), histone H1 is much less so and it is the most variable histone class (Baatout & Derradji, 2006; Cole, 1984). There are eleven known subtypes of histone H1 in humans, some are present in all somatic cells, while others are only expressed in oocytes and spermatids (Table 1.1; Happel & Doenecke, 2009). The main somatic subtypes of histone H1 are H1.1 through to H1.5 (Figure 1.4), which are expressed solely in S phase of the cell cycle (Dalton & Wells, 1988). The remaining six, H1.0, H1x, H1t, H1T2, H1LS1, and H1oo, are germ-line and specialised subtypes (Happel & Doenecke, 2009). Linker histones H1.1 to H1.5 are found in a gene cluster alongside the core histone genes on chromosome 6, as is H1t (Albig *et al.*, 1993), while the remaining linker histone genes are individually located in different genomic regions (Happel & Doenecke, 2009).

In mice, gene disruption studies have revealed that the loss of one or two main H1 subtypes can be compensated for by the remaining subtypes of histone H1 (Fan *et al.*, 2001). However, the simultaneous disruption of three of the main linker histones H1c, H1d, H1e (human homologues of H1.2, H1.3 and H1.4) led to abnormal development, a low H1 stoichiometry, and death around midgestation (Fan *et al.*, 2003). Decreased nucleosome spacing and a reduction in chromatin condensation were seen in embryonic stem cells derived from the triple-null mice (Fan *et al.*, 2005). Overall, this suggests that there is some redundancy in H1 function, particularly with regards to structural roles in chromatin; although the reduced stoichiometry seen with the loss of the three histone genes is embryonic lethal implying that these linker histones have essential roles (Fan *et al.*, 2003).

Little is known about the individual function of the histone H1 subtypes, although mounting evidence suggests they have some non-redundant functions (Clausell *et al.*, 2009; Konishi *et al.*, 2003; Millán-Ariño *et al.*, 2014). A specific function has been identified for H1.2 in the activation of apoptosis (Konishi *et al.*, 2003). In this role H1.2 acts as a messenger, transmitting that DNA damage is present in the nucleus to the

mitochondria (Konishi *et al.*, 2003). This stimulates the release of cytochrome c from the mitochondria triggering the apoptotic signalling pathway (Konishi *et al.*, 2003).

Of the main linker histones, H1.2 to H1.5 are present in the majority of somatic cells, with H1.1 showing little to no expression (Meergans *et al.*, 1997). These linker histones have different chromatin binding properties, with the binding determinants primarily in the C-terminus where the majority of amino acid divergence is seen (Clausell *et al.*, 2009; Hendzel *et al.*, 2004; Th'ng *et al.*, 2005). H1.1 and H1.2 bind to chromatin weakly, and H1.3 shows intermediate binding (Clausell *et al.*, 2009; Th'ng *et al.*, 2005). In contrast, histone H1.4 and H1.5 show a strong chromatin binding profile with lower mobility in fluorescence recovery after photobleaching (FRAP) experiments (Th'ng *et al.*, 2005). With H1.0 as the exception, these binding profiles correlate with the length of the C-terminal tail (Th'ng *et al.*, 2005). Thus H1.1 and H1.2, with shorter C-terminal tails show reduced binding compared to the subtypes H1.4 and H1.5 that have longer C-termini (Th'ng *et al.*, 2005). Additionally, H1 subtypes show differences in their ability to condense chromatin (Clausell *et al.*, 2009). As for chromatin binding, H1.1 and H1.2 are weak condensers, H1.3 has intermediate condensation properties, and H1.4 and H1.5 are the strongest condensers of chromatin (Clausell *et al.*, 2009). Differences also occur in the DNA binding affinity for the H1 subtypes from rat, with H1.1 having the lowest affinity, H1.2 and H1.5 with intermediate affinities, and H1.3 and H1.4 with the highest affinity (Orrego *et al.*, 2007). Taken together, these data indicate that the H1 subtypes have variable binding and condensation capacities for DNA and chromatin, suggesting they may contribute differentially to the regulation of chromatin compaction.

Table 1.1. H1 subtypes and their properties

H1 Subtype	H1 Type[a]	Expression (Level)[b]	Chromatin affinity and compaction[c]	% Identity (H1.4)[d]	C-terminal tail length[e]	CDK sites[f]
H1.1	Main	Ubiquitous (Low)	Weak	70.7	103	2
H1.2	Main	Ubiquitous (High)	Weak	84.5	104	4
H1.3	Main	Ubiquitous	Intermediate	86.0	111	4
H1.4	Main	Ubiquitous (High)	Strong	100	110	5
H1.5	Main	Ubiquitous	Strong	83.8	114	5
H1.0	Variant	Differentiated cells	Intermediate	41.9	97	3
H1x	Variant	Ubiquitous	ND	34.1	ND	ND
H1t	Germline	Spermatocytes	ND	52.0	ND	ND
H1T2	Germline	Spermatids	ND	20.7	ND	ND
H1LS1	Germline	Spermatids	ND	14.7	ND	ND
H1oo	Germline	Oocytes	ND	22.4	ND	ND

[a,b] From Happel and Doenecke (2009).
[c] From Th'ng *et al.* (2005) and Clausell *et al.* (2009).
[d] Relative to H1.4; from Pan and Fan (2016).
[e] From Harshman *et al.* (2013).
[f] From Uniprot.
ND Not determined.

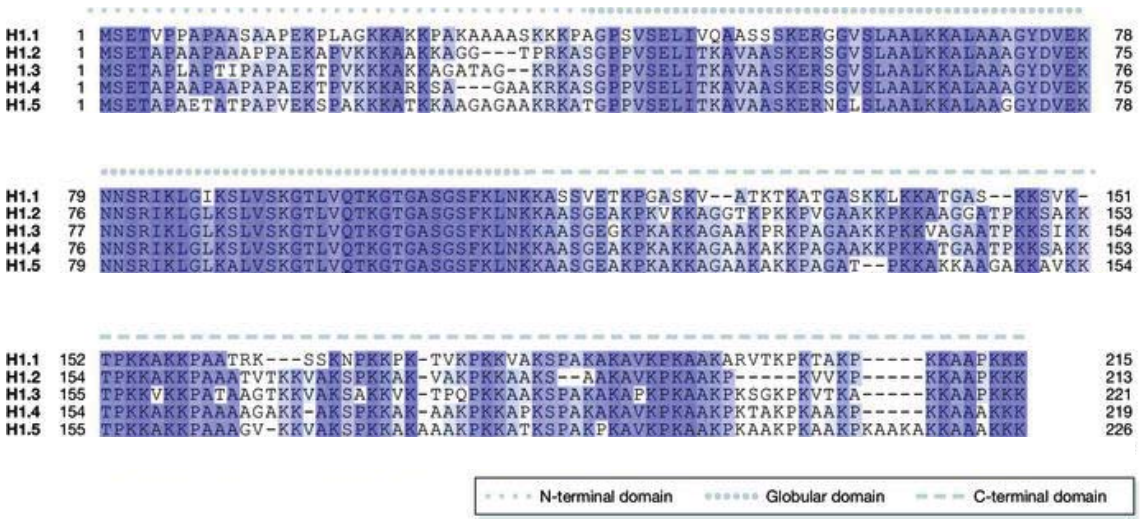

Figure 1.4. Sequence alignment of the somatic main H1 subtypes.
Amino acid alignment for the main somatic H1 subtypes. Conserved and similar residues are highlighted. The N-terminus, globular domain, and C-terminus are indicated, with the globular domain showing the highest sequence conservation. Adapted from Hergeth and Schneider (2015).

Of the somatic subtypes of H1, histone H1.4 is the most highly expressed, alongside H1.2, and both have ubiquitous expression across many cell types, suggesting that they play an important role in chromatin organisation (Meergans *et al.*, 1997). H1.4 and H1.2 are the only linker histones expressed in all cell lines tested to date (Kratzmeier *et al.*, 1999; Meergans *et al.*, 1997). Histone H1.2, with its low chromatin binding affinity, is enriched in euchromatin (Th'ng *et al.*, 2005). In contrast, histone H1.4 shows one of the highest affinities for binding DNA and chromatin (Th'ng *et al.*, 2005), and is a strong condenser of chromatin (Clausell *et al.*, 2009). It is not surprising then that histone H1.4 is preferentially located in heterochromatic regions of the genome compared to the other subtypes (Th'ng *et al.*, 2005). Reduction of histone H1.4 expression in the T47D breast cancer cell line resulted in cell death, thus histone H1.4 is the first linker histone identified to be essential for survival in human cells, although MCF7 and HeLa cells were able to survive with this shRNA-mediated H1.4 knockdown (Sancho *et al.*, 2008).

1.4.3 The function of histone H1

In chromatin studies H1 is often overlooked (Happel & Doenecke, 2009; Izzo *et al.*, 2008). There are a number of factors that have contributed to this omission of H1, including early work where knock out of the lone H1 gene in unicellular organisms was often asymptomatic (Barra *et al.*, 2000; Escher & Schaffner, 1997; Ramón *et al.*, 2000). Consequently, histone H1 was considered to be dispensable for several years (Ausió, 2000; Fan *et al.*, 2001; Shen *et al.*, 1995), resulting in a focus on the core histones (Happel & Doenecke, 2009; Kouzarides, 2007). Unlike for H1 and the chromatosome, the structure of the core histones in the nucleosome particle is well understood (Luger *et al.*, 1997). This structural detail has allowed investigation into subtype roles and post-translational modifications of core histones, and the changes in gene regulation that result (Kouzarides, 2007). More recently the importance of H1 has been reaffirmed (Fan *et al.*, 2003; Lu *et al.*, 2009; Maresca *et al.*, 2005). In mice, the knock out of three H1 subtypes is lethal at the embryonic stage (Fan *et al.*, 2003). In addition, chromosomes are aberrantly long, align poorly at metaphase and don't segregate evenly upon mitotic cell division in the absence of H1 in *Xenopus* egg extracts (Maresca et al., 2005).

As H1 contributes to chromatin condensation, it was anticipated that H1 may repress transcription globally (Happel & Doenecke, 2009; Shen & Gorovsky, 1996), however, data from study of H1 in several unicellular organisms illustrated that this is not the case (Hellauer *et al.*, 2001; Shen & Gorovsky, 1996). When the only H1 gene in *Tetrahymena thermophila* was knocked out, a limited number of genes were differentially expressed (Shen & Gorovsky, 1996). Despite lack of evidence as a global repressor, H1 has been demonstrated in some instances to regulate gene expression (Koop *et al.*, 2003; Lee *et al.*, 2004; Shen & Gorovsky, 1996). For example, mouse H1b (H1.2 in humans) has been reported to interact with Msx1, a transcriptional repressor, resulting in cooperative repression of MyoD and inhibition of muscle differentiation (Lee *et al.*, 2004). Chromatin that is being actively transcribed is generally depleted of H1 (Kamakaka & Thomas, 1990), particularly at the transcription start site (Millán-Ariño *et al.*, 2014).

1.5 Histone phosphorylation regulates chromatin structure during the cell cycle

Chromatin structure is regulated by multiple mechanisms during the cell cycle, including remodelling complexes, histone variants, and post-translational modification of the histones (Bannister & Kouzarides, 2011). A diverse array of histone modifications have been described and these occur on both core and linker histone tails (Garcia *et al.*, 2004; Kouzarides, 2007; Zhang *et al.*, 2003). These modifications can alter the charge of the modified residue, which alters their affinity for the DNA or adjacent nucleosomes, or serve as binding sites where proteins are recruited to the chromatin (Bannister & Kouzarides, 2011). Histone post-translational modifications include acetylation, methylation, ubiquitination, citrullination and phosphorylation (Kouzarides, 2007).

Phosphorylation is a common modification of histones that occurs mainly on serine and threonine residues within the histone tails (Rossetto *et al.*, 2012). Phosphorylation,

catalysed by kinases, is the addition of a phosphoryl (PO_3^{2-}) group that imparts a negative charge (Bannister & Kouzarides, 2011). This modification is transient and is removed by phosphatases (Bannister & Kouzarides, 2011). The role of histone phosphorylation *in vivo* is still being established, although *in vitro* studies have shown it can weaken the association between the positively charged histones and the DNA (Green *et al.*, 1993).

1.5.1 Histone phosphorylation and mitotic chromosome condensation

The timing of maximal histone H1 phosphorylation is coincident with the massive condensation of chromosomes that occurs at the onset of mitosis (Gurley *et al.*, 1978; Y.-I. Matsumoto *et al.*, 1980). In order for the complex division that occurs during mitosis, dramatic condensation of the chromosomes is required (Belmont, 2006; Maresca & Heald, 2006). This allows the DNA that has been replicated during S phase to be accurately separated, so that one complete copy of the genome is allotted to each daughter cell (Maresca & Heald, 2006). This compaction is massive, there is an estimated 10,000 fold compaction over naked DNA and up to 50 times over interphase chromosomes (Belmont, 2006). Little is understood about how condensation of mitotic chromosomes occurs, some even describe the process as a "riddle, wrapped in a mystery, inside an enigma" (Belmont, 2006; p. 632); nevertheless a few key players in the process have been identified. These include the condensins, topoisomerases and phosphorylation of histones H1 and H3 (Ajiro *et al.*, 1983; Hirano & Mitchison, 1994; K. Kimura & Hirano, 1997; Maresca *et al.*, 2005; Uemura *et al.*, 1987).

The association of both histone H1 and H3 phosphorylation with premature chromosome condensation was first observed in temperature sensitive mutants of baby hamster kidney cells by Ajiro *et al.* (1983). At the non-permissive temperature, premature chromosome condensation occurred and histones H1 and H3 were as extensively phosphorylated as they are in mitotic cells (Ajiro *et al.*, 1983). Also, when mitotic and interphase cells were fused, premature chromosome condensation in interphase nuclei correlated with an increase in hyperphosphorylated H1 and H3

(Hanks *et al.*, 1983). Inhibition of the phosphorylation of histone H1 and H3 using the kinase inhibitor staurosporine prevented cells entering mitosis (Th'ng *et al.*, 1994). When mitotic cells were treated with this drug rapid dephosphorylation of histone H1 and H3 occurred, concordant with the premature decondensation of mitotic chromosomes (Th'ng *et al.*, 1994). While these results show a close correlation between histone phosphorylation and chromosome condensation, another study suggested H1 isn't necessary for mitotic chromosome compaction, as when H1 was depleted from *Xenopus laevis* egg extracts, sperm chromatin was able to form condensed metaphase chromosomes (Ohsumi *et al.*, 1993). However, more recent studies have supported a role for histone H1 in the chromosome compaction process (Maresca *et al.*, 2005). Histone H1 was shown to be essential for the longitudinal compaction of replicated metaphase chromosomes, as metaphase chromosomes depleted of H1, which would normally be phosphorylated, had increased in length by 50% (Maresca *et al.*, 2005; Maresca & Heald, 2006).

1.5.2 CDK-mediated histone H1 phosphorylation

The most prominent post-translational modification of H1 is its cell cycle associated phosphorylation that was first described in the 1960's and 1970's (Gurley *et al.*, 1974; Ord & Stocken, 1966). Histone H1 is a substrate of the cyclin dependent kinases, and one of the most highly phosphorylated subtypes is H1.4 (Table 1.1; Swank *et al.*, 1997; Talasz *et al.*, 1996). There are five CDK motifs of (S/T)-P-X-K (where X is any amino acid) within H1.4 that occur at T18, T146, T154, S172, and S187 (Figure 1.5; Contreras *et al.*, 2003; Garcia *et al.*, 2004). Of these, one CDK phosphorylation site is in the N-terminus of H1.4, with the remaining four sites located in the C-terminal tail (Contreras *et al.*, 2003; Garcia *et al.*, 2004). The cell cycle pattern of the CDK phosphorylation on histone H1.4 is one phosphate is present in G_1, two phosphates in S phase, and the maximum of five phosphate groups in mitosis (Garcia *et al.*, 2004; Talasz *et al.*, 1996). During interphase CDK2/cyclin A phosphorylates histone H1.4 on S172 and S187 (Sarg *et al.*, 2006). When chromosomes are most compact during mitosis H1.4 becomes hyperphosphorylated with the remaining sites, T18, T146 and T154, phosphorylated by

CDK1/cyclin B (Langan *et al.*, 1989; Sarg *et al.*, 2006; Swank *et al.*, 1997; Talasz *et al.*, 1996). Phosphorylation is lost during telophase to reset levels for interphase (Gurley *et al.*, 1978), and Protein phosphatase 1 (PP1) is one phosphatase known to be responsible for this dephosphorylation (Paulson *et al.*, 1996).

Partial phosphorylation of histone H1.4 during interphase destabilises its interaction with chromatin, and increases the mobility of H1.4 (Contreras *et al.*, 2003; Lopez *et al.*, 2015). A non-phosphorylatable CDK mutant of histone H1 was shown to be less mobile during interphase using FRAP (Contreras *et al.*, 2003). Interphase phosphorylated H1 therefore has higher mobility, reducing chromatin condensation and resulting in greater access to chromatin for factors involved in transcription and DNA replication (Bhattacharjee *et al.*, 2001; Dou *et al.*, 1999; Halmer & Gruss, 1996; Lopez *et al.*, 2015). For instance, the presence of phosphorylated H1 at the mouse mammary tumour virus promotor is known to enhance transcriptional activation by improving the positioning of the nucleosomes (Koop *et al.*, 2003; Vicent *et al.*, 2002). The plasticity of chromatin is lost as cells differentiate and lose growth potential (Reik, 2007). One role of the CDK phosphorylation of histone H1 is its inhibition of erythroid differentiation in a model system (Yellajoshyula & Brown, 2006). A constitutive CDK phosphorylation mimic of H1 prevented cells committing to terminal differentiation, whereas cells with hypophosphorylated histone H1 differentiated normally (Yellajoshyula & Brown, 2006).

The interaction between histone H1 and chromatin is highly dynamic (Misteli *et al.*, 2000), and this relates to the phosphorylation status of H1 (Contreras *et al.*, 2003; Lever *et al.*, 2000). FRAP has shown that the residence time of H1 on chromatin is 3 – 4 minutes during interphase, after which H1 dissociates and then rapidly interacts at another binding site (Misteli *et al.*, 2000). This residence time is rapid relative to that of the core histones, which have a residence time of several hours (H. Kimura & Cook, 2001; Phair *et al.*, 2004), but is much slower than the 5 – 25 seconds of transcription factors (Phair *et al.*, 2004). The residence time of H1 during mitosis is increased and can reach 15 minutes, but this varies according to the mitotic phase (Chen *et al.*, 2005).

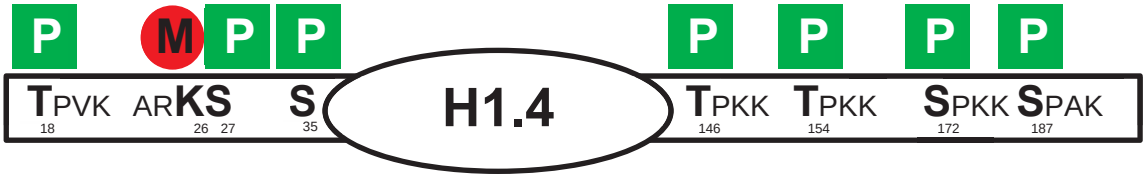

Figure 1.5. A diagram of H1.4 and its key post-translational modifications.
Schematic diagram of the tripartite structure of histone H1.4. The circular proportion indicates the globular winged-helix domain, with the flanking N-terminal (left), and C-terminal (right) tails. The locations of the five CDK phosphorylation sites (P) in the CDK consensus sequences [S/T]-P-X-[K/R], the single methylation site (M), and the Aurora B phosphorylation site (P) in the 'ARKS' motif are shown, as is the Protein kinase A phosphorylation site (P) on serine 35.

It is somewhat contradictory that when H1 is hyperphosphorylated, chromatin is at its most compact (Gurley *et al.*, 1978), considering that chromatin structure is more relaxed with partial H1 phosphorylation in interphase (Contreras *et al.*, 2003; Lopez *et al.*, 2015). It has been suggested that hyperphosphorylation of histone H1 during chromosome condensation allows brief decondensation to grant access to condensation factors (Roth & Allis, 1992). However, Roque *et al.* (2008) showed that the DNA compaction ability of the fully phosphorylated H1 C-terminus is restored to that of the unphosphorylated form, as mediated by structural changes in the C-terminus of histone H1, rather than through charge differences. Since these findings, this group have extended their results using chromatin isolated from chicken erythrocytes (Lopez *et al.*, 2015). This showed that partial phosphorylation of H1, achieved using CDK2 on a chromatin template, led to an increase in β-sheet structures in H1 and a decrease in α-helices (Lopez *et al.*, 2015). These conformational changes in H1 and H5 (an avian erythrocyte H1 subtype) resulted in a more relaxed chromatin structure as detected by sucrose gradient sedimentation (Lopez *et al.*, 2015). This could be due to the increase in β-sheet structure in H1 reducing the interaction with DNA, decreasing the linker histones residence time (Lopez *et al.*, 2015). So, it seems that partial phosphorylation of H1 reduces its ability to bind and aggregate DNA and chromatin, not through charge differences, but instead through structural changes (Lopez *et al.*, 2015; Roque *et al.*, 2008). This condensation capacity is then restored upon hyperphosphorylation of histone H1, indicating how phosphorylation of H1 can be involved in the condensation of mitotic chromosomes (Roque *et al.*, 2008).

Phosphorylation of histone H1 could directly change its ability to compact chromatin, or this could be brought about indirectly by the recruitment of other key players, such as the condensins (Maresca *et al.*, 2005). Factors known to be involved in chromosome condensation have been shown to localise normally in *Xenopus laevis* extracts depleted of histone H1, that have aberrantly long mitotic chromosomes (Maresca *et al.*, 2005). This indicates that histone H1 depletion could in itself lead to destabilisation of the 30 nm fibre, with downstream consequences for compaction of mitotic chromosomes that lack hyperphosphorylated H1 (Maresca *et al.*, 2005).

1.5.3 Aberrant phosphorylation of histone H1 in cancer

Cancer cells exhibit altered nuclear morphology, chromatin patterning and increased chromatin plasticity (Komitowski & Janson, 1990; Reik, 2007; Umbricht *et al.*, 1989). Compared to normal tissue, tumour tissue has high levels of histone H1 phosphorylation (Burstein *et al.*, 2002; Harshman *et al.*, 2014; Telu *et al.*, 2013), which could be an early event in tumour progression. Pre-malignant tissue that appears histologically normal from mouse models of breast, prostate, and skin tissue has significantly higher levels of histone H1 phosphorylation when compared to normal tissue (A. Contreras, personal communication). Furthermore, cells transformed with oncogenes, or those lacking the retinoblastoma tumour suppressor gene, display high levels of histone H1 phosphorylation during interphase, and a more relaxed chromatin structure (Chadee *et al.*, 1995; Herrera *et al.*, 1996). Additionally, recent work in *Drosophila* has shown that H1 itself may act to suppress tumourigenesis in the context of hyperactive growth signalling (Xu *et al.*, 2014).

Phosphorylation of H1.2, H1.3, and H1.4 at the mitotic CDK phosphorylation site threonine 146 (H1T146p) has been observed in both human breast tumour tissue and bladder cancer cell lines and tissue (Harshman *et al.*, 2014; Telu *et al.*, 2013). Increased H1 phosphorylation was detected by mass spectrometry of bladder cancer cell lines and this correlated with invasive potential (Telu *et al.*, 2013). There is a significant increase in phosphorylation of H1.2, H1.4, and H1.5 in invasive bladder cancer cell lines when compared to low grade non-invasive, or normal bladder epithelial cells (Telu *et al.*, 2013). The usefulness of H1 phosphorylation as a biomarker for bladder tumour grade was supported by immunohistochemical screening with the H1T146p antibody, which showed increasing positivity with increased tumour severity, and also correlated well with the established proliferative marker Ki67 (Telu *et al.*, 2013). Similar results were found when the same H1T146p antibody was used to screen breast tumour samples (Harshman *et al.*, 2014). Thus phosphorylated H1T146 may be a suitable biomarker for mitotic index given its association with cells that are actively dividing (Harshman *et al.*, 2014; Telu *et al.*, 2013). As increased H1 phosphorylation is likely to result from increased CDK activity in hyperproliferative cells, this could create

a ‘mutator phenotype’ with inappropriate derepression of gene expression and genomic instability.

1.5.4 Non-CDK phosphorylation of histone H1.4

In addition to CDK-mediated phosphorylation, histone H1.4 is also phosphorylated by other kinases (Figure 1.5; C.-S. Chu *et al.*, 2011; Garcia *et al.*, 2004; Hergeth *et al.*, 2011; Swank *et al.*, 1997; Talasz *et al.*, 1996). Two non-CDK phosphorylation sites are present in the N-terminal tail of H1.4, these are S27 and S35 (C.-S. Chu *et al.*, 2011; Garcia *et al.*, 2004; Hergeth *et al.*, 2011). In 2011, H1.4S35 was found to be phosphorylated by c-AMP dependent Protein kinase A (PKA) during mitosis (C.-S. Chu *et al.*, 2011). When H1.4 was phosphorylated at S35 it dissociated from the mitotic chromosomes, as shown in cell fractionation and immunofluorescence experiments (C.-S. Chu *et al.*, 2011). The remaining non-CDK phosphorylation site in H1.4 on serine 27 is within an ‘ARKS’ sequence motif and is of particular interest given its similarity to the ‘binary methylation-phosphorylation switch’ in H3 (Figure 1.6; Daujat *et al.*, 2005; Garcia *et al.*, 2004; Hergeth *et al.*, 2011). H1.4 is the only linker histone with this ‘ARKS’ motif (Garcia *et al.*, 2004), and it is not known whether it is regulated in the same manner with that in H3.

1.5.4.1 The similarities between the ‘ARKS’ motifs at H1.4K26S27 and H3K9S10

Phosphorylation of H1.4 at serine 27 cannot be considered in isolation as it resides within an ‘ARKS’ motif, where the adjacent lysine 26 can be methylated (Garcia *et al.*, 2004). The similarity between the motifs in the N-terminus of the core histone H3 at K9S10 and K27S28, with that in H1.4K26S27 was reported in 2004 by Garcia *et al.* (2004), who first detected the dual modification on H1.4 using mass spectrometry. The well-known ‘ARKS’ motif in the core histone H3 at K9S10 serves as a binding site for Heterochromatin Protein 1 (HP1) when lysine 9 is methylated (Bannister *et al.*, 2001; Jacobs *et al.*, 2001; Lachner *et al.*, 2001). However, phosphorylation of the adjacent serine 10 has been shown to disrupt this interaction, resulting in the release of HP1 from mitotic chromosomes (Fischle *et al.*, 2005; Hirota *et al.*, 2005). Similarly to H3, H1.4

has been shown to recruit HP1 when K26 is methylated, while phosphorylation on the adjacent serine 27 disrupts this interaction, as shown in *in vitro* peptide binding assays (Daujat *et al.*, 2005). The similarity between these sites is illustrated in Figure 1.6. Thus, histone H1.4 may operate as a 'binary methylation-phosphorylation switch' to regulate HP1 binding, in a similar manner to that proposed for histone H3 (Figure 1.6; Fischle *et al.*, 2005; Fischle *et al.*, 2003; Hirota *et al.*, 2005).

The enzymes that modify the H3 'ARKS' motif have been identified (Hsu *et al.*, 2000; Tachibana *et al.*, 2001), whereas they are still being elucidated for H1.4. Methylated H3K9 is associated with heterochromatin, and the histone methyltransferases G9a and SUV39H1 methylate this residue (Rea *et al.*, 2000; Tachibana *et al.*, 2001). As these enzymes also methylate H1.4K26 (Rea *et al.*, 2000; Trojer *et al.*, 2009; Weiss *et al.*, 2010), then phosphorylation of the adjacent H1.4S27 may also occur through a common kinase.

Mitotic H3S10 phosphorylation is mediated by the kinase, Aurora B, which resides in the Chromosomal passenger complex (CPC; Adams *et al.*, 2001; Giet & Glover, 2001; Hsu *et al.*, 2000). It has been demonstrated that Aurora B kinase is necessary for axial shortening of chromosomes, accurate chromosome segregation, and completion of cytokinesis (Kallio *et al.*, 2002; Mora-Bermudez *et al.*, 2007; Terada *et al.*, 1998). H3S10 is phosphorylated by Aurora B kinase during mitosis from prophase until anaphase (Hergeth *et al.*, 2011; Hirota *et al.*, 2005). While the function of H3S10 phosphorylation is thought to be the dislodgement of HP1, it is also associated with mitotic chromosome condensation (Ajiro *et al.*, 1983; Fischle *et al.*, 2005; Hendzel *et al.*, 1997; Hirota *et al.*, 2005). However, the mechanism through which H3S10 phosphorylation contributes to this compaction is unknown (Prigent & Dimitrov, 2003). Whether Aurora B also phosphorylates the 'ARKS' motif in H1.4, and if this regulates HP1 dislodgement or chromosome compaction during mitosis is worthy of further investigation.

A

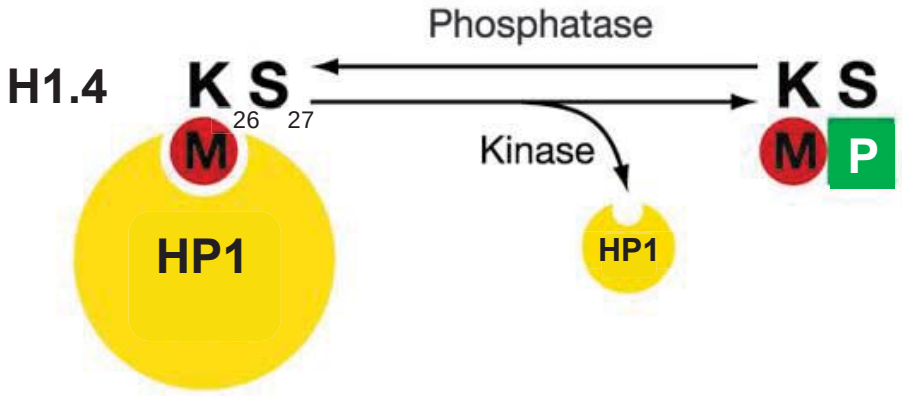

B

Histone H1.4

$ARK_{26}S_{27}$

Histone H3

$ARK_{9}S_{10}$

$ARK_{27}S_{28}$

Figure 1.6. The mechanism of HP1 dislodgement from H1.4.
A. A depiction of the model 'binary methylation-phosphorylation switch' for displacing Heterochromatin Protein 1 (HP1) family members from H1.4. When methylated at K26 (M), H1.4 serves as a binding site for HP1. When H1.4 methylated at K26 is also phosphorylated (P) at S27, HP1 can no longer bind. When H1.4S27 is dephosphorylated the HP1 binding site is re-established. A similar mechanism operates on the core histone H3 at 'ARKS' motifs. Figure adapted from Fischle *et al.* (2003).
B. Comparison of the 'ARKS' sequence in histone H1.4 and histone H3. Both histones can be post-translationally modified by lysine (K) methylation, and serine (S) phosphorylation. There is one motif in H1.4 at $K_{26}S_{27}$, and two motifs in H3 at $K_{9}S_{10}$ and at $K_{27}S_{28}$, that are subject to this 'binary methylation-phosphorylation switch'.

The association of H1.4K26 methylation with heterochromatin and HP1 is not surprising in light of the strong chromatin condensation capacity of the H1.4 subtype (Table 1.1; Clausell *et al.*, 2009; Daujat *et al.*, 2005; Th'ng *et al.*, 2005). HP1 interacts with di-methylated lysine 26 in H1.4 through its chromo domain, and promotes heterochromatin formation and maintenance through the adjoining related chromo shadow domain (Bannister *et al.*, 2001; Daujat *et al.*, 2005). As methylation is a stable heritable modification through cell division (Bannister *et al.*, 2002), it is possible that H1.4S27 phosphorylation is required for the transient dissociation of HP1 during mitosis (Daujat *et al.*, 2005; Fischle *et al.*, 2003). As phosphorylation is highly labile, its removal would allow HP1 to reassociate with the preserved H1.4K26 methylation mark without risk of losing domains of heterochromatin (Daujat *et al.*, 2005; Dormann *et al.*, 2006; Fischle *et al.*, 2003).

While the lysine in H1.4 at position 26 is conserved in all main H1 subtypes (Happel & Doenecke, 2009; Hergeth & Schneider, 2015), it has only been reported to be methylated in H1.2 and H1.4 (Garcia *et al.*, 2004; Kuzmichev *et al.*, 2004; Ohe *et al.*, 1986; Wiśniewski *et al.*, 2007), although H1.4 is the only H1 subtype in which this conserved lysine is adjacent to a serine that can be phosphorylated (Garcia *et al.*, 2004). Additionally, H1.4S27 phosphorylation can occur adjacent to K26 acetylation in mitosis (Terme *et al.*, 2014). While histone acetylation is associated with transcriptional activation, H1.4K26 acetylation has not been functionally characterised (Kouzarides, 2007; Terme *et al.*, 2014; Vaquero *et al.*, 2004). This modification is removed by SirT1, a histone deacetylase (HDAC) found in Polycomb repressive complex 4 (PRC4), which also contains the H1.4K26 methyltransferase Ezh2 (Kuzmichev *et al.*, 2004; Kuzmichev *et al.*, 2005; Vaquero *et al.*, 2004). Thus, when H1.4K26 acetylation is replaced with methylation, by SirT1 and Ezh2 in PRC4, this promotes heterochromatin formation and transcriptional repression (Vaquero *et al.*, 2004).

Elucidation of the function of the 'ARKS' motif in H1.4 *in vivo* and whether this and the 'ARKS' motif in H3 function in concert, or act independently is yet to be established. There is potential for similar roles, although with the more mobile H1.4 present on the outside of the nucleosome (Misteli *et al.*, 2000; Phair *et al.*, 2004), they may also have distinct functions.

1.6 The interacting partners of Histone H1.4

Few histone H1 interacting proteins have been identified to date, and of those that have, most are enzymes known to modify H1, including the H1.4K26 histone deacetylase, SirT1, and the H1.4K26 methyltransferase, G9a (Trojer *et al.*, 2009; Vaquero *et al.*, 2004). Interestingly, two proteins involved in higher order chromatin structure, HP1 and CAPD2, have been shown to interact with histone H1 (Ball *et al.*, 2002; Daujat *et al.*, 2005; Hale *et al.*, 2006).

1.6.1 Heterochromatin protein 1

There are three paralogs of HP1 in mammals, HP1α, HP1β, and HP1γ, all of which are involved in heterochromatin formation and maintenance (Maison & Almouzni, 2004; Singh *et al.*, 1991). Heterochromatin has been described as 'self-maintaining', as H3 methylated at lysine 9 recruits HP1, which in turn brings in the methyltransferase SUV39H1, which methylates nearby H3 at K9, a modification that acts as a dock to recruit further HP1 (Bannister *et al.*, 2001; Jacobs *et al.*, 2001; Lachner *et al.*, 2001; Rea *et al.*, 2000). HP1 is chromatin bound throughout the majority of the cell cycle, and is only displaced from the chromosomes during mitosis (Hayakawa *et al.*, 2003; Minc *et al.*, 1999; Terada, 2006), which is thought to allow access for factors involved in chromatin condensation (Fischle *et al.*, 2005; Hirota *et al.*, 2005). This mitotic dislodgment of HP1 is brought about through phosphorylation of H3S10, which prevents the interaction between methylated H3K9 and the chromo domain of HP1 (Fischle *et al.*, 2005; Hirota *et al.*, 2005).

In vitro, HP1α, HP1β, and HP1γ can each be dislodged from H1.4 methylated at K26 when also phosphorylated at H1.4S27 as described in Section 1.5.4.1 (Daujat *et al.*, 2005). Phosphorylation of H1.4S27 may therefore remove HP1 from the mitotic chromosomes while maintaining K26 methylation, signalling that the area should form heterochromatin following re-entry into interphase (Daujat *et al.*, 2005; Dormann *et al.*, 2006; Fischle *et al.*, 2003). There has been some conflicting results over the mitotic

displacement of HP1, with some demonstrating H3S10 phosphorylation as sufficient (Fischle *et al.*, 2005; Hirota *et al.*, 2005), while other groups showed this is inadequate for displacement of full length HP1 (Fass *et al.*, 2002; Terada, 2006), or that concomitant H3K14 acetylation is also required (Mateescu *et al.*, 2004). It has also been demonstrated that the correct localisation of HP1 depends not only on the methyl binding of the chromo domain, but also on binding to RNA through its hinge (Muchardt *et al.*, 2002).

Only HP1α has been demonstrated to interact with H1 independently of methylated K26 *in vitro* (Hale *et al.*, 2006; Meehan *et al.*, 2003; A. Nielsen *et al.*, 2001). This interaction with HP1α instead occurs between its hinge domain and the C-terminal tail of H1.4 (Hale *et al.*, 2006). Additionally, there may be a requirement for RNA to mediate this interaction, for which three adjacent lysine residues from position 104 – 106 in HP1α are necessary (Muchardt *et al.*, 2002; T.K. Hale, personnal communication). This is supported by studies indicating that localisation of HP1α to heterochromatin *in vivo* requires both H3 methylated at K9, and the hinge domain of HP1α binding to RNA (Maison *et al.*, 2002; Muchardt *et al.*, 2002). Interestingly, *Xenopus laevis* HP1α does not bind to methylated H3K9 from isolated chicken chromatin, due to its inaccessibility, but rather to histone H1, through the hinge of HP1α (Meehan *et al.*, 2003). Together, these results suggest that histone H1.4, in addition to H3, may have an important role in regulating HP1 localisation during the cell cycle, especially in mitosis.

1.6.2 CAPD2, a component of Condensin I, interacts with histone H1

Both histone H1 and H3 have been shown to interact with the Condensin I subunit Condensin complex subunit 1 (CAPD2) *in vitro* (Ball *et al.*, 2002). Condensin I is involved in mitotic chromosome condensation and is thought to compact chromatin in conjunction with topoisomerase activity (K. Kimura *et al.*, 2001). This occurs through the Structural maintenance of chromosome (SMC) subunits of Condensin I which have ATPase activity that can introduce positive supercoils into circular DNA (K. Kimura & Hirano, 1997). The CAPD2 subunit is involved in the regulation and recruitment of

Condensin I to chromatin through its chromosome targeting domain, which doesn't require the remaining Condensin I subunits (Ball *et al.*, 2002). To date, the only evidence of an *in vivo* interaction between CAPD2 and a histone is that it immunoprecipitates with H3 (Ball *et al.*, 2002; Schmiesing *et al.*, 2000). Ball *et al.* (2002) demonstrated an *in vitro* interaction between CAPD2 and histone H1 via Far-Western analysis using a HeLa chromatin fraction, and purified bovine H1 (Ball *et al.*, 2002). However, this work has not identified the subtype of H1 that interacts with CAPD2, the interacting region in H1, or how the status of H1 phosphorylation affects this interaction.

1.7 Research Aims

During mitosis histone H1.4 is hyperphosphorylated, and the majority of this phosphorylation is mediated by the cyclin dependent kinases (CDKs; Garcia *et al.*, 2004; Swank *et al.*, 1997; Talasz *et al.*, 1996). The function of the CDK phosphorylation of H1.4 remains unclear, although, its timing is coincident with mitotic chromosome condensation, and high levels of H1 phosphorylation are seen in tumours and cell lines with active oncogenes (Burstein *et al.*, 2002; Chadee *et al.*, 1995; Gurley *et al.*, 1978; Herrera *et al.*, 1996). The non-CDK phosphorylation site in the N-terminus of H1.4 on serine 27 bears similarity to the 'ARKS' motif in histone H3 at serine 10, which is phosphorylated by Aurora B kinase (Crosio *et al.*, 2002; Garcia *et al.*, 2004; Hsu *et al.*, 2000). Methylation occurs on the adjacent H3K9 which serves as a docking site for HP1, while phosphorylation at H3S10 abolishes this interaction (Bannister *et al.*, 2001; Fischle *et al.*, 2005; Hirota *et al.*, 2005; Lachner *et al.*, 2001). Histone H1.4 also has the neighbouring lysine residue methylated within an 'ARKS' motif and therefore it may function similarly as a 'binary methylation-phosphorylation switch' (Daujat *et al.*, 2005; Fischle *et al.*, 2003; Garcia *et al.*, 2004).

The aims of this research are:

- To determine the kinase that phosphorylates histone H1.4S27 in HeLa cells.
- To establish if aberrantly high histone H1.4S27 phosphorylation is present in breast tumour tissue.
- To characterise the function of histone H1.4S27 phosphorylation, and whether this plays a role in mitotic chromosome condensation.
- To explore whether histone H1.4 phosphorylation regulates HP1 localisation.
- To investigate the interaction between histone H1.4 and CAPD2 and whether this is regulated by phosphorylation of histone H1.4.

Chapter Two

Materials and Methods

2.1 Materials

Analytical or molecular biology grade reagents were purchased from Bio-Rad, Sigma, Thermo Fisher Scientific or Merck Millipore unless otherwise specified. Corning or Becton Dickinson (BD) tissue culture plasticware was obtained from In Vitro Technologies. Sterile Axygen® and Finn filter tips were purchased from Global Science or Thermo Fisher Scientific respectively.

2.2 DNA and RNA manipulations

2.2.1 Determining the concentration of DNA and RNA

The concentration of DNA and RNA was determined with 1 μL of sample on the NanoDrop ND-1000 spectrophotometer. The ratio of absorbance at 260 nm/280 nm was measured to establish if it was near 1.8 for DNA and 2.0 for RNA.

2.2.2 Agarose gel electrophoresis

Agarose gels were prepared by melting agarose in 1 x Tris acetate EDTA (TAE buffer; 40 mM Tris, 20 mM acetate, 1 mM EDTA) in a microwave oven, ethidium bromide (Sigma) was added to the molten agarose to a final concentration of 0.5 μg/mL. BlueJuice™ Gel Loading Buffer (Thermo Fisher Scientific) or TrackIt™ Cyan/Orange Loading Buffer (Thermo Fisher Scientific) was mixed with samples of equal volume to give a 1 x solution prior to loading. The 1 kb Plus DNA Ladder (5 μL; Thermo Fisher Scientific) was diluted according to the manufacturer's instructions and was loaded for size estimation of DNA bands. Samples were subject to electrophoresis at approximately 90 volts for 1 hour. Visualisation and photography were carried out by

examination under ultraviolet (UV) light using a UV transilluminator Gel Documentation system (Bio-Rad).

2.2.3 RNA extraction

Total RNA was extracted from HeLa cells using the High Pure RNA Isolation kit (Roche) according to the manufacturer's instructions.

2.2.4 Complementary DNA synthesis

Total RNA from HeLa cells (Section 2.2.3) was reverse transcribed into complementary DNA (cDNA) using the Transcriptor First Strand cDNA Synthesis Kit (Roche) according to the manufacturer's instructions. Anchored-oligo $(dT)_{18}$ primers were used to prime cDNA synthesis.

2.2.5 Polymerase chain reaction

The polymerase chain reaction (PCR) was used to amplify Condensin complex subunit 1 (CAPD2) cDNA from HeLa cells (Section 2.2.4) using sequence specific primers (Section 2.2.5.1). PCR reactions were carried out using *PfuUltra* Hotstart DNA Polymerase (Agilent Technologies) according to the manufacturer's instructions. PCR was performed using an Eppendorf Mastercycler® Gradient thermocycler.

2.2.5.1 Primers used in this study

To clone CAPD2 cDNA into the SmaI site of the pGEX2TK plasmid for later GST-CAPD2 expression, the forward primer: AATGGCTCCCCAAATGTATGAGTTCC, and reverse primer: ATACCCTGCACAGGGAGGAC were used, producing an amplicon of 4,240 bp. To produce the plasmid to express the GST-CTD fusion protein, inverse PCR was performed on the pGEX2TK-CAPD2 plasmid utilising the primers CTTCGGGCCTGTCATACCAG (forward) and TGGGGATCCAACAGATGCAC

(reverse), which produced an amplicon of 5,345 bp. Primers were purchased from Integrated DNA Technologies (IDT).

2.2.6 Site-directed mutagenesis

Site-directed mutagenesis (SDM) was performed to create the pET3d-H1.4S27E-FLAG construct from pET3d-H1.4-FLAG, and to correct a point mutation in CAPD2 cDNA from HeLa cells using the QuikChange II Site-Directed Mutagenesis Kit (Agilent Technologies) according to the manufacturer's instructions. Primers used to attain the H1.4S27E mutation in the pET3d-H1.4-FLAG plasmid were GAAGAAGGCCCGC AAG**GAG**GCAGGTGCG (forward) and CGCACCTGC**CTC**CTTGCGGGCCTTCTTC (reverse), with the underlined codon being that changed from serine to alanine. The amplicon produced was 5,343 bp. The primers used for site-directed mutagenesis of CAPD2 cDNA from HeLa cells that had been cloned into the pGEX2TK plasmid were GCCTCAAAGAAGATACTCTG**CAA**TTCCTGATAAAAGTGGTA (forward) and TACCACTTTTATCAGGAA**TTG**CAGAGTATCTTCTTTGAGGC (reverse). The underlined codon indicates the point mutation corrected from glutamate to glutamine at position 83, the amplicon was 9,209 bp. Primers were purchased from IDT.

2.2.7 Cloning

Restriction endonuclease digestions were performed according to the manufacturer's instructions. The QIAquick PCR Purification Kit (Qiagen) was used to purify the digested plasmid or insert. Products were analysed by agarose gel electrophoresis (Section 2.2.2) to verify whether digestion was complete. Phosphate groups were removed from vector ends using rAPid Alkaline Phosphatase (Roche), phosphate groups were added to the PCR products where required using T4 Polynucleotide Kinase (Thermo Fisher Scientific), and ligations were carried out using T4 DNA Ligase (Thermo Fisher Scientific) according to the manufacturer's instructions.

2.2.8 Transformation of competent *Escherichia coli* cells

Up to 100 ng of ligation reactions or plasmid DNA (Table 2.1) were added to 50 μL of the indicated competent *E. coli* strains. DH5α cells (Thermo Fisher Scientific) or JM110 cells (kindly supplied by Dr Jeong Park; Massey University) were used for plasmid amplification, and BL21 or BL21(DE3) cells (Agilent Technologies) were used for protein expression. Cells were incubated on ice for 30 minutes followed by heat shock at 42 °C for 45 seconds, incubation on ice for 2 minutes followed by the addition of 500 μL of sterile S.O.C Medium (Thermo Fisher Scientific). The cells were incubated at 37 °C for 1 hour with shaking at 225 rpm. The cell suspension (50 μL) was plated on LB (lysogeny broth) agar plates which contained ampicillin (100 μg/mL); if necessary the cells were concentrated by centrifugation at 5,000 rpm for 5 minutes and cells were resuspended and plated after removal of 450 μL of supernatant. The plates were incubated overnight at 37 °C, and then stored at 4 °C.

2.2.9 Plasmid purification

Following transformation (Section 2.2.8) and bacterial culture in LB medium, plasmids were extracted using the ChargeSwitch Pro Plasmid MiniPrep Kit (Thermo Fisher Scientific) for screening of clones via restriction endonuclease digestion. Once DNA sequencing (Section 2.2.10) confirmed that the plasmid of the correct identity was attained the PureLink HiPure Plasmid Filter Midiprep Kit (Thermo Fisher Scientific) was used to obtain high quality plasmid DNA.

2.2.10 DNA sequencing

Sanger sequencing of DNA was performed at the Massey Genome Service (MGS, Massey University, Palmerston North), using the BigDye™ Terminator Version 3.1 Ready Reaction Cycle Sequencing Kit (Thermo Fisher Scientific) on the ABI3730 DNA Analyzer using specific sequencing primers. Sequencing reactions contained 600 ng of plasmid DNA and 4 pmol of primer in 20 μL.

2.1. Plasmids used in this study

Plasmid	Manufacturer	Expression system	Plasmid Source
pTRE-Tight-H1.4-FLAG	Clontech	HeLa Tet-On	CRG laboratory
pTRE-Tight-H1.4S27A-FLAG	Clontech	HeLa Tet-On	CRG laboratory
pTRE-Tight-H1.4S27E-FLAG	Clontech	HeLa Tet-On	CRG laboratory
pET-3d-H1.4-FLAG	Merck Millipore	BL21(DE3)	CRG laboratory
pET-3d-H1.4S27A-FLAG	Merck Millipore	BL21 (DE3)	CRG laboratory
pET-3d-H1.4S27E-FLAG	Merck Millipore	BL21 (DE3)	This study
pET-3d-H1.4K26A-FLAG	Merck Millipore	BL21 (DE3)	CRG laboratory
pET-3d-H1.4/H1.2-FLAG	Merck Millipore	BL21 (DE3)	Dr Nicole Happel, University of Göttinggen
pET-3d-A1.5-FLAG	Merck Millipore	BL21 (DE3)	CRG laboratory
pET-3d-A2345-FLAG	Merck Millipore	BL21 (DE3)	CRG laboratory
pET-3d-E1.5-FLAG	Merck Millipore	BL21 (DE3)	CRG laboratory
pGEX-2T	GE Healthcare	BL21	GE Healthcare
pGEX-2T-HP1β	GE Healthcare	BL21	CRG laboratory
pGEX-2TK	GE Healthcare	BL21	GE Healthcare
pGEX-2TK-CAPD2	GE Healthcare	BL21	This study
pGEX-2TK-CTD	GE Healthcare	BL21	This study

2.3 Protein manipulations

Protein samples were kept at 4 °C at all times during manipulation to protect their integrity. In addition all solutions and buffers for cell lysis or protein storage had cOmplete™ or cOmplete™ ULTRA Mini Protease Inhibitor Cocktail Tablets containing EDTA (Roche) added according to the manufacturer's instructions. The phosphatase inhibitor sodium fluoride (NaF) was added to a final concentration of 1 mM where phosphorylation was being investigated.

2.3.1 Protein quantification

Purified proteins or lysates were quantified in duplicate using the bicinchoninic acid (BCA) microplate assay (Pierce). Protein was quantified using standards of known concentration prepared from bovine serum albumin (BSA; Thermo Fisher Scientific), or in the case of purified histones, calf thymus H1 (Sigma). Protein standards were prepared with the buffer used for lysis. In instances where the quantification of protein was not suitable cells were counted using a haemocytometer and equal cell concentrations were used.

2.3.2 SDS-PAGE

For protein electrophoresis using sodium dodecyl sulphate-polyacrylamide gel electrophoresis (SDS-PAGE), equivalent amounts of protein were set up in equal volumes of 1 x Laemmli buffer (62.5 mM Tris pH 6.8, 7.5% glycerol, 1.67% SDS, 0.0025% bromophenol blue, 35.75 mM β-mercaptoethanol; Laemmli, 1970) and were boiled for 5 minutes. Samples were subject to discontinuous gel electrophoresis through a 5% stacking gel before resolution in a 12% gel (Davis, 1964; Ornstein, 1964) in 1 x Tris-glycine-SDS running buffer (TGS; 25 mM Tris, 192 mM glycine, 1% SDS) at 100 V for 2 – 3 hours. Where required, gels were stained with 0.1% Coomassie blue R-

350 (PlusOne Coomassie PhastGel® Blue R-350 tablets; Sigma) in 30% methanol and 10% acetic acid. Gels were destained in 10% methanol and 10% acetic acid.

2.3.3 Autoradiography

Following separation by SDS-PAGE and Coomassie staining (Section 2.3.2) the gel was dried in a Model 583 Gel dryer (Biorad). The dried gel was exposed to Biomax MS film (Kodak) overnight at -80 °C under a Biomax Transcreen LE (Kodak) and then developed on the ALLPRO Imaging 100Plus X-ray Film Processor.

2.3.4 Western blotting

Following separation by SDS-PAGE (Section 2.3.2) protein was electrophoretically transferred to 0.1 μm nitrocellulose in 25 mM CAPSO buffer pH 10, 20% methanol for basic histone proteins, or for general transfer, Towbin buffer (25 mM Tris, 192 mM glycine, 20% methanol; Towbin *et al.*, 1979). The membrane was blocked in 5% non-fat milk (NFM; Anchor) for 1 hour at room temperature (RT) and incubated with the primary antibody (in 5% NFM) overnight at 4 °C. After washing in TBST (1 x Tris-buffered saline [20 mM Tris pH 7.6, 150 mM NaCl], 0.1% Tween 20 [Sigma]) the membrane was incubated with the HRP (horseradish peroxidase)-conjugated secondary antibody for 1 hour at RT. Further washing was followed by signal development using ECL Prime (enhanced chemiluminescence; GE Healthcare); the membrane was exposed to Hyperfilm ECL (GE Healthcare), and developed on the ALLPRO Imaging 100Plus X-ray Film Processor and/or imaged with a Fujifilm LAS-1000 CCD camera in an Intelligent Dark Box II. See Tables 2.3 and 2.4 for antibody details.

2.2. Primary antibodies used in this study

Antibody	Manufacturer (code)	Raised In	Dilutions		
			WB	IF	IHC
α-H1.4	Sigma (H7665)	Rabbit	1:1,000	1:500	-
α-H1.4K26ac	Sigma (H7789)	Rabbit	1:1,400	-	-
α-H1.4K26me2	Sigma (H8289)	Rabbit	1:2,000	-	-
α-H1.4K26me2S27p	Sigma (H8164)	Rabbit	1:10,000	-	-
α-H1.4S27p	Sigma (H7664)	Rabbit	1:10,000	1:1,000	1:10,000
α-H1.4K26me3	Abcam (ab17347)	Rabbit	1:500	-	-
α-Total H1	Abcam (ab1938)	Sheep	1:1,000	-	-
α-Phospho H1	Millipore (06-597)	Rabbit	1:1,000	-	-
α-H3S10p	Abcam (ab5176)	Rabbit	1:1,000	-	1:200
α-H4	Abcam (ab10158)	Rabbit	1:1,000	-	-
α-HP1α	Millipore (05-689)	Mouse	1:1,000	-	-
α-HP1α	Cell Signaling (2616)	Rabbit	1:1,000	-	-
α-HP1β	Abcam (ab10478)	Rabbit	1:500	-	-
α-Ki67	Dako (M7240)	Mouse	-	-	1:100
α-Aurora A	Abcam (ab12875)	Rabbit	1:500	-	-
α-Aurora B	Abcam (ab10735)	Mouse	1:900	1:100	-
α-CENPA	Abcam (ab13939)	Mouse	1:1,000	-	-
α-CAPD2	Abcam (ab34338)	Rabbit	1:500	-	-
α-FLAG	Sigma (F1804)	Mouse	1:1,000	1:1,000	-
α-FLAG	Sigma (F7425)	Rabbit	1:1,000	1:1,000	-
α-Tubulin (α)	Thermo Fisher (A11126)	Mouse	-	1:400	-
α-Tubulin (α)	Abcam (ab4074)	Rabbit	1:2,300	1:400	-
α-Tubulin (α)	Sigma (T6199)	Mouse	1:1,200	-	-

2.3. Secondary antibodies used in this study

Antibody	Type	Company	Code	Dilutions		
				WB	IF	IHC
α-Mouse	HRP	GE Healthcare	NA931	1:10,000	-	-
α-Rabbit	HRP	GE Healthcare	NA934	1:10,000	-	-
α-Sheep	HRP	Abcam	ab6900	1:4,000	-	-
α-Mouse	Cy3	Thermo Fisher	A10521	-	1:1,000	-
α-Mouse	Cy5	Thermo Fisher	A10524	-	1:1,000	-
α-Rabbit	Cy3	Thermo Fisher	A10520	-	1:1,000	-
α-Rabbit	Cy5	Thermo Fisher	A10523	-	1:1,000	-

2.3.5 Expression of mammalian proteins in bacteria

BL21 or BL21 (DE3; for expression from the T7 promoter) strains of *E. coli* (Agilent Technologies) were used for expression of recombinant proteins from the pET-3d, pGEX-2T, or pGEX-2TK vectors (Table 2.1). Following transformation (Section 2.2.8; 2.1) and overnight culture in LB (or to A_{600} of 0.6 – 1 in the case of H1.4-FLAG expression) of clonal cultures, 200 mL cultures were inoculated with the starter culture (1:40 – 1:100; maintained with 150 μg/mL carbenicillin). After growth until A_{600} of 0.6 – 1 at 30 °C (or 37 °C for H1.4-FLAG proteins) cultures were induced by the addition of IPTG (0.4 mM; Sigma) and growth was continued for a further 2 – 4 hours. Cells were pelleted by centrifugation at 4,000 x *g* for 10 minutes at 4 °C, then washed (10 mM Tris pH 8.0, 100 mM NaCl), and the cell pellet was stored at -80 °C until harvest (Section 2.3.6).

2.3.6 Harvest of bacterially expressed protein

The bacterial cell pellet was resuspended in 1 x CSB buffer (1 x phosphate buffered saline [PBS; Thermo Fisher Scientific], 100 mM EDTA), or 1 x ELB buffer (50 mM HEPES pH 7.5 [Thermo Fisher Scientific], 150 mM NaCl, 5 mM EDTA, 0.1% IGEPAL® CA-630 [Sigma]) for H1.4-FLAG proteins prior to acid extraction (Section 2.3.7). Cells were lysed via sonication at 20% amplitude for 3 x 30 second pulses using the Misonix Sonicator S-4000, and were rotated with 1% Triton™ X-100 (Sigma) for 30 minutes at 4 °C for protein solubilisation. Lysates were centrifuged at 10,000 rpm to remove insoluble components and the supernatant was stored at -80 °C until use in GST (glutathione S-transferase) pull-down assays (Section 2.3.12), or acid extraction for H1.4-FLAG proteins (Section 2.3.7).

2.3.7 Acid extraction from bacterial cell pellets

Following harvest of bacterial lysates (Section 2.3.6), H1.4-FLAG proteins were acid extracted. Perchloric acid (60%) was added to lysates to a final concentration of 5%,

then incubated at 4 °C for 10 minutes, and centrifuged at 10,000 rpm for 10 minutes. Trichloroacetic acid (TCA; 100%) was added to the supernatant to a final concentration of 18% and samples were rotated at 4 °C overnight. Following centrifugation at 14,000 rpm for 30 minutes at 4 °C, the histone pellet was washed with acidified acetone (0.05% HCl), and twice more with acetone. The histone pellet was resuspended in 1 x TBS (Tris-buffered saline) and 1 M Tris pH 8.0 was used to neutralise the solution. Histones were stored at -80 °C until affinity purification (Section 2.3.8).

2.3.8 Protein purification

Bacterially expressed recombinant protein (Section 2.3.5) was affinity purified. For the purification of H1.4-FLAG proteins, partial purification using acid extraction (Section 2.3.7) was performed, followed by column purification using ANTI-FLAG® M2 Affinity Gel (Sigma) according to the manufacturer's instructions. Glutathione sepharose 4B (GE Healthcare) was used to batch purify GST-tagged proteins during each GST pull-down assay according to the manufacturer's instructions.

2.3.9 *In vitro* methylation assays

Bacterially expressed (Section 2.3.5) and purified (Section 2.3.8) H1.4-FLAG (1 μg) was incubated with 166.67 ng of the histone methyltransferase G9a (Abcam) and 40 nCi of ^{14}C-SAM (Adenosyl-L-Methionine, S-[methyl-^{14}C]; PerkinElmer) in methyltransferase buffer (50 mM Tris pH 8.0, 5 mM $MgCl_2$, 4 mM DTT) at 37 °C for 1.5 hours. Methylated H1.4-FLAG was then used in kinase assays with Aurora B or CDK1/cyclin B (Cyclin dependent kinase; Section 2.3.10), and in GST pull-down assays (Section 2.3.12), or analysed by SDS-PAGE (Section 2.3.2) and autoradiography (Section 2.3.3).

2.3.10 *In vitro* kinase assays

Bacterially expressed (Section 2.3.5) and purified (Section 2.3.8) H1.4-FLAG (1 μg) was incubated with 100 ng of Aurora A kinase (Sigma), Aurora B kinase (Abcam) and/or CDK1/Cyclin B (Thermo Fisher Scientific) and 200 μM ATP (adenosine triphosphate; Thermo Fisher Scientific) in kinase assay buffer (20 mM Tris pH 7.5, 10 mM $MgCl_2$, 0.5 mM DTT, 0.1 mM EDTA, 1 mM NaF) at 30 °C for a minimum of 10 minutes. EDTA was added to a final concentration of 30 mM to stop the reaction when required. Phosphorylated H1.4-FLAG proteins were then used in GST pull-down assays (Section 2.3.12), or analysed by western blotting (Section 2.3.4).

2.3.11 Radioactive *in vitro* kinase assays

Bacterially expressed and purified H1.4-FLAG and H1.4S27A-FLAG (1 μg) were incubated with 100 ng of Aurora B kinase (Abcam) and 100 μM ATP and 5 μCi of [γ-^{33}P] ATP (PerkinElmer) in kinase assay buffer at 30 °C for 30 minutes. Phosphorylated H1.4-FLAG was analysed by SDS-PAGE (Section 2.3.2) and autoradiography (Section 2.3.3).

2.3.12 GST pull-down assays

Glutathione Sepharose™ 4B (GE Healthcare) was washed according to the manufacturer's instructions, and GST-tagged proteins in bacterial lysate (Section 2.3.6) were bound to 10 μL of beads. Beads were pelleted at 500 x *g* for 5 minutes then washed 3 x in 10 bead volumes of NEB buffer (25 mM Tris pH 8.0, 250 mM NaCl [unless otherwise indicated], 10% glycerol, 1 mM EDTA, 0.5% NP40, and 1 mM NaF for reactions involving phosphorylation). For phosphorylation of the GST-tagged C-terminal domain of CAPD2 (final 113 amino acids; GST-CTD) by CDK1/cyclin B 10 μL of beads with GST-CTD bound were added to the kinase reaction in the place of the H1.4-FLAG proteins (Section 2.3.10). CDK phosphorylated bead bound GST-CTD was then included in the GST pull-down reaction. For the GST pull-down assay 10 μL of

beads with the bound GST-tagged protein were incubated with 0.75 μg (for HP1β assays; Heterochromatin protein 1β) or 0.5 μg (for CAPD2 CTD assays) of the H1.4-FLAG proteins, which had been included in methylation and kinase assays (Sections 2.3.9 and 2.3.10) where indicated, and 30 μg of acetylated BSA (Thermo Fisher Scientific) in NEB buffer overnight with rotation. For RNase A treatments the indicated amount of RNase A (Sigma) was added to the GST pull-down reaction then incubated at room temperature for 30 minutes with rotation prior to overnight incubation at 4 °C. Beads were washed 4 x in 75 bead volumes of NEB buffer and bound protein was eluted by boiling for 5 minutes in 15 μL of 1.5 x Laemmli buffer. Samples were then analysed by western blotting (Section 2.3.4).

2.4 Tissue analysis

2.4.1 Immunohistochemistry

Formalin fixed paraffin embedded (FFPE) human breast tissue samples were kindly supplied by Assistant Professor Alejandro Contreras, MD Anderson Cancer Center. Samples were incubated overnight at 60 °C, then dewaxed and rehydrated with successive 5 minute incubations in 2 x xylene, 1 x xylene: ethanol (1:1), 2 x 100% ethanol, 1 x 95% ethanol, 1 x 70% ethanol, 1 x 50% ethanol, and finally 1 x in water. Endogenous peroxidase activity was blocked with 0.3% hydrogen peroxide for 15 minutes and then epitope retrieval was performed in 10 mM sodium citrate pH 6.0 for 3 minutes at 121 °C in a Decloaking Chamber (NxGen). Samples were blocked in 10% normal goat serum (Dako) for 1 hour, followed by overnight incubation at 4 °C with the primary antibody (2.2). Antibodies were diluted in Dako Antibody Diluent. Subsequent to 2 x 5 minute washes in TBST and TBS, samples were incubated with secondary antibodies (Dako EnVision+ Kit) for 1 hour at RT. After 5 minute washes in 2 x TBST, then 2 x TBS the slides were developed using DAB+ chromogen (Dako EnVision+ Kit). Samples were counterstained in haematoxylin and dehydrated, then

mounted using a Leica CV5030 Automated Glass Coverslipper. Images were captured using a Zeiss Axiophot Light Microscope at the Manawatu Microscopy and Imaging Centre. Histological analysis was kindly provided by Dr Bruce Lockett, Medlab Central and Assistant Professor Alejandro Contreras, MD Anderson Cancer Center.

2.5 Cell culture and techniques

Standard cell culture procedures and aseptic technique were followed. All manipulations were carried out in an ESCO Biological Safety Cabinet (Model: LA24A1) after brief UV exposure. Sterile solutions and equipment were used. Once harvested cell lysates were kept in the presence of cOmplete Protease Inhibitor Cocktail Tablets with EDTA (Roche) used according to the manufacturer's instructions and at 4 °C at all times unless otherwise stated.

2.5.1 Cell lines

HeLa and HeLa Tet-On Advanced cells were used in this study. Adherent HeLa cells, a human epithelial cervical adenocarcinoma cell line, were obtained from the ATCC. The HeLa Tet-On Advanced cells (Clontech) were a generous gift from Dr Jeong Park (Massey University). These cells were derived from HeLa cells that have been stably transfected with the pTet-On regulatory plasmid that allows inducible expression of a gene of interest from the pTRE-Tight plasmid in response to doxycycline.

2.5.2 Maintenance of cells

Cells were maintained in 75 cm^2 flasks at 37 °C with 5% CO_2 in a humid Hera cell 150 incubator. Cells were passaged as confluence was reached every three days by washing

twice with 10 mL PBS (Thermo Fisher Scientific), followed by incubation with 1.5 mL of 0.25% Trypsin-EDTA (Thermo Fisher Scientific) to detach cells. Trypsin was inactivated by addition of 8.5 mL Dulbecco's Modified Eagle Medium (DMEM, with L-glutamine, 4.5 g/L glucose and 110 mg/L sodium pyruvate) supplemented with 10% fetal bovine serum (FBS; Thermo Fisher Scientific) and 1% penicillin/streptomycin (Thermo Fisher Scientific; supplemented DMEM), the standard culture medium.

2.5.3 Cell synchronisation

To synchronise cells in the phases of the cell cycle several methods were employed.

2.5.3.1 Mitotic arrest

Cells were treated with colcemid (100 ng/mL; Thermo Fisher Scientific) from times ranging from 2 hours, for metaphase spreads, or up to 24 hours. Alternatively cells were blocked in mitosis using nocodazole (50 ng/mL; Sigma) for 2 – 18 hours.

2.5.3.2 The double thymidine block

For cells synchronised in G_1, S or M phase the double thymidine block was used as adapted from Pederson and Robbins (1971). Briefly, at 25% confluence 2 mM thymidine was added to the media and cells were incubated for 19 – 24 hours, thymidine was removed with 3 x PBS washes, and medium without thymidine was added. After 7.5 hours, 2 mM thymidine was again added to the cells, which were incubated for a further 16 hours. The thymidine was removed with 3 washes in PBS, and fresh media without thymidine was added. To obtain cells in G_1, cells were harvested immediately following completion of the second block. Cells in S phase were harvested four hours after release of the second thymidine block. To obtain cells in mitosis, cells were monitored and harvested when a large proportion of cells were rounded up (approximately 6 – 8 hours), or colcemid (100 ng/mL) or nocodazole (50 μg/mL) was added to the media to arrest cells in mitosis after release from the second thymidine block. Alternatively cells were harvested at various times following release from the second thymidine block for flow cytometry (Section 2.5.14) to analyse the proportion of cells in each phase of the cell cycle.

2.5.3.3 Mitotic shake-off

To harvest mitotic cells exclusively, cells were synchronised in mitosis using colcemid, nocodazole (Section 2.5.3.1) or the double thymidine block (Section 2.5.3.2) and the mitotic shake-off method adapted from Terasima and Tolmach (1963) was used. Briefly, the media was pipetted over the cell surface repeatedly to detach rounded mitotic cells.

2.5.4 Cell lysis

Following detachment of cells using trypsin or by scraping, cells were resuspended in high salt lysis buffer (50 mM HEPES pH 8.0, 400 mM NaCl, 1% NP40 and 1 mM NaF) or RIPA (Radioimmunoprecipitation assay buffer; 50 mM Tris pH 8.0, 150 mM NaCl, 1% NP40, 0.5% sodium deoxycholate, 0.1% SDS). Cells were rotated in lysis buffer for 30 minutes at 4 °C before removal of debris and insoluble material by centrifugation at 12,000 rpm for 10 minutes at 4 °C.

2.5.5 Acid extraction from eukaryotic cells

To acid extract histones from HeLa cells the method adapted from Shechter *et al.* (2007) was used. Briefly, cells were detached using trypsin or the mitotic shake-off (Sections 2.5.2 and 2.5.3.3) and were washed with PBS, then resuspended in hypotonic lysis buffer (10 mM Tris pH 8.0, 1 mM KCl, 1.5 mM $MgCl_2$, 1 mM DTT, 10 mM NaF, 10 mM nicotinamide, 5 mM sodium butyrate) and incubated at 4 °C with rotation for 30 minutes. Intact nuclei were pelleted by centrifugation at 10,000 x *g* for 10 minutes, and the pelleted nuclei were incubated in 0.4 N sulphuric acid at 4 °C overnight with rotation. Nuclear debris was removed by centrifugation at 16,000 x *g* for 10 minutes. The histone containing supernatant was transferred to a clean tube and TCA was added to a final concentration of 33%. Histones were precipitated overnight at 4 °C, with rotation, and then pelleted by centrifugation at 16,000 x *g* for 30 minutes at 4 °C,

then washed twice in acetone. Histones were air dried and resuspended in distilled water and stored at -80 °C.

2.5.6 Acid etch and poly-D-lysine coating of coverslips

Coverslips (Electron Microscopy Sciences; 8 mm, #1.5 thickness) were etched in 1 M hydrochloric acid overnight at 60 °C, washed 5 x for 5 minutes in distilled water, then incubated in poly-D-lysine (1 mg/mL) for 1 hour at RT. Coverslips were washed 3 x 5 minutes in distilled water, then 2 x 10 minutes in 70% ethanol, and 2 x 10 minutes in absolute ethanol prior to exposure to UV for 20 minutes on each side.

2.5.7 Immunofluorescence

Cells on poly-D-lysine coated coverslips (Section 2.5.6) in 6 well plates were grown asynchronously or synchronised in mitosis using the double thymidine block (Section 2.5.3.2). Cells were harvested by washing 3 x 5 minutes in PBS (containing $CaCl_2$ and $MgCl_2$; Thermo Fisher Scientific). Cells were fixed in 2 mL of 2% PFA (paraformaldehyde; in PBS) for 15 minutes and washed 2 x 10 minutes in 2 mL of PBS. Cells were permeabilised for 5 minutes in 2 mL of PBS containing 0.2% Triton™ X-100, then washed a further 2 x 10 minutes in 2 mL of PBS, and coverslips were transferred to individual wells in a 24 well plate. Following blocking in 300 µL of 5% BSA/0.5% Tween 20 for 30 minutes at RT, cells were incubated with primary antibodies (Table 2.2) in 300 µL of blocking buffer (1 x PBS, 5% BSA, 0.5% Tween 20) at 4 °C overnight. Cells were washed 3 x 5 minutes in 0.5 mL of wash buffer (0.1% Triton™ X-100 in PBS) then incubated with Cy3 or Cy5 labelled secondary antibodies (Table 2.3) in 300 µL of blocking buffer for 1 hour at RT with agitation. Cells were washed a further 3 x 5 minutes in 0.5 mL of wash buffer, then 1 x 5 minutes in 0.5 mL of PBS. Cells were fixed in 0.5 mL of 2% PFA (in PBS) for 15 minutes at RT, then washed 2 x 10 minutes in 0.5 mL of PBS, and 1 x 5 minutes in 0.5 mL of wash buffer. Cells were incubated with 300 µL of 300 nM DAPI (Thermo Fisher Scientific; in PBS), then washed a further 2 x 5 minutes in 0.5 mL of PBS before being mounted on a microscope slide in SlowFade®

Gold Antifade Mountant (Thermo Fisher Scientific). Images were captured using a Leica SP5 Scanning Confocal Microscope at the Manawatu Microscopy and Imaging Centre.

2.5.8 Metaphase spread immunofluorescence

HeLa Tet-On cells were grown in 25 cm^2 flasks in the presence or absence of doxycycline (1 μg/mL), and arrested in mitosis with colcemid (100 ng/mL) for 2 hours. Cells were harvested using the mitotic shake-off (Section 2.5.3.3) to collect loosely attached rounded mitotic cells, and then remaining cells were detached using trypsin (Section 2.5.2). Metaphase spreads were then prepared using the method adapted from Jeppesen (2000), briefly, the cells were swelled in 75 mM KCl (5 x 10^5 cells/mL) at 37 °C for 15 minutes. Cells were resuspended in 75 mM KCl/0.1% Tween 20 (5 x 10^5 cells/mL) and 50 μL was added to a Shandon Cytospin 4 Centrifuge Chamber then centrifuged at 1,000 rpm for 5 minutes. For immunofluorescence, samples were incubated in 50 μL of potassium chromosome medium (KCM buffer; 10 mM Tris pH 7.5, 120 mM KCl, 20 mM NaCl, 0.5 mM EDTA, 0.1% Triton™ X-100 and 1 mM NaF) for 15 minutes at RT. Samples were blocked with 50 μL of 5% BSA (in KCM buffer) for 30 minutes at RT, then incubated with primary antibodies (Table 2.2) in 50 μL of 5% BSA (in KCM buffer) overnight at 4 °C. Slides were rinsed, then washed 2 x 5 minutes in 40 mL of KCM buffer, and incubated with secondary antibodies (Table 2.3) in 50 μL of 5% BSA (in KCM buffer) for 1 hour at RT. Samples were rinsed, washed 2 x 5 minutes in 40 mL of KCM buffer, and then fixed in 40 mL of 2% PFA (in KCM buffer) for 15 minutes at RT. Samples were washed for 5 minutes in water, followed by incubation in 40 mL of 300 nM DAPI for 5 minutes. Slides were then washed 2 x 5 minutes in water and a coverslip was mounted over the metaphase spread preparation with SlowFade® Gold Antifade Mountant (Thermo Fisher Scientific). Images were captured using a Leica SP5 Scanning Confocal Microscope at the Manawatu Microscopy and Imaging Centre.

2.5.9 Transient transfection of siRNA targeting Aurora A and Aurora B kinase

HeLa cells were seeded at 1 x 10^5 cells per well in 6 well plates. The following day, 0.5 μg of siRNA targeting Aurora A or Aurora B kinase, or the non-targeting Negative Control #1 (Sigma) were transiently transfected using the X-tremeGENE™ siRNA Transfection Reagent (Roche). Transfection mixtures were set up using a ratio of 2.5 μL of transfection reagent to 0.5 μg of siRNA according to the manufacturer's instructions. After incubation for 20 minutes at RT the transfection mixture was added to the cells. Twenty-four hours post transfection colcemid (100 ng/mL) was added to arrest cells in mitosis. Cells were harvested 48 hours after transfection by washing with 2 mL of PBS and scraping cells into 200 μL of high salt lysis buffer. After incubation on ice for 30 minutes, lysates were centrifuged at 12,000 rpm at 4 °C to remove debris. The concentration of the protein extract was determined (Section 2.3.1) and was then analysed by western blotting (Section 2.3.4). Alternatively, when western blotting for histones the mitotic transfected cells were subjected to acid extraction (Section 2.5.5).

2.5.10 Inhibition of PP1 with calyculin A

HeLa cells were seeded on poly-D-lysine coated coverslips (Section 2.5.6) at 1.2 x 10^5 cells per well in 6 well plates. Following the synchronisation of cells in mitosis using the double thymidine block (Section 2.5.3.2), the Protein phosphatase 1 (PP1) inhibitor, calyculin A (100 nM final concentration; 20 μL of 10 μM stock), or the diluent DMSO (20 μL), was added to the cells for 1 hour prior to processing by immunofluorescence (Section 2.5.7).

2.5.11 Creation of stable H1.4-FLAG phosphorylation mutant inducible cell lines

Cell lines that inducibly expressed H1.4-FLAG, the non-phosphorylatable H1.4S27A-FLAG, or the phosphomimetic H1.4S27E-FLAG, were created. Cloning of wild-type human H1.4 or H1.4S27A or H1.4S27E with a C-terminal FLAG-tag into the pTRE-Tight vector (Clontech) was performed by laboratory colleagues using standard

techniques (Section 2.2.7; Table 2.1). These vectors were then co-transfected into HeLa Tet-On cells, with a linear hygromycin marker, to give inducible expression of the H1.4-FLAG proteins in response to doxycycline. Selection of transfected cells with hygromycin B produced cell lines with the construct stably incorporated.

2.5.11.1 Determining the effective concentration of hygromycin B for selection

HeLa Tet-On cells that were not resistant to hygromycin B were seeded at 0.6 x 10^5 cells per well in a 6-well plate, and hygromycin B was added 24 hours later at the following concentrations: 0, 50, 200, 400, 600 and 800 μg/mL. Media containing the appropriate concentration of hygromycin B was replaced every three days. Levels of cell death were recorded for 14 days. The concentration of 400 μg/mL hygromycin B caused most cells to die within 3 – 6 days, with all cells non-viable after 14 days, so was used to select cells following transfection with the H1.4-FLAG constructs (Section 2.5.11.2).

2.5.11.2 Transfection of the H1.4-FLAG constructs

HeLa Tet-On cells were seeded at 1.5 x 10^5 cells per well in 6 well plates. Transfection was performed in triplicate 24 hours later using X-tremeGENE™ 9 DNA Transfection Reagent (Roche). Plasmid DNA (1 μg) was co-transfected with a linear hygromycin selection marker (50 ng) using a 3:1 ratio of X-tremeGENE™ 9 DNA Transfection Reagent to plasmid DNA in Opti-MEM® I Reduced Serum Medium (Thermo Fisher Scientific). The transfection mixture was incubated at RT for 20 minutes, and then added to each of the wells. In addition, transfection without the hygromycin selection marker and no selection controls were used to verify that only transfected cells survived selection.

2.5.11.3 Selection and maintenance of stable H1.4-FLAG cell lines

Cells were trypsinised 24 hours after transfection, and transferred into 10 cm dishes with supplemented DMEM, then 400 μg/mL hygromycin B was added after a further 24 hours. The selection media was replaced every two days, until surviving cells began to form colonies. After selection for 8 – 9 days, individual colonies were transferred to 24 well plates following trypsinisation with cloning discs, at this time no healthy surviving cells were seen in dishes that had been transfected in the absence of the

linear hygromycin selection marker. Both uninduced and induced (1 μg/mL doxycycline) clonal cell populations were tested for inducible expression by western blotting cell lysates with the FLAG antibody (Section 2.3.4). Cell lines that showed low background expression, and strong induction were moved into progressively larger vessels, and were then routinely passaged (Section 2.5.2) and maintained in 200 μg/mL hygromycin B. Frozen stocks for the three inducible cell lines were maintained at all times.

2.5.11.4 Induction of the H1.4-FLAG proteins

Cells were seeded in the presence of, or had doxycycline added the following day. The concentration of doxycycline required for induction was determined by titration, with 1 μg/mL used for routine induction. Cells were incubated in doxycycline for 48 – 72 hours; fresh doxycycline was added to the media when replaced. Cells were maintained in hygromycin B during induction.

2.5.12 Quantitative analysis of mitotic defects and micronuclei

The H1.4-FLAG HeLa Tet-On cells were grown on coverslips in the presence or absence of doxycycline (1 μg/mL) and were synchronised in mitosis using the double thymidine block (Section 2.5.3.2), then processed for immunofluorescence (Section 2.5.7). Fields of cells were captured at 400x magnification using a Leica SP5 Scanning Confocal Microscope at the Manawatu Microscopy and Imaging Centre. Images were analysed for mitotic cells with defects including multipolar mitosis, misaligned chromosomes at metaphase, and lagging and bridging chromosomes during anaphase. A minimum of 50 mitotic cells were analysed in duplicate in two independent experiments. Interphase cells were also scored for abnormalities including cells undergoing apoptosis, cells that were multinucleate and cells that contained a micronucleus. A minimum of 500 cells were analysed in two independent experiments. P values were calculated using the Students T test.

2.5.13 Cell proliferation assay

Cells were seeded in duplicate in 5 x 96 well plates at a concentration of 1.5 x 10^4 cells per well, with or without doxycycline (1 μg/mL). The first plate was harvested 24 hours later, and one plate was harvested daily to day 4, with the final plate harvested on day 6. To harvest cells the medium was aspirated and the plate was stored at -80 °C. The proliferation time course was then assayed using the CyQUANT Cell Proliferation Assay Kit (Thermo Fisher Scientific) according to the manufacturer's instructions. Following incubation for 2 – 5 minutes after reagent addition the plates were read using the FLUOstar Galaxy, with an excitation of 485 nm and emission detection at 520 nm.

2.5.14 Flow cytometry

Cells were seeded in 6 well plates at a concentration of 1.5 x 10^5 cells per well, with or without doxycycline (1 μg/mL). Where required the double thymidine block was used to synchronise cells in the same phase of the cell cycle (Section 2.5.3.2). After 72 hours with or without doxycycline cells were detached with 0.5 mL of 0.25% trypsin and washed 2 x with 3 mL of PBS. For analysis of apoptotic cells using the fluorescent nucleic acid stain YO-PRO®-1 iodide, the cells were resuspended in 1 mL of PBS containing 1 μg/mL propidium iodide (PI; Thermo Fisher Scientific) and 0.1 μg/mL YO-PRO®-1 Iodide (Thermo Fisher Scientific). The cells were incubated on ice for 30 minutes and analysed on a Partec CyFlow® Space Flow Cytometer. For all other flow cytometry where fixation was required, cells were resuspended in 0.9 mL PBS then 2.1 mL of absolute ethanol was added dropwise with agitation, to a final concentration of 70%. Fixed cells were stored at -20 °C until they were prepared for analysis. Following 2 x PBS washes, cells were resuspended in 1 mL of PBS containing 50 μg/mL PI and 50 μg/mL RNase A. Cells were analysed by flow cytometry after incubation at 37 °C for 30 minutes on a FACSCalibur™ Flow Cytometer (BD).

2.5.15 Subcellular fractionation

Cells seeded in 75 cm^2 flasks (1 x 10^6 cells) in the presence or absence of doxycycline (1 μg/mL) underwent the double thymidine block (Section 2.5.3.2) and on removal of the second thymidine block, nocodazole (50 ng/mL) was added. Eight hours after mitotic arrest, cells were harvested using the mitotic shake-off (Section 2.5.3.3), washed in PBS and processed using the method adjusted from Kapoor *et al.* (2005). Briefly, cells were resuspended in buffer A (2 x 10^7 cells/mL; 20 mM Tris pH 7.5, 75 mM KCl, 30 mM $MgCl_2$, 1 mM DTT, 0.5 mM EDTA, 1 mM NaF and 0.5% NP40), and were incubated for 10 minutes with rotation, then half of the volume was removed for total cell lysate samples (T). The remaining lysate was centrifuged at 10,000 x rpm for 10 minutes, and the supernatant (soluble fraction) was transferred to a clean tube. The insoluble fraction was resuspended in an equal volume of buffer A.

2.5.16 Preparing soluble chromatin arrays for immunoprecipitation

Soluble chromatin arrays were prepared using methods adapted from Méndez and Stillman (2000), and the SimpleChIP Enzymatic Chromatin IP Kit (Cell Signaling). Briefly, cells grown in 15 cm dishes in the presence (1 μg/mL) or absence of doxycycline were detached using trypsin in the case of asynchronously grown cells, or by the mitotic shake (Section 2.5.3.3) following arrest in mitosis with colcemid (Section 2.5.3.1). Cells were fixed in 20 mL of 1% PFA (in supplemented DMEM) for 2.5 minutes with rotation, which was quenched with 125 mM glycine for 5 minutes. Washed cells were resuspended in buffer A (10 mM HEPES pH 7.9, 10 mM KCl, 1.5 mM $MgCl_2$, 340 mM sucrose, 10% glycerol, 1 mM DTT, 0.1% Triton™ X-100, 1 mM NaF) at a concentration of 5 x 10^6 cells/mL, and rotated for 30 minutes. Nuclei were collected by centrifugation at 2000 x *g* for 5 minutes, then resuspended in buffer A (5 x 10^6 cells/mL). Chromatin was digested by incubation with 500 U of micrococcal nuclease (MNase; NEB)/1 x 10^6 nuclei for 12 minutes at 37 °C after addition of $CaCl_2$ to 5 mM. To stop the reaction EGTA was added to a concentration of 10 mM. Nuclei were collected by centrifugation at 3000 x *g* for 5 minutes. Prior to nuclear lysis nuclei were

resuspended in buffer B (3 mM EDTA, 0.2 mM EGTA, 1 mM NaF; 5 x 10^6 cells/mL) with rotation for 30 minutes. Nuclei were sonicated at 20% amplitude for 4 x 15 second pulses using the Misonix Sonicator S-4000. Insoluble material was collected by centrifugation at 1700 x *g* for 5 minutes; the supernatant containing soluble chromatin arrays was transferred to a clean 15 mL tube for preparation of nucleosome ladders (Section 2.5.16.1), or use in immunoprecipitation experiments (Section 2.5.16.2). Fixation and sonication steps were introduced after initial optimisation experiments as indicated in Chapter 4.

2.5.16.1 Nucleosome ladders

Following preparation of soluble chromatin arrays (Section 2.5.16) a 50 µL aliquot (from 2.5 x 10^5 cells) was incubated in 190 mM NaCl with 135 µg/mL RNase A for 30 minutes at 37 °C. Proteinase K (Roche) was added to 250 µg/mL and samples were incubated for 2 hours at 65 °C. DNA fragments were purified using the Wizard SV Gel and PCR Clean-Up System (Promega). The entire eluate was then analysed by agarose gel electrophoresis (Section 2.2.2).

2.5.16.2 Immunoprecipitation

Soluble chromatin arrays (Section 2.5.16) were subject to immunoprecipitation (IP) using 10 µL ANTI-FLAG® M2 Affinity Gel (Sigma) washed according to the manufacturer's instructions. Conditions used for optimisation are indicated in Figure 4.18. Binding reactions took place at 4 °C overnight with rotation in IP buffer (50 mM Tris pH 7.5, 150 mM NaCl, 1 mM NaF initially, adapted to include 0.5% Triton™ X-100 following optimisation). Beads were then washed 4 x with at least 20 bead volumes of 1 x TBS (with 1 mM NaF, adapted to include 0.5% Triton™ X-100 following optimisation). After removal of the supernatant the bound protein was eluted from the beads by boiling for 5 minutes in 15 µL of 1.5 x Laemmli buffer (without β-mercaptoethanol). Samples were then analysed by western blotting (Section 2.3.4).

Chapter Three

Post-translational modification of the 'ARKS' motif within the N-terminus of histone H1.4

3.1 Introduction

The histone H1 subtypes are post-translationally modified at residues beyond the well-studied Cyclin dependent kinase (CDK) phosphorylation sites (Garcia *et al.*, 2004). The unique phosphorylation site on histone H1.4 at serine 27 (H1.4S27) is of particular interest, as it is similar to the 'binary methylation-phosphorylation switch' described in the N-terminus of the core histone, H3 (Fischle *et al.*, 2005; Fischle *et al.*, 2003; Garcia *et al.*, 2004; Hirota *et al.*, 2005). H1.4 is the only subtype of linker histone that possesses this sequence (Garcia *et al.*, 2004). Both H1.4 and H3 share the 'ARKS' motif (Figure 1.6), where dual modification of lysine and serine, by methylation and phosphorylation respectively, has been detected using mass spectrometry of histones from HeLa cells (Fischle *et al.*, 2005; Garcia *et al.*, 2004). These modifications can occur independently or together on one histone tail (Fischle *et al.*, 2005; Garcia *et al.*, 2004). In H3 when lysine 9 is methylated, it serves as a binding site for the Heterochromatin protein 1 (HP1) family members, and phosphorylation of serine 10 during mitosis disrupts this interaction (Bannister *et al.*, 2001; Fischle *et al.*, 2005; Hirota *et al.*, 2005; Lachner *et al.*, 2001).

The phosphorylation of H3 at serine 10 (H3S10p) is a hallmark of mitosis that has been associated with mitotic chromosome condensation (Prigent & Dimitrov, 2003). Kinases that phosphorylate H3S10 include Mitogen- and stress-activated protein kinase 1 (MSK1) and Aurora B, with Protein phosphatase 1 (PP1) reported to remove this transient phosphorylation (Crosio *et al.*, 2002; Hsu *et al.*, 2000; Soloaga *et al.*, 2003). Although H3S10 phosphorylation peaks during mitosis, this site is also phosphorylated at other times in the cell cycle (Hans & Dimitrov, 2001; Thomson *et al.*, 1999). Somewhat contradictory to its proposed mitotic role, phosphorylation of H3S10 during interphase facilitates gene activation and opens chromatin structure (Prigent & Dimitrov, 2003). It has been suggested that this can be brought about by the removal of HP1 in each situation (Fischle *et al.*, 2005). During interphase HP1 removal may allow access to histone acetyltransferases (HATs) and other factors that facilitate transcription, whereas during mitosis this could allow cohesin or the condensins to access the DNA (Dormann *et al.*, 2006; Fischle *et al.*, 2005).

Of the kinases that phosphorylate H3S10, Aurora B kinase is responsible for this modification during mitosis (Crosio *et al.*, 2002; Hsu *et al.*, 2000). Aurora B kinase is a chromosomal passenger protein that localises to mitotic chromosomes, particularly at the centromere, and then transfers to the central spindle during anaphase (Sun *et al.*, 2008). This kinase plays key roles during mitosis contributing to both chromosome condensation, and the attachment of the sister chromatids to the opposing spindle poles for their segregation (Adams *et al.*, 2001; Giet & Glover, 2001; Hsu *et al.*, 2000; Kallio *et al.*, 2002). Aurora B kinase is also necessary for the completion of cytokinesis as its depletion disrupts this process (Kallio *et al.*, 2002; Terada *et al.*, 1998). Aurora B is often found to be overexpressed in cancer, leading to aneuploidy, through missegregation, and tetraploidy, through failure of cytokinesis (Ota *et al.*, 2002).

The 'binary methylation-phosphorylation switch' in H3, so described for the ability of the transient phosphorylation of serine 10 to dislodge HP1 from methylated lysine 9, is the classic example of a binary switch in the histone code hypothesis (Fischle *et al.*, 2003). The association between HP1 and trimethylated H3K9 (H3K9me3) was reported in 2001 (Bannister *et al.*, 2001; Lachner *et al.*, 2001), with methyltransferases Suppressor of variegation 3-9 homolog 1 (SUV39H1) and G9a found to modify this residue (Rea *et al.*, 2000; Tachibana *et al.*, 2002). However, HP1 binding was found to be weak ($K_d = 10^{-4} – 10^{-6}$ M) and the presence of H3K9me3 did not always lead to the colocalisation of HP1, suggesting more complex mechanisms operate *in vivo* (Fischle *et al.*, 2005; Muchardt *et al.*, 2002). Fischle *et al.* (2005) revealed that the mitotic dislodgement of HP1 occurred despite the maintenance of H3K9 methylation throughout the cell cycle. Transient phosphorylation of the adjacent H3S10 displaced HP1 in peptide binding assays, and inhibition of Aurora B led to the retention of HP1 on the mitotic chromosomes (Fischle *et al.*, 2005; Hirota *et al.*, 2005; Terada, 2006). Together, this suggested that H3S10 phosphorylation was key for releasing HP1 from the chromosomes as they condense early in mitosis (Fischle *et al.*, 2005; Hirota *et al.*, 2005).

While the H3K9S10 motif in H3 has been studied extensively, the site in H1.4 at serine 27 is often disregarded. Exploration of this similarly modified 'ARKS' site in H1.4 revealed its ability to interact with HP1 in peptide binding assays (Daujat *et al.*, 2005).

The HP1 family members interacted with H1.4 when lysine 26 was dimethylated (H1.4K26me2), and phosphorylation of serine 27 (H1.4S27p) abolished this interaction (Daujat *et al.*, 2005). As anticipated from its association with the HP1 paralogs, H1.4K26me2 is considered to be a transcriptionally repressive modification, and has been shown to be methylated by both G9a and the polycomb repressive complex 2 (PRC2) member EZH2 (Enhancer of zeste homolog 2; Kuzmichev *et al.*, 2004; Trojer *et al.*, 2009). Identification of the kinase that phosphorylates H1.4S27, and the timing of this modification during the cell cycle will enable better understanding of the role of this phosphorylation in the cell and how this relates to the interaction between HP1 and H1.4.

The aim of this chapter is to examine the phosphorylation of H1.4S27 during the cell cycle, and investigate if this site is regulated in the same manner as that in histone H3 at serine 10. This will establish the relevance of H1.4S27 phosphorylation and its effect on the interaction with HP1 *in vitro*.

3.2 Results

3.2.1 H1.4S27 phosphorylation is cell cycle regulated

To establish if phosphorylation of H1.4 at S27 is regulated in a cell cycle dependent manner, HeLa cells were synchronised in G_1, S or M phase of the cell cycle using the double thymidine block (Section 2.5.3.2; See Figure 4.13 for an example of verification of synchronisation), and post-translational modifications of extracted histones were analysed by western blotting using commercial antibodies (Sections 2.3.4 and 2.5.5; Table 2.2 and 2.3; Full annotated western blots are located in Appendix One). The level of H1.4S27 phosphorylation was low in G_1 and S phase, but markedly increased during mitosis (Figure 3.1; Figure 3.9B illustrates that this antibody is specific for H1.4 phosphorylated at serine 27). H1.4 was detected in each phase, but H1.4 from mitotic cells displayed retarded migration due to its hyperphosphorylation by CDK. Phosphorylation of H3 at S10, like H1.4S27, was low during interphase (G_1 and S phase) and increased in mitosis. The core histones were present in equal amounts as indicated by histone H4. Taken together, this data indicates that, like for H3S10, phosphorylation at H1.4S27 occurs predominantly in mitosis, and is thus regulated in a cell cycle dependent manner.

To examine the cell cycle post-translational modification of the H1.4K26S27 bivalent site, western blotting of histones extracted from cells in G_1, S and M phase was performed (Sections 2.3.4, 2.5.3.2 and 2.5.5). H1.4K26 was di- and tri-methylated in G_1 and S phase, although, this appeared to be reduced during mitosis (Figure 3.1). This pattern could be caused by the inability of the H1.4 methylation specific antibodies to recognise their epitope when the adjacent H1.4S27 is phosphorylated. An antibody that recognised dimethylation and phosphorylation only when present together confirmed this, detecting H1.4K26me2S27p during mitosis. Acetylation of H1.4 at lysine 26 was present during both G_1 and S phase, but was reduced in mitosis. Together, these results show that as H1.4S27 phosphorylation can occur adjacent to methylation on lysine 26, like with H3K9S10, then there is potential for H1.4K26S27 to act as a binary switch *in vivo* for the displacement of HP1 during mitosis.

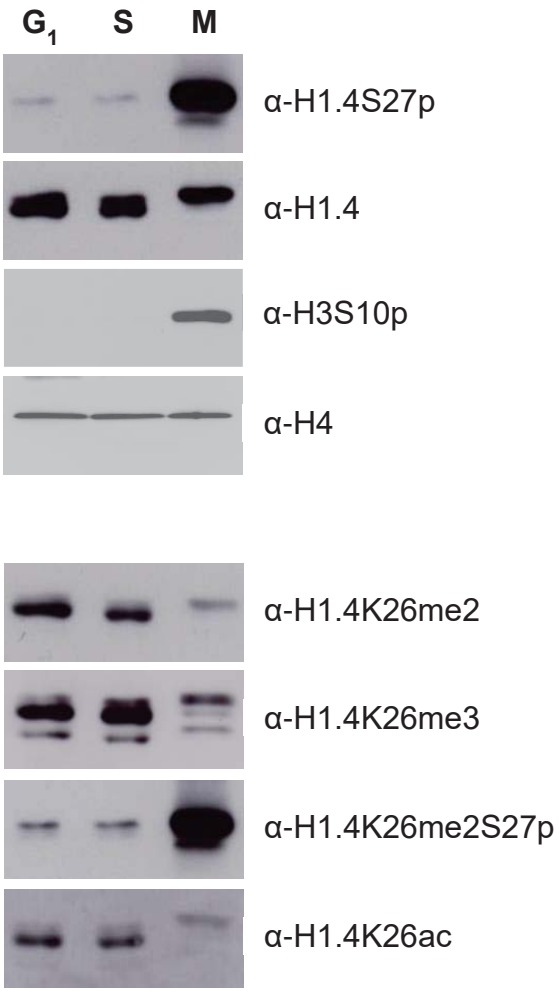

Figure 3.1. Post-translational modification of H1.4 during the cell cycle. Western blotting of acid-extracted histones (2 µg) from HeLa cells synchronised in G_1, S or M phase. The antibodies used for western blotting are indicated.

3.2.1.1 The localisation of phosphorylated H1.4S27 during mitosis

To determine the localisation and timing of H1.4S27 phosphorylation during mitosis, immunofluorescent confocal microscopy was carried out (Section 2.5.7). HeLa cells synchronised in mitosis (Section 2.5.3.2) were incubated with antibodies against histone H1.4S27p and α-tubulin for mitotic staging. During mitosis, H1.4S27 phosphorylation was present on the condensed chromosomes (Figure 3.2). This phosphorylation appeared early, as the chromosomes underwent condensation in prophase. This H1.4S27 phosphorylation was maintained along the length of the chromosomes, until early anaphase. From this stage onwards phosphorylation remained only on the tips of the chromosome arms and was lost from the regions of the chromosomes closest to the spindle poles. There was some exclusion of the H1.4S27p antibody indicating hindrance to antibody penetration into the condensed mitotic chromosomes. By telophase H1.4S27 phosphorylation was lost completely as the nuclear membrane reformed and the chromosomes began to decondense. In agreement with western blotting results in Figure 3.1, there was very little phosphorylated H1.4S27 in an interphase nucleus, indicating that histone H1.4S27 phosphorylation is exclusive to mitosis.

Metaphase spreads were then used to establish how H1.4S27 phosphorylation is distributed along metaphase chromosomes. Cells expressing H1.4-FLAG were synchronised in mitosis, spun onto coverslips using a cytocentrifuge and then screened with antibodies against H1.4S27p and FLAG using immunofluorescence (Section 2.5.8). While the arms of each chromosome were coated with phosphorylated H1.4S27, there was a marked enrichment of phosphorylation at the centromere, where the two replicated sister chromatids are attached (Figure 3.3). This demonstrates that the distribution of H1.4S27 phosphorylation on chromosomes changes during mitosis.

Figure 3.2

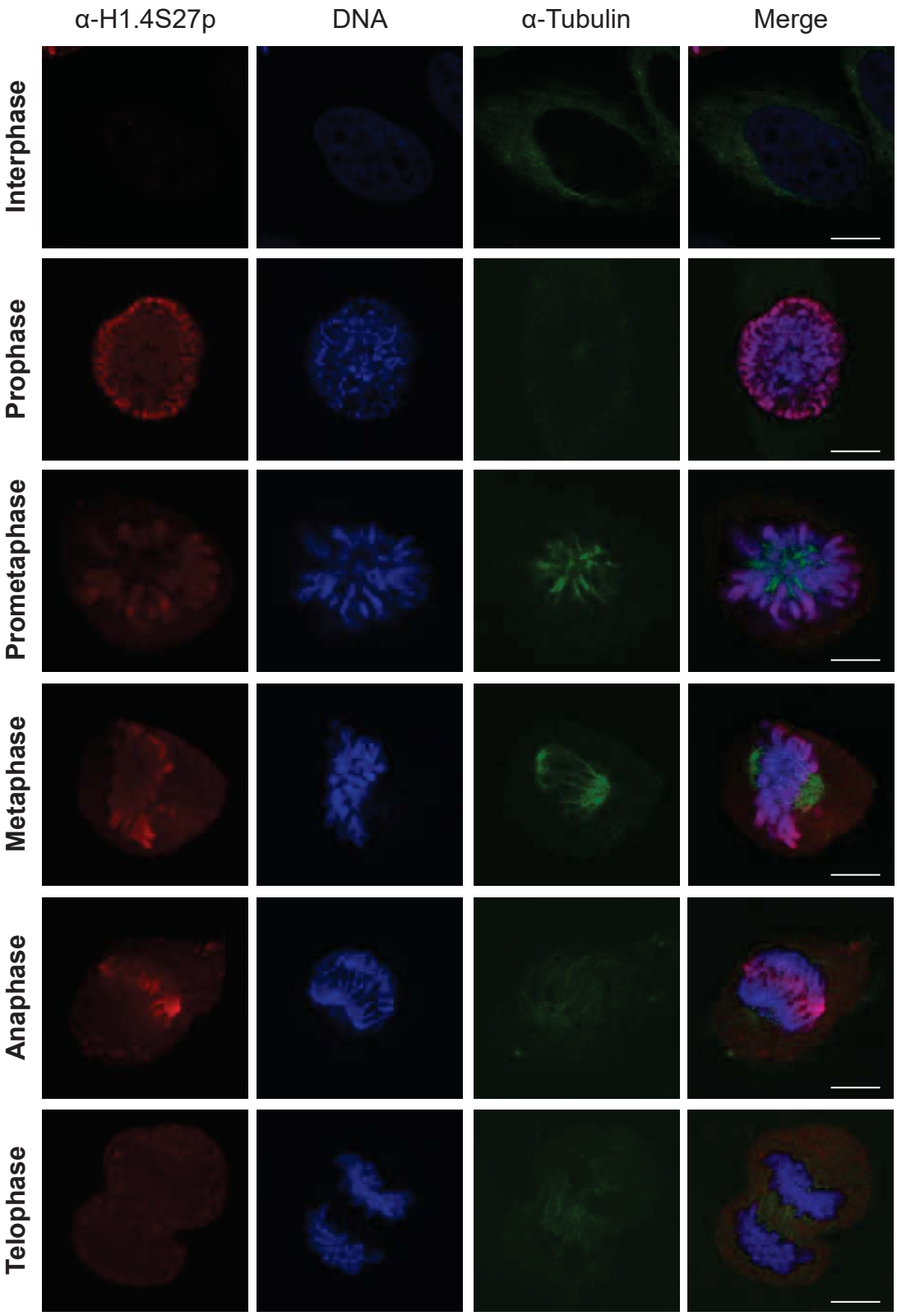
α-H1.4S27p
DNA
α-Tubulin
Merge
Interphase
Prophase
Prometaphase
Metaphase
Anaphase
Telophase

Figure 3.2. H1.4 is phosphorylated on serine 27 within the mitotic chromosomes.
Immunofluorescence of HeLa cells synchronised in mitosis using the double thymidine block. Antibodies against H1.4S27p (red) and α-Tubulin (green) were used; DNA was stained with DAPI (blue). Mitotic cells were imaged on a confocal microscope at 400x magnification with the same exposure time and settings. Representative cells are shown. Scale bar, 10 μm.

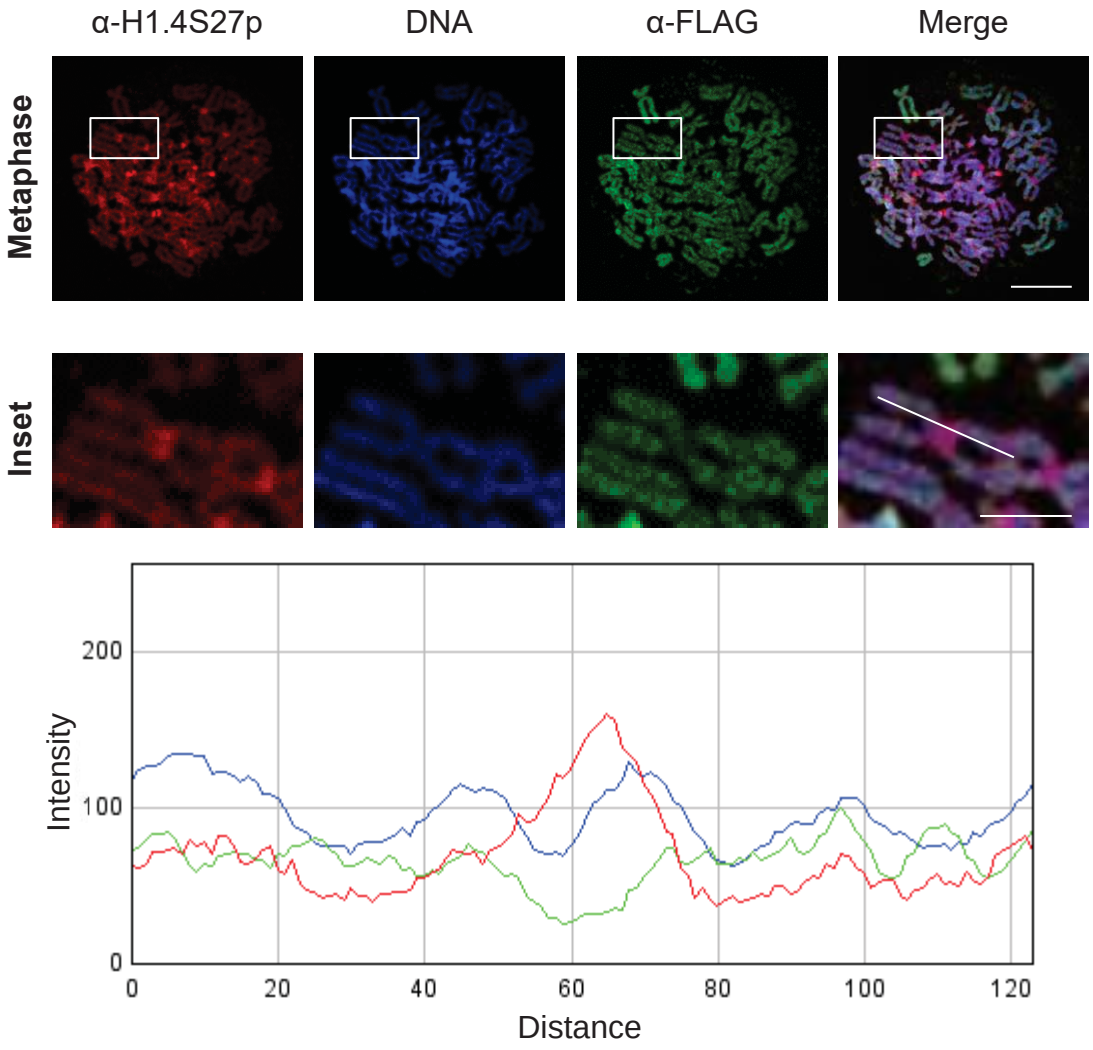

Figure 3.3. H1.4 serine 27 phosphorylation is enriched at the centromere.
Immunofluorescence of metaphase spreads from HeLa Tet-On cells expressing H1.4-FLAG arrested in mitosis using colcemid. Metaphase spreads were produced by cytocentrifugation onto coverslips then processed for immunofluorescence with antibodies against H1.4S27p (red) and FLAG (green); DNA was stained with DAPI (blue). Metaphase spreads were imaged on a confocal microscope at 400x magnification with the same exposure time and settings. A representative metaphase spread is shown. Image J RGB Profiler analysis shows the enrichment of H1.4S27p in the centromeric region. Scale bar, 10 μm and 5 μm (inset).

3.2.1.2 H1.4S27 phosphorylation is a potential marker of mitosis

H3S10 phosphorylation is used as a marker of mitosis when screening tumours (Yang, 2011); however, phosphorylation of H1.4S27 in tumours has not been explored. To determine if H1.4S27 phosphorylation could be used as a mitotic marker, formalin-fixed, paraffin-embedded breast invasive lobular carcinoma and normal tissue were subject to immunohistochemistry (Section 2.4.1). Examination of the breast tumour tissues shown in Figure 3.4 revealed positive staining of phosphorylated H1.4S27 and H3S10 in mitotic cells in invasive lobular carcinoma, which was not seen in normal tissue. Ki67, which detects actively cycling cells and is used routinely as a proliferation marker in pathological screening (Urruticoechea *et al.*, 2005), showed strong positivity in the invasive lobular carcinoma, but was negative in normal breast. This initial result indicates that as for H3S10 phosphorylation, H1.4S27p antibodies can detect mitotic cells in human breast tumours, and thus there is potential for their use in determining the mitotic index in breast tumours. Further optimisation will be required as background staining of H1.4S27 phosphorylation was seen in non-mitotic tumour cells and in the stromal cells in normal tissue.

3.2.2 Enzymes responsible for the mitotic phosphorylation of H1.4S27

To understand the regulation of the mitotic specific phosphorylation of H1.4S27, the enzymes that regulate this modification were explored. Of particular focus were the enzymes known to modify the similar site in H3, Aurora B kinase and PP1.

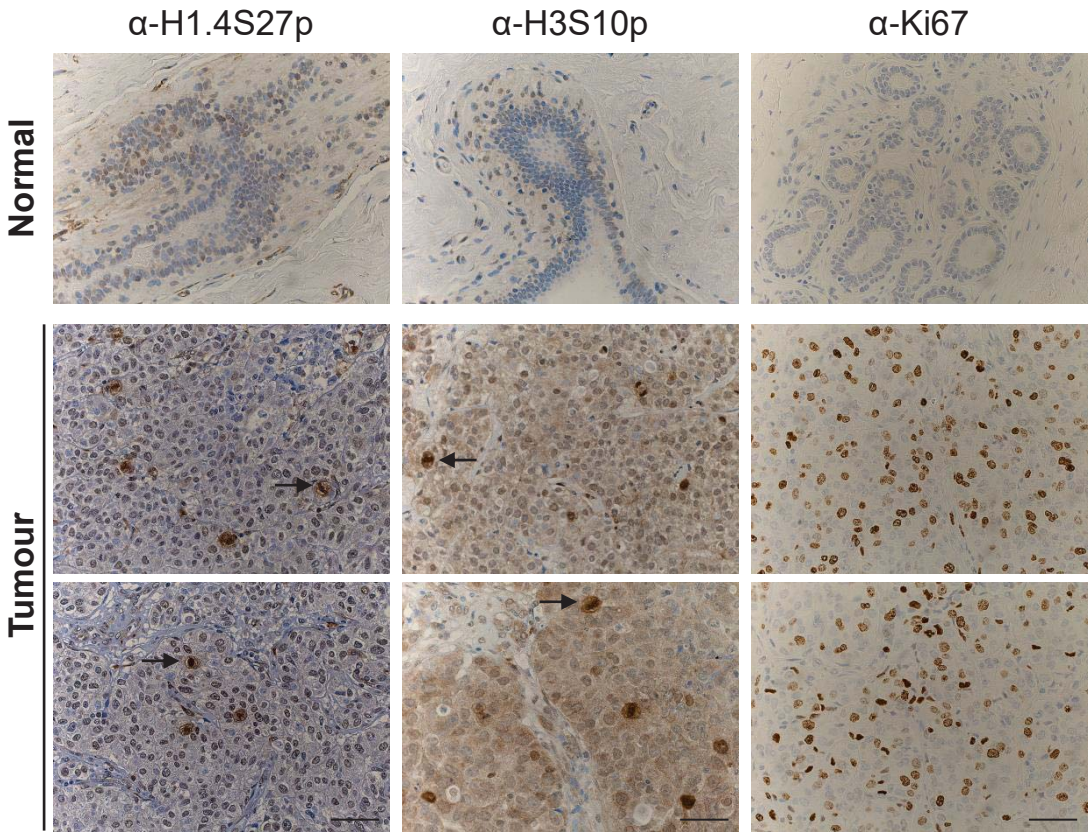

Figure 3.4. H1.4S27 phosphorylation as a mitotic marker in breast tumour tissue.
Immunohistochemistry of normal breast or invasive lobular carcinoma tissue (tumour) processed with antibodies against H1.4S27p, H3S10p or the proliferative marker Ki67 (brown). Nuclei were counterstained with haematoxylin (blue). Arrows indicate examples of mitotic cells positive for H1.4S27p or H3S10p. Tissue was imaged on a light microscope at 400x magnification with the same exposure time and settings. Representative tissue is shown. Scale bar, 50 μm.

3.2.2.1 Histone H1.4S27 is phosphorylated by the Aurora kinases

To determine if the Aurora kinases are able to phosphorylate histone H1.4 at S27, an *in vitro* kinase assay was performed (Section 2.3.10). Purified FLAG-tagged histone H1.4 and H1.4 in which serine 27 was replaced with alanine (H1.4S27A), to prevent phosphorylation, were used as substrates for commercially sourced Aurora A and Aurora B kinase. Following the assay, western blotting was performed with antibodies against histone H1.4, and H1.4S27p (Section 2.3.4), to detect total H1.4 protein and its phosphorylation respectively. Both Aurora A and Aurora B kinase phosphorylated H1.4 at S27 *in vitro* (Figure 3.5A). There was some weak phosphorylation detected with H1.4S27A under the assay conditions used here. However, no other Aurora kinase consensus sequences are present in histone H1.4; and this could be due to non-optimal *in vitro* kinase assay conditions.

To establish whether Aurora B kinase can phosphorylate histone H1.4 at sites other than serine 27, a kinase assay using ^{33}P-labelled ATP was used (Section 2.3.11) and following SDS-PAGE, the gel was examined by autoradiography (Sections 2.3.2 and 2.3.3). Figure 3.5B shows that in the presence of Aurora B kinase, ^{33}P was incorporated onto H1.4-FLAG, but was barely detectable for H1.4S27A. This indicates that the predominant site in H1.4 that Aurora B kinase phosphorylates is serine 27, although there may be an additional site that is poorly phosphorylated *in vitro*. From these results it can be concluded that both Aurora A and Aurora B kinase phosphorylate histone H1.4S27 *in vitro*.

3.2.2.2 Aurora B kinase phosphorylates histone H1.4S27 *in vivo*

Knockdown of Aurora A and B kinase using siRNA was carried out to determine whether these kinases phosphorylate histone H1.4 at serine 27 *in vivo*. HeLa cells were transiently transfected with siRNA targeting either Aurora A or Aurora B kinase, and a scrambled siRNA as a negative control (Section 2.5.9). Firstly, to verify whether the siRNA was effective, the level of Aurora A and Aurora B was identified by western blotting of mitotic cell lysates (Sections 2.3.4 and 2.5.3.1). As shown in Figure 3.5C, both

Aurora A and Aurora B kinase were efficiently targeted by their respective siRNAs. This demonstrated that the RNA interference was successful, and that each siRNA was specific for the targeted Aurora family member.

To identify whether the siRNA knockdown of Aurora A or B kinase led to a change in H1.4S27 phosphorylation, histones were acid-extracted and screened with the H1.4S27p antibody during western blotting (Sections 2.3.4 and 2.5.5). A small reduction in H1.4S27 phosphorylation (30%) was observed when Aurora B kinase was targeted by siRNA following normalisation to H1.4 (Figure 3.5C; Refer to Appendix Two for Quantitation). H3S10 phosphorylation was reduced with knockdown of Aurora B kinase, but was unaffected by reduced levels of Aurora A kinase as expected. This result shows that while both Aurora A and Aurora B kinase can phosphorylate H1.4S27 *in vitro*, it is Aurora B kinase that phosphorylates H1.4 at S27 *in vivo* in HeLa cells. As this reduction was only partial, then it is possible that other kinases also phosphorylate H1.4 at serine 27.

3.2.2.3 The localisation of Aurora B kinase overlaps with phosphorylated H1.4S27

To determine if the chromosomal localisation of Aurora B kinase during mitosis overlaps that of phosphorylated H1.4S27, the location of Aurora B in mitotic cells was established. Cells induced to express H1.4-FLAG were examined using immunofluorescence and confocal microscopy (Sections 2.5.3.2 and 2.5.7). From early prophase through to metaphase, Aurora B was seen on the condensing chromosomes, with brighter punctate staining at centromeres (Figure 3.6). However, by anaphase Aurora B shifted to the central mitotic spindle as the chromosomes moved toward the spindle poles. The exogenous H1.4-FLAG localised to the chromosomes, where it colocalised with the DNA. The localisation of Aurora B with the chromosomes was similar to that of phosphorylated H1.4S27 until metaphase, and the movement of Aurora B to the mitotic spindle could explain the retention of H1.4S27 phosphorylation in the centre of the cell in early anaphase (Figure 3.2). Together, this and RNA interference results (Figure 3.5C) strongly suggest that Aurora B kinase contributes to the phosphorylation of H1.4 at S27.

Figure 3.5

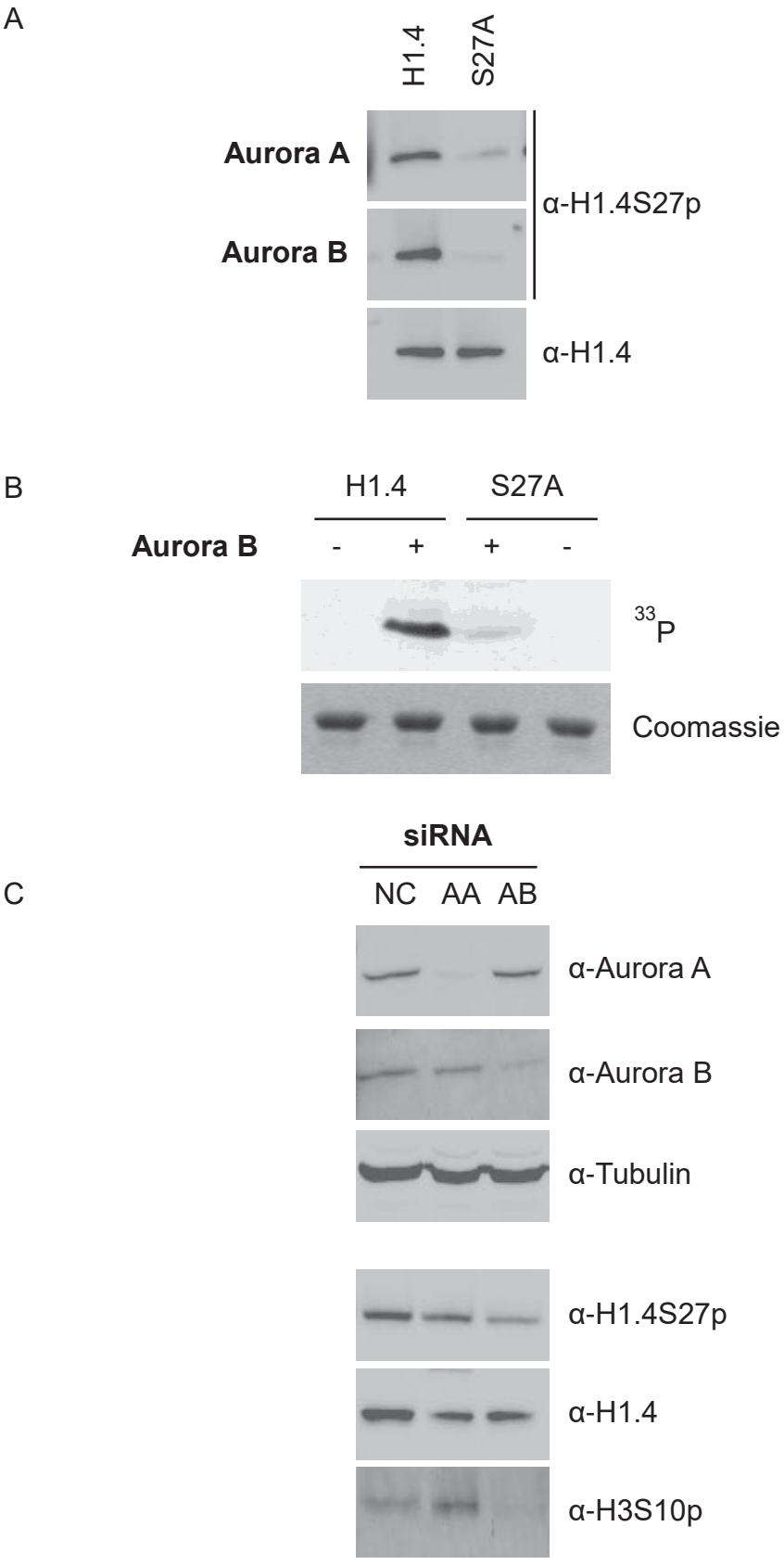
A
H1.4
S27A
Aurora A
Aurora B
α-H1.4S27p
α-H1.4
B
H1.4
S27A
Aurora B
-
+
+
-
33P
Coomassie
siRNA
C
NC
AA
AB
α-Aurora A
α-Aurora B
α-Tubulin
α-H1.4S27p
α-H1.4
α-H3S10p

Figure 3.5. Aurora B kinase phosphorylates H1.4 at serine 27.
A. *In vitro* kinase assay and western blotting of 1 µg of bacterially expressed and purified H1.4-FLAG (H1.4) or the phosphorylation mutant, H1.4S27A-FLAG (S27A), with Aurora A or B kinase. Total protein was detected with the H1.4 antibody; phosphorylation was detected with the H1.4S27p antibody.
B. Radioactive *in* vitro kinase assay with ^{33}P-labelled ATP where 1 µg of H1.4-FLAG (H1.4) or H1.4S27A-FLAG (S27A) were incubated with or without Aurora B kinase. The Coomassie Blue stained SDS-PAGE gel was developed using autoradiography.
C. Western blotting of siRNA treated lysates (30 µg) from HeLa cells. Cells transfected with siRNA targeting Aurora A (AA) or Aurora B (AB) kinase, or a non-targeting control (NC) arrested in mitosis were analysed using western blotting with antibodies against the kinases or α-tubulin to control for loading. For detection of histones or their modifications acid-extracts (1 µg) from siRNA transfected HeLa cells were western blotted with the antibodies indicated.

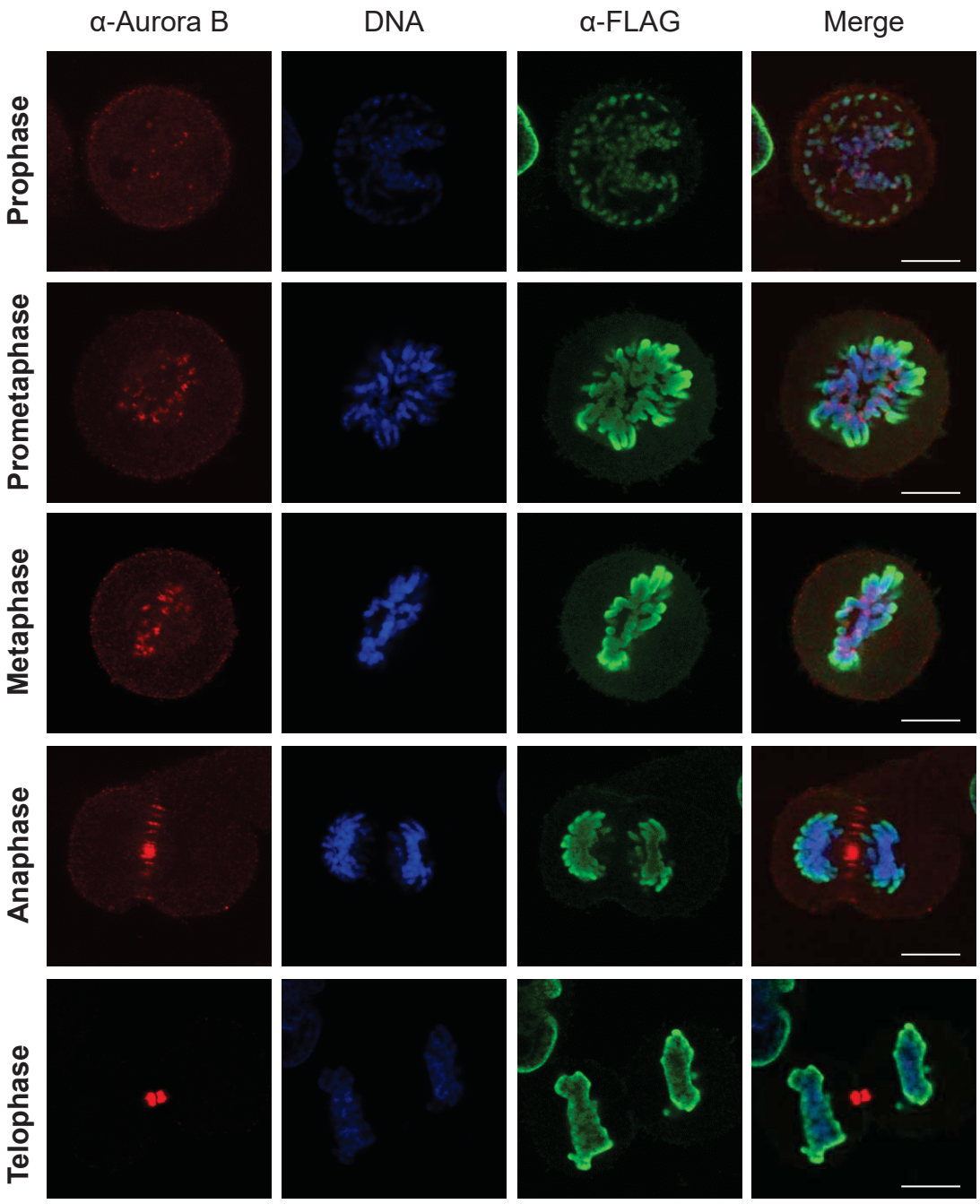

Figure 3.6. Aurora B localisation during mitosis.
Immunofluorescence of mitotic HeLa Tet-On cells that express H1.4-FLAG. Cells were processed for immunofluorescence using antibodies against Aurora B kinase (red) and FLAG (green); DNA was stained with DAPI (blue). Cells in mitosis were imaged on a confocal microscope at 400x magnification with the same exposure time and settings. Representative cells are shown. Scale bar, 10 μm.

3.2.2.4 Protein phosphatase 1 dephosphorylates H1.4 at serine 27

As PP1 works in concert with Aurora B to regulate the level of phosphorylation (Hsu *et al.*, 2000), it was determined if PP1 could dephosphorylate H1.4S27. HeLa cells were exposed to the PP1 inhibitor, calyculin A, and immunofluorescent confocal microscopy was performed (Sections 2.5.7 and 2.5.10). With constant intensity settings across captured images, levels of H1.4S27 phosphorylation were consistently higher in metaphase cells treated with the PP1 inhibitor when compared to the control (Figure 3.7). Inhibition of PP1 affects the phosphorylation of H1.4S27, so this phosphatase acts in concert with Aurora B kinase to regulate H1.4S27 phosphorylation.

3.2.3 Aurora B phosphorylation of H1.4S27 regulates the interaction with HP1

In the bivalent site, H1.4K26 is also methylated during mitosis, serving as a binding site for HP1. To determine if Aurora B phosphorylation of H1.4S27 can dislodge HP1 from this site, a glutathione S-transferase (GST) pull-down was performed. The HP1β family member was chosen for this, as it is known to be completely dislodged from mitotic chromosomes (Hayakawa *et al.*, 2003), whereas HP1α is retained at the centromere in a manner thought to be dependent on its chromo shadow domain, and HP1γ localises to euchromatic sites (Hayakawa *et al.*, 2003; Minc *et al.*, 1999). To perform the GST pull-down assay, proteins were first expressed and then their post-translational modification was optimised before binding assays could commence.

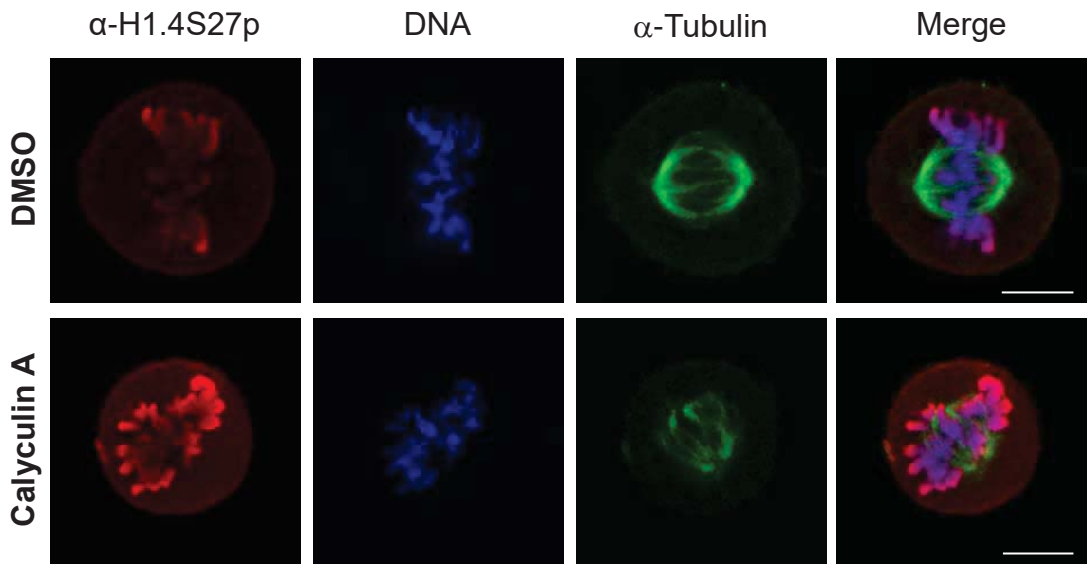

Figure 3.7. PP1 inhibition increases H1.4 serine 27 phosphorylation.
Immunofluorescence of HeLa cells treated with the PP1 inhibitor calyculin A. Mitotic cells were treated with calyculin A (100 nM) or the diluent DMSO for 1 hour, then processed for immunofluorescence with antibodies against H1.4S27p (red) and α-tubulin (green); DNA was stained with DAPI (blue). Metaphase cells were imaged on a confocal microscope at 400x magnification with the same exposure time and settings. Representative cells are shown. Scale bar, 10 μm.

3.2.3.1 Preparation of histone H1.4-FLAG and GST-HP1β

To obtain the H1.4 and HP1β required for GST pull-down assays, a bacterial expression system was used to produce protein free of post-translational modifications (Sections 2.3.5 and 2.3.6). Expression of H1.4 with a C-terminal FLAG-tag (H1.4-FLAG) was induced and lysates were visualised using SDS-PAGE. A band was present at the expected molecular weight of 35 kDa after induction (Figure 3.8A). The basic nature of H1.4-FLAG enabled its partial purification by acid extraction (Section 2.3.7). This was then further purified using an affinity column with FLAG M2 Affinity gel, and the protein was eluted in fractions (Section 2.3.8). Equal aliquots of each fraction were analysed by SDS-PAGE to assess their purity (Section 2.3.2). H1.4-FLAG was present in fractions 4 through 10, with the largest amounts seen in fractions 5 and 6 (Figure 3.8B). This bacterially expressed H1.4-FLAG was then able to be post-translationally modified enzymatically to explore the interaction with HP1β.

To produce GST-HP1β and GST, expression was induced in bacteria (Section 2.3.5), and these protein were then purified from lysates with Glutathione Sepharose 4B (Sections 2.3.6 and 2.3.8). To determine the amount of GST (26 kDa) or GST-HP1β (50 kDa) that was present in each pull-down assay, the purified protein was visualised using SDS-PAGE (Section 2.3.2). The purified proteins were observed at the expected molecular weight (Figure 3.8C), and the amount of protein loaded was used in subsequent GST pull-downs to investigate interaction between HP1β and H1.4.

Figure 3.8

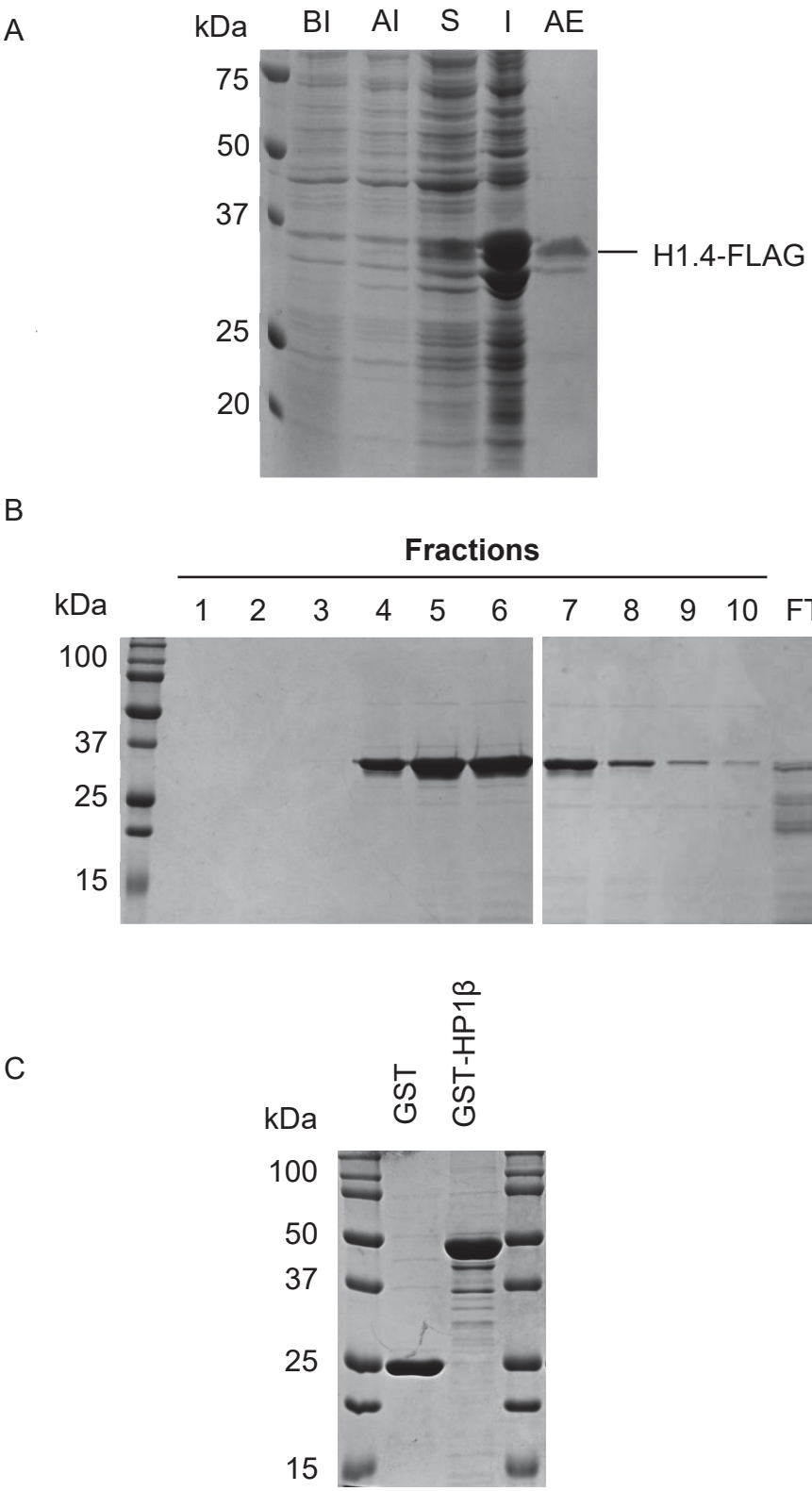
A
kDa
BI
AI
S
I
AE
75
50
37
25
20
H1.4-FLAG
B
Fractions
kDa
1
2
3
4
5
6
7
8
9
10
FT
100
37
25
15
C
GST
GST-HP1β
kDa
100
50
37
25
15

Figure 3.8. Expression and purification of H1.4-FLAG and GST-HP1β.
A. Coomassie Blue stained SDS-PAGE gel of lysates from *E. coli* cells transformed with an expression vector for H1.4-FLAG. Cells (50 µL) sampled before induction (BI) and after induction (AI). Following sonication, 2 µL of soluble (S) and insoluble (I) fractions were analysed. The soluble fraction was acid-extracted (AE; 2 µL). The left lane contains protein standards with molecular weights shown in kDa. The expressed H1.4-FLAG is indicated (35 kDa).
B. Coomassie Blue stained SDS-PAGE gel of bacterially expressed H1.4-FLAG purified using an anti-FLAG affinity column. Eluted fractions (1-10; 10 µL) were analysed alongside the column flow-through (FT). Outer lanes show protein standards with molecular weights indicated in kDa.
C. Coomassie Blue stained SDS-PAGE gel of bacterially expressed GST (26 kDa; 23 µL) and GST-HP1β (50 kDa; 15 µL) purified with Glutathione Sepharose 4B. Outer lanes show protein standards with molecular weights indicated in kDa.

3.2.3.2 *In vitro* post-translational modification of H1.4

Purified H1.4-FLAG was methylated at lysine 26 with G9a, a histone methyltransferase (HMT), and then phosphorylated by Aurora B kinase at serine 27 *in vitro* for use in subsequent GST pull-downs. H1.4-FLAG and H1.4K26A (where lysine 26 was substituted with alanine to prevent K26 methylation) were used as substrates for G9a (Section 2.3.9) and the reactions were analysed using SDS-PAGE and autoradiography (Sections 2.3.2 and 2.3.3). Methylation of H1.4-FLAG occurred only in the presence of G9a as shown by detection of the ^{14}C-labelled methyl group (Figure 3.9A). In contrast, H1.4K26A was not methylated, showing that lysine 26 is the only site in H1.4 that G9a can methylate.

Following methylation, H1.4S27 was phosphorylated using Aurora B kinase (Section 2.3.10), and western blotting with the H1.4S27p antibody was performed (Section 2.3.4). Aurora B kinase phosphorylated H1.4S27 regardless of the methylation status of H1.4K26 (Figure 3.9B). Phosphorylation was not seen in the absence of Aurora B kinase. This indicates that H1.4-FLAG was successfully post-translationally modified, and can therefore be used to test the interaction with HP1β.

3.2.3.3 H1.4S27 phosphorylation disrupts the interaction between methylated H1.4 and HP1β

To establish whether Aurora B phosphorylation of H1.4S27 affects the interaction between HP1β and H1.4 methylated at K26, a GST pull-down was performed (Section 2.2.12). H1.4-FLAG that was incubated with or without G9a and/or Aurora B kinase was incubated in a GST pull-down reaction with GST or GST-HP1β, then bound H1.4 was detected by western blotting for FLAG (Section 2.3.4). Methylated H1.4 interacted with HP1β, while unmodified H1.4 did not (Figure 3.9C). The affinity of HP1β for methylated H1.4 was reduced by 46% when S27 was phosphorylated by Aurora B (Refer to Appendix Two for Quantitation). This result shows that HP1β can directly interact with H1.4 methylated at lysine 26 *in vitro*, and that phosphorylation of S27 by Aurora B kinase can partially disrupt this interaction.

Figure 3.9

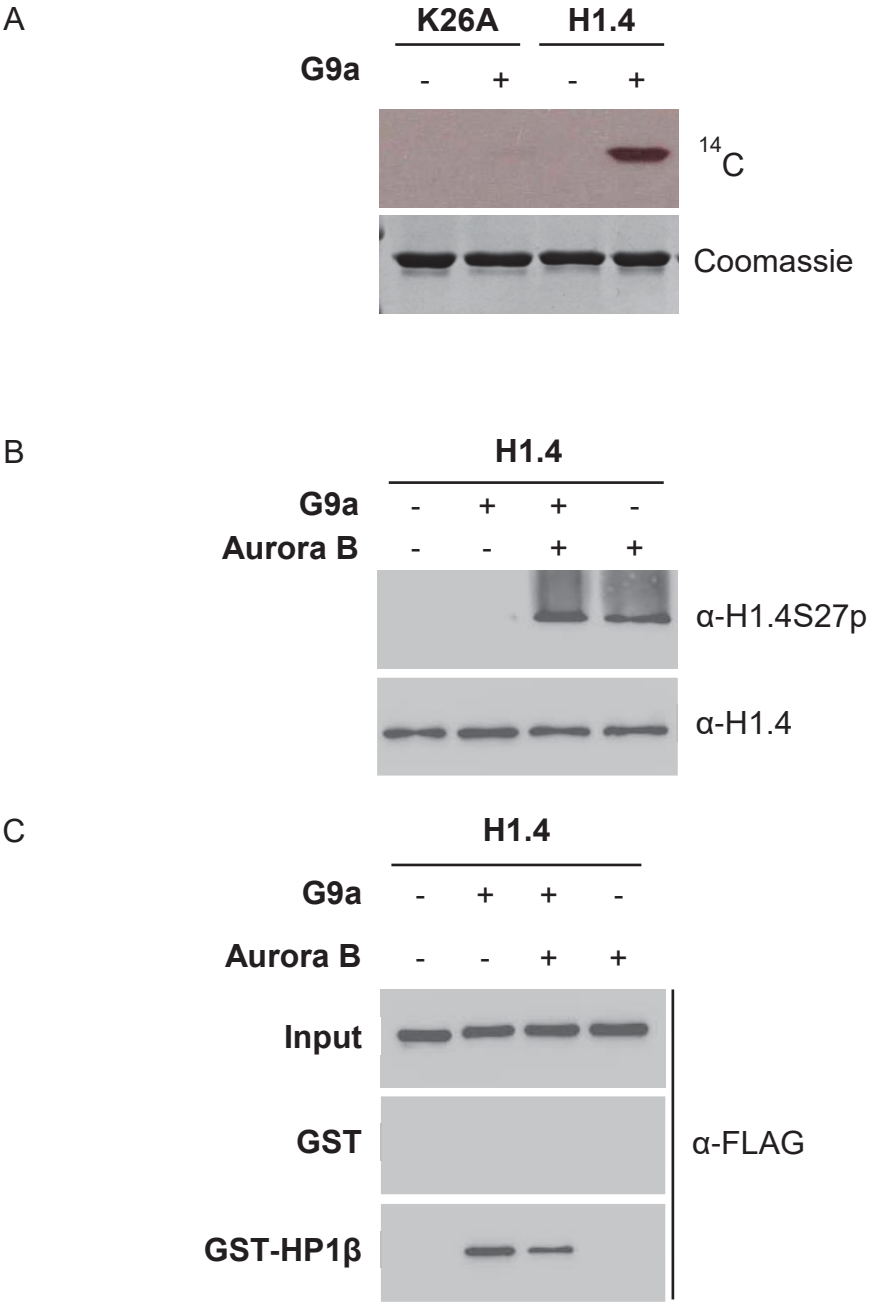
A
K26A
H1.4
G9a
- + - +
14C
Coomassie
B
H1.4
G9a
- + + -
Aurora B
- - + +
α-H1.4S27p
α-H1.4
C
H1.4
G9a
- + + -
Aurora B
- - + +
Input
GST
GST-HP1β
α-FLAG

Figure 3.9. H1.4S27 phosphorylation reduces the interaction with HP1β.
A. *In vitro* methylation assay where 1 µL of bacterially expressed and purified H1.4-FLAG (H1.4) or the methylation mutant H1.4K26A-FLAG (K26A) were analysed by Coomassie Blue stained SDS-PAGE gel following incubation with (+) or without (-) G9a and ^{14}C-labelled SAM. Autoradiography was used to detect the ^{14}C-methyl group.
B. Western blotting of an *in vitro* methylation assay and kinase assay where H1.4-FLAG (H1.4; 1 µg) was incubated with (+) or without (-) the histone methyltransferase G9a and Aurora B kinase. The antibodies used for western blotting are indicated.
C. GST pull-down assay where H1.4-FLAG (1 µg) was incubated with (+) or without (-) the histone methyltransferase G9a and Aurora B kinase, then with GST or GST-HP1β (0.75 µg modified H1.4-FLAG). The bound fraction was subject to western blotting with the FLAG antibody. 20% of the protein in the reaction was represented in the inputs.

3.3 Discussion

The data presented in this chapter demonstrates that like H3S10, H1.4S27 is phosphorylated during mitosis, but levels are low in G_1 and S phase. Confocal analysis of metaphase spreads revealed that H1.4S27 phosphorylation occurs on mitotic chromosomes and is enriched at the centromere. Aurora B kinase was identified as a kinase of this site, first *in vitro*, and then via RNA interference and through its similar localisation throughout the phases of mitosis. In addition, the Aurora B phosphorylation of serine 27 adjacent to methylated H1.4K26 partially displaced HP1β *in vitro*, providing support for the hypothesis that this 'ARKS' motif may act as a binary switch during mitosis.

Exploration of the phosphorylation of H1.4S27 has revealed that in addition to the sequence similarity shared with H3, there are also parallels in the timing and in the enzyme systems that add and remove this modification. As both H3S10 and H1.4S27 are phosphorylated by Aurora B kinase, then the attempts at elucidating the function of H3S10 phosphorylation with kinase inhibitors (Ota *et al.*, 2002; Terada, 2006), would also have directly impacted H1.4S27 phosphorylation. Thus there is a need to separate out the respective roles of these phosphorylation sites and establish if they act in concert or play differing roles during mitosis. The importance of H3S10 phosphorylation in dislodging HP1 from the chromatin also needs to be reconsidered, as the Aurora B phosphorylation of S27 on H1.4 methylated at K26 can also partially dislodge HP1β, although further investigation is required to determine if this occurs in the context of chromatin.

As H1.4S27 phosphorylation is a modification that occurs predominantly in mitosis this suggests it plays a specific role during this orchestrated phase. The Aurora B phosphorylation of H1.4S27 seen here in HeLa cells, and that explored in MCF7 breast cancer cells by Hergeth *et al.* (2011) shows that this modification is regulated in the same way in these human cell lines. Additionally, Aurora B kinase and H1.4 are located similarly in the cell, whereas despite phosphorylating H1.4S27 *in vitro*, Aurora A does not colocalise with the mitotic chromosomes, instead it resides on the mitotic spindle (Carmena *et al.*, 2009). Despite this, the use of siRNA to decrease Aurora B

kinase levels both here, and by Hergeth *et al.* (2011), did not result in the complete loss of H1.4S27 phosphorylation. As residual phosphorylation occurred it is possible that another mitotic kinase may also contribute to H1.4S27 phosphorylation. Although, this group did verify that H1.4 was the only somatic subtype of H1 to be phosphorylated by Aurora B (Hergeth *et al.*, 2011). Dephosphorylation of H1.4S27 by PP1 may also require further investigation, as the inhibitor used here can also inhibit the related enzyme, Protein phosphatase 2A (PP2A; Ishihara *et al.*, 1989).

The detection of H1.4S27 phosphorylation on metaphase spreads along the chromosome arms and its enrichment at the centromere mirrors where Aurora B kinase is present during metaphase. In addition to the centromeric population of Aurora B kinase there is a dynamic cytoplasmic pool of Aurora B, as detected when tagged with GFP (Murata-Hori & Wang, 2002), which could maintain the H1.4S27 phosphorylation along the chromosome arms. Studies of H1 distribution throughout the genome have not shown any enrichment of the somatic H1 subtypes at the centromere, although it is present, like elsewhere in the genome (Orthaus *et al.*, 2009). HP1α, while largely dislodged from the chromosomes remains at the centromere (Hayakawa *et al.*, 2003), suggesting it can be present despite the enrichment of H1.4S27 phosphorylation. Thus phosphorylation of H1.4S27 doesn't always exclude the presence of the HP1 paralogs. The HP1α present at the centromere during mitosis may localise through its hinge, or through proteins with PxVxL motifs and the chromo shadow domain, rather than via the chromo domain (Hayakawa *et al.*, 2003).

Given the mitotic specificity of H1.4S27 phosphorylation, there is potential for its use as a mitotic marker in tumour tissue. As shown here, mitotic cells in invasive lobular breast carcinoma were positive for phosphorylation of H1.4S27, as well as H3S10. The widely used Ki67 proliferative marker was much more abundant in tumour tissue, as expected given it detects all cells that are actively cycling (Gerdes *et al.*, 1983). Other recent work on the CDK phosphorylation site T146, in both H1.4 and H1.2, found that the incidence of this modification correlated with tumour grade (Harshman *et al.*, 2014; Telu *et al.*, 2013). Similar results were seen when H1.2, H1.4 and H1.5 phosphorylation were found to be increased in invasive bladder cancer cell lines relative to non-invasive

or normal bladder cell lines (Telu *et al.*, 2013). Together, these results suggest that H1 phosphorylation could aid pathologists in staging of tumours alongside other markers, with H1.4S27 phosphorylation particularly useful in determining the mitotic index of tumour tissue.

Investigation of the *in vitro* interaction between H1.4 and HP1β showed that when H1.4 methylated on K26 was also phosphorylated at S27 by Aurora B, there was partial displacement of HP1β. This differs to that seen in peptide binding assays performed by Daujat *et al.* (2005) where HP1α, β or γ did not detectably bind to the H1.4K26me2S27p peptide on affinity columns. However, differences in the experimental conditions and the use of short peptides containing amino acids from 20 – 33 of H1.4 may contribute to the differences seen here, where whole proteins were used. Additionally, given the enzyme mediated modification, it is possible that some of the H1.4 was not dually modified following the methylation and kinase assays used here, resulting in partial dissociation of HP1β. Similar differences also occurred when assaying the interaction between HP1 and an H3K9meS10p peptide, where only the chromo domain of HP1, and not the full length protein could be dislodged (Mateescu *et al.*, 2004; Terada, 2006), while others showed that HP1 did not bind to H3 peptides containing a phosphate group on S10 (Fischle *et al.*, 2005; Hirota *et al.*, 2005). Exploration of the interaction between HP1 and H1.4 *in vivo* is required to establish the role of H1.4S27 in dislodging HP1 during mitosis.

Overall, these data indicate a functional role for H1.4S27 phosphorylation in regulating the localisation of HP1 during mitosis, which will be further explored in the following chapter.

Chapter Four

Functional analysis of H1.4S27 phosphorylation during mitosis

4.1 Introduction

As demonstrated in Chapter 3, Aurora B kinase phosphorylates H1.4 at serine 27 (H1.4S27) during mitosis. Aside from the *in vitro* peptide binding assays showing that H1.4S27 phosphorylation can dislodge Heterochromatin protein 1 (HP1) from H1.4 methylated at K26 (Daujat *et al.*, 2005), there has been limited investigation into the function of H1.4S27 phosphorylation. This chapter will explore the function of the mitotic phosphorylation of H1.4 at serine 27.

The similar bivalent 'ARKS' motif in H3 at K9S10 has been more extensively studied than that in H1.4 at K26S27, and phosphorylation of H3S10 is known as a marker of mitosis, and for its dislodgement of HP1 at this time (Fischle *et al.*, 2005; Hirota *et al.*, 2005; Johansen & Johansen, 2006). Phosphorylation of H3S10 is not restricted to mitosis like H1.4S27 phosphorylation (Hans & Dimitrov, 2001; Thomson *et al.*, 1999). In interphase, H3S10 is phosphorylated by Mitogen- and stress-activated kinase 1 (MSK1) and this facilitates transcription of the immediate early genes (Soloaga *et al.*, 2003; Thomson *et al.*, 1999). This interphase H3S10 phosphorylation is often accompanied by acetylation at H3K9 or H3K14, which recruits 14-3-3 proteins and leads to transcriptional activation through SWI/SNF (Switch/Sucrose non-fermentable) remodelling (Drobic *et al.*, 2010; Winter *et al.*, 2008). In *Drosophila melanogaster*, ectopic H3S10 phosphorylation by JIL-1 in causes chromatin reorganisation from the heterochromatic state to euchromatin (Deng *et al.*, 2008).

In contrast, during mitosis, H3S10 phosphorylation by Aurora B kinase is associated with chromosome condensation, and this is highly conserved from yeast through to mammals (Hans & Dimitrov, 2001; Hendzel *et al.*, 1997; Hsu *et al.*, 2000). In organisms with only one copy of H3, mutation of serine 10 to alanine resulted in mitotic defects and impaired chromosome segregation, both in *Saccharomyces pombe* and *Tetrahymena thermophila* (Mellone *et al.*, 2003; Wei *et al.*, 1999). This phenotype also occurred in HeLa cells expressing H3S10A, where the incidence of lagging and bridging chromosomes was increased relative to cells expressing wild-type H3 (Terada, 2006). Interestingly, the expression of H3S10E, which mimics constitutive phosphorylation, led to an increase in the proportion of lagging and bridging chromosomes, which also occurred when Aurora B was overexpressed (Ota *et al.*, 2002). The way in which H3S10

phosphorylation leads to chromosome condensation or how its dysregulation brings about mitotic defects is not clear. One consequence of the dysregulation of H3S10 phosphorylation is the altered chromosome association of HP1 (Terada, 2006).

When the non-phosphorylatable mutant H3S10A was overexpressed in HeLa cells, HP1α was retained on mitotic chromosomes (Terada, 2006). Depletion of Aurora B using siRNA also resulted in the retention of HP1α (Terada, 2006), suggesting that Aurora B phosphorylation of H3S10 led to release of HP1α from the mitotic chromosomes. However, more HP1α was retained on chromosomes upon Aurora B depletion than in the presence of H3S10A (Terada, 2006), which implies that additional Aurora B phosphorylation sites also contribute. Given that H1.4S27 is also phosphorylated by this kinase, studies employing knock down of Aurora B will have reduced both H3S10 and H1.4S27 phosphorylation (Ota *et al.*, 2002; Terada, 2006), and thus decreased H1.4S27 phosphorylation may have contributed to this phenotype. Taken together, these data suggest that phosphorylation of H1.4 at serine 27 may contribute to the displacement of HP1 paralogs during mitosis.

The *in vitro* dislodgment of HP1 from methylated H1.4K26 has been attributed to the phosphorylation of H1.4S27 (Figure 3.9; Daujat *et al.*, 2005). Additionally, mimicking H1.4S27 phosphorylation with a glutamic acid substitution altered the affinity of H1.4 for chromatin in Fluorescence recovery after photobleaching (FRAP) experiments (Hergeth *et al.*, 2011). Green fluorescent protein (GFP)-tagged H1.4S27E exhibited delayed recovery kinetics on mitotic chromosomes following photobleaching, indicating it has increased chromatin affinity, whereas both H1.4 and non-phosphorylatable H1.4S27A showed similar recovery times (Hergeth *et al.*, 2011). Thus, further investigation into the role of H1.4S27 phosphorylation is necessary.

The aim of this chapter is to explore the function of H1.4S27 phosphorylation during mitosis, using cell lines that are mutant for this phosphorylation. The effect of this aberrant H1.4S27 phosphorylation on cellular proliferation and progression through mitosis will be investigated. Additionally, the effect of mutation of H1.4S27 phosphorylation on the interaction with HP1 will be investigated both *in vitro* and in the context of chromatin *in vivo*.

4.2 Results

4.2.1 Construction of cell lines to explore H1.4S27 phosphorylation

To elucidate the *in vivo* role of the mitotic phosphorylation of H1.4S27, clonal HeLa Tet-On cell lines were created that inducibly express wild-type H1.4, or H1.4 mutant at serine 27. To distinguish the exogenous constructs from endogenous H1.4, the C-terminus was tagged with FLAG (Section 2.5.11). The wild-type histone H1.4-FLAG overexpression control cell line was used to verify that changes seen in the mutant H1.4-FLAG expressing cell lines were not due to excess H1.4. The first H1.4 mutant had serine 27 substituted with alanine (H1.4S27A-FLAG), to prevent phosphorylation. The second mutant, H1.4S27E-FLAG, had glutamic acid at position 27, in the place of serine to mimic phosphorylation. Figure 4.1 shows the constitutive negative charge carried on H1.4S27E and how this compares to phosphoserine, and the non-phosphorylatable alanine in H1.4S27A.

4.2.1.1 Selection of inducible H1.4S27 phosphorylation mutant cell lines

To establish the cell lines described above, plasmids carrying H1.4-FLAG, H1.4S27A and H1.4S27E were transfected into HeLa Tet-On cells and were selected with hygromycin B (Sections 2.5.11.2 and 2.5.11.3). Once established, stable clonal cell lines grown with or without 1 μg/mL doxycycline, the inducer, were screened by western blotting for FLAG and α-tubulin (Sections 2.3.4 and 2.5.11.4). While the levels of α-tubulin were consistent across the cell lines examined regardless of induction, the level of H1.4-FLAG expression increased in the presence of doxycycline for each clone (Figure 4.2). Without induction, the H1.4-FLAG proteins could be detected in the H15, A7 and E1 populations. The E24 cell line was omitted, as immunofluorescence confocal microscopy showed that a low proportion of induced cells expressed H1.4S27E. The following clonal populations were selected based on their high induction of expression and minimal basal expression: H9, A10 and E1. These H1.4-FLAG cell lines were used to investigate the function of H1.4S27 phosphorylation and will be referred to as H1.4-FLAG, H1.4S27A and H1.4S27E respectively.

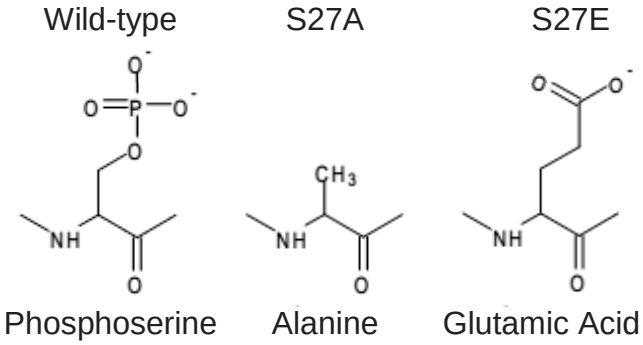

Figure 4.1 Comparing H1.4S27 phosphorylation and the mutations that prevent or mimic this phosphorylation.

The structure of serine in the phosphorylated state (phosphoserine) alongside the substituted amino acids in the H1.4S27A-FLAG (S27A) and H1.4S27E-FLAG (S27E) phosphorylation mutant cell lines. In the H1.4S27A expressing cells, serine 27 is replaced by alanine. This has a similar structure but is more hydrophobic due to the lack of the hydroxyl group, which also prevents phosphorylation. In the cells expressing H1.4S27E, glutamic acid replaces serine 27. As glutamic acid carries a negative charge and has a similar structure it mimics the constitutively phosphorylated state. Figure adapted from Anthis *et al.* (2009).

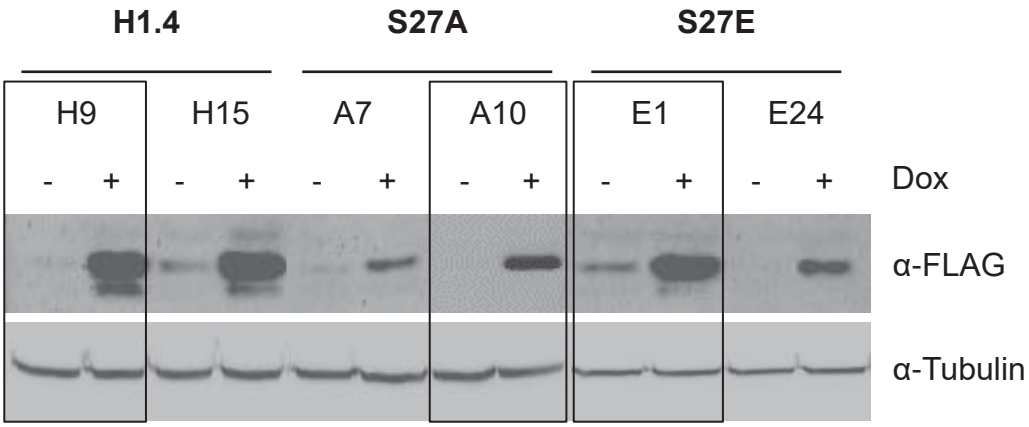

Figure 4.2. Screening the H1.4S27 phosphorylation mutant cell lines. Western blotting of cell lysates (15 µg protein) prepared from inducible HeLa Tet-On cell lines grown with (+; 1 µg/mL) or without (-) doxycycline (Dox). Cell lines: H9 and H15 express H1.4-FLAG (H1.4); A7 and A10 express non-phosphorylatable H1.4S27A-FLAG (S27A); E1 and E24 express the phosphomimetic H1.4S27E-FLAG (S27E). The H1.4-FLAG proteins were detected with an antibody against FLAG, and α-tubulin was detected to control for loading. Boxes indicate the clonal cell populations that were used through the rest of this study.

4.2.2 Characterisation of histone H1.4-FLAG phosphorylation mutant cell lines

The HeLa Tet-On cell lines, with inducible expression of the exogenous H1.4-FLAG control, the non-phosphorylatable H1.4S27A, or the phosphomimetic H1.4S27E, were induced and their location, effect on proliferation and progression through mitosis was explored.

4.2.2.1 Localisation of the H1.4-FLAG proteins

The expression of H1.4-FLAG was examined to determine whether the exogenous H1.4-FLAG localised to the chromatin, as endogenous H1.4 does. Firstly, a titration was performed to determine the concentration of doxycycline that resulted in nuclear localisation of H1.4-FLAG. Immunofluorescent confocal microscopy was used to visualise the H1.4-FLAG expressing cells that had been examined with antibodies against FLAG and histone H1.4 (Section 2.5.7). Nuclear localisation of H1.4-FLAG was seen in an increasing proportion of cells as the concentration of doxycycline increased (Figure 4.3). In cells grown without doxycycline there was minimal detection of H1.4-FLAG, although it was present in a few cells. Increasing the concentration of doxycycline increased the number of cells expressing H1.4-FLAG, rather than increasing the amount present within each cell, and despite their clonal origin not all cells in the population expressed H1.4-FLAG. With 1 μg/mL doxycycline H1.4-FLAG localised to the nucleus, as endogenous H1.4 does. Therefore this concentration of doxycycline was chosen for subsequent inductions (unless otherwise stated).

The expression and subcellular localisation of H1.4-FLAG was then compared to the H1.4S27A and H1.4S27E cell lines, via immunofluorescence using antibodies against FLAG and α-tubulin (Section 2.5.7). In cells expressing H1.4S27A or H1.4S27E, the exogenous protein colocalised with the nuclear DNA or the mitotic chromosomes (Figure 4.4). Minimal H1.4S27A or H1.4S27E was detected in the absence of induction, and the exogenous proteins were expressed in the induced population. As for H1.4-FLAG, H1.4S27A and H1.4S27E were not detected within all cells in the clonal population in the presence of doxycycline. This result shows that for each cell line the H1.4-FLAG proteins colocalise with the chromatin in the nucleus, as endogenous H1.4 does.

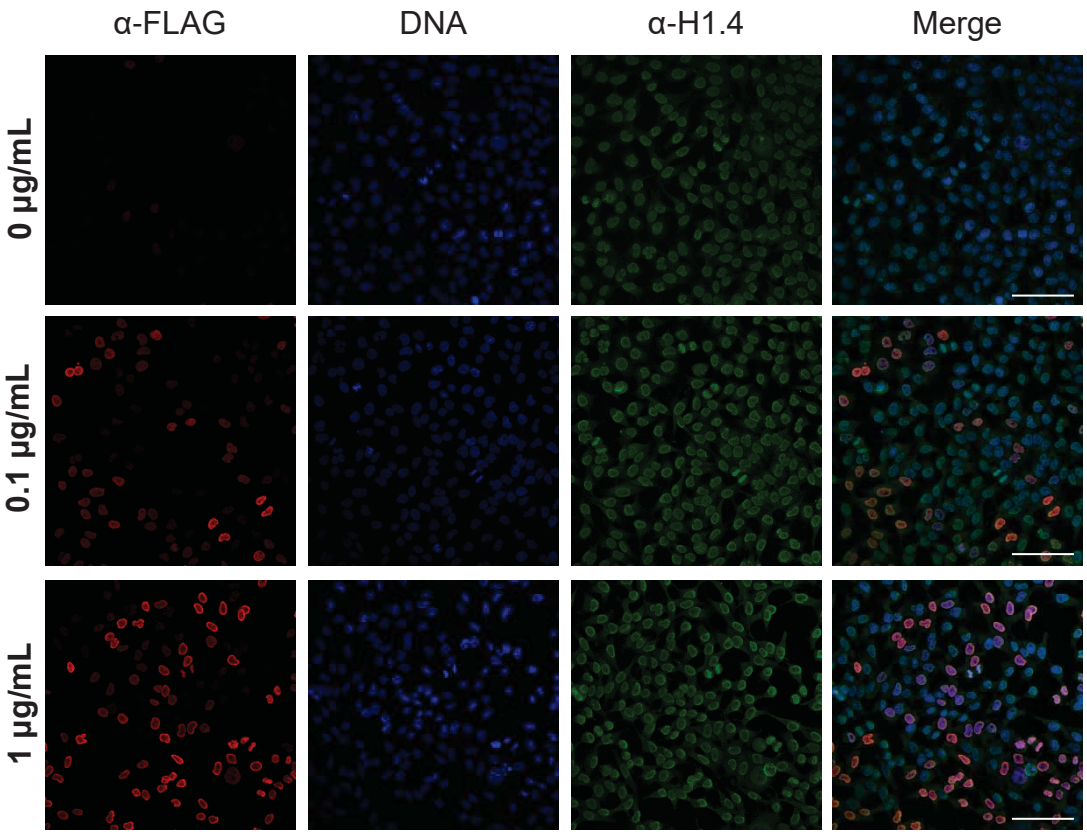

Figure 4.3. H1.4-FLAG colocalises with endogenous H1.4.
Immunofluorescence of H1.4-FLAG inducible cells grown with 0 µg/mL, 0.1 µg/mL or 1 µg/mL of doxycycline. Cells were analysed using antibodies against FLAG (red) or H1.4 (green); DNA was stained with DAPI (blue). Cells were imaged on a confocal microscope at 200x magnification with the same exposure time and settings. Representative fields are shown. Scale bar, 100 µm.

Figure 4.4

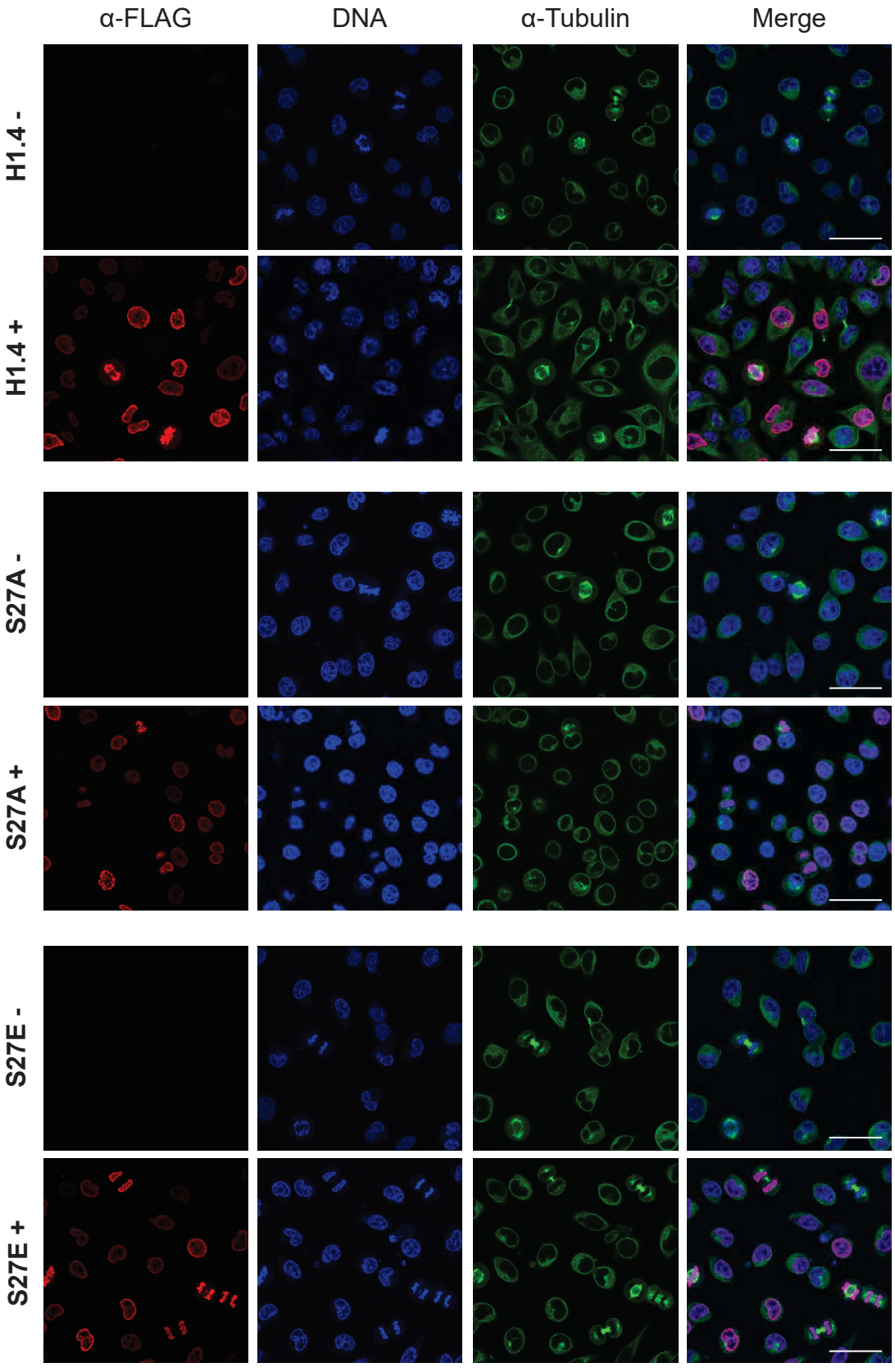

Figure 4.4. Exogenous H1.4-FLAG, H1.4S27A and H1.4S27E localise to the nucleus.
Immunofluorescence of H1.4-FLAG (H1.4), H1.4S27A-FLAG (S27A) and H1.4S27E-FLAG (S27E) cells grown with (+; 1 μg/mL) or without (-) doxycycline. Cells were analysed with antibodies against FLAG (red) or α-tubulin (green); DNA was stained with DAPI (blue). Cells were imaged on a confocal microscope at 400x magnification with the same exposure time and settings. Representative fields are shown. Scale bar, 50 μm.

4.2.2.2 Mitotic defects occur when H1.4S27 phosphorylation is aberrant

As histone H1.4S27 phosphorylation is exclusive to mitosis, the H1.4-FLAG cell lines were examined to determine if dysregulation of phosphorylation altered the transit through mitosis. The induced or uninduced H1.4-FLAG cell lines were synchronised in mitosis and immunofluorescence confocal microscopy with antibodies against FLAG and α-tubulin was performed (Sections 2.5.3.2 and 2.5.7). The incidence of mitotic defects such as multi-nucleated cells, lagging chromosomes and cells with tripolar spindles was recorded (Section 2.5.12). When either the non-phosphorylatable H1.4S27A or phosphomimetic H1.4S27E were expressed, an increase in the occurrence of mitotic defects occurred (Figure 4.5A). The increase in mitotic defects was greater when H1.4S27A was expressed, compared to H1.4S27E, although both cell lines had a small increase in defects when uninduced compared to the control cell line. While there was a range of defects seen in mitotic cells for each of the induced cell lines, there were changes in the relative proportions of the type of defect seen. In particular, when H1.4S27A was expressed there was an increase in the percentage of cells with chromosomes that didn't align to the equatorial plate in metaphase; or that possessed more than two spindle poles. In contrast, expression of H1.4S27E resulted in an increased proportion of cells with chromosomes that bridged the separating chromosomes in anaphase, leading to an increase in lagging chromosomes that were not included in the cell nucleus as it reformed. Examples of these defects are shown in Figure 4.5B. This is the first report to show that mutation of H1.4S27 phosphorylation causes defects to occur during the transit through mitosis.

During this analysis it was observed that interphase cells were also atypical, particularly for the H1.4S27E cell line. As such, interphase cells were also scored for each of the three cell lines (Section 2.5.12). In interphase cells expressing H1.4S27E there was an increase in the proportion of cells with DNA excluded from the nucleus, in a micronucleus (Figure 4.6). Such changes were not observed upon induction of the H1.4-FLAG or H1.4S27A cell lines, which showed similar levels to uninduced cells. This shows that regulation of H1.4S27 phosphorylation is required for accurate chromosome segregation, and for the normal transit through mitosis.

Figure 4.5

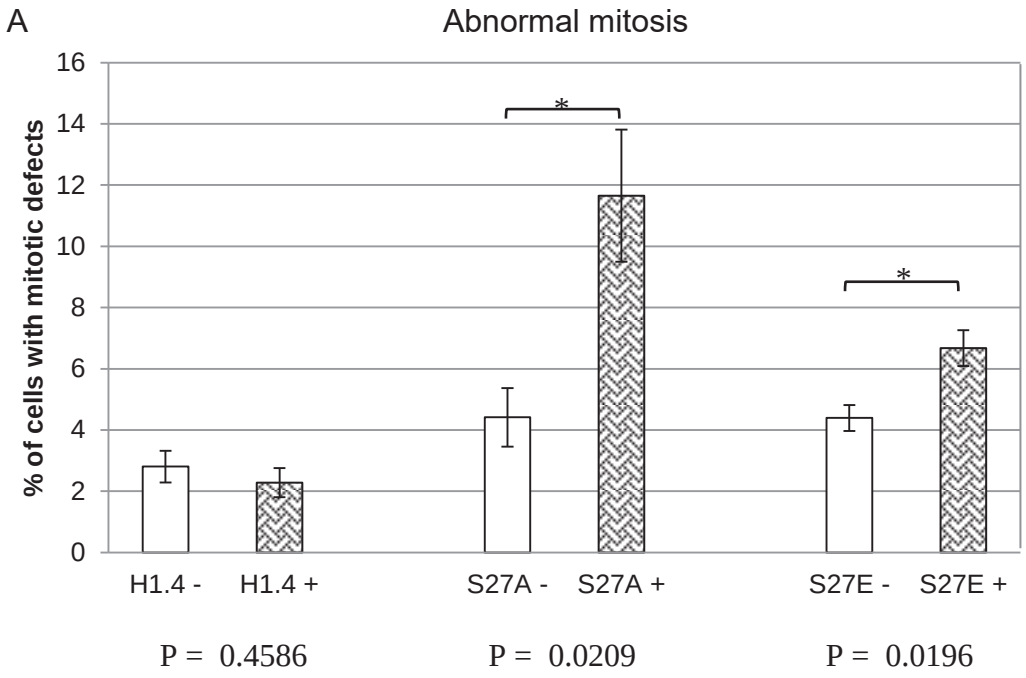
A
Abnormal mitosis
% of cells with mitotic defects
16
14
12
10
8
6
4
2
0
*
*
H1.4 -
H1.4 +
S27A -
S27A +
S27E -
S27E +
P = 0.4586
P = 0.0209
P = 0.0196

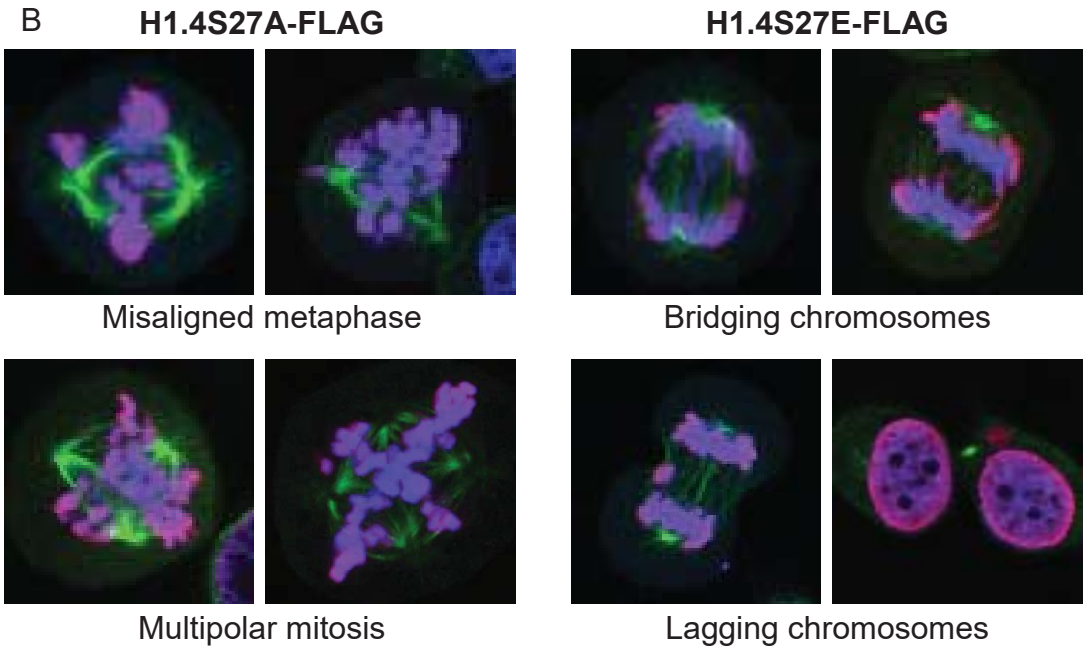
B
H1.4S27A-FLAG
H1.4S27E-FLAG
Misaligned metaphase
Bridging chromosomes
Multipolar mitosis
Lagging chromosomes

Figure 4.5. Mitotic defects occur with expression of H1.4S27A or H1.4S27E.

A. Quantification of abnormal mitosis from immunofluorescent analysis of H1.4-FLAG (H1.4), H1.4S27A-FLAG (S27A) and H1.4S27E-FLAG (S27E) cells. Cells grown with (+; 1 µg/mL) or without (-) doxycycline were synchronised in mitosis, then analysed with antibodies against FLAG (red) or α-tubulin (green); DNA was stained with DAPI (blue). Abnormal mitoses were analysed quantitatively in two independent experiments and the percentage of abnormal mitosis was calculated with the mean displayed; bars show standard error. P values (Students T test) are indicated below the graph, * denotes that $P < 0.05$.

B. Examples of abnormal mitosis from cells expressing non-phosphorylatable H1.4S27A-FLAG, and the phosphomimetic H1.4S27E-FLAG. Representative merged images of cells prepared as described in **A** were captured using a confocal microscope at 400x magnification with the same exposure time and settings. Misaligned metaphases and multipolar mitoses increased when H1.4S27A-FLAG was expressed, whereas bridging and lagging chromosomes increased when H1.4S27E-FLAG was expressed.

Figure 4.6. Cells that express H1.4S27E have an increased incidence of micronuclei.

A. Quantification of interphase cells containing a micronucleus from immunofluorescent analysis of H1.4-FLAG (H1.4), H1.4S27A-FLAG (S27A) and H1.4S27E-FLAG (S27E) cells. Cells grown with (+; 1 µg/mL) or without (-) doxycycline were synchronised in mitosis, then analysed with antibodies against FLAG (red) or α-tubulin (green); DNA was stained with DAPI (blue). Fields of interphase cells were analysed quantitatively for abnormalities in two independent experiments and the percentage of interphase cells with a micronucleus was calculated with the mean displayed; bars show standard error. P values (Students T test) are indicated below the graph, * denotes that $P < 0.05$.

B. Examples of cells containing a micronucleus from cells expressing the phosphomimetic H1.4S27E-FLAG. Representative merged images of cells prepared as described in **A** were captured using a confocal microscope at 400x magnification with the same exposure time and settings. There was an increased incidence of micronuclei when H1.4S27E-FLAG was expressed.

Figure 4.6

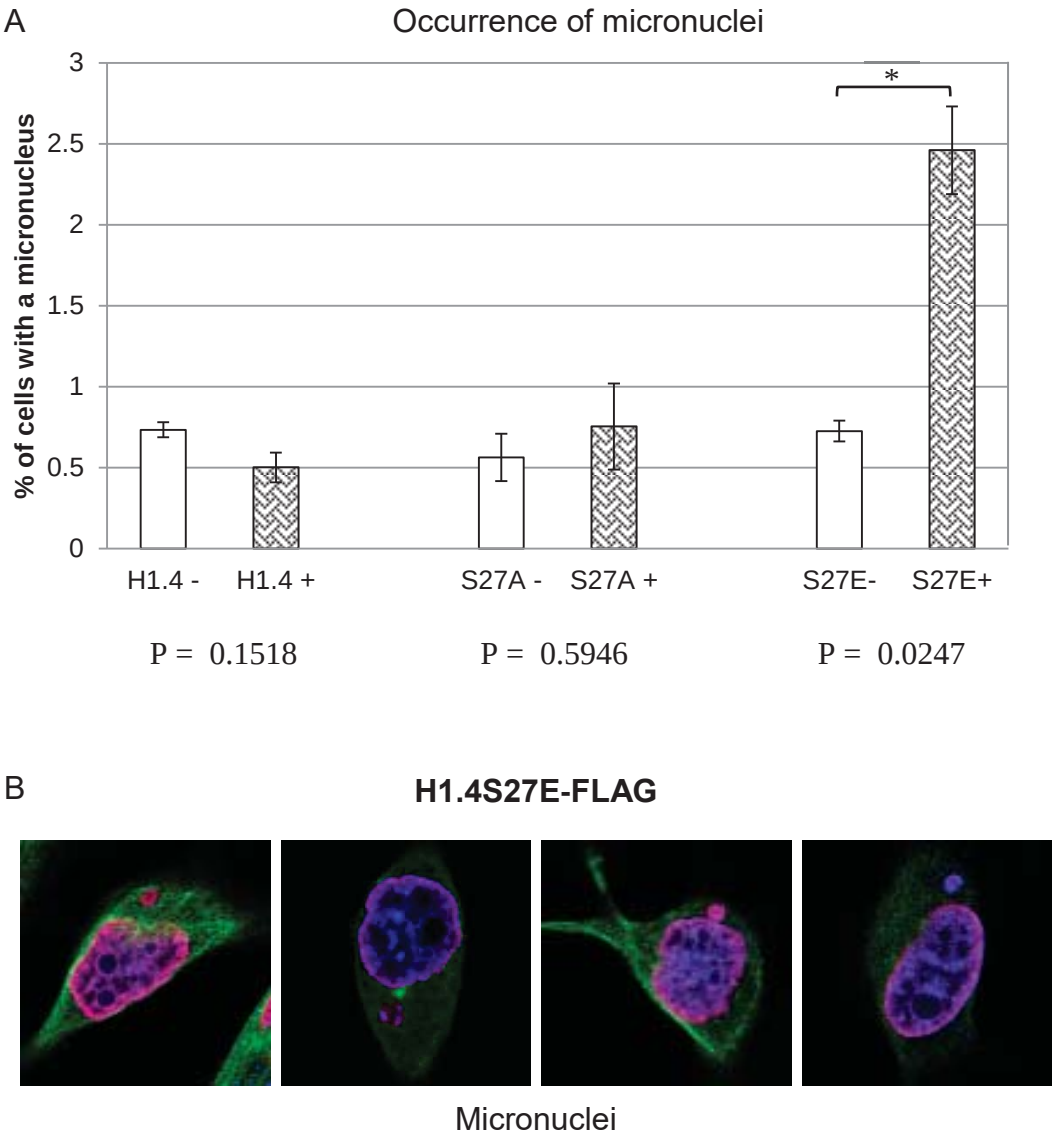
A
Occurrence of micronuclei
% of cells with a micronucleus
3
2.5
2
1.5
1
0.5
0
*
H1.4 -
H1.4 +
S27A -
S27A +
S27E-
S27E+
P = 0.1518
P = 0.5946
P = 0.0247
B
H1.4S27E-FLAG
Micronuclei

4.2.2.3 Expression of the H1.4S27 phosphorylation mutants does not alter cell proliferation or viability

To ascertain if expression of the exogenous H1.4S27 phosphorylation mutants altered cell growth, a proliferation assay was performed (Section 2.5.13). Each cell line was grown in the presence or absence of doxycycline over the course of the experiment and cells were harvested daily, and then assayed with the CyQUANT Cell Proliferation Assay kit. This measured the cell density using the CyQUANT GR dye that fluoresces when bound to nucleic acids. Cellular proliferation was not altered when the exogenous H1.4-FLAG control or H1.4S27 mutant proteins were expressed (Figure 4.7). Thus overexpression of H1.4-FLAG or H1.4 which is non-phosphorylatable or phosphomimetic at serine 27 does not alter cellular proliferation.

Flow cytometry was then performed to establish if the mitotic defects resulting from expression of the H1.4S27 phosphorylation mutants led to apoptosis when expressed for 72 hours (Section 2.5.14). The nucleic acid intercalating fluorescent dyes, YO-PRO®-1 iodide and propidium iodide (PI), were used in combination to distinguish apoptotic and non-viable cells from living cells. Apoptotic cells are permeable to YO-PRO®-1 iodide, and not PI, whereas non-viable cells are permeable to both stains. Although viable cells are impermeable to both stains they could be detected as they scattered light. No difference was found in the level of apoptosis or non-viable cells for each of the cell lines when induced, relative to uninduced cells (Figure 4.8). This indicates that the level of expression used in H1.4-FLAG, H1.4S27A or H1.4S27E cell lines did not induce cell death.

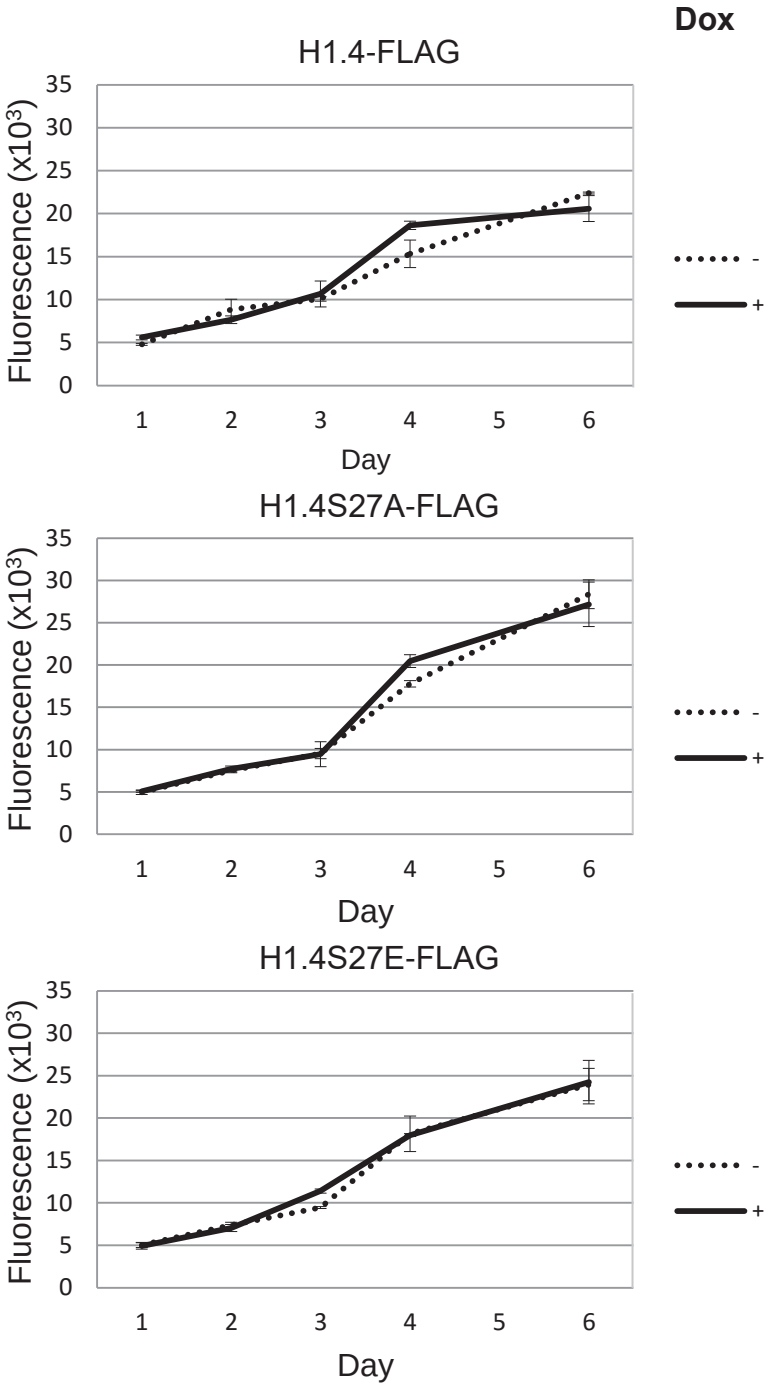

Figure 4.7. Expression of the H1.4S27 phosphorylation mutants does not alter cellular proliferation.
Proliferation assay for H1.4-FLAG, H1.4S27A-FLAG and H1.4S27E-FLAG inducible cells. Cells were grown in duplicate in five 96-well plates in the presence (+; 1 μg/mL) or absence (-) of doxycycline (Dox), one plate was harvested each day for days 1 – 4, then for day 6. The total cellular nucleic acid content was evaluated as a measure of proliferation, the mean is displayed, and bars show standard error.

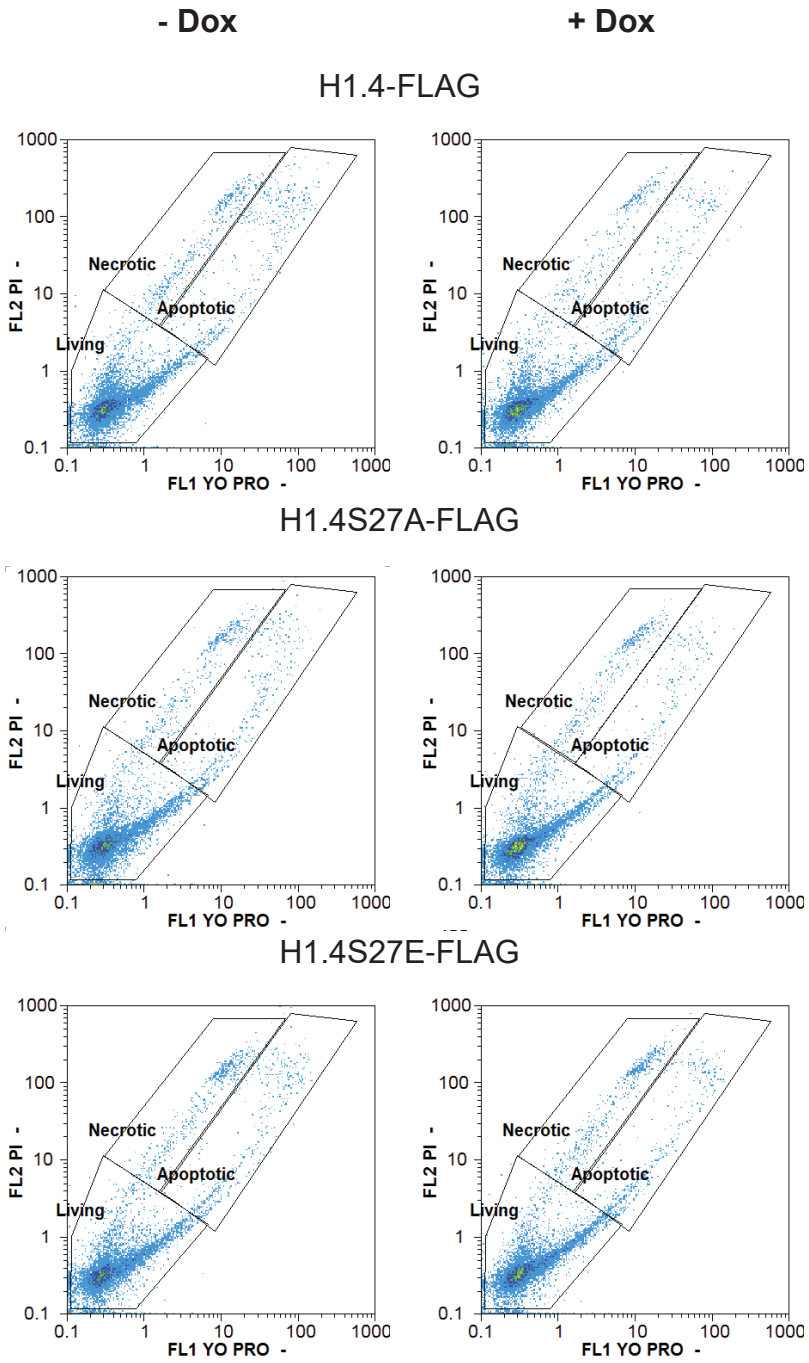

Figure 4.8. Expression of the H1.4S27 phosphorylation mutants does not affect programmed cell death.
Flow cytometry of H1.4-FLAG, H1.4S27A-FLAG and H1.4S27E-FLAG cell lines. Cells grown with (+; 1 µg/mL) or without (-) doxycycline (Dox) were stained with the fluorescent nucleic acid stains Propidium iodide (PI) and YO-PRO®-1 iodide. A minimum of 10,000 cells were analysed on the Partec CyFlow® Space Flow Cytometer. Living, apoptotic and necrotic populations are indicated.

4.2.2.4 Characterisation of endogenous histone H1 protein levels and phosphorylation in the H1.4-FLAG cell lines

As expression of exogenous histones often causes a reduction in endogenous H1 expression to compensate (Brown *et al.*, 1996), it was determined if expression of the H1.4-FLAG proteins altered levels of H1.4 or its post-translational modification. Asynchronous cells grown in the absence of, or with 0.1 μg/mL (+) or 1 μg/mL (++) of doxycycline were harvested for total protein and western blotting was performed (Sections 2.3.4 and 2.5.4). All three of the cell lines expressed the H1.4-FLAG proteins with 1 μg/mL doxycycline (Figure 4.9). When detected with the FLAG antibody the H1.4-FLAG control cell line showed the highest expression, the level of H1.4S27E expression was less, with the H1.4S27A cell line showing the lowest expression. These results are consistent with the prior screen in Figure 4.2, although background expression of H1.4S27E appears to have decreased with regular passaging of the cells.

Overall, endogenous H1 levels were unchanged upon induction, as shown with the total H1 antibody which recognises multiple subtypes of histone H1. With 1 μg/mL of doxycycline the exogenous H1.4-FLAG protein was detected above the endogenous H1 doublet due to the added weight of FLAG (1 kDa). This band was most prominent with H1.4-FLAG then H1.4S27E; while detection of H1.4S27A was weaker. H1.4 shows a similar pattern to that of total H1, where the level of endogenous H1.4 remained unchanged regardless of the H1.4-FLAG expressed. The exogenous H1.4-FLAG was also detected with the H1.4 antibody at 1 μg/mL doxycycline, although the equivalent bands were not seen for H1.4S27A or H1.4S27E. As this antibody was raised against a peptide of H1.4 containing amino acids 22 to 33, the alteration of serine 27 to alanine or glutamic acid may hinder epitope recognition. Endogenous dimethylation at H1.4K26 was constant, although there was reduced dimethylation of both exogenous H1.4S27A and H1.4S27E, when compared to the H1.4-FLAG control. This result shows that the alteration of serine 27, to either alanine or glutamic acid, may impede the enzyme that methylates lysine 26. However, this result could also be obtained by loss of epitope recognition, thus further investigation will be required to establish if K26 methylation can occur on H1.4S27A or H1.4S27E.

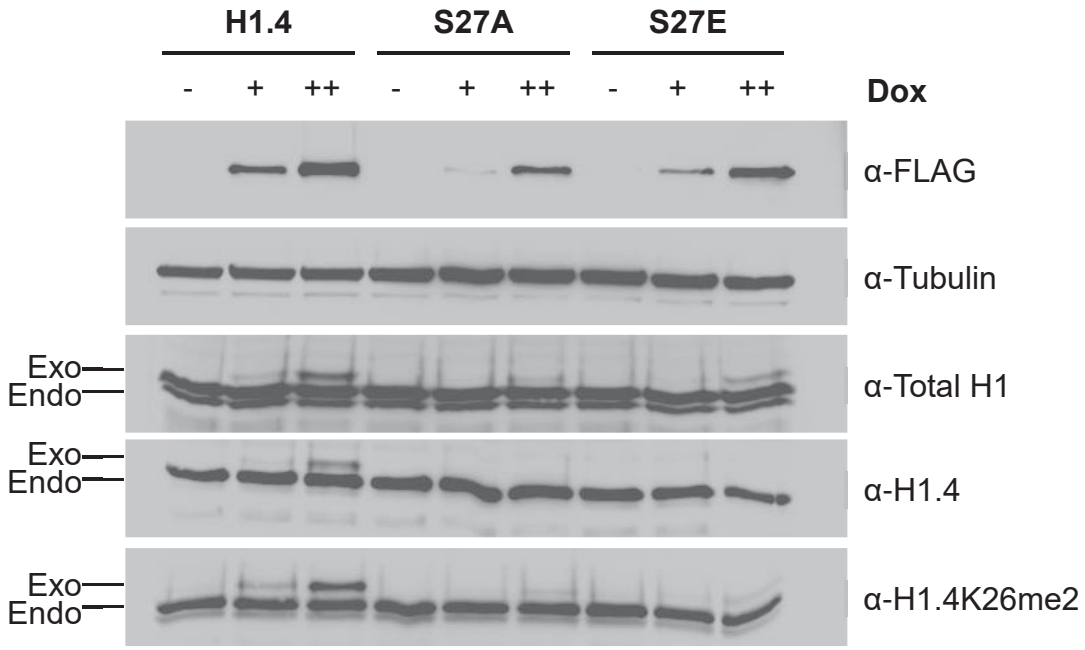

Figure 4.9. Reduced K26 methylation of the H1.4S27 phosphorylation mutants in asynchronously grown cells.
Western blotting of asynchronous lysates (25 µg of protein) from H1.4-FLAG (H1.4), H1.4S27A-FLAG (S27A), and H1.4S27E-FLAG (S27E) cell lines. Cells grown asynchronously with 1 µg/mL (++), 0.1 µg/mL (+) or without (-) doxycycline (Dox) were harvested and the antibodies used for western blotting are indicated. The exogenous H1.4-FLAG proteins (Exo) are indicated, as is endogenous H1 (Endo). α-tubulin was used as a loading control.

Mitotic cells were also analysed by western blotting, given that H1.4S27 phosphorylation normally occurs during mitosis. Cells grown in the absence of, or with doxycycline at 0.1 μg/mL (+) or 1 μg/mL (++) were arrested in mitosis and total protein was harvested and analysed by western blotting (Sections 2.3.4, 2.5.3.1 and 2.5.4). Detection of the exogenous proteins with the antibody against FLAG in mitotic cells in Figure 4.10, gave a similar expression profile to that seen in asynchronously grown cells (Figure 4.9). The level of total H1 was unchanged with expression of the H1.4-FLAG proteins. Endogenous H1.4K26me2 was also not altered, but this methylation was absent on the exogenous H1.4S27A and H1.4S27E from mitotic cells.

In mitotic cells, endogenous H1.4S27 phosphorylation was detected. This was highest in the H1.4S27A cell line and increased slightly with expression of H1.4S27A. As exogenous H1.4-FLAG is wild-type at serine 27 it was able to be phosphorylated at this site, and as expected, H1.4S27A was not phosphorylated. The exogenous H1.4S27E protein was not detected by the H1.4S27p antibody, despite mimicking S27 phosphorylation. Finally, an increase in H3S10 phosphorylation was detected in the H1.4S27A cell line similar to H1.4S27 phosphorylation, and while H3S10 phosphorylation was reduced with H1.4S27E expression at 1 μg/mL of doxycycline, this was not observed consistently. In summary, expression of the H1.4-FLAG proteins did not appreciably affect levels of endogenous H1 protein, H1.4K26 methylation or H1.4S27 phosphorylation in asynchronous or mitotic cells, and thus did not contribute to the occurrence of mitotic defects. However, reduced methylation of the exogenous H1.4S27 mutants was observed, which is investigated further in Section 4.2.3.

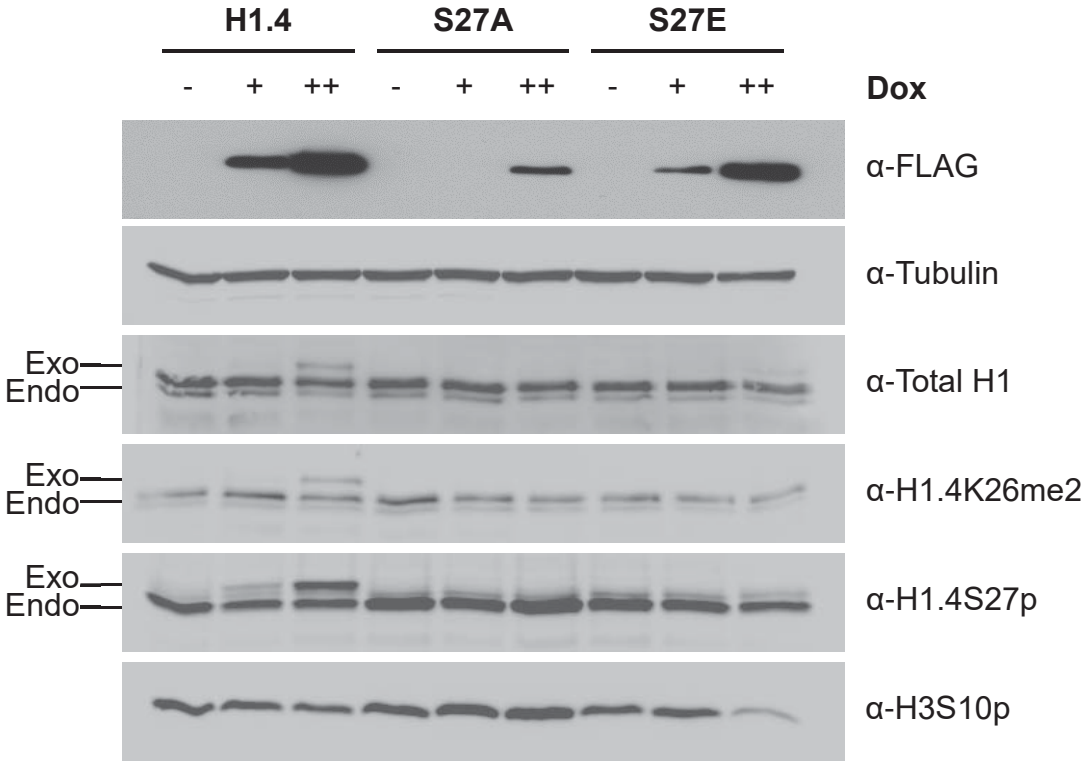

Figure 4.10. H1 protein levels are not altered by expression of the H1.4S27 phosphorylation mutants in mitotic cells.
Western blotting of mitotic lysates (25 µg of protein) from H1.4-FLAG (H1.4), H1.4S27A-FLAG (S27A), and H1.4S27E-FLAG (S27E) cell lines. Mitotic cells grown with 1 µg/mL (++), 0.1 µg/mL (+) or without (-) doxycycline (Dox) were harvested and the antibodies used for western blotting are indicated. The exogenous H1.4-FLAG proteins (Exo) are indicated, as is endogenous H1 (Endo). α-tubulin was detected as a loading control.

4.2.2.5 Localisation of the H1.4-FLAG proteins on metaphase chromosomes

To examine whether the phosphorylation state of H1.4S27 modulates mitotic chromosome condensation, which could contribute to the observed defects, metaphase spreads were generated. Both induced and uninduced mitotic cells were spun onto slides in a cytocentrifuge, then processed for immunofluorescence and examined by confocal microscopy (Sections 2.5.3.1 and 2.5.8). For the three cell lines, H1.4S27 phosphorylation was present along the metaphase chromosomes, and was enriched at the centromere (Figure 4.11), as previously observed (Figure 3.3). When expressed, the exogenous H1.4-FLAG proteins localised to the chromosomes. No gross morphological or structural changes to chromosomes were observed for cells expressing the H1.4-FLAG control, the non-phosphorylatable H1.4S27A, or the phosphomimetic H1.4S27E. This indicates that gross chromosome structural alterations did not contribute to the mitotic defects that occurred when the H1.4S27 phosphorylation mutants were expressed.

4.2.3 Does mutation of H1.4S27 alter the interaction with HP1β *in vitro*?

The ability of HP1β to interact with the H1.4S27 phosphorylation mutants when methylated at K26 was tested to investigate if the dysregulation of HP1β could cause the mitotic defects observed in their presence.

Figure 4.11

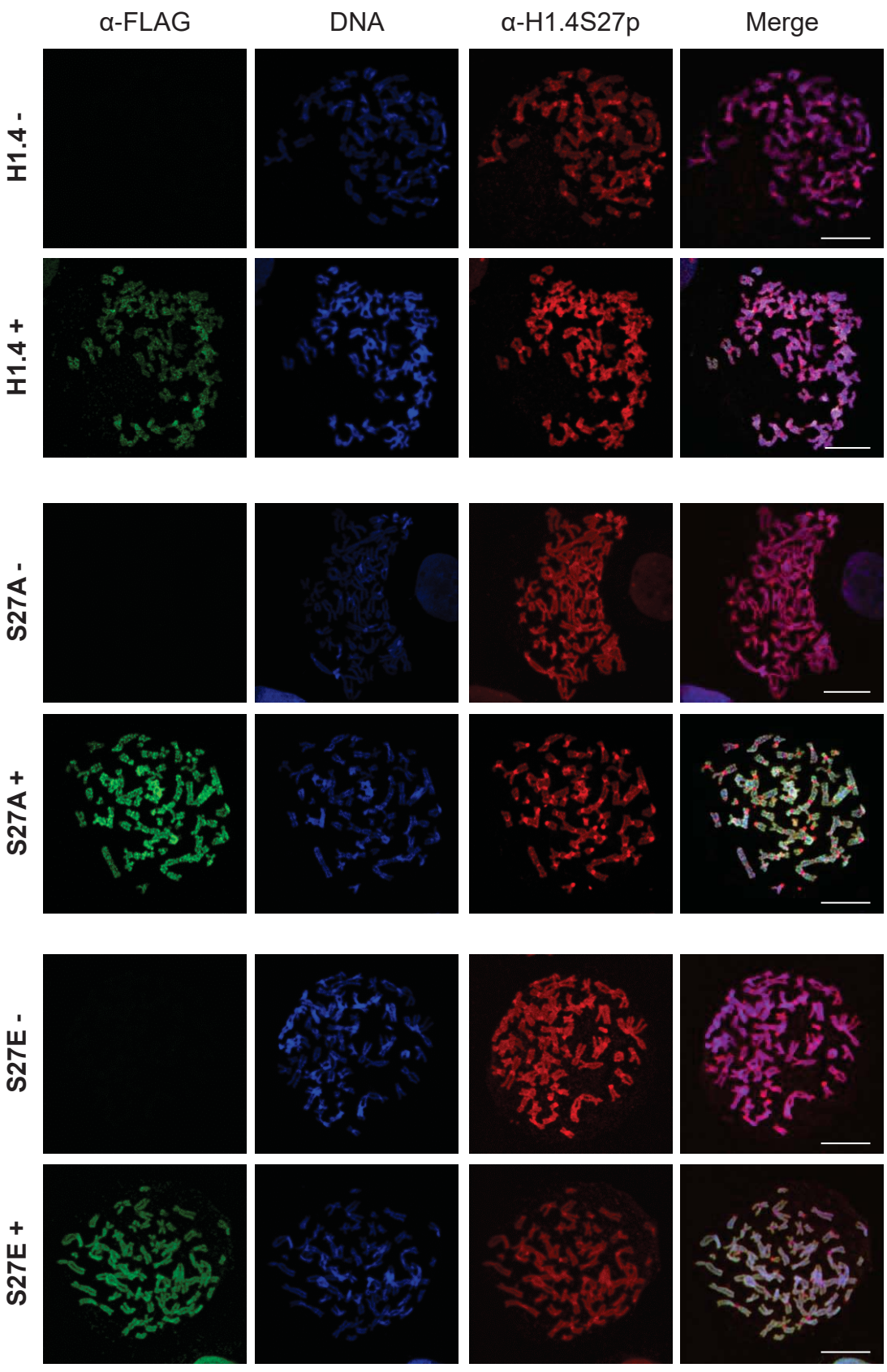

Figure 4.11. Expression of the H1.4S27 phosphorylation mutants does not affect metaphase chromosome structure.
Immunofluorescence of metaphase spreads from H1.4-FLAG (H1.4), H1.4S27A-FLAG (S27A) and H1.4S27E-FLAG (S27E) cell lines. Cells grown in the presence (+; 1 μg/mL) or absence (-) of doxycycline were arrested in mitosis then cytocentrifuged onto microscope slides. Metaphase spreads were analysed using antibodies against FLAG (green) and H1.4S27p (red); DNA was stained with DAPI (blue). Images were captured on a confocal microscope at 400x magnification with the same exposure time and settings. Scale bar, 100 μm.

4.2.3.1 Mutation of H1.4S27 reduces K26 methylation by G9a *in vitro*

Firstly, the ability of the H1.4S27 phosphorylation mutants to be methylated *in vitro* by G9a was confirmed. Following the methylation assay (Section 2.3.9), the reactions were analysed by SDS-PAGE and autoradiography (Sections 2.3.2 and 2.3.3). Methylation was reduced on both H1.4S27A and H1.4S27E when compared to H1.4-FLAG as determined by the incorporation of the ^{14}C-labelled methyl group (Figure 4.12A). As H1.4K26 is the only site in H1.4 methylated by G9a (Figure 3.9A), reduced H1.4K26 methylation occurred when the adjacent S27 was mutated to alanine, and this level was further reduced with the phosphomimetic H1.4S27E. This result confirms that the alteration of serine 27 to alanine or glutamic acid hinders H1.4K26 methylation by G9a *in vitro*, supporting the *in vivo* methylation reduction seen in Figures 4.9 and 4.10.

4.2.3.2 Decreased methylation of the H1.4S27 phosphorylation mutants reduces the interaction with HP1β

To determine whether mutation of H1.4S27 affects the interaction with HP1β, the methylated H1.4S27A and H1.4S27E proteins were included in a GST pull-down with GST-HP1β. Given that K26 methylation of the H1.4S27 phosphorylation mutants was reduced compared to wild-type H1.4 (Figure 4.12A), this is expected to reduce the interaction with HP1β, which is dependent on H1.4K26 methylation. Despite this reduced methylation of H1.4S27A and H1.4S27E, the amount of protein in the reactions was kept constant. Following methylation by G9a (Section 2.3.9), the methylated H1.4-FLAG proteins were incubated with GST-HP1β and the bound protein was detected by western blotting with the FLAG antibody (Section 2.3.12). As shown in Figure 4.12B, the interaction with HP1β showed a similar pattern to the methylation status of the H1.4-FLAG proteins (Figure 4.12A). The H1.4S27E phosphomimetic reduced the interaction with HP1β corresponding to that expected from the reduction in methylation only, no further reduction was seen from mimicking H1.4S27 phosphorylation. Together, the results in Figure 4.12 indicate that the mitotic defects caused by the presence of H1.4S27A or H1.4S27E (Figures 4.5 and 4.6) could be due to their methylation level affecting the interaction with HP1β.

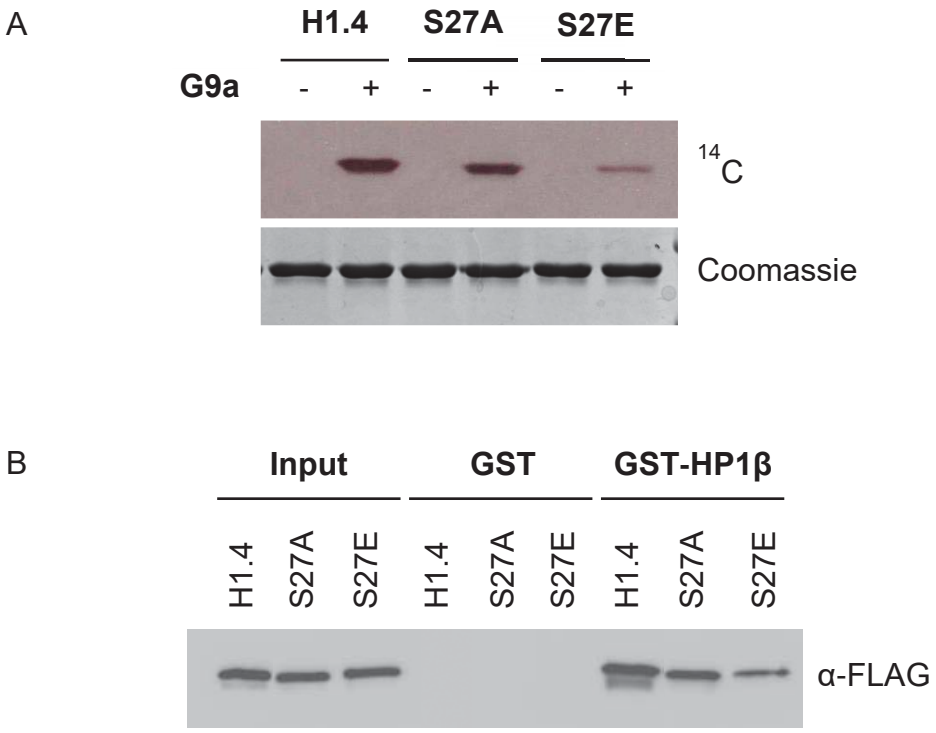

Figure 4.12. Reduced H1.4K26me in the H1.4S27 phosphorylation mutants led to a concomitant reduction in the interaction with HP1β.
A. Autoradiography of an *in* vitro methylation assay where 1 µg of bacterially expressed and purified H1.4-FLAG (H1.4), H1.4S27A-FLAG (S27A) and H1.4S27E-FLAG (S27E) were incubated with (+) or without (-) G9a and ^{14}C-labelled SAM. The reactions were analysed by Coomassie Blue stained SDS-PAGE gel and autoradiography was used to detect the ^{14}C-methyl group.
B. GST pull-down assay with protein treated in a methylation assay as described in **A**. GST or GST-HP1β were incubated with the methylated H1.4-FLAG proteins (0.75 µg) and the bound fraction was subject to western blotting with an antibody against FLAG. The interaction was specific as it did not occur when GST replaced GST-HP1β. The input represents 10% of the protein in the reaction.

4.2.4 The effect of H1.4S27A or H1.4S27E expression on HP1 localisation *in vivo*

Since the level of methylation of H1.4S27A or H1.4S27E alters the interaction with HP1β *in vitro*, this interaction was explored in the context of chromatin isolated from mitotic or asynchronous cells.

4.2.4.1 HP1α localisation is not affected by the presence of H1.4S27A or H1.4S27E

Mitotic cells were subjected to subcellular fractionation (Section 2.5.15) to establish if expression of the non-phosphorylatable H1.4S27A, or phosphomimetic H1.4S27E altered the release of HP1 from the mitotic chromosomes. The HP1 paralogs are transiently released from the chromosomes in mitosis, and therefore should be present in the soluble fraction (Terada, 2006). However, in preliminary experiments HP1α and HP1β remained in the insoluble fraction, possibly due to poor synchronisation of cells in mitosis. Initially, to optimise the synchronisation of cells in mitosis, flow cytometry was performed. Induced and uninduced H1.4S27A cells were synchronised using the double thymidine block and at several time points following release, cells were harvested and processed for flow cytometry using the intercalating DNA dye, propidium iodide (Sections 2.5.3.2 and 2.5.14). When H1.4S27A was expressed there was no change in the cell cycle distribution across the analysed time points, indicating that its expression did not lead to alterations in progression through the cell cycle (Figure 4.13). At the earliest time point, 6.5 hours post-thymidine release; 48% of cells were in G_2 or mitosis (4N). At each subsequent time point a smaller G_2/M peak was detected, indicating that cells were progressing through mitosis and returning to G_1 (2N), with almost all cells synchronised in G_1 11 hours after thymidine was removed. This indicated that the double thymidine block led to cell cycle synchrony, and that the optimal time point for obtaining the highest proportion of cells in G_2 or mitosis was 6.5 hours following release, and as such, cells were harvested at this time.

Figure 4.13

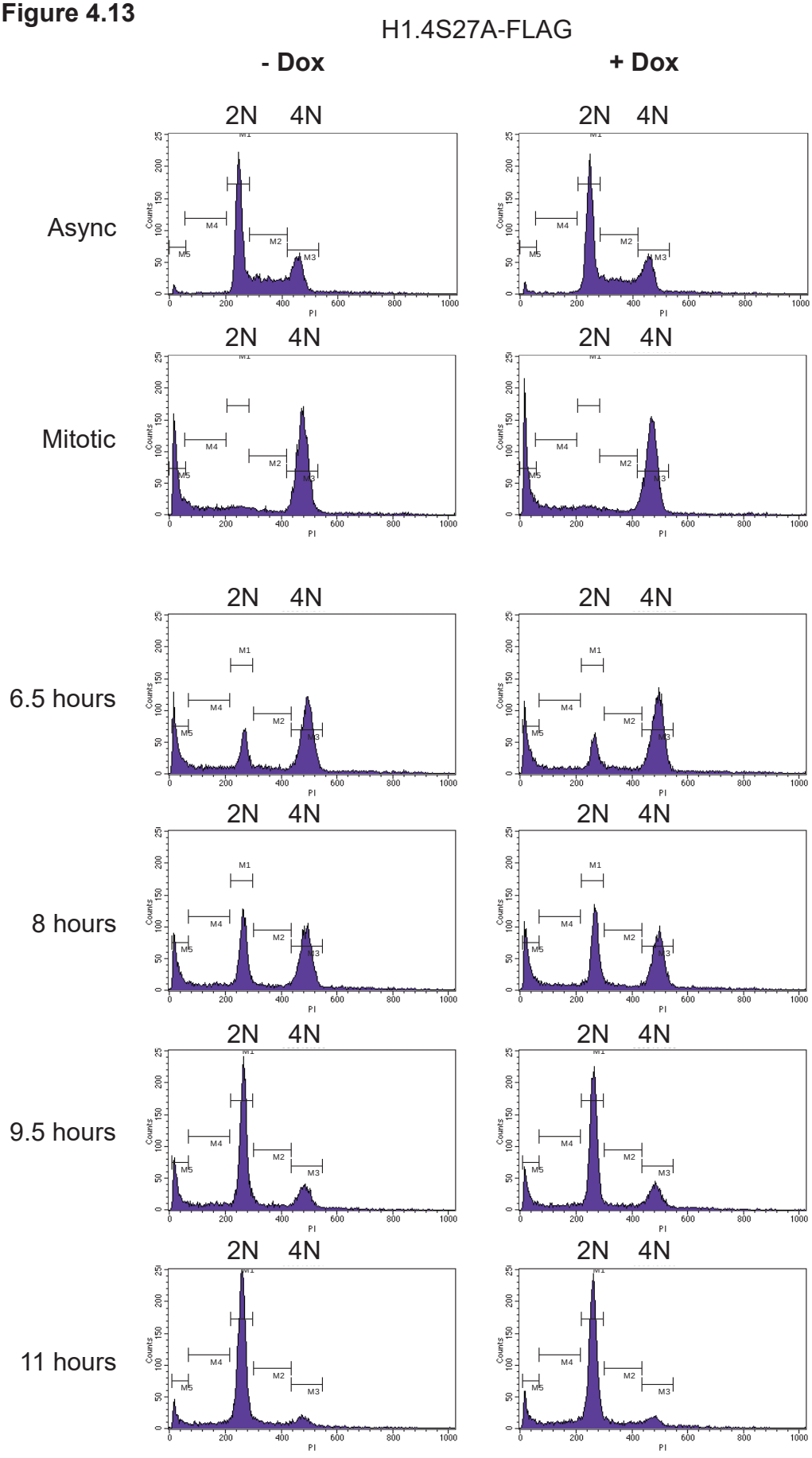
H1.4S27A-FLAG
- Dox
+ Dox
2N 4N
Async
Mitotic
6.5 hours
8 hours
9.5 hours
11 hours
Counts
PI
M1
M2
M3
M4
M5

Figure 4.13. Cells in G_2/M peak 6.5 hours after release from the double thymidine block.
Flow cytometry of H1.4S27A-FLAG inducible cells grown with (+; 1 µg/mL) or without (-) doxycycline (Dox). Asynchronous (Async), nocodazole arrested (Mitotic), or cells synchronised using the double thymidine block were cultured for 6.5, 8, 9.5 or 11 hours after removal of the second block. Cells were stained with propidium iodide (PI) and a minimum of 10,000 cells were analysed using the BD FACSCalibur Flow Cytometer. Gating indicates cell cycle stage: M1, G1 phase; M2, S phase; M3, G2/Mitosis; M4, Sub-G1; M5, Apoptotic.

Following cell fractionation under the optimised conditions (Section 2.5.15), the three H1.4-FLAG cell lines were subjected to western blotting to determine which fraction contained the H1.4 and HP1 proteins (Section 2.3.4). The H1.4-FLAG proteins were all found in the insoluble chromosome fraction, and endogenous H1.4S27 phosphorylation was detected in the insoluble chromosome pellet regardless of induction (Figure 4.14). However, in the presence of doxycycline, S27 phosphorylation was also detected on the exogenous H1.4-FLAG and H1.4S27E proteins, while it was absent for H1.4S27A. Despite optimisation to obtain the majority of cells in mitosis (Figure 4.13), HP1α was still predominantly present in the chromosomal pellet for each of the cell lines regardless of induction. This indicates that there was little effect on the localisation of HP1α when the H1.4S27 phosphorylation mutants were expressed, and thus mislocalisation of HP1α did not appear to contribute to the mitotic defects in cells expressing H1.4S27 phosphorylation mutants.

4.2.4.2 Investigating the interaction between HP1 and chromatin in the presence of H1.4S27A or H1.4S27E

As HP1α localisation was not altered in the context of global chromatin containing H1.4S27A or H1.4S27E, an alternative approach was trialled. Here short chromatin arrays were enriched for exogenous H1.4S27A-FLAG or H1.4S27E-FLAG by immunoprecipitation with an antibody against FLAG, and then the presence of HP1 in the immunoprecipitate was investigated.

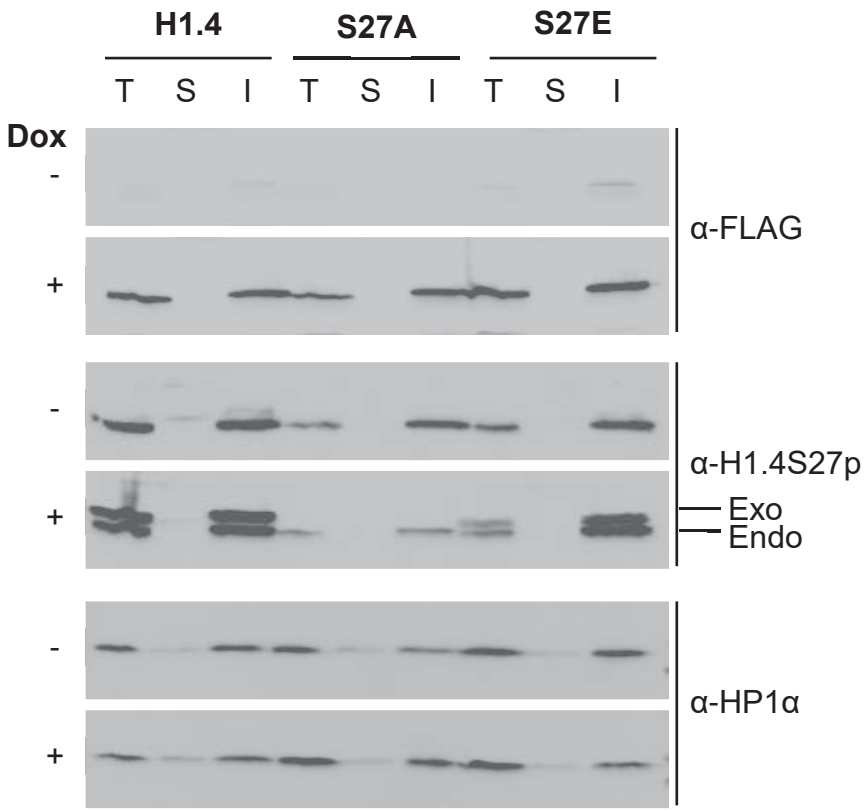

Figure 4.14. Expression of H1.4S27A or H1.4S27E does not change HP1α localisation.
Western blotting of fractionated H1.4-FLAG (H1.4), H1.4S27A-FLAG (S27A) and H1.4S27E-FLAG (S27E) cells. Cells grown in the presence (+; 1 μg/mL) or absence (-) of doxycycline (Dox) were arrested in mitosis then fractionated into total cell lysate (T), soluble protein (S) or insoluble protein (I; each from 2 x 10^5 cells) and analysed with the antibodies indicated. The exogenous H1.4-FLAG proteins (Exo) are indicated, as is endogenous H1 (Endo).

4.2.4.2.1 Preparation of chromatin arrays for immunoprecipitation of the H1.4S27 phosphorylation mutants

To obtain short chromatin arrays that were soluble and therefore able to be analysed using an immunoprecipitation reaction, micrococcal nuclease (MNase) was utilised. Nuclei extracted from cells were digested with MNase, then lysed and analysed by western blotting (Sections 2.3.4 and 2.5.16). From Figure 4.15A H1.4S27A was insoluble; as nuclear lysis may have been incomplete, an alternate lysis method was used where the nuclei were sonicated following MNase digestion (Section 2.5.16). After separation of the soluble and insoluble fractions, H1.4S27A from asynchronous or mitotic cells was detected using western blotting (Section 2.3.4). With sonication, the H1.4S27A protein was present in the soluble fraction across the range of MNase concentrations tested (Figure 4.15B). As sonication can shear chromatin into short fragments, sonication in the absence of MNase also resulted in soluble H1.4S27A.

The success of this procedure is illustrated by the nucleosome ladder in Figure 4.15C, where increasing concentrations of MNase resulted in an increased proportion of smaller DNA fragments. The size of the smallest mononucleosome fragments produced was just below 200 bp, consistent with the size of DNA expected from a single nucleosome from H1 containing chromatin of approximately 168 bp (Orthaus *et al.*, 2009; Simpson, 1978), with larger fragments increasing at multiples of this interval. The concentration of MNase chosen was 500 U/1 x 10^6 cells, as this resulted in chromatin fragments with the majority of arrays containing 2 – 6 nucleosomes. This indicates that MNase digestion, combined with sonication to lyse the nuclei, resulted in soluble chromatin arrays.

Figure 4.15

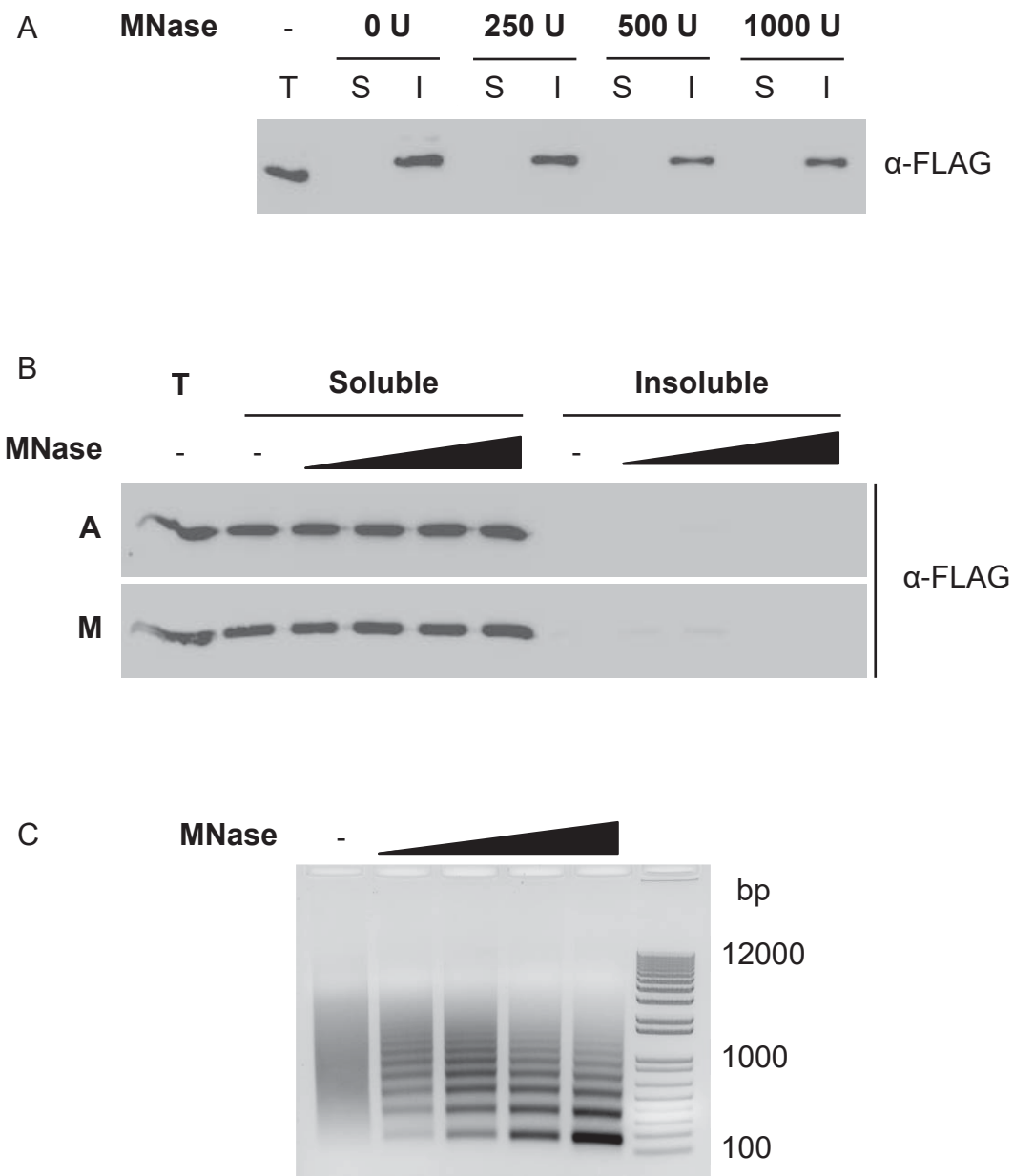
A
MNase
-
0 U
250 U
500 U
1000 U
T S I S I S I S I
α-FLAG
B
T
Soluble
Insoluble
MNase
- - -
A
M
α-FLAG
C
MNase
-
bp
12000
1000
100

Figure 4.15. Obtaining chromatin arrays for immunoprecipitation.
A. Western blotting of soluble (S) and insoluble (I) chromatin arrays alongside total cell lysate (T; each from 2.5 x 10^5 cells) from induced H1.4S27A-FLAG cells. Nuclei from cells grown asynchronously with doxycycline (1 µg/mL) were digested with micrococcal nuclease (MNase) at the indicated concentrations. Nuclei lysed in hypotonic buffer were centrifuged to produce soluble and insoluble fractions. The antibody against FLAG was used to detect H1.4S27A-FLAG.
B. Western blotting of induced H1.4S27A-FLAG cells that had been treated as described in **A**, except that a sonication step was introduced following MNase digestion to lyse nuclei from cells grown asynchronously (A), or arrested in mitosis (M). Concentrations of MNase used were 0 U (-), 250 U, 500 U, 1000 U and 2000 U from low to high as indicated. Soluble and insoluble chromatin fractions were analysed alongside total cell lysate (T; each from 2.5 x 10^5 cells) with an antibody against FLAG.
C. Nucleosome ladders from induced mitotic H1.4S27A-FLAG cells (4 x 10^5 cells) were prepared from soluble chromatin arrays as described in **B**. Soluble chromatin arrays were digested with RNase A and Proteinase K. The DNA was purified and analysed on an agarose gel stained with ethidium bromide. The right lane shows the 1 kb Plus DNA Ladder, size (bp).

Given the introduction of sonication to lyse nuclei, fixation was required to preserve the chromatin state, as shearing forces may disrupt weak chromatin interactions. To optimise the fixation conditions, the duration of fixation in 1% paraformaldehyde (PFA) was titrated, together with sonication. Following processing to obtain a nucleosome ladder, the DNA was analysed on an agarose gel stained with ethidium bromide (Section 2.5.16.1). While DNA was seen after one sonication pulse, the amount of DNA increased with additional sonication (Figure 4.16). As fixation times from 1 – 5 minutes yielded similar results, a fixation time of 2.5 minutes was selected, as were 3 sonication pulses, and the fixed chromatin arrays were then able to be used in the immunoprecipitation reaction.

4.2.4.2.2 Optimising the immunoprecipitation reaction

The chromatin arrays containing the H1.4-FLAG proteins were immunoprecipitated using anti-FLAG affinity gel (Section 2.5.16.2). The immunoprecipitate was then examined by western blotting with antibodies against FLAG and H3S10p (Section 2.3.4). The H1.4-FLAG proteins were successfully immunoprecipitated, as was histone H3 phosphorylated at S10, verifying that the chromatin remained in nucleosome arrays (Figure 4.17). Three control reactions were analysed alongside the test immunoprecipitation reactions. Firstly, a 'no protein' reaction, where lysate was not added was performed, to establish if immunoglobulin G (IgG) released from the affinity gel was detected. This was important as the IgG light chains migrate near the HP1 paralogs (both 25 kDa). Next, bacterially expressed and purified H1.4-FLAG was used as a positive control to verify that H1.4-FLAG was immunoprecipitated. Finally, lysate from the uninduced H1.4-FLAG cell line was used to control for non-specific binding of protein to the affinity gel. As phosphorylated H3S10 was present in the uninduced control, despite the absence of H1.4-FLAG, histone H3 bound non-specifically to the affinity gel.

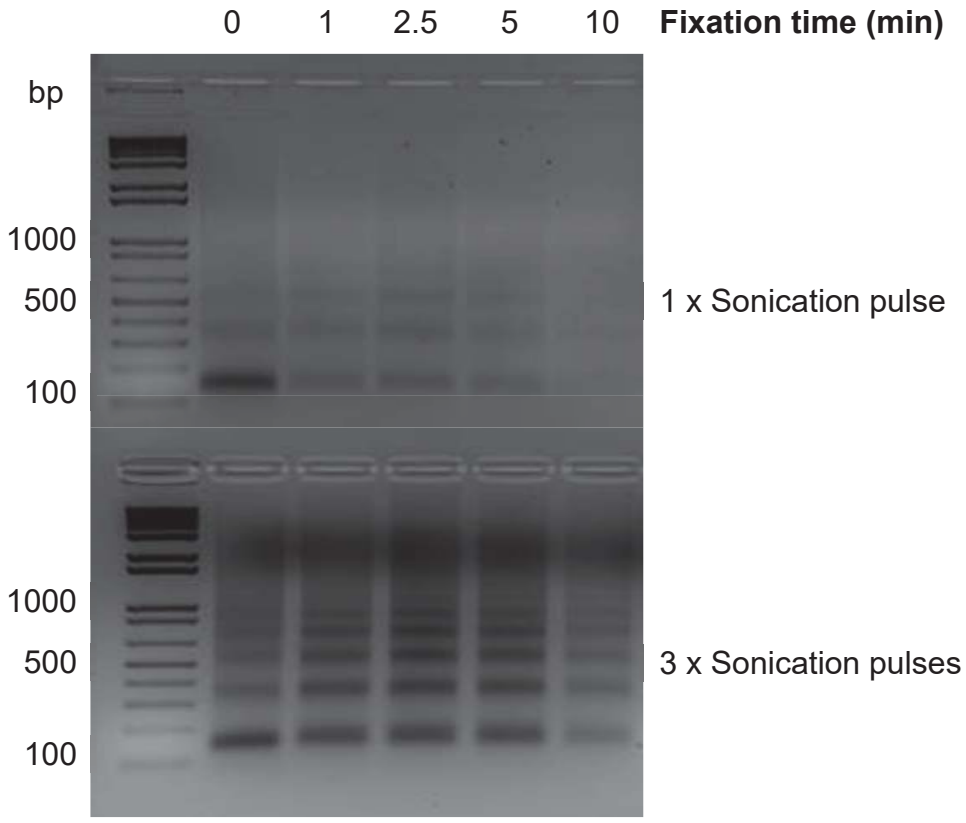

Figure 4.16. Optimisation of fixation for immunoprecipitation.
Nucleosome ladders of chromatin arrays from H1.4-FLAG inducible cells where fixation was titrated. Asynchronous cells grown without doxycycline were fixed in 1% PFA for the indicated duration in minutes (min). Nuclei were digested with micrococcal nuclease (500 U/1 x 10^6 cells), sonicated with one or three pulses and were centrifuged to produce soluble chromatin arrays. Chromatin arrays (from 2.5 x 10^5 cells) were digested with RNase A and Proteinase K and the DNA was purified and analysed on an agarose gel stained with ethidium bromide. The left lane shows the 1 kb Plus DNA Ladder, size (bp).

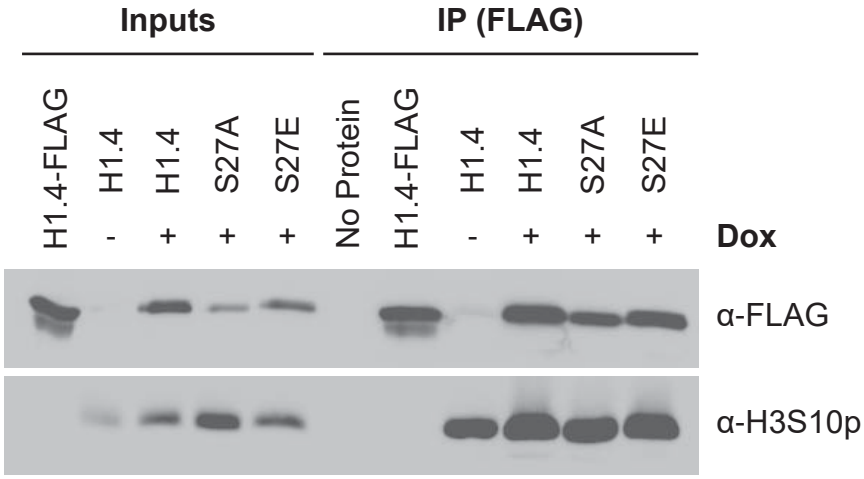

Figure 4.17. Non-specific binding in the immunoprecipitation reaction. Immunoprecipitation and western blotting of chromatin arrays produced from H1.4-FLAG (H1.4), H1.4S27A-FLAG (S27A) and H1.4S27E-FLAG (S27E) cells. Cells grown with (+; 1 µg/mL) or without (-) doxycycline (Dox) were arrested in mitosis and fixed in 1% PFA for 2.5 minutes. Extracted nuclei were digested with micrococcal nuclease (500 U/1 x 10^6 cells), sonicated and centrifuged to produce soluble chromatin arrays. Mitotic chromatin arrays (from 1 x 10^6 cells) were immunoprecipitated with affinity gel against FLAG. Bound protein was analysed by western blotting with the indicated antibodies. Inputs represent 5% of the chromatin arrays in the reaction. Bacterially expressed H1.4-FLAG was used as a positive control and 50% of this protein was analysed in the input. The buffer without chromatin (No Protein) was analysed to control for detection of the anti-FLAG immunoglobulins from the affinity gel used in the immunoprecipitation reaction.

To reduce this non-specific binding in the immunoprecipitation reaction a range of binding and wash conditions were tested. Mitotic chromatin arrays from the uninduced H1.4-FLAG cell line were immunoprecipitated alongside that of induced H1.4-FLAG, then detected by western blotting for H3S10 phosphorylation. Of the conditions tested only the use of detergent reduced the amount of phosphorylated H3S10 in the reaction, while retaining specific binding in the presence of H1.4-FLAG (Figure 4.18A). When the chromatin was pre-cleared with Protein A/G, free antibody fragments were introduced which bound to the affinity gel and were then detected on the western blot. After testing further types of detergent, 0.5% Triton X-100 gave low non-specific background yet enabled chromatin arrays containing H1.4-FLAG to be immunoprecipitated (Figure 4.18B), and was thus used in subsequent immunoprecipitations.

4.2.4.3 Exploring the interaction between HP1β and chromatin in asynchronous cells

To establish if the expression of H1.4S27A or H1.4S27E resulted in changes in the interaction with HP1β that may have resulted in the phenotypic changes seen in these cells during the transition through mitosis (Figures 4.5 and 4.6), soluble chromatin arrays were obtained, fixed and used for immunoprecipitation. Firstly, to verify whether the chromatin arrays produced were similar in size from cells expressing the H1.4-FLAG control or the H1.4S27 phosphorylation mutants, nucleosome ladders were prepared (Section 2.5.16.1). Nucleosome ladders were obtained from both asynchronous and mitotic cells, with a size range from mononucleosomes through to pentanucleosomes (Figure 4.19). As chromatin arrays were consistent for each H1.4-FLAG cell line the soluble chromatin was examined by immunoprecipitation.

Figure 4.18

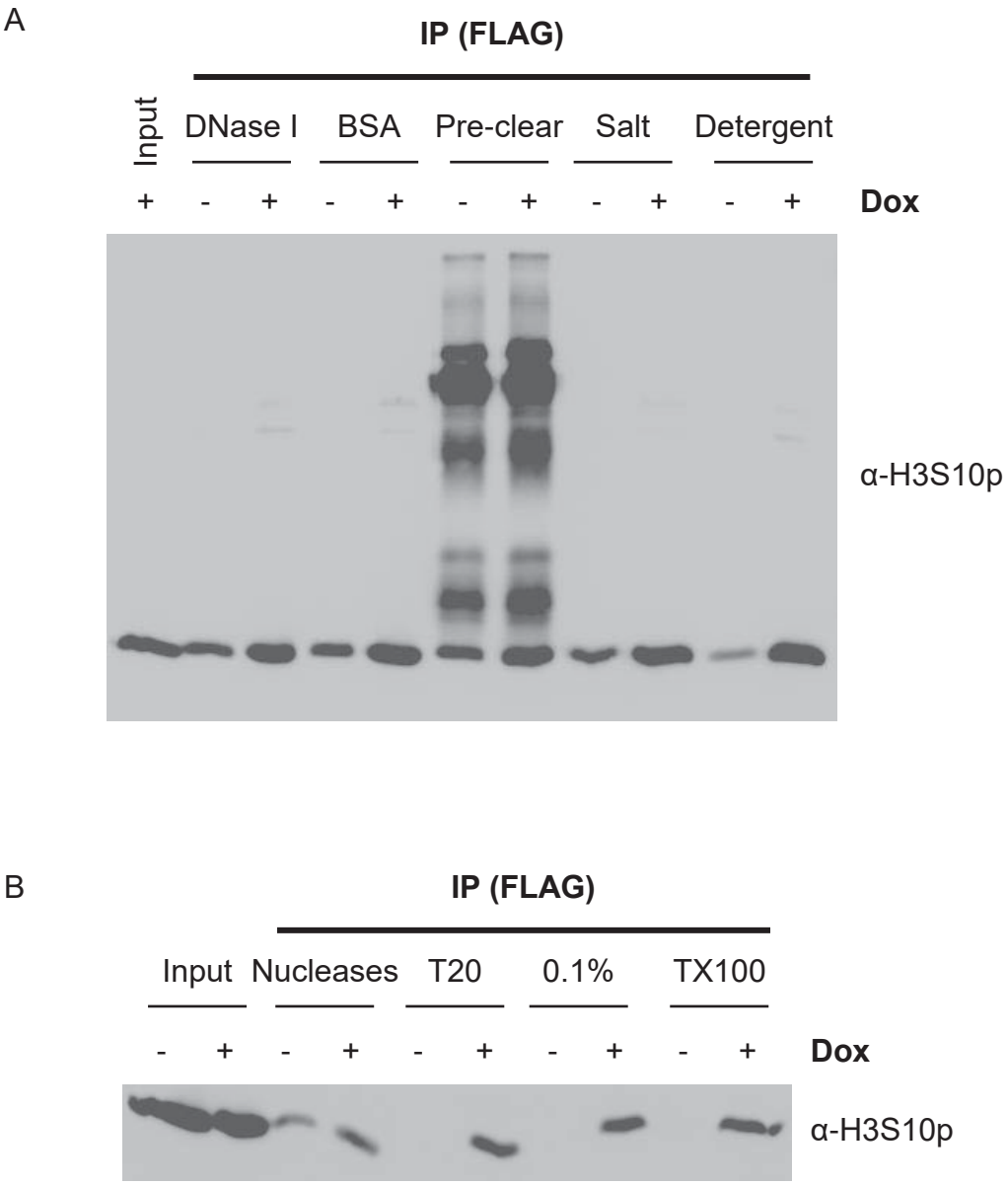
A
IP (FLAG)
Input
DNase I
BSA
Pre-clear
Salt
Detergent
+ - + - + - + - + - +
Dox
α-H3S10p
B
IP (FLAG)
Input
Nucleases
T20
0.1%
TX100
- + - + - + - + - +
Dox
α-H3S10p

Figure 4.18. Triton X-100 in the immunoprecipitation reaction reduced non-specific binding.
A. Immunoprecipitation and western blotting of mitotic chromatin arrays from H1.4-FLAG inducible cells grown with (+; 1 μg/mL) or without (-) doxycycline (Dox). Nuclei extracted from cells arrested in mitosis and fixed in 1% PFA for 2.5 minutes were digested with MNase (500 U/1 x 10^6 cells), sonicated and centrifuged to produce soluble chromatin arrays. Mitotic chromatin arrays (from 1 x 10^6 cells) were immunoprecipitated with affinity gel against FLAG. The immunoprecipitation reaction was digested with DNase I, or 5% BSA was used to block the affinity gel before use (BSA). Alternatively the chromatin arrays were pre-cleared using Protein A/G PLUS Agarose (Pre-clear), or washes included an additional 100 mM sodium chloride (250 mM total; Salt) or 0.1% Triton X-100 (Detergent). Bound protein was analysed by western blotting for H3S10p, 7.5% of the chromatin arrays in the reaction were represented in the input.
B. Immunoprecipitation and western blotting were carried out as in **A** but with different optimisation conditions. A combination of DNase I, MNase and RNase A was used to digest the immunoprecipitation reaction (Nucleases), or detergents included were 0.1% Tween 20 (T20), 0.1% Tween 20 and 0.1% Triton X-100 (0.1%), or 0.5% Triton X-100 (TX100). Bound protein was analysed by western blotting with the H3S10p antibody, 15% of the chromatin arrays in the reaction were represented in the input.

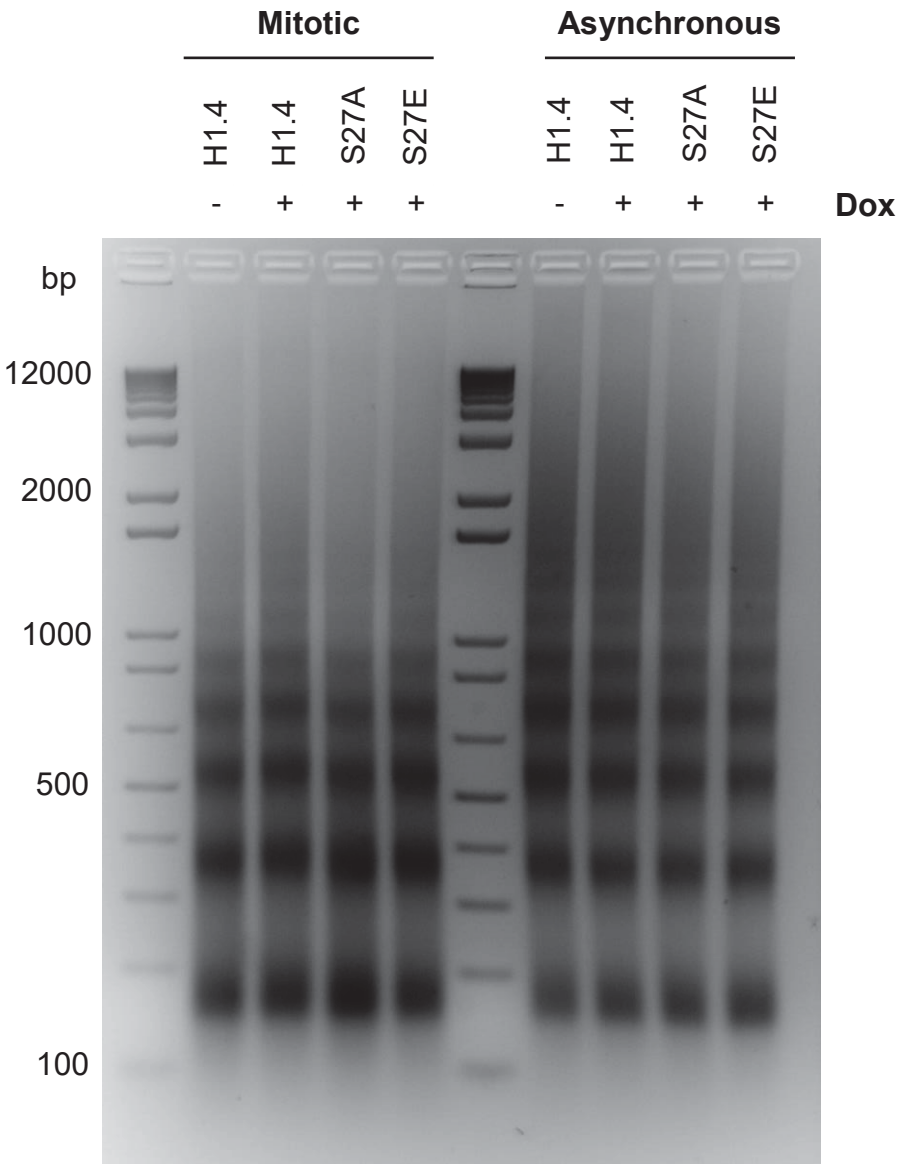

Figure 4.19. Nucleosome ladders for fixed immunoprecipitation.
Nucleosome ladders from H1.4-FLAG (H1.4), H1.4S27A-FLAG (S27A) and H1.4S27E-FLAG (S27E) cells. Cells grown asynchronously (right) or arrested in mitosis (left), with (+; 1 µg/mL) or without (-) doxycycline (Dox) were fixed in 1% PFA for 2.5 minutes and nuclei were digested with micrococcal nuclease (500 U/1 x 10^6 cells), then sonicated and centrifuged to produce soluble chromatin arrays. Chromatin arrays (from 2.5 x 10^5 cells) were digested with RNase A and Proteinase K and the DNA was purified and analysed on an agarose gel stained with ethidium bromide. The left and middle lanes show the 1 kb Plus DNA Ladder, size (bp).

While the defects occurred during mitosis, chromatin arrays from asynchronously grown cells were first analysed to establish whether chromatin bound HP1β could be detected in the immunoprecipitate, as during interphase HP1β is chromatin bound (Hayakawa *et al.*, 2003). Following immunoprecipitation (Section 2.5.16.2), western blots were screened with antibodies for FLAG, H1.4K26me2, HP1β and H4. HP1β was present in the immunoprecipitate in the presence of the exogenous H1.4-FLAG proteins (Figure 4.20). While a greater amount of HP1β was present in the immunoprecipitate of H1.4S27E expressing cells, this increase may be due uneven loading as indicated by the corresponding increase in H4. H1.4K26me2 was examined as reduced G9a methylation of H1.4S27A and H1.4S27E occurred *in vitro* (Figure 4.12A). Dimethylation of H1.4K26 on the exogenous H1.4-FLAG proteins was detected strongly for H1.4-FLAG, while H1.4S27A and H1.4S27E were minimally dimethylated in agreement with Figure 4.12A. The endogenous H1.4 was equally dimethylated in each sample. Overall, no appreciable change in the HP1β associated with the H1.4-FLAG proteins was observed in chromatin from asynchronous cells, although reduced methylation of the phosphorylation mutants did occur.

4.2.4.4 The mitotic chromatin landscape with H1.4S27A and H1.4S27E expression

As HP1β was detected in asynchronous immunoprecipitate with the H1.4-FLAG proteins, mitotic chromatin arrays were explored to establish if HP1 interacted differentially with chromatin containing H1.4S27A or H1.4S27E during mitosis. It was hypothesised that HP1 would remain associated with chromosomes containing the H1.4S27A phosphorylation mutant during mitosis, however the change from serine to alanine at position 27 interfered with the ability to methylate the adjacent lysine 26 in this mutant meaning less HP1 would be bound. Chromatin arrays were prepared from mitotic cells and FLAG affinity gel was used to immunoprecipitate the H1.4-FLAG proteins (Section 2.5.16.2). Minimal HP1α or HP1β was co-immunoprecipitated with the H1.4-FLAG proteins (Figure 4.21). As observed for asynchronously grown cells,

mitotic cells also showed reduced H1.4K26me2 on the exogenous H1.4S27A and H1.4S27E compared to the H1.4-FLAG control. There were additional discrete bands for H1.4K26me2 that may correspond to differing degrees of mitotic hyperphosphorylation of H1.4 by the cyclin dependent kinases. To determine whether H1.4K26 was able to be acetylated when H1.4S27 was mutated H1.4K26 acetylation was examined. Reduced H1.4K26 acetylation was observed in both the input and in the immunoprecipitate for the exogenous H1.4S27A and H1.4S27E proteins. The H4 control verified that core histones were present in both the input and immunoprecipitate with the H1.4-FLAG proteins, confirming they were incorporated in chromatin arrays and were evenly loaded. Thus while HP1 was present in the soluble mitotic chromatin arrays, it was only weakly associated with the H1.4-FLAG containing nucleosome arrays. Although the signal is weak, there is a reduction in the amount of HP1β present in the H1.4S27E immunoprecipitate. This may be indicative of an effect of H1.4S27 phosphorylation of the dislodgement of HP1β during mitosis. Further work will be necessary to confirm the relationship between H1.4 and HP1β *in vivo*.

Other proteins of interest were also explored for alterations in the presence of H1.4S27A and H1.4S27E. As H1.4S27 phosphorylation is enriched at the centromere (Figure 3.3), changes in this modification here could affect centromeric proteins. As such the centromeric variant, Centromere protein A (CENPA), which replaces H3 in nucleosomes at the centromere (Shelby *et al.*, 1997), was examined. Also explored was the condensin component, Condensin complex subunit 1 (CAPD2), which has been reported to interact with H1 (Ball *et al.*, 2002). While both CENPA and CAPD2 were detected in the soluble mitotic chromatin arrays, they were not present in the immunoprecipitate with the H1.4-FLAG proteins. In summary, little change in the tested chromatin bound proteins in mitosis could be detected upon immunoprecipitation of the H1.4S27 phosphorylation mutants.

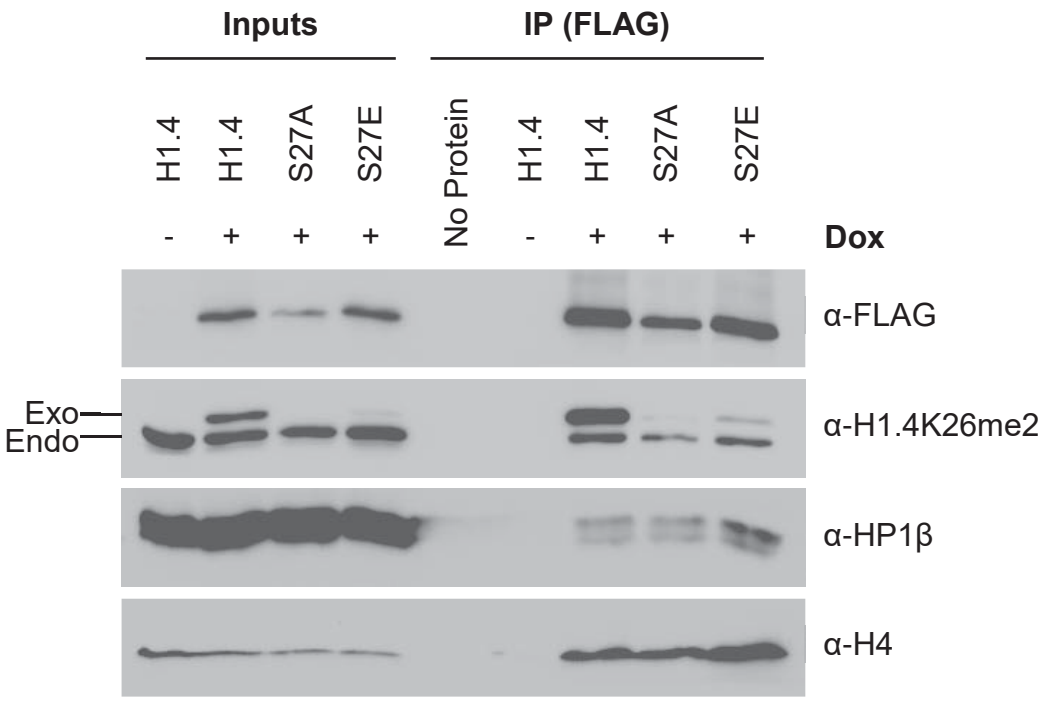

Figure 4.20. HP1β interacts with chromatin containing the H1.4S27 phosphorylation mutants from asynchronous cells.
Immunoprecipitation and western blotting of chromatin arrays from asynchronous H1.4-FLAG (H1.4), H1.4S27A-FLAG (S27A) and H1.4S27E-FLAG (S27E) cells. Cells grown asynchronously with (+; 1 µg/mL) or without (-) doxycycline (Dox) were fixed in 1% PFA for 2.5 minutes; nuclei were digested with micrococcal nuclease (500 U/1 x 10^6 cells) and were sonicated and centrifuged to produce soluble chromatin arrays. Chromatin arrays (from 2.5 x 10^6 cells) were immunoprecipitated with affinity gel against FLAG. Bound protein was analysed by western blotting with the indicated antibodies. Inputs represent 3% of the chromatin arrays in the reaction. Buffer without chromatin (No Protein) was analysed to control for detection of the anti-FLAG immunoglobulins from the affinity gel used in the immunoprecipitation reaction. The exogenous H1.4-FLAG proteins (Exo) are indicated, as is endogenous H1 (Endo).

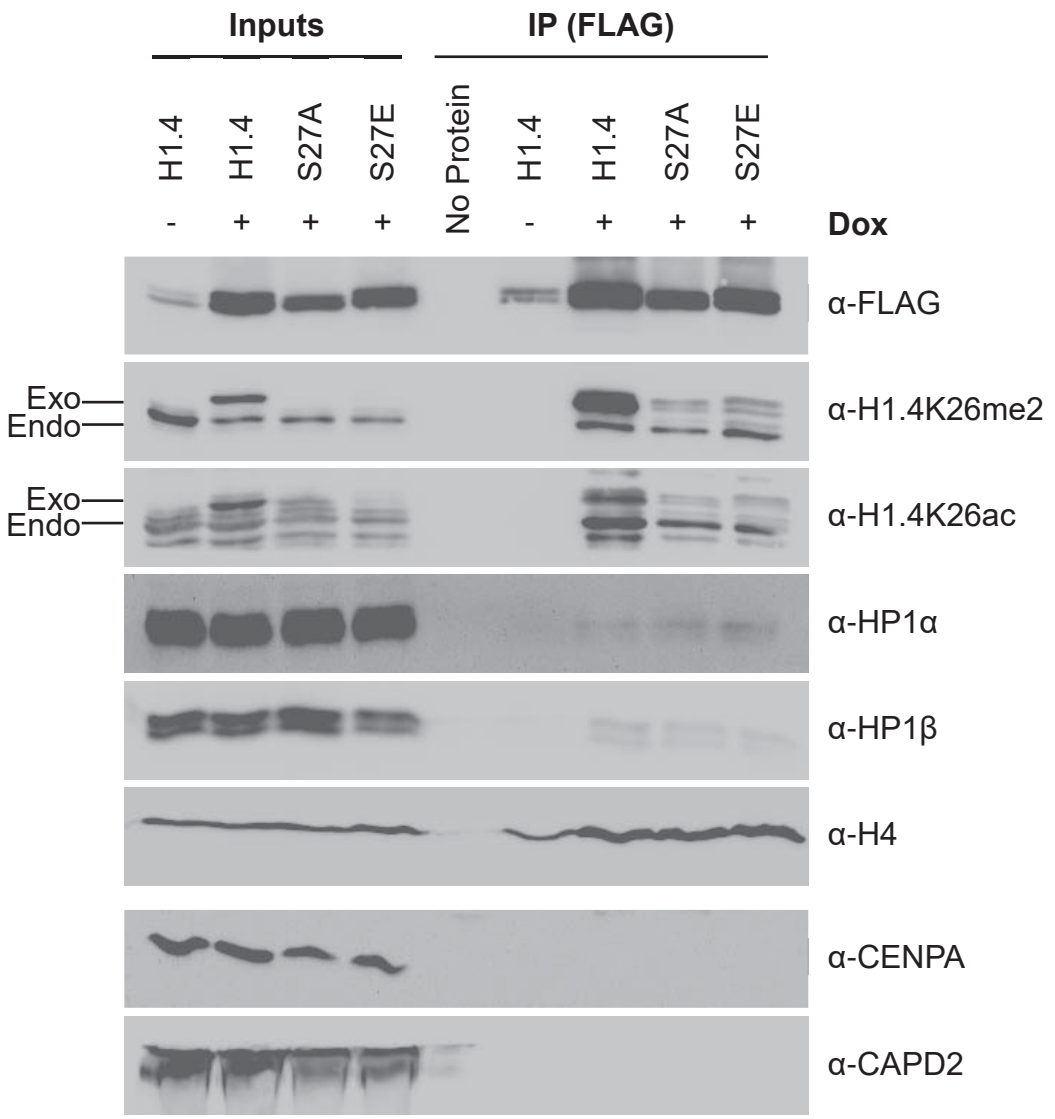

Figure 4.21. The chromatin landscape in mitotic cells expressing the H1.4S27 phosphorylation mutants.
Immunoprecipitation and western blotting of mitotic chromatin arrays from H1.4-FLAG (H1.4) H1.4S27A-FLAG (S27A) and H1.4S27E-FLAG (S27E) cells. Cells grown with (+; 1 μg/mL) or without (-) doxycycline (Dox) were arrested in mitosis then fixed in 1% PFA for 2.5 minutes; nuclei were digested with micrococcal nuclease (500 U/1 x 10^6 cells), sonicated and centrifuged to produce soluble chromatin arrays. Chromatin arrays (from 2.5 x 10^6 cells) were immunoprecipitated with affinity gel against FLAG. The immunoprecipitate was analysed by western blotting with the indicated antibodies. Inputs represent 3% of the chromatin arrays in the reaction. Buffer without chromatin (No Protein) was analysed to control for detection of the anti-FLAG immunoglobulins from the affinity gel used in the immunoprecipitation reaction. The exogenous H1.4-FLAG proteins (Exo) are indicated, as is endogenous H1 (Endo).

4.3 Discussion

Here, for the first time I have shown that the dysregulation of H1.4S27 phosphorylation leads to mitotic defects. Mutation of H1.4S27 to prevent phosphorylation, or to constitutively mimic phosphorylation, both resulted in abnormal mitosis. The nature of the defects differed however, with the type of H1.4S27 phosphorylation mutant expressed. In the presence of non-phosphorylatable H1.4S27A defects occurred early in mitosis, whereas the phosphorylation mimic H1.4S27E led to defects in late mitosis, when H1.4S27 is dephosphorylated.

The phosphorylation of H1.4S27 usually occurs from prophase, early in mitosis, until the chromosomes begin to segregate during anaphase (Figure 3.2). The inability to phosphorylate H1.4S27A during this time led to an increase in chromosomes that were misaligned in metaphase. While no gross defects in chromosome structure were apparent in metaphase spreads in the presence of H1.4S27A, there may be changes that could not be detected at this scale. As H1.4S27 phosphorylation is enriched at the centromere, where the mitotic spindle attaches to the chromosomes, the presence of a population of non-phosphorylatable H1.4S27A at this location may lead to errors in spindle attachment resulting in misalignment of chromosomes at the equatorial plate in metaphase. However, normal alignment at metaphase was also seen in cells expressing H1.4S27A indicating that in some instances mitosis can proceed normally. Examination of mitosis in real time in these cells would enable a more detailed picture, and establish if this misalignment could be resolved. Whether there was an increase in the duration of mitosis, or an increase in aneuploidy in these cells may also be revealed.

Additionally, the incidence of multipolar spindles increased when H1.4S27A was expressed. This result is unexpected as multipolar mitoses usually arise from excess centrosome duplication or by previous failure of cytokinesis (Kops *et al.*, 2005). Both CDK2 and Aurora A kinase are involved in the duplication and maturation of centrosomes (Hannak *et al.*, 2001; Y. Matsumoto *et al.*, 1999), while Aurora B kinase is implicated in cytokinesis failure (Kallio *et al.*, 2002; Terada *et al.*, 1998). The presence of H1.4S27A, which cannot be phosphorylated by Aurora B, could hinder completion of

cytokinesis. Although evidence of this was not observed, so further analysis is required to establish how expression of H1.4S27A could lead to centrosome duplication and concomitant formation of excess spindles.

The increase in abnormal mitosis when the constitutive phosphorylation mimic H1.4S27E was expressed was small, but affected the late stages of mitosis. Thus, the constitutive phosphorylation mimic may lead to defects in mitosis after anaphase onset when dephosphorylation should have occurred. While this cell line mimicked phosphorylation during mitosis, this may not adequately represent the phosphorylated state hindering the progression through mitosis. Alternatively, these defects could arise due to aberrant timing of H1.4S27 phosphorylation. Another consideration is the report of the relative abundance of H1.4S27 phosphorylation being 3% (Hergeth *et al.*, 2011). Thus expression of H1.4S27E could mimic phosphorylation to a degree that is aberrantly high. The occurrence of bridging and lagging chromosomes in cells where H1.4S27E was expressed shows that the dephosphorylation of H1.4S27 in anaphase is necessary for proper segregation of chromosomes. The increased affinity for chromatin displayed by H1.4S27E (Hergeth *et al.*, 2011), may also contribute to the defects seen here. Interestingly, when H3S10E was transiently overexpressed in CHE cells, segregation defects occurred (Ota *et al.*, 2002), although the percentage of cells affected here with H1.4S27E expression was much lower. This similar phenotype also occurs when Aurora B kinase is overexpressed (Ota *et al.*, 2002), so this phenotype could occur through a pathway that involves H1.4S27 phosphorylation.

The increase in the incidence of cells in interphase that contained a micronucleus when the phosphomimetic H1.4S27E was expressed may stem from the bridging and lagging chromosomes seen during mitosis. A micronucleus is formed when chromosomal DNA is not incorporated into the nucleus following its reformation near the completion of mitosis (Fenech *et al.*, 2011). This erroneous DNA outside of the cell nucleus can be caused by lagging chromosomes that fail to segregate with the rest of the chromosomes, resulting in the formation of its own small nucleus (Fenech *et al.*, 2011). Thus the increased incidence of lagging chromosomes in cells expressing H1.4S27E could have formed a micronucleus as mitotic cells re-entered interphase. The

aneuploidy that can result from micronuclei formation suggests that erroneous H1.4S27 phosphorylation contributes to the way in which overexpression of Aurora B kinase results in increased aneuploidy and tumourigenesis.

The occurrence of mitotic defects upon expression of H1.4S27A or H1.4S27E could also be brought about indirectly. The presence of mutant H1.4 in the cell may interfere with the function of chromatin modifying enzymes. Additionally, the expression of or deposition of other core or linker histones into chromatin may be altered by the presence of the over-expressed H1.4S27 mutant proteins. It is possible that such indirect effects resulting from H1.4S27A or H1.4S27E expression could also contribute to the mitotic defects that were observed.

While mitotic defects were observed in the presence of H1.4S27A and H1.4S27E, these defects did not lead to an increase in apoptosis or slower proliferation. Since the inducible H1.4-FLAG proteins were only present for 72 hours before mitotic defects were analysed this allowed for only three cycles of cell division before cells were harvested. Despite the defects that occurred in this time frame, there was no change in apoptosis or proliferation (Figures 4.7 and 4.8). The presence of endogenous H1.4 that was able to be modified, in addition to the exogenous phosphorylation mutants may have minimised the effect of their presence. In contrast, Terme *et al.* (2014) showed that cells stably expressing a mutant of the adjacent H1.4K26A were out competed by the parental T47D cell line suggesting that H1.4K26A impairs proliferation, presumably through its inability to be acetylated or methylated.

Only minor changes in the interaction of HP1 with the chromatin occurred when H1.4S27A or H1.4S27E was expressed, as seen here in cell fractionation and immunoprecipitation experiments. The mitotic time point in which the HP1 proteins are released from the chromosomes may not have been captured, making it difficult to establish if there was an increase in the chromosomal retention of HP1α with expression of non-phosphorylatable H1.4S27A. In addition, the unexpected reduction in H1.4K26 methylation on the phosphorylation mutants may have caused reduced binding of HP1 to the exogenous H1.4-FLAG proteins. Thus HP1 may have favoured binding to endogenous H1.4, resulting in normal regulation of HP1 throughout the cell

cycle. H3 was also present, and its phosphorylation at S10 may also have contributed to the normal dissociation of HP1 (Terada, 2006). Despite the normal localisation of HP1, the expression of H1.4S27A and H1.4S27E still had an impact on the progression through mitosis, perhaps through their reduced H1.4K26 methylation. This indicates that H1.4S27 phosphorylation does play an important role in mitosis, although further research will be required to elucidate the mechanism through which this occurs.

There are additional post-translational modifications on H1.4, particularly its CDK phosphorylation. As one of these CDK phosphorylation sites is near the 'ARKS' motif, then the CDK phosphorylation of H1.4 during mitosis may also affect the interaction between HP1 and H1.4 methylated at K26. Thus the CDK phosphorylation of H1.4 during mitosis and the effect that this has on protein interactions was explored further as documented in Chapter Five.

Chapter Five

Investigating the contribution of CDK phosphorylation of H1.4 on the interaction with HP1β and CAPD2 during mitosis

5.1 Introduction

In addition to the post-translational modification of K26 and S27, H1.4 is hyperphosphorylated by Cyclin dependent kinase (CDK) during mitosis (Garcia *et al.*, 2004; Langan *et al.*, 1989; Swank *et al.*, 1997; Talasz *et al.*, 1996). This hyperphosphorylation of H1.4 by CDK has been implicated in regulation of the chromosome condensation that occurs in mitosis (Bradbury *et al.*, 1973; Gurley *et al.*, 1995; Th'ng *et al.*, 1994). However, it is not understood whether this is brought about by the change in charge of H1.4 through its hyperphosphorylation, or if it is due to the recruitment of other protein factors.

Whether CDK phosphorylation of H1.4 alters the interaction between H1.4 and heterochromatin protein 1β (HP1β) has not been investigated. While the interaction of H1.4 with HP1β is dependent on the chromodomain binding to methylated H1.4K26, the hinge of HP1α can interact with the C-terminus of H1.4 and this interaction is abolished by the CDK phosphorylation of H1.4 (Hale *et al.*, 2006). There is a single N-terminal CDK phosphorylation site within H1.4 on threonine 18 that is in the vicinity of the 'ARKS' motif and is phosphorylated exclusively during mitosis (Zheng *et al.*, 2010). When unmodified, this CDK site may be spatially orientated such that it facilitates the HP1β interaction through hydrogen bonding as previously shown for HP1γ (Ruan *et al.*, 2012). The spatial arrangement and the concurrent timing of H1.4T18 phosphorylation with that of serine 27 suggests that both may contribute to the dislodgement of HP1β from methylated H1.4, therefore the effect of CDK phosphorylation of H1.4T18 on the interaction with HP1β was investigated.

While it is unknown how the CDK phosphorylation of H1 induces chromosome condensation during mitosis it has been reported that H1 interacts with the Condensin I subunit, CAPD2 (Condensin complex subunit I), *in vitro* (Ball *et al.*, 2002). Condensin I is a large five protein complex which is critical for correct chromosome condensation (Hirano & Mitchison, 1994). It consists of SMC2 and SMC4, Structural maintenance of chromosome (SMC) subunits, which are ATPases (Hirano & Mitchison, 1994). The additional three regulatory subunits are CAPD2, NCAPG (non-SMC Condensin I complex, subunit G) and NCAPH (non-SMC Condensin I complex, subunit H; Hirano

& Mitchison, 1994). When combined in the Condensin I complex these proteins are thought to introduce positive supercoiling into DNA and work together with topoisomerases to rearrange the chromosome structure into its mitotic condensed form (K. Kimura *et al.*, 1999). The interaction between H1 and CAPD2 has been shown previously *in vitro*, using far-western blotting with the chromatin fraction from HeLa cells (Ball *et al.*, 2002). Like the HP1 family (Bannister *et al.*, 2001; Daujat *et al.*, 2005; Lachner *et al.*, 2001), CAPD2 can also interact with both H1 and the core histone H3 (Ball *et al.*, 2002). However, the subtype of H1 that interacts with CAPD2 has not yet been identified. Although the region of CAPD2 that interacts with H1 has been mapped to its C-terminus (Ball *et al.*, 2002), the interacting region of H1 has not yet been determined. The effect of post-translational modification of either protein on their interaction has also not been determined. Condensin I, and therefore CAPD2, is excluded from the nucleus until the nuclear envelope breaks down in prometaphase, thus the interaction with H1 is limited to mitosis, a time when H1 is hyperphosphorylated (Hirota *et al.*, 2004; Talasz *et al.*, 1996). CAPD2 itself is also phosphorylated by CDK in the C-terminal region, which is thought to activate the supercoiling function of Condensin I (K. Kimura *et al.*, 1998). As the CAPD2 subunit targets Condensin I to the chromosomes (Ball *et al.*, 2002), its interaction with linker histones could be one way that the hyperphosphorylation of H1 could contribute to mitotic chromosome condensation.

The aim of this chapter is to investigate whether CDK phosphorylation alters the interaction between methylated H1.4 and HP1β, to establish if this can also contribute to the dislodgement of HP1β. Additionally, an interaction between CAPD2 and H1.4 was investigated with and without CDK phosphorylation of each protein to determine whether CDK phosphorylated H1 can recruit Condensin I to facilitate chromosome condensation.

5.2 Results

5.2.1 Total mitotic phosphorylation of H1.4 abolishes the interaction with HP1β

As H1.4 is also phosphorylated in mitosis by CDK, the interaction between HP1β and H1.4 methylated at K26 and phosphorylated by CDK was explored. Initially, in an *in vitro* kinase assay, the mitotic kinase CDK1/cyclin B (CDK1/B) was used to phosphorylate H1.4-FLAG (Section 2.3.10). Western blotting of the *in vitro* kinase assay presented in Figure 5.1A shows that unmodified H1.4 was phosphorylated in the presence of CDK1/B, as detected by the Phospho H1 antibody. The CDK hyperphosphorylated H1.4 has a small retardation in migration due to the additional weight of these phosphate moieties, when compared to unmodified H1.4.

Next, a GST pull-down was performed to investigate whether the CDK phosphorylation of H1.4-FLAG alters the interaction with HP1β (Section 2.3.12). Following methylation of H1.4K26 by the histone methyltransferase, G9a, H1.4 was phosphorylated by CDK and incubated with HP1β. As shown in Figure 5.1B, HP1β interacts with H1.4 methylated at K26 and CDK phosphorylation of H1.4 completely abolished this interaction. In contrast, phosphorylation of S27 by Aurora B kinase caused only an approximate two-fold reduction in binding of HP1β to methylated H1.4 (46% reduction; Refer to Appendix Two for Quantitation), as seen previously (Figure 3.9C). This shows that CDK1/cyclin B phosphorylation of methylated H1.4 was sufficient to abolish the interaction with HP1β.

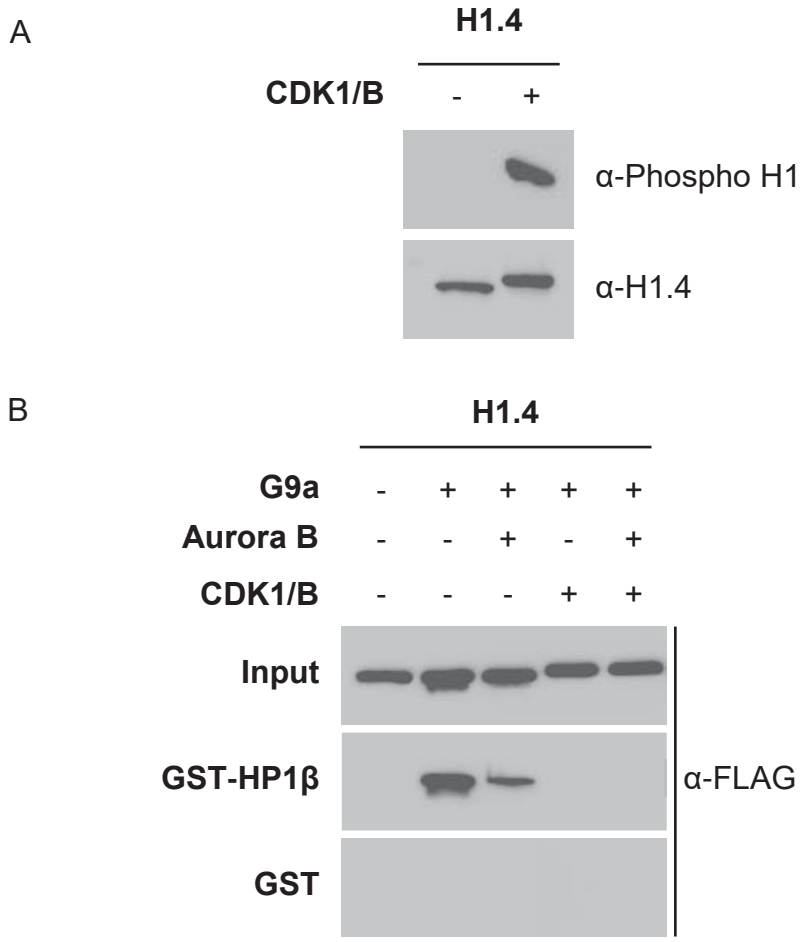

Figure 5.1. CDK phosphorylation of H1.4 abolishes the interaction with HP1β.
A. Western blotting of an *in vitro* kinase assay. Bacterially expressed and purified H1.4-FLAG (H1.4; 0.25 µg) incubated with (+) or without (-) CDK1/cyclin B (CDK1/B) was detected with the antibodies indicated.
B. GST pull-down assay of GST-HP1β and H1.4-FLAG (H1.4). H1.4-FLAG was incubated with (+) or without (-) the histone methyltransferase, G9a, Aurora B kinase, and CDK1/cyclin B (CDK1/B). Modified H1.4-FLAG (0.75 µg) was then incubated with GST or GST-HP1β and bound protein was analysed by western blotting with the FLAG antibody. The interaction was specific as it did not occur when GST replaced GST-HP1β. Equal protein was present in each reaction as shown by the inputs (20%).

5.2.1.2 CDK phosphorylation of H1.4T18 disrupts the interaction with HP1β

To determine whether phosphorylation of the CDK site at H1.4T18 is responsible for abolishing the interaction with HP1β, CDK phosphorylation mutants of H1.4 were used in a GST pull-down assay (Section 2.3.12). The H1.4 A1.5 mutant, in which all CDK phosphorylation sites are substituted with alanine to prevent phosphorylation, was compared to the A2345 mutant, where only the T18 site is able to be phosphorylated. The interaction of HP1β with methylated A2345 was reduced approximately two-fold upon phosphorylation of T18 by CDK (Figure 5.2; Refer to Appendix Two for Quantitation). CDK phosphorylation of methylated H1.4 resulted in loss of the interaction with GST-HP1β, as shown previously (Figure 5.1B), while phosphorylation of methylated A1.5 did not disrupt this interaction. Thus CDK phosphorylation of T18 in the N-terminus of H1.4 can also contribute to the disruption of HP1β binding. Further mutagenesis of the C-terminal CDK phosphorylation sites in H1.4 would establish the contribution of each site in disrupting the interaction with HP1β.

5.2.2 The interaction between the Condensin I subunit, CAPD2, and H1.4

The Condensin I regulatory subunit CAPD2 interacts with the linker histone H1 (Ball *et al.*, 2002), but whether this interaction can be mediated by the H1.4 subtype is not known. CAPD2 was cloned and expressed to investigate if CAPD2 and H1.4 interact *in vitro*.

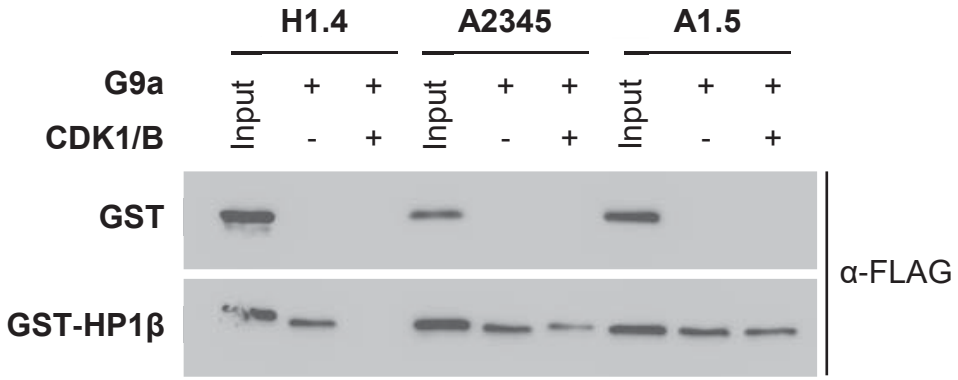

Figure 5.2. H1.4T18 phosphorylation contributes to the loss of HP1β binding.
GST pull-down assay of GST-HP1β with H1.4-FLAG (H1.4), A2345-FLAG (A2345), with only T18 able to be CDK phosphorylated, or the CDK phosphorylation mutant A1.5-FLAG (A1.5). The H1.4-FLAG proteins (0.75 µg) were incubated with (+) or without (-) the histone methyltransferase, G9a, and CDK1/cyclin B (CDK1/B). The modified proteins were incubated with GST or GST-HP1β and bound protein was analysed by western blotting with the FLAG antibody. The interaction was specific as it did not occur when GST replaced GST-HP1β. Equal protein was present in each reaction represented by the inputs (20%).

5.2.2.1 H1.4 interacts with the C-terminal domain of CAPD2

Firstly the 4.2 kb CAPD2 cDNA from HeLa cells was amplified using the polymerase chain reaction (PCR; Section 2.2.5). This was then cloned into the pGEX-2TK bacterial expression vector such that CAPD2 was produced with a GST-tag at the N-terminus (GST-CAPD2; Section 2.2.7). GST-CAPD2 is 183 kDa, and as proteins of this size may not fold correctly upon bacterial expression, the region of this protein known to interact with histone H1, the C-terminal domain (CTD; Ball *et al.*, 2002), was also cloned (GST-CTD). Once DNA sequencing confirmed their correct identity (Section 2.2.10), expression of GST-CAPD2 and GST-CTD was induced and bacterial lysates were tested for the presence of CAPD2 using SDS-PAGE (Sections 2.2.2 and 2.3.5). GST-CTD (38 kDa) was observed after induction (Figure 5.3A, arrow), whereas GST-CAPD2 (183 kDa) was not expressed, and its expression was not pursued further. To determine if the GST-CTD expressed was soluble, the soluble and insoluble fractions were analysed using SDS-PAGE (Section 2.3.2). As the majority of the GST-CTD produced was soluble (Figure 5.3B, arrow), GST and GST-CTD were batch purified and amounts were normalised for use in the GST pull-down assay (Section 2.3.8). As seen in Figure 5.3C, increasing amounts of GST-CTD were batch purified from increasing amounts of supernatant, with the amounts of GST and GST-CTD shown on the right chosen for use in each GST pull-down.

A GST pull-down was then performed to determine if CAPD2 can interact with the H1.4 subtype. GST-CTD bound to Glutathione Sepharose 4B was incubated with H1.4-FLAG, and the bound protein was analysed by western blotting with the FLAG antibody (Section 2.3.12). When GST-CTD was pulled-down, H1.4-FLAG was copurified, indicating that H1.4 can interact with the CTD of CAPD2 (Figure 5.4).

Figure 5.3

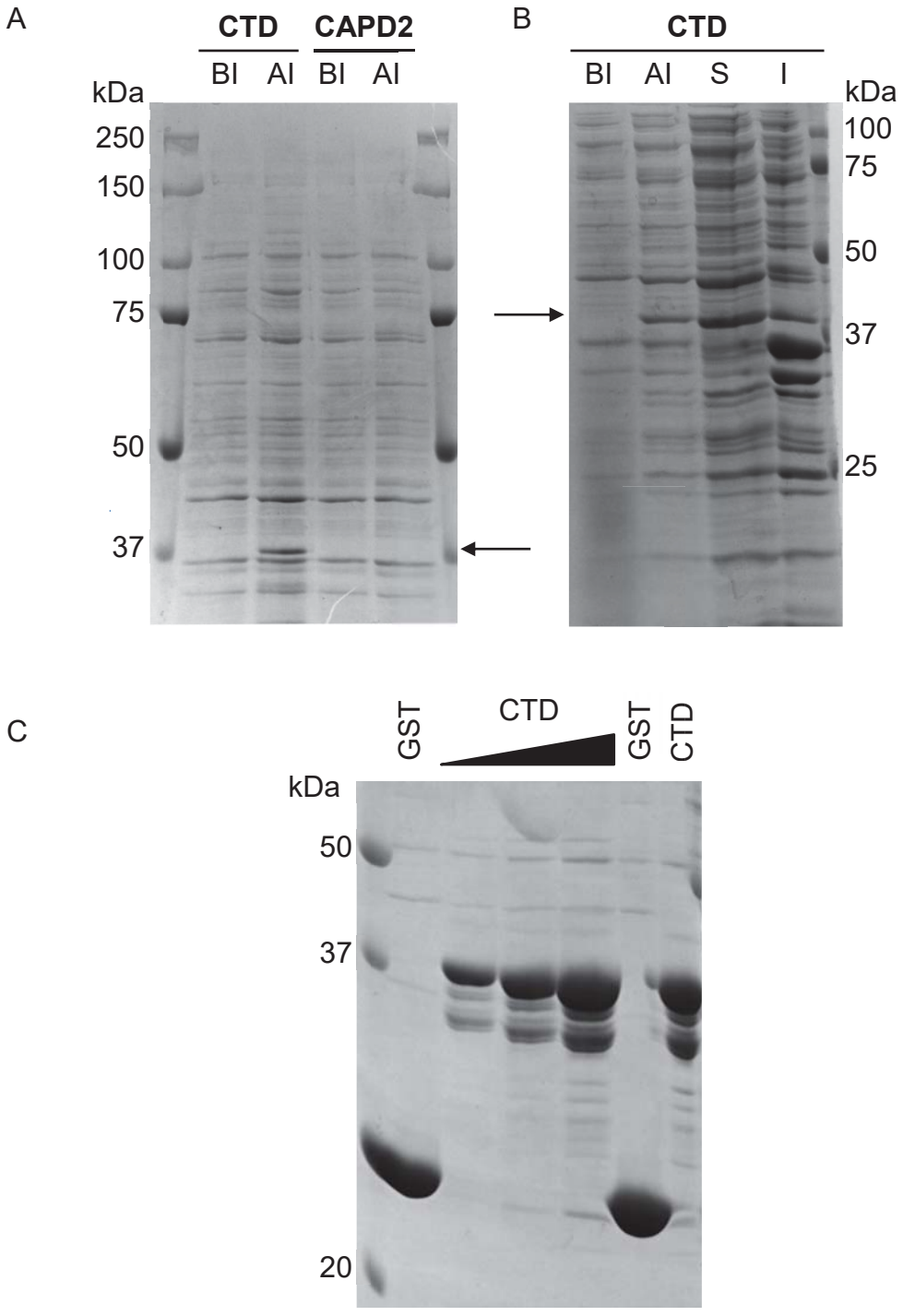
A
CTD
CAPD2
Bl
Al
Bl
Al
kDa
250
150
100
75
50
37
B
CTD
Bl
Al
S
I
kDa
100
75
50
37
25
C
GST
CTD
GST
CTD
kDa
50
37
20

Figure 5.3. Expression and purification of GST-CAPD2 and GST-CTD.
A. Coomassie Blue stained SDS-PAGE gel of lysates from transformed *E. coli* induced to express GST-CAPD2 (CAPD2) or GST-CTD (CTD; which included the 113 amino acids at the C-terminus of CAPD2). Samples (50 µL) from before induction (BI) and after induction (AI) are shown. The outer lanes show protein standards with molecular weights indicated in kDa. The arrow indicates GST-CTD (38 kDa).
B. Coomassie Blue stained SDS-PAGE gel of lysates from transformed *E. coli* cells that express GST-CTD (CTD). Samples (50 µL) from before induction (BI) and after induction (AI) are shown. Following lysis, soluble (S) and insoluble (I) fractions (5 µL) were separated by centrifugation. The right lane contains protein standards with molecular weights shown in kDa. The arrow indicates GST-CTD (38 kDa).
C. Coomassie Blue stained SDS-PAGE gel of GST (26 kDa) or GST-CTD (CTD; 38 kDa) purified with Glutathione Sepharose 4B. Increasing amounts of GST-CTD (50 µL, 100 µL, 200 µL) were compared to GST (5 µL); and the GST (7 µL) and GST-CTD (80 µL) on the right were used in pull-down assays. The left lane contains protein standards with molecular weights shown in kDa.

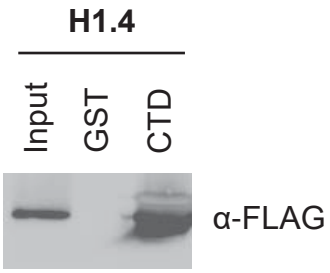

Figure 5.4. H1.4 interacts with CAPD2.
GST pull-down assay of H1.4-FLAG (H1.4; 0.5 µg) with GST-CTD (CTD) at a sodium chloride concentration of 150 mM. The bound fraction was subject to western blotting and bound H1.4-FLAG was detected with the FLAG antibody. The interaction was specific, as it did not occur when GST replaced GST-CTD. The protein in the reaction was represented in the input (18%).

5.2.2.2 The C-terminal tail in H1.4 mediates the interaction with CAPD2

To identify the domain of H1.4 that interacts with the CTD of CAPD2, GST-CTD was incubated with the N-terminus, central globular domain, or the C-terminus of H1.4 or combinations of these domains in GST pull-down assays, then the bound protein was analysed by western blotting with an antibody against FLAG (Section 2.3.12). When the C-terminus of H1.4 was present in the reaction, it bound to GST-CTD (Figure 5.5). This region together with the globular domain of H1.4 was also copurified with GST-CTD, whereas no interaction was detected when the globular domain or the N-terminus was present. Full-length H1.4-FLAG interacted with the CTD of CAPD2, consistent with the previous pull-down (Figure 5.4). Thus, the determinants required for the interaction between CAPD2 and H1.4 can be found in the C-terminus of both proteins.

5.2.2.3 H1.4 is not the only linker histone subtype that can interact with CAPD2

As the C-terminal tail of H1.4 interacts with CAPD2, this part of H1.4 was replaced with the C-terminus of H1.2 (H1.4/H1.2-FLAG; kindly provided by Nicole Happel, University of Göttinggen) to determine if H1.2 could also mediate this interaction. Alongside H1.4, H1.2 is a ubiquitous linker histone subtype present in somatic cells; however H1.2 is more prevalent in euchromatin and is among the more mobile H1 subtypes (Clausell *et al.*, 2009; Happel & Doenecke, 2009; Th'ng *et al.*, 2005). GST pull-downs with H1.4-FLAG and H1.4/H1.2-FLAG were performed followed by western blotting for FLAG (Section 2.3.12). In both cases the FLAG-tagged proteins were present in the bound fraction, indicating that the interaction between linker histones and CAPD2 is not limited to the H1.4 subtype (Figure 5.6). Thus the other prominent subtype of H1, H1.2 can also mediate the interaction with CAPD2 via its C-terminal tail, which shares high amino acid sequence identity with the C-terminus of H1.4 (Figure 5.6).

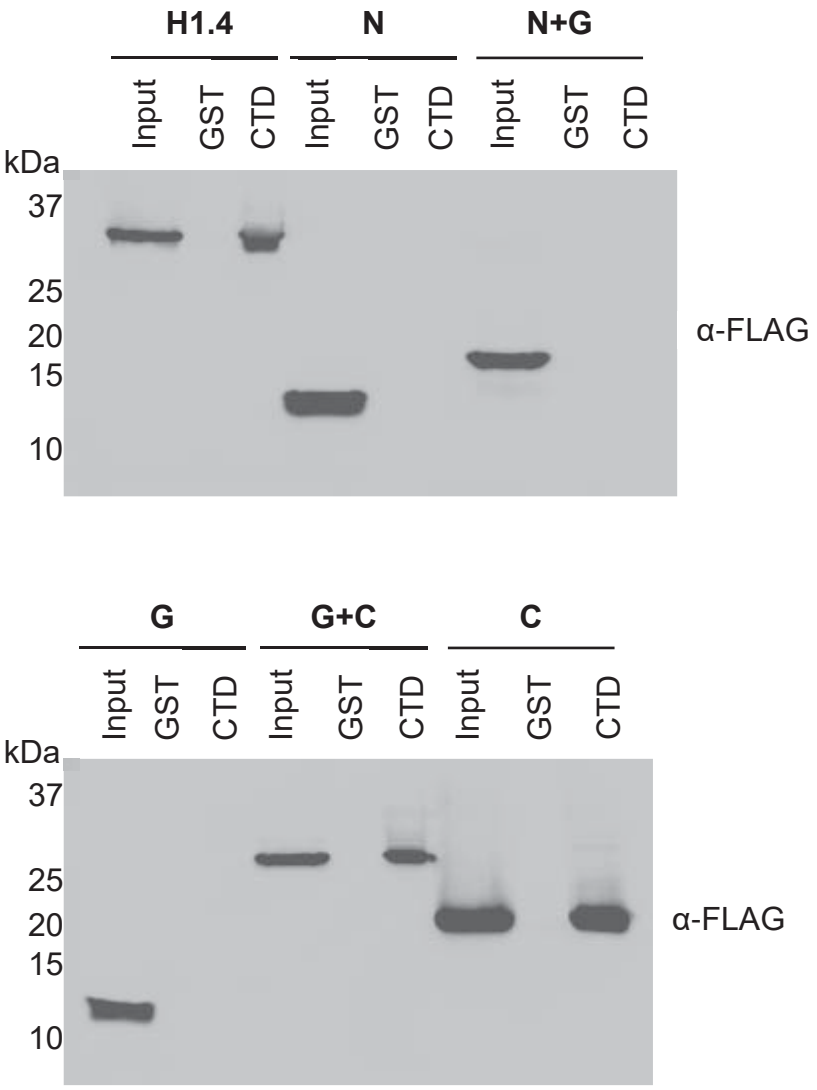

Figure 5.5. The C-terminus of H1.4 interacts with CAPD2.
GST pull-down assay of 0.5 µg of H1.4-FLAG (H1.4), or individual or adjoining domains thereof, with GST-CTD (CTD). FLAG-tagged domains of H1.4 included the N-terminal tail (N), the N-terminal tail with the globular domain (N+G), the globular domain (G), the globular domain with the C-terminal tail (G+C), and the C-terminal tail (C). Bound protein was analysed by western blotting for FLAG. The interaction was specific, as it did not occur when GST replaced GST-CTD. Inputs (50%) show similar amounts of protein were present in the reactions. The molecular weights indicated on the left in kDa were established using a protein standard.

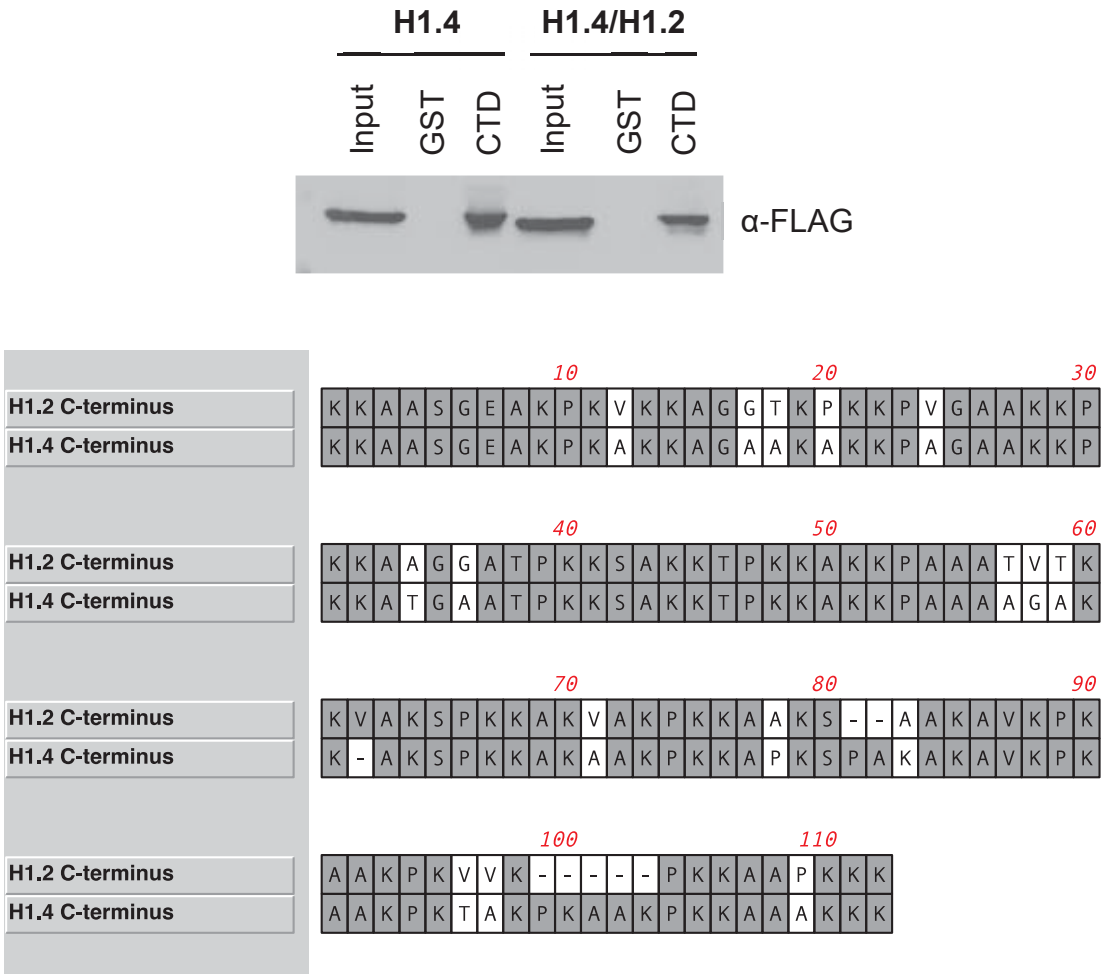

Figure 5.6. The C-terminus of H1.2 interacts with CAPD2.
GST pull-down assay of 0.5 µg of H1.4-FLAG (H1.4) and H1.4/H1.2-FLAG (H1.4/H1.2), where the C-terminus of H1.4 was replaced with the C-terminus of H1.2, with GST-CTD (CTD). Bound protein was analysed by western blotting with an antibody against FLAG. The interaction was specific, as it did not occur when GST replaced GST-CTD. Equal protein was included in each reaction as shown by the inputs (50%). An alignment of the amino acid sequence of the C-terminus of H1.2 and H1.4 is included.

5.2.2.4 H1.4 and CAPD2 interact when phosphorylated by CDK

To establish if CAPD2 can interact with hyperphosphorylated H1.4, the CDK phosphorylation mimic E1.5-FLAG, where the five CDK phosphorylation sites in H1.4 were mutated to glutamic acid, was tested for its ability to bind the CTD of CAPD2 in a GST pull-down over a range of sodium chloride concentrations (Section 2.3.12). While there appeared to be no difference in the amount of H1.4 and E1.5 interacting with the CTD of CAPD2 at 150 mM, as the sodium chloride concentration increased to 300 mM there was a decrease in the amount of interacting E1.5, relative to H1.4 (Figure 5.7). As the E1.5 phosphorylation mimic was able to interact with the CTD of CAPD2 under stringent conditions then this indicates that mitotic hyperphosphorylation of H1.4 is not likely to prevent the interaction between H1.4 and CAPD2.

To determine if this interaction occurs with hyperphosphorylation of H1.4, H1.4-FLAG was incubated with or without CDK1/cyclin B in the kinase assay established in Figure 5.1A, then a GST pull-down was performed with GST-CTD and bound protein was analysed using western blotting (Sections 2.3.10 and 2.3.12). A similar reduction in the interaction between the CTD of CAPD2 and H1.4-FLAG occurred when H1.4 was phosphorylated on its CDK sites when 300 mM of sodium chloride was present in the binding buffer (Figure 5.8A), when compared to the E1.5 phosphorylation mimic (Figure 5.7). Next, both H1.4 and the CTD of CAPD2 were phosphorylated by CDK, and their binding was examined in a GST pull-down (Section 2.3.12). As shown in Figure 5.8B, after western blotting for FLAG, H1.4 and the CTD of CAPD2 were still able to interact when CDK phosphorylated individually, and when both proteins had been phosphorylated. These *in vitro* results suggest that H1.4 and CAPD2 can interact when phosphorylated during mitosis.

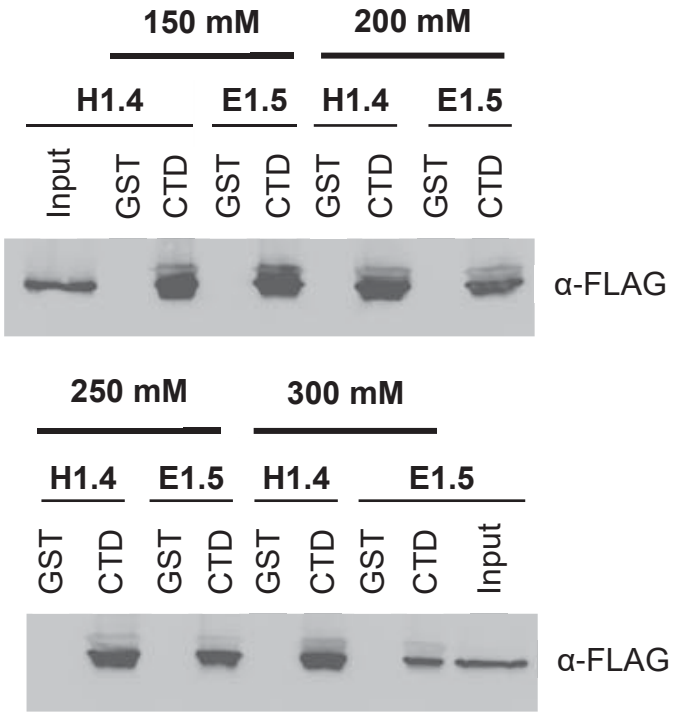

Figure 5.7. H1.4 and the CDK phosphorylation mimic E1.5 interact with CAPD2.

GST pull-down assay of 0.5 µg of H1.4-FLAG (H1.4) and E1.5-FLAG (E1.5) with GST-CTD (CTD). Sodium chloride in binding and washing steps was titrated from 150 mM to 300 mM as indicated. The bound fraction was subject to western blotting with an antibody against FLAG. The interaction was specific, as it did not occur when GST replaced GST-CTD. Equal amounts of H1.4-FLAG or E1.5-FLAG in the reactions were represented in the inputs (25%).

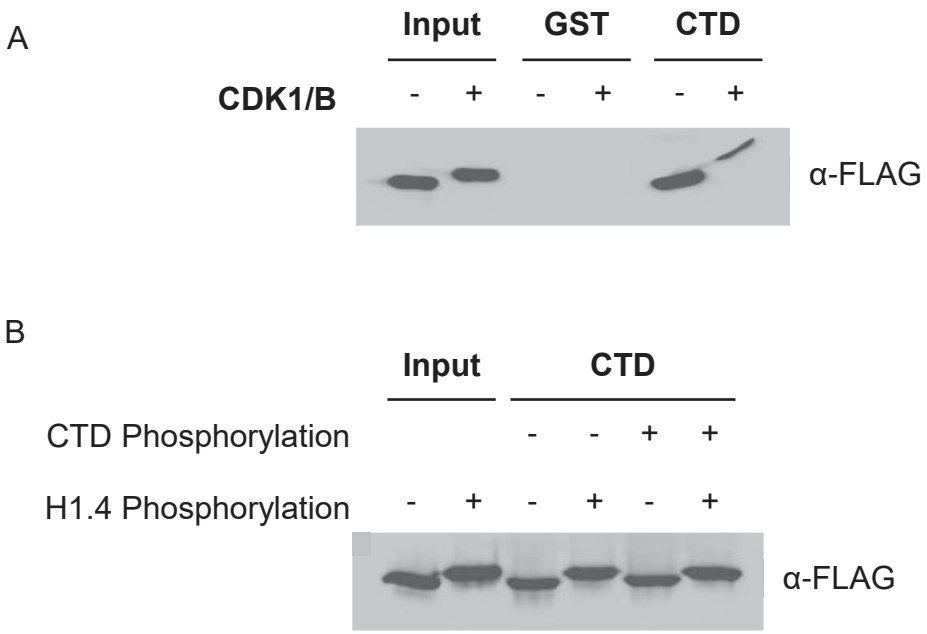

Figure 5.8. H1.4 and CAPD2 still interact when phosphorylated by CDK.
A. GST pull-down assay of H1.4-FLAG (0.5 µg) with GST-CTD (CTD) at 300 mM sodium chloride. H1.4-FLAG was incubated in a kinase assay with (+) or without (-) CDK1/cyclin B (CDK1/B). Modified H1.4-FLAG was then incubated with GST or GST-CTD and bound protein was subject to western blotting with an antibody against FLAG. The interaction was specific, as it did not occur when GST replaced GST-CTD. Inputs (50%) showed equal amounts of protein in each reaction.
B. GST pull-down assay of H1.4-FLAG (H1.4; 0.5 µg) with GST-CTD (CTD). H1.4-FLAG and GST-CTD were incubated in kinase assays with (+) or without (-) CDK1/cyclin B. The protein was then used in a GST pull-down assay as described for **A** but with 150 mM sodium chloride. Equal amounts of H1.4-FLAG in the reactions were represented in the input (50%).

5.2.2.5 RNA is required for the interaction between H1.4 and CAPD2

Unpublished results from this laboratory have shown that the C-terminus of H1.4 can mediate the interaction with other proteins through RNA. To establish if the interaction between the C-terminus of H1.4 and the CTD of CAPD2 requires RNA, which may have been copurified with GST-CTD, RNase A was added to the pull-down reaction and the bound protein was analysed by western blotting for FLAG (Section 2.3.12). As shown in Figure 5.9, the interaction between H1.4 and the CTD of CAPD2 was lost upon degradation of RNA. The interaction was only maintained when low concentrations of RNase A were used (0.01 μg/mL or less). Below this concentration some of the bacterial RNA copurified with the proteins may have remained intact, and was therefore able to mediate the interaction. This result suggests that H1.4 and CAPD2 require an RNA component to interact *in vitro*, although, further investigation will be required to establish if this interaction occurs through a specific RNA species *in vivo*.

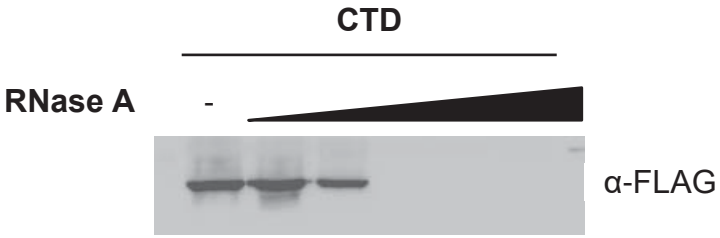

Figure 5.9. RNA is required to mediate the interaction between H1.4 and CAPD2.
GST pull-down assay of H1.4-FLAG (0.5 µg) and GST-CTD (CTD) at 150 mM sodium chloride with RNase A. RNase A was added to each reaction at the following concentrations from lane 1 through 6; 0, 0.001, 0.01, 0.1, 1 and 10 µg/mL. Bound H1.4-FLAG was analysed by western blotting for FLAG.

5.3 Discussion

The hyperphosphorylation of H1.4 by the Cyclin dependent kinases that occurs during mitosis abolished the interaction with HP1β, whereas the interaction with the Condensin I subunit CAPD2 was maintained. While phosphorylation of the CDK sites in the C-terminus of H1.4 did affect the ability of HP1β to interact with methylated H1.4K26, phosphorylation of H1.4T18 also contributed. H1.4T18 is in the immediate vicinity of the methylated 'ARKS' motif to which HP1β binds, and H1.4T18 has been shown to be spatially orientated form hydrogen bonds with HP1γ bound to methylated H1.4 (Ruan *et al.*, 2012). Thus phosphorylation of H1.4T18 may disrupt weak interactions important for facilitating the interaction between the HP1β chromo domain and H1.4 methylated at lysine 26. As the H1.4T18 phosphorylation site contributes to the displacement of HP1β as much as H1.4S27 phosphorylation does, then it will be interesting to establish if simultaneous phosphorylation of both sites together is sufficient to dislodge HP1β from methylated H1.4

CDK phosphorylation itself has been shown to induce conformational changes in H1 that may contribute to changes in the wider chromatin landscape (Lopez *et al.*, 2015; Roque *et al.*, 2008), although, the contribution of other protein factors acting together with H1 has not been well investigated. The report by Ball *et al.* (2002) linking the Condensin I regulatory subunit, CAPD2, and histone H1, provided an additional mechanism through which H1 could be implicated in chromosome condensation. While the localisation and histone interaction domains of CAPD2 were explored, the interaction with H1 was shown only via far-western blotting and in a GST pull-down assay with bovine H1 (Ball *et al.*, 2002). As shown here, the H1.4 subtype could interact with CAPD2, regardless of its CDK phosphorylation status, through its C-terminal tail. However, this interaction was also mediated by the equivalent region in H1.2, which has a lesser condensation capacity relative to H1.4 (Clausell *et al.*, 2009; Th'ng *et al.*, 2005). This indicates that these two ubiquitous subtypes of H1 can mediate the interaction with CAPD2 through their C-terminal tail. Although the C-terminal tail is the most divergent region within H1, the other subtypes are yet to be tested for their ability to interact with CAPD2.

Not only is H1.4 phosphorylated by CDK (Langan *et al.*, 1989; Swank *et al.*, 1997), but CAPD2 has also been reported to be a substrate for CDK (K. Kimura *et al.*, 1998). This phosphorylation has been reported to activate the supercoiling activity in *Xenopus laevis* 13S condensin, leading to chromosome condensation (K. Kimura *et al.*, 1998). Both H1.4 and CAPD2 can interact regardless of their phosphorylation status, suggesting that phosphorylation does not regulate this interaction. Regulation of the interaction by phosphorylation may not be necessary given that the Condensin I complex is excluded from the nucleus until the nuclear envelope disassembles (Hirota *et al.*, 2004). The observation that H1 and CAPD2 can interact when Condensin I is in its active state, suggests that H1 could aid in the targeting and maintenance of Condensin I to the chromatin to perform its condensation function indicating that phosphorylated H1 plays a role in chromosome condensation.

Most intriguing is the potential requirement for RNA to mediate the interaction between CAPD2 and H1.4, as shown here. The interaction through the C-terminal tail of H1.4 and the dependence on RNA bears similarity to the interaction between H1.4 and the hinge domain of HP1α (T.K. Hale, personnal communication; Hale *et al.*, 2006). In addition, as for the hinge in HP1α, there are three adjacent lysine residues in the region of CAPD2 that mediates the interaction with H1 (Ball *et al.*, 2002); these lysines may facilitate an interaction through RNA. Although mutation of these residues in CAPD2 was not attempted here, the dependence on RNA shown here, together with the failure of the lysine to alanine mutant tested by Ball *et al.* (2002) to localise to the nucleus suggests that these residues may mediate their nuclear localisation effect through an interaction between RNA and H1.4, or even H3. Establishing if CAPD2 and H1.4 do in fact interact in an RNA-dependent manner *in vivo*, and whether this is important for the correct localisation of the Condensin I complex requires further investigation. While attempts were made to study the *in vivo* interaction between CAPD2 and H1.4 using fluorescently tagged proteins, this was hindered by the inability to obtain cotransfected cells that were in mitosis. Future exploration could establish if this RNA mediated interaction occurs *in vivo* and if there is specificity in the type of RNA required to facilitate the interaction between CAPD2 and H1.4.

Together, this *in vitro* data indicates that further exploration is required to elucidate whether these mechanisms occur in the context of chromatin in the nucleus during mitosis.

Chapter Six

Discussion

Among linker histones the H1.4 subtype has a unique 'ARKS' motif that is methylated and phosphorylated during mitosis (Garcia *et al.*, 2004). Phosphorylation within this motif in the N-terminus of H1.4 at serine 27 (H1.4S27) is mediated by Aurora B kinase (Section 3.2.2), a master regulator of mitosis (Carmena *et al.*, 2009). That Aurora B kinase phosphorylates H1.4S27 in HeLa cells corroborates the finding of Hergeth *et al.* (2011) in MCF7 cells. Phosphorylation occurs on H1.4S27 from prophase until early anaphase, and while it is present along the arms of metaphase chromosomes, it is enriched at the centromere (Section 3.2.1). Disruption of this phosphorylation resulted in defective mitosis indicating the fundamental role H1.4S27 phosphorylation plays during this key stage in the cell cycle (Section 4.2.2.2).

When phosphorylation of H1.4 at serine 27 was prevented by substitution with alanine (H1.4S27A), chromosomes failed to align on the equatorial plate in metaphase (Section 4.2.2.2). Misalignment of chromosomes during metaphase could arise by improper attachment between the kinetochore, assembled at the centromere, and the spindle microtubules (Guo *et al.*, 2013). This attachment ultimately results in the segregation of the duplicated sister chromatids to the daughter cells (Kops *et al.*, 2005). The bipolar attachment of each sister chromatid to opposing spindle poles is regulated by Aurora B kinase in several model organisms, and when Aurora B was inhibited chromosome congression during metaphase failed (Adams *et al.*, 2001; Kallio *et al.*, 2002). Prevention of H1.4S27 phosphorylation by Aurora B kinase also resulted in an increased incidence of multipolar spindles during mitosis (Section 4.2.2.2). Aurora B activity is necessary for completion of cytokinesis, and its failure can lead to excessive centrosome duplication and multipolar spindles (Kops *et al.*, 2005; Maiato & Logarinho, 2014). Additionally, H1 subtypes are closely associated with inner kinetochore proteins, including the motor protein CENP-C (Centromere protein C; Orthaus *et al.*, 2009). As similar phenotypes occur when Aurora B is inhibited, and when its phosphorylation of H1.4S27 is prevented, then this phosphorylation that is enriched at the centromere may contribute to the regulation of attachments between the kinetochore and the spindle apparatus. Real time imaging of cells expressing the non-phosphorylatable H1.4S27 mutant could be performed to establish whether the chromosome congression during metaphase was able to be resolved, and if this resulted in an extended mitotic duration.

When the H1.4 mutant that is constitutively phosphorylated at serine 27 during the cell cycle (H1.4S27E) was present, bridging and lagging chromosomes were observed (Section 4.2.2.2). This phenotype is also characteristic of improper attachment between the chromosome kinetochore and the spindle microtubules that is regulated by Aurora B kinase (Adams *et al.*, 2001). Overexpression of Aurora B kinase can cause lagging chromosomes and lead to aneuploidy in mammalian cells (Ota *et al.*, 2002). Thus the persistence of H1.4S27 phosphorylation beyond anaphase, when this phosphorylation is removed, may cause merotelic attachments, where the chromatid is attached to both spindle poles and lags (Kops *et al.*, 2005). This could be further exasperated by sustained levels of H1.4S27 phosphorylation that are high, particularly with the 3% relative abundance of H1.4S27 phosphorylation reported using mass spectrometry (Hergeth *et al.*, 2011). Lagging chromosomes not enclosed in the nucleus when it reforms are incorporated into a micronucleus (Fenech *et al.*, 2011; Kirsch-Volders *et al.*, 2011), and micronuclei were frequently observed in cells expressing H1.4 constitutively phosphorylated on serine 27. These micronuclei can be lost in subsequent rounds of cell division leading to monosomy of the remaining chromosome (Kirsch-Volders *et al.*, 2011). Together, these similar phenotypes support a role for Aurora B kinase phosphorylation of H1.4S27 contributing to the attachment of sister chromatids to the spindle microtubules. Karyotyping of cells in the presence or absence of the H1.4S27 phosphorylation mimic could reveal whether the increased proportion of lagging chromosomes and micronuclei cause aneuploidy.

Both the N-terminal tails of the core histone H3, and H1.4 have 'ARKS' motifs that are regulated by common enzymes (Fischle *et al.*, 2003; Garcia *et al.*, 2004; Hergeth *et al.*, 2011; Hsu *et al.*, 2000; Tachibana *et al.*, 2001; Trojer *et al.*, 2009). Not only does Aurora B kinase phosphorylate both H1.4S27 and H3S10 (Section 3.2.2; Crosio *et al.*, 2002; Hergeth *et al.*, 2011; Hsu *et al.*, 2000), but both H3K9 and H1.4K26 are methylated by G9a and SUV39H1 (Rea *et al.*, 2000; Tachibana *et al.*, 2001; Tachibana *et al.*, 2002; Trojer *et al.*, 2009; Weiss *et al.*, 2010). Methylation of the lysine within the 'ARKS' motif in H3 and H1.4 is a post-translational modification that is characteristic of heterochromatin

and transcriptional repression (Daujat *et al.*, 2005; Kuzmichev *et al.*, 2004). This is due to methylated H3K9 and H1.4K26 providing a binding platform for the chromo domain of the Heterochromatin protein 1 (HP1) family members (Bannister *et al.*, 2001; Daujat *et al.*, 2005; Lachner *et al.*, 2001).

While H3 and H1.4 are methylated within the 'ARKS' motif throughout the cell cycle (Section 3.2.1; Bannister *et al.*, 2002; Fischle *et al.*, 2005; Terme *et al.*, 2014), the phosphorylation of the adjacent serine occurs predominantly during mitosis (Section 3.2.1; Fischle *et al.*, 2005; Hergeth *et al.*, 2011; Hirota *et al.*, 2005; Hsu *et al.*, 2000). As for the common phosphorylation of H1.4S27 and H3S10 by Aurora B kinase (Section 3.2.2; Crosio *et al.*, 2002; Hergeth *et al.*, 2011; Hsu *et al.*, 2000), similar phenotypes occur when this phosphorylation is aberrant (Section 4.2.2.2; Ota *et al.*, 2002). In *Schizosaccharomyces pombe* and *Tetrahymena thermophila* possessing a single H3 gene with serine 10 substituted with alanine to prevent H3S10 phosphorylation, segregation defects occurred, which lead to chromosome loss (Mellone *et al.*, 2003; Wei *et al.*, 1999). Lagging and bridging chromosomes were present in mitotic Chinese hamster embryo cells expressing the H3S10E phosphorylation mimic (Ota *et al.*, 2002). The misalignment of chromosomes in the presence of H1.4S27A and lagging chromosomes in the presence of H1.4S27E correlate with this, and this phenotype is also seen when Aurora B kinase is impaired or over-expressed (Section 4.2.2.2; Adams *et al.*, 2001; Kallio *et al.*, 2002; Ota *et al.*, 2002). The occurrence of these parallel phenotypes indicate that phosphorylation of the 'ARKS' motifs in H1.4 and H3 by Aurora B could be regulated in concert, thus this motif in H1.4 should also be considered in studies that explore the site in H3, while omitting that in H1.4. A limitation of this study was the presence of endogenous H1.4 that was able to be phosphorylated, in addition to the exogenous phosphorylation mutants. Using recent advances in genome editing technology, including CRISPR/Cas, could allow replacement of serine 27 within endogenous H1.4 with alanine or glutamic acid (Cong *et al.*, 2013). This is feasible given that H1.4 is the only H1 subtype to possess the 'ARKS' motif.

The HP1 family members dissociate from the condensed chromosomes during mitosis (Hayakawa *et al.*, 2003; Minc *et al.*, 1999; Murzina *et al.*, 1999), and this has been attributed to the activity of Aurora B kinase (Fischle *et al.*, 2005; Hirota *et al.*, 2005; Terada, 2006). Phosphorylation of H3S10 within the 'ARKS' motif in H3 by Aurora B kinase is proposed to displace HP1 from H3 methylated at lysine 9, transiently, from prophase to anaphase (Fischle *et al.*, 2005; Hirota *et al.*, 2005). As for H3K9S10, the dissociation of HP1 from H1.4 methylated at K26 upon S27 phosphorylation has been reported by Daujat *et al.* (2005). Unlike for Daujat *et al.* (2005) where a 13 amino acid peptide was used, when full length H1.4 was employed here the dissociation of HP1 upon S27 phosphorylation of methylated H1.4 was incomplete (Section 3.2.3.3). This suggests that Aurora B phosphorylation of H1.4 may be insufficient to displace HP1β from H1.4 methylated at lysine 26. Additional mechanisms may be required for the mitotic displacement of HP1 *in vivo*, including the Cyclin dependent kinase (CDK) phosphorylation of H1.4 (Section 5.2.1). Similar partial displacement of HP1 from methylated H3 upon S10 phosphorylation has been reported when peptides were enzymatically phosphorylated by Aurora B kinase (Fass *et al.*, 2002; Terada, 2006). Exploration of cell lines with phosphorylation mutants of both H1.4S27 and H3S10 could reveal if their phosphorylation is the sole mechanism to displace HP1 paralogs from the chromosomes during mitosis.

While each of the HP1 family members are displaced from the chromosomes during mitosis, there are differences between the paralogs across the length of the chromosome (Hayakawa *et al.*, 2003; Minc *et al.*, 1999). HP1β and HP1γ are displaced entirely from the chromosomes, whereas a small population of HP1α is retained at the centromere (Hayakawa *et al.*, 2003; Minc *et al.*, 1999). The displacement of HP1α along the arms of the mitotic chromosomes is proposed to occur through Aurora B phosphorylation of H3S10, and potentially H1.4S27, and involves the conserved chromo domain (Daujat *et al.*, 2005; Fischle *et al.*, 2005; Hirota *et al.*, 2005). A different mechanism is responsible for the HP1α retained at the centromere, which occurs through the chromo shadow domain that binds to proteins containing a PxVxL motif (L. Chu *et al.*, 2014; Hayakawa *et al.*, 2003; Smothers & Henikoff, 2000). HP1α present at the centromere may be important for the maintenance of cohesion at the centromere, as

is the case in fission yeast (Bernard *et al.*, 2001; Nonaka *et al.*, 2002), although results in humans have proved contradictory thus far (Inoue *et al.*, 2008; Kang *et al.*, 2011; Koch *et al.*, 2008; Yamagishi *et al.*, 2008). Determining how HP1β and HP1γ are displaced at the centromere, whilst HP1α persists is yet to be established as each paralog can interact with proteins via the conserved chromo shadow domain (Smothers & Henikoff, 2000). Thus there may be paralog specificity where the Aurora B phosphorylation of methylated H1.4 displaces HP1α along the chromosome arms only, while displacing HP1β and HP1γ from the arms and the centromere, where this phosphorylation is enriched (Section 3.2.1.1).

Aurora B and CDK phosphorylation of H1.4 occur concurrently during mitosis, and at this time H1.4 is phosphorylated at each of the five CDK motifs. Here, the *in vitro* CDK phosphorylation of H1.4 methylated at K26 was able to displace HP1β more efficiently than Aurora B phosphorylation of H1.4S27 (Section 5.2.1). Phosphorylation of the single N-terminal CDK phosphorylation site at H1.4T18 contributed to dislodging HP1β from H1.4 methylated at lysine 26, although not to the extent of phosphorylation of all CDK sites. As the combination of H1.4T18 and H1.4S27 phosphorylation together was not examined here, then this will need to be carried out to establish if HP1β can interact with H1.4 when both of these N-terminal sites are phosphorylated. While the phosphorylation of the C-terminus of H1.4 contributed to HP1 dislodgement *in vitro*, in the context of chromatin this H1.4 domain may not be free to influence HP1 binding. From the crystal structure of the interaction between HP1γ and an H1.4 peptide methylated at K26, both H1.4T18 and H1.4S27 were able to form hydrogen bonds with amino acid residues in the chromo domain of HP1γ (Ruan *et al.*, 2012). The residues in HP1γ that form these hydrogen bonds and salt bridges are conserved in HP1α and HP1β, as is the hydrophobic pocket for methylated H1.4K26 (P. Nielsen *et al.*, 2002; Ruan *et al.*, 2012). This suggests that the combination of CDK and Aurora B phosphorylation of H1.4 act together to displace bound HP1. This interaction may be further regulated by post-translational modification of HP1β, as the HP1 family members are also phosphorylated in a cell cycle dependent manner (Minc *et al.*, 1999).

Establishing whether H1.4S27 phosphorylation could displace HP1 *in vivo* was inconclusive (Section 4.2.4), however, from GST pull-down experiments it is clear that the CDK phosphorylation of H1.4 also plays a role in displacing HP1β (Section 5.2.1). As the dissociation of HP1α from the mitotic chromosomes was not detectable in cell fractionation experiments with exogenous wild-type H1.4 (Section 4.2.4.1), then this suggests that further optimisation of this technique, together with immunoprecipitation, is required to capture the timeframe where the HP1 family members are displaced. Difficulty was encountered as the mutation of H1.4S27 to alanine or glutamic acid also disrupted the consensus for the methyltransferase G9a, resulting in reduced H1.4K26 methylation on the H1.4S27 phosphorylation mutants (Sections 4.2.2.4, 4.2.3.1, 4.2.4.3 and 4.2.4.4). This together with the CDK phosphorylation of T18 on the exogenous H1.4S27 phosphorylation mutants could explain the difficulty in detecting changes in HP1 localisation through the cell cycle. However, as methylation of H1.4K26 was reduced on the H1.4S27 phosphorylation mutants, and this would reduce bound HP1, then this could explain the defects that occurred during mitosis. Thus examining HP1 localisation in the presence of the H1.4S27 phosphorylation mutants warrants further exploration, and cell lines that are mutant for both Aurora B and CDK phosphorylation of H1.4 could be used to investigate their interplay with regards to regulating the interaction with HP1 family members.

The significance of the transient release of HP1 family members from the chromosome arms during mitosis is not known. One possibility is that HP1 release is necessary to facilitate access of factors involved in chromosome condensation (Fischle *et al.*, 2005; Hirota *et al.*, 2005). The release of HP1 through the transient phosphorylation of H1.4S27 would enable reestablishment of HP1 at the preserved methylation on H1.4K26, ensuring that heterochromatin is restored at the appropriate locations following cell division (Daujat *et al.*, 2005; Dormann *et al.*, 2006; Fischle *et al.*, 2003). The timing of HP1 dispersal into the cytoplasm is coincident with CDK phosphorylation of H1 (Gurley *et al.*, 1974; Hayakawa *et al.*, 2003), and both of these may facilitate access of condensation factors to the chromatin for mitotic chromosome condensation.

Structural changes occur within the C-terminal tail of H1 upon its CDK phosphorylation (Roque *et al.*, 2008), and whether this alters the interaction with other proteins to bring about chromosome condensation needs to be identified. While the CDK phosphorylation of H1.4 abolished the interaction with HP1β (Section 5.2.1), it did not affect that with the Condensin I subunit, CAPD2. The C-terminal domain (CTD) of CAPD2 and H1.4 were able to interact while both were phosphorylated by CDK, as they are during mitosis (Section 5.2.2.4). The C-terminus of both H1.2 and H1.4, the most ubiquitous and abundant H1 subtypes (Kratzmeier *et al.*, 1999; Meergans *et al.*, 1997), interacted with CAPD2 indicating that linker histones could target the Condensin I complex to the chromatin, alongside H3 (Ball *et al.*, 2002). As CAPD2 was able to interact with H1.4 equally well regardless of its phosphorylation status, then CDK phosphorylation of H1.4 does not regulate the interaction with CAPD2, however, regulation through H1.4 phosphorylation is unnecessary given that Condensin I is excluded from the nucleus until the nuclear envelope breaks down in prometaphase (Hirota *et al.*, 2004).

The interaction between H1.4 and the CTD of CAPD2 was facilitated by bacterial RNA that may have been co-purified with GST-CTD (Section 5.2.2.5). While attempts were made to transiently transfect mammalian cells with expression constructs for fluorescently tagged CAPD2 and H1.4, establishing whether these proteins interact within the cell during mitosis requires further optimisation. If this interaction can be confirmed *in vivo* using Förster resonance energy transfer (FRET), then the requirement for an RNA element can be further explored. Electromobility shift assays could confirm whether there is specificity for the type, or sequence of the RNA, in addition to whether the interaction between H1.4 and CAPD2 could also be mediated by double or single stranded DNA. RNA pull-down assays could then be used to determine the identity of the mediating eukaryotic RNA species. A number of non-coding RNAs that are associated with mouse mitotic chromosomes have been identified recently (Meng *et al.*, 2016) and it will be interesting to establish whether these function in chromosome condensation by guiding factors such as CAPD2 to the chromosomes.

In summary, the interactions of H1.4 both in interphase and during mitosis are proposed in the model in Figure 6.1. During interphase HP1 is able to interact with methylated K26 in the N-terminus of H1.4. At this time Aurora B kinase is minimally active, and H1.4S27 is not modified (Section 3.2.1; Bischoff *et al.*, 1998; Hergeth *et al.*, 2011). CDK2/Cyclin A is able to phosphorylate H1.4 on serine 172 and 187 during interphase, while the remaining CDK consensus sequences are not phosphorylated at this time (Sarg *et al.*, 2006). Meanwhile, Condensin I and its subunit CAPD2 are present in the cytoplasm, excluded from the nucleus until the nuclear envelope breaks down (Hirota *et al.*, 2004; Ono *et al.*, 2004). Upon entry into mitosis H1.4 is hyperphosphorylated by CDK, which includes phosphorylation of the N-terminal CDK site at T18 (Garcia *et al.*, 2004; Talasz *et al.*, 1996). This, together with phosphorylation of H1.4S27 by Aurora B, inhibits the interaction of HP1β with the methyl group present on H1.4K26 (Sections 3.2.3.3 and 5.2.1; Daujat *et al.*, 2005; Hergeth *et al.*, 2011). In contrast, when CAPD2 gains entry to the nucleus in prometaphase it can interact with the C-terminus of H1.4 at a time when both are CDK phosphorylated, in a manner dependent on RNA (Section 5.2.2).

In conclusion, this study has highlighted the importance of H1.4 and its phosphorylation by Aurora B kinase during mitosis. When this phosphorylation on H1.4S27 was aberrant, defects occurred during mitosis, indicating that this phosphorylation regulates mitotic events. Further experimentation is required to determine how this comes about, although, defects may arise through the reduction in methylation of the adjacent lysine 26 that reduces the association with the HP1 family members throughout the cell cycle. These results indicate that the 'ARKS' motif in H1.4 in which these modifications occur warrants attention, together with the motif in the core histone H3. H1.4 that has been hyperphosphorylated by the Cyclin dependent kinases interacts with the Condensin I subunit CAPD2, and thus may be linked to the condensation of mitotic chromosomes through recruitment of the Condensin I complex. Overall, H1.4 is a ubiquitous and abundant linker histone subtype and its cell cycle dependent phosphorylation by Aurora B kinase and the Cyclin dependent kinases is fundamental for the proper execution of mitosis.

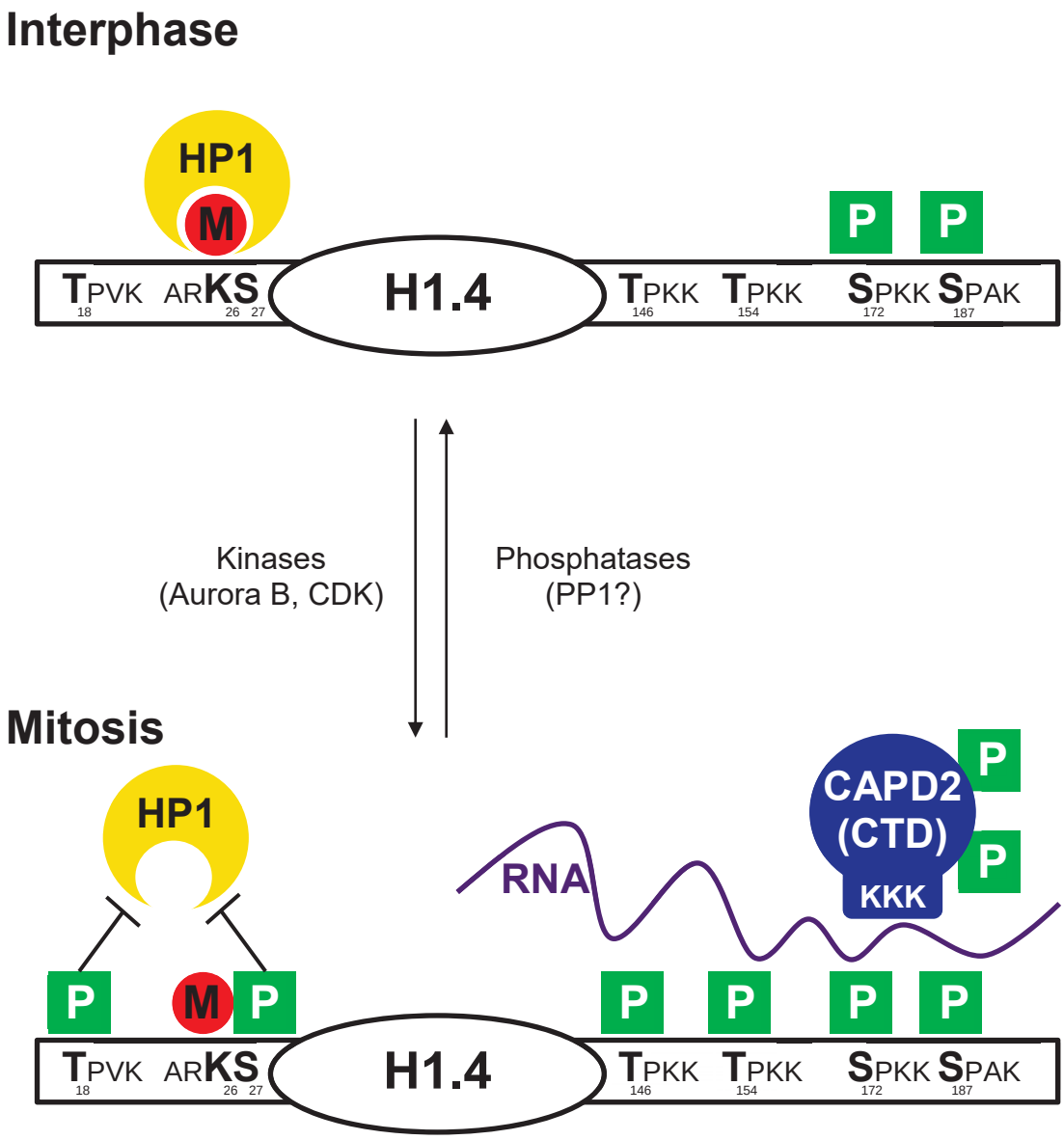

Figure 6.1. Model for the interactions of H1.4 during mitosis.
During interphase HP1 interacts with H1.4 that is methylated at K26 (M). H1.4 is free from phosphorylation in early interphase but can be phosphorylated on S172 and S187 during G_2 and S phase (Sarg *et al.*, 2006). At this time in the cell cycle the Condensin I subunit CAPD2 is excluded from the nucleus (!!! INVALID CITATION !!! (Ball et al., 2002; Hirota et al., 2004)), and cannot interact with H1.4. In contrast, during mitosis H1.4 becomes hyperphosphorylated, both on the CDK consensus phosphorylation sites ([S/T]-P-X-[K/R]), and on the Aurora B kinase phosphorylation site in the 'ARKS' motif, as denoted by P. Upon hyperphosphorylation of H1.4, the binding of HP1 to H1.4 methylated at K26 is inhibited by CDK phosphorylation of H1.4T18 and by Aurora B phosphorylation of H1.4S27. When the nuclear envelope breaks down in late prophase, the C-terminal domain (CTD) of CAPD2, which has been phosphorylated by CDK, interacts with the C-terminal tail of H1.4 in a manner reliant on RNA. It is yet to be established if these interactions occur *in vivo.*

6.1 Conclusions

The work presented here has illustrated that histone H1.4 is phosphorylated on serine 27 exclusively during mitosis, and that this phosphorylation is mediated by Aurora B kinase *in vivo*. The enrichment of H1.4 serine 27 phosphorylation on mitotic chromosomes in the vicinity of the centromere, together with the occurrence of segregation defects during mitosis, indicates that this post-translational modification may play a role in centromere function. Whether H1.4 serine 27 phosphorylation disrupts the interaction between chromatin and the HP1 family members requires further interrogation *in vivo*. *In vitro* experiments suggest that additional phosphorylation sites in H1.4, particularly threonine 18, also contribute to dislodging HP1 family members during mitosis.

An interaction between the linker histone subtype H1.4 and the Condensin I subunit, CAPD2, has been demonstrated. This *in vitro* interaction was unaffected by the phosphorylation status of either protein, suggesting this interaction occurs *in vivo* during mitosis when both proteins are hyperphosphorylated and present on the condensed chromosomes. Preliminary results indicate that the C-terminal tail of H1.4 and the C-terminal domain of CAPD2 require RNA to mediate this interaction and future exploration of this requirement *in vivo* will be of interest in establishing the role of RNA in the formation of high order chromatin structures.

References

Adams, R. R., Maiato, H., Earnshaw, W. C., & Carmena, M. (2001). Essential roles of *Drosophila* inner centromere protein (INCENP) and Aurora B in histone H3 phosphorylation, metaphase chromosome alignment, kinetochore disjunction, and chromosome segregation. *The Journal of Cell Biology, 153*(4), 865-880.

Ajiro, K., Nishimoto, T., & Takahashi, T. (1983). Histone H1 and H3 phosphorylation during premature chromosome condensation in a temperature-sensitive mutant (tsBN2) of baby hamster kidney cells. *Journal of Biological Chemistry, 258*(7), 4534-4538.

Albig, W., Drabent, B., Kunz, J., Kalff-Suske, M., Grzeschik, K.-H., & Doenecke, D. (1993). All known human H1 histone genes except the H1 0 gene are clustered on chromosome 6. *Genomics, 16*(3), 649-654.

Allan, J., Mitchell, T., Harborne, N., Bohm, L., & Crane-Robinson, C. (1986). Roles of H1 domains in determining higher order chromatin structure and H1 location. *Journal of Molecular Biology, 187*(4), 591-601.

Anthis, N. J., Haling, J. R., Oxley, C. L., Memo, M., Wegener, K. L., Lim, C. J., Ginsberg, M. H., & Campbell, I. D. (2009). β integrin tyrosine phosphorylation is a conserved mechanism for regulating talin-induced integrin activation. *Journal of Biological Chemistry, 284*(52), 36700-36710.

Arents, G., & Moudrianakis, E. N. (1995). The histone fold: A ubiquitous architectural motif utilized in DNA compaction and protein dimerization. *Proceedings of the National Academy of Sciences, 92*(24), 11170-11174.

Ausió, J. (2000). Are linker histones (histone H1) dispensable for survival? *BioEssays, 22*(10), 873-877.

Baatout, S., & Derradji, H. (2006). About histone H1 phosphorylation during mitosis. *Cell Biochemistry and Function, 24*(2), 93-94.

Bak, A. L., Bak, P., & Zeuthen, J. (1979). Higher levels of organization in chromosomes. *Journal of Theoretical Biology, 76*(2), 205-217.

Ball, A. R., Jr, Schmiesing, J. A., Zhou, C., Gregson, H. C., Okada, Y., Doi, T., & Yokomori, K. (2002). Identification of a chromosome-targeting domain in the human condensin subunit CNAP1/hCAP-D2/Eg7. *Molecular and Cellular Biology, 22*(16), 5769.

Bannister, A. J., & Kouzarides, T. (2011). Regulation of chromatin by histone modifications. *Cell Research, 21*(3), 381-395.

Bannister, A. J., Schneider, R., & Kouzarides, T. (2002). Histone methylation: Dynamic or static? *Cell, 109*(7), 801-806.

Bannister, A. J., Zegerman, P., Partridge, J. F., Miska, E. A., Thomas, J. O., Allshire, R. C., & Kouzarides, T. (2001). Selective recognition of methylated lysine 9 on histone H3 by the HP1 chromo domain. *Nature, 410*(6824), 120-124.

Barra, J. L., Rhounim, L., Rossignol, J.-L., & Faugeron, G. (2000). Histone H1 is dispensable for methylation-associated gene silencing in *Ascobolus immersus* and essential for long life span. *Molecular and Cellular Biology, 20*(1), 61-69.

Bates, D. L., & Thomas, J. O. (1981). Histories H1 and H5: One or two molecules per nucleosome? *Nucleic Acids Research, 9*(22), 5883-5894.

Bednar, J., Hamiche, A., & Dimitrov, S. (2016). H1–nucleosome interactions and their functional implications. *Biochimica et Biophysica Acta (BBA) - Gene Regulatory Mechanisms, 1859*(3), 436-443.

Bednar, J., Horowitz, R. A., Grigoryev, S. A., Carruthers, L. M., Hansen, J. C., Koster, A. J., & Woodcock, C. L. (1998). Nucleosomes, linker DNA, and linker histone form a unique structural motif that directs the higher-order folding and compaction of chromatin. *Proceedings of the National Academy of Sciences, 95*(24), 14173-14178.

Belmont, A. S. (2006). Mitotic chromosome structure and condensation. *Current Opinion in Cell Biology, 18*(6), 632-638.

Belmont, A. S., Sedat, J. W., & Agard, D. A. (1987). A three-dimensional approach to mitotic chromosome structure: Evidence for a complex hierarchical organization. *The Journal of Cell Biology, 105*(1), 77-92.

Bernard, P., Maure, J.-F., Partridge, J. F., Genier, S., Javerzat, J.-P., & Allshire, R. C. (2001). Requirement of heterochromatin for cohesion at centromeres. *Science, 294*(5551), 2539-2542.

Bhattacharjee, R. N., Banks, G. C., Trotter, K. W., Lee, H.-L., & Archer, T. K. (2001). Histone H1 phosphorylation by Cdk2 selectively modulates mouse mammary tumor virus transcription through chromatin remodeling. *Molecular and Cellular Biology, 21*(16), 5417-5425.

Bischoff, J. R., Anderson, L., Zhu, Y., Mossie, K., Ng, L., Souza, B., Schryver, B., Flanagan, P., Clairvoyant, F., & Ginther, C. (1998). A homologue of *Drosophila* Aurora kinase is oncogenic and amplified in human colorectal cancers. *The EMBO Journal, 17*(11), 3052-3065.

Bradbury, E. M., Inglis, R. J., Matthews, H. R., & Sarner, N. (1973). Phosphorylation of very-lysine-rich histone in *Physarum polycephalum*. *European Journal of Biochemistry, 33*(1), 131-139.

Brown, D. T., Alexander, B. T., & Sittman, D. B. (1996). Differential effect of H1 variant overexpression on cell cycle progression and gene expression. *Nucleic Acids Research, 24*(3), 486-493.

Burstein, D. E., Oami, S., Dembitzer, F., Chu, C., Cernaianu, G., Leytin, A., Misilim, E., Jammula, S. R., Strauchen, J., & Kohtz, D. S. (2002). Monoclonal antibody specific for histone H1 phosphorylated by cyclin-dependent kinases: A novel immunohistochemical probe of proliferation and neoplasia. *Modern Pathology, 15*(7), 705-711.

Carmena, M., Ruchaud, S., & Earnshaw, W. C. (2009). Making the Auroras glow: Regulation of Aurora A and B kinase function by interacting proteins. *Current Opinion in Cell Biology, 21*(6), 796-805.

Chadee, D. N., Taylor, W. R., Hurta, R. A. R., Allis, C. D., Wright, J. A., & Davie, J. R. (1995). Increased phosphorylation of histone H1 in Mouse fibroblasts transformed with oncogenes or constitutively active Mitogen-activated protein kinase kinase. *Journal of Biological Chemistry, 270*(34), 20098-20105.

Chen, D., Dundr, M., Wang, C., Leung, A., Lamond, A., Misteli, T., & Huang, S. (2005). Condensed mitotic chromatin is accessible to transcription factors and chromatin structural proteins. *The Journal of Cell Biology, 168*(1), 41-54.

Chu, C.-S., Hsu, P.-H., Lo, P.-W., Scheer, E., Tora, L., Tsai, H.-J., Tsai, M.-D., & Juan, L.-J. (2011). Protein kinase A-mediated serine 35 phosphorylation dissociates histone H1.4 from mitotic chromosome. *Journal of Biological Chemistry, 286*(41), 35843-35851.

Chu, L., Huo, Y., Liu, X., Yao, P., Thomas, K., Jiang, H., Zhu, T., Zhang, G., Chaudhry, M., & Adams, G. (2014). The spatiotemporal dynamics of chromatin protein HP1α is essential for accurate chromosome segregation during cell division. *Journal of Biological Chemistry, 289*(38), 26249-26262.

Clausell, J., Happel, N., Hale, T. K., Doenecke, D., & Beato, M. (2009). Histone H1 subtypes differentially modulate chromatin condensation without preventing ATP-dependent remodeling by SWI/SNF or NURF. *PLoS One, 4*(10), e0007243.

Cole, R. D. (1984). A minireview of microheterogeneity in H1 histone and its possible significance. *Analytical Biochemistry, 136*(1), 24-30.

Cong, L., Ran, F. A., Cox, D., Lin, S., Barretto, R., Habib, N., Hsu, P. D., Wu, X., Jiang, W., & Marraffini, L. A. (2013). Multiplex genome engineering using CRISPR/Cas systems. *Science, 339*(6121), 819-823.

Contreras, A., Hale, T. K., Stenoien, D. L., Rosen, J. M., Mancini, M. A., & Herrera, R. E. (2003). The dynamic mobility of histone H1 is regulated by cyclin/CDK phosphorylation. *Molecular and Cellular Biology, 23*(23), 8626.

Crosio, C., Fimia, G. M., Loury, R., Kimura, M., Okano, Y., Zhou, H., Sen, S., Allis, C. D., & Sassone-Corsi, P. (2002). Mitotic phosphorylation of histone H3: Spatio-temporal regulation by mammalian Aurora kinases. *Molecular and Cellular Biology, 22*(3), 874.

Dalton, S., & Wells, J. (1988). A gene-specific promoter element is required for optimal expression of the histone H1 gene in S-phase. *The EMBO Journal, 7*(1), 49.

Daujat, S., Zeissler, U., Waldmann, T., Happel, N., & Schneider, R. (2005). HP1 binds specifically to Lys26-methylated histone H1.4, whereas simultaneous Ser27 phosphorylation blocks HP1 binding. *Journal of Biological Chemistry, 280*(45), 38090.

Davis, B. J. (1964). Disc electrophoresis-II: Method and application to human serum proteins*. *Annals of the New York Academy of Sciences, 121*(2), 404-427.

De, S., Brown, D. T., Lu, Z. H., Leno, G. H., Wellman, S. E., & Sittman, D. B. (2002). Histone H1 variants differentially inhibit DNA replication through an affinity for chromatin mediated by their carboxyl-terminal domains. *Gene, 292*(1), 173-181.

Deng, H., Bao, X., Cai, W., Blacketer, M. J., Belmont, A. S., Girton, J., Johansen, J., & Johansen, K. M. (2008). Ectopic histone H3S10 phosphorylation causes chromatin structure remodeling in *Drosophila*. *Development, 135*(4), 699-705.

Dimitrov, S., Russanova, V., & Pashev, I. (1987). The globular domain of histone H5 is internally located in the 30 nm chromatin fiber: An immunochemical study. *The EMBO Journal, 6*(8), 2387.

Dormann, H. L., Tseng, B. S., Allis, C. D., Funabiki, H., & Fischle, W. (2006). Dynamic regulation of effector protein binding to histone modifications: The biology of HP1 switching. *Cell Cycle, 5*(24), 2842-2851.

Dou, Y., Mizzen, C. A., Abrams, M., Allis, C. D., & Gorovsky, M. A. (1999). Phosphorylation of linker histone H1 regulates gene expression *in vivo* by mimicking H1 removal. *Molecular Cell, 4*(4), 641-647.

Drobic, B., Pérez-Cadahía, B., Yu, J., Kung, S. K.-P., & Davie, J. R. (2010). Promoter chromatin remodeling of immediate-early genes is mediated through H3 phosphorylation at either serine 28 or 10 by the MSK1 multi-protein complex. *Nucleic Acids Research, 38*(10), 3196-3208.

Dubochet, J., Adrian, M., Chang, J.-J., Homo, J.-C., Lepault, J., McDowall, A. W., & Schultz, P. (1988). Cryo-electron microscopy of vitrified specimens. *Quarterly reviews of biophysics, 21*(02), 129-228.

Earnshaw, W. C., Halligan, B., Cooke, C. A., Heck, M., & Liu, L. F. (1985). Topoisomerase II is a structural component of mitotic chromosome scaffolds. *The Journal of Cell Biology, 100*(5), 1706-1715.

Earnshaw, W. C., & Laemmli, U. K. (1983). Architecture of metaphase chromosomes and chromosome scaffolds. *The Journal of Cell Biology, 96*(1), 84-93.

Eickbush, T. H., & Moudrianakis, E. N. (1978). The histone core complex: An octamer assembled by two sets of protein-protein interactions. *Biochemistry, 17*(23), 4955-4964.

Eltsov, M., MacLellan, K. M., Maeshima, K., Frangakis, A. S., & Dubochet, J. (2008). Analysis of cryo-electron microscopy images does not support the existence of 30-nm chromatin fibers in mitotic chromosomes in situ. *Proceedings of the National Academy of Sciences, 105*(50), 19732-19737.

Escher, D., & Schaffner, W. (1997). Gene activation at a distance and telomeric silencing are not affected by yeast histone H1. *Molecular and General Genetics, 256*(4), 456-461.

Evans, T., Rosenthal, E. T., Youngblom, J., Distel, D., & Hunt, T. (1983). Cyclin: A protein specified by maternal mRNA in sea urchin eggs that is destroyed at each cleavage division. *Cell, 33*(2), 389-396.

Fan, Y., Nikitina, T., Morin-Kensicki, E. M., Zhao, J., Magnuson, T. R., Woodcock, C. L., & Skoultchi, A. I. (2003). H1 linker histones are essential for mouse development and affect nucleosome spacing *in vivo*. *Molecular and Cellular Biology, 23*(13), 4559.

Fan, Y., Nikitina, T., Zhao, J., Fleury, T. J., Bhattacharyya, R., Bouhassira, E. E., Stein, A., Woodcock, C. L., & Skoultchi, A. I. (2005). Histone H1 depletion in mammals alters global chromatin structure but causes specific changes in gene regulation. *Cell, 123*(7), 1199-1212.

Fan, Y., Sirotkin, A., Russell, R. G., Ayala, J., & Skoultchi, A. I. (2001). Individual somatic H1 subtypes are dispensable for mouse development even in mice lacking the H10 replacement subtype. *Molecular and Cellular Biology, 21*(23), 7933.

Fass, E., Shahar, S., Zhao, J., Zemach, A., Avivi, Y., & Grafi, G. (2002). Phosphorylation of histone H3 at serine 10 cannot account directly for the detachment of human heterochromatin protein 1γ from mitotic chromosomes in plant cells. *Journal of Biological Chemistry, 277*(34), 30921-30927.

Felsenfeld, G., & Groudine, M. (2003). Controlling the double helix. *Nature, 421*(6921), 448-453.

Fenech, M., Kirsch-Volders, M., Natarajan, A., Surralles, J., Crott, J., Parry, J., Norppa, H., Eastmond, D., Tucker, J., & Thomas, P. (2011). Molecular mechanisms of micronucleus, nucleoplasmic bridge and nuclear bud formation in mammalian and human cells. *Mutagenesis, 26*(1), 125-132.

Finch, J. T., & Klug, A. (1976). Solenoidal model for superstructure in chromatin. *Proceedings of the National Academy of Sciences of the United States of America, 73*(6), 1897-1901.

Fischle, W., Tseng, B. S., Dormann, H. L., Ueberheide, B. M., Garcia, B. A., Shabanowitz, J., Hunt, D. F., Funabiki, H., & Allis, C. D. (2005). Regulation of HP1–chromatin binding by histone H3 methylation and phosphorylation. *Nature, 438*(7071), 1116-1122.

Fischle, W., Wang, Y., & Allis, C. D. (2003). Binary switches and modification cassettes in histone biology and beyond. *Nature, 425*(6957), 475-479.

Garcia, B. A., Busby, S. A., Barber, C. M., Shabanowitz, J., Allis, C. D., & Hunt, D. F. (2004). Characterization of phosphorylation sites on histone H1 isoforms by tandem mass spectrometry. *Journal of Proteome Research, 3*(6), 1219-1227.

Gerdes, J., Schwab, U., Lemke, H., & Stein, H. (1983). Production of a mouse monoclonal antibody reactive with a human nuclear antigen associated with cell proliferation. *International Journal of Cancer, 31*(1), 13-20.

Giet, R., & Glover, D. M. (2001). *Drosophila* Aurora B kinase is required for histone H3 phosphorylation and condensin recruitment during chromosome condensation and to organize the central spindle during cytokinesis. *The Journal of Cell Biology, 152*(4), 669-682.

Graziano, V., Gerchman, S. E., Schneider, D. K., & Ramakrishnan, V. (1994). Histone H1 is located in the interior of the chromatin 30-nm filament. *Nature, 368*(6469), 351-354.

Green, G. R., Lee, H. J., & Poccia, D. L. (1993). Phosphorylation weakens DNA binding by peptides containing multiple "SPKK" sequences. *Journal of Biological Chemistry, 268*(15), 11247-11255.

Grigoryev, S. A., Arya, G., Correll, S., Woodcock, C. L., & Schlick, T. (2009). Evidence for heteromorphic chromatin fibers from analysis of nucleosome interactions. *Proceedings of the National Academy of Sciences, 106*(32), 13317-13322.

Guo, Y., Kim, C., & Mao, Y. (2013). New insights into the mechanism for chromosome alignment in metaphase. *International Review of Cell and Molecular Biology, 303*, 237.

Gurley, L. R., D'Anna, J. A., Barham, S. S., Deaven, L. L., & Tobey, R. A. (1978). Histone phosphorylation and chromatin structure during mitosis in Chinese hamster cells. *European Journal of Biochemistry, 84*(1), 1-15.

Gurley, L. R., Valdez, J. G., & Buchanan, J. S. (1995). Characterization of the mitotic specific phosphorylation site of histone H1. *Journal of Biological Chemistry, 270*(46), 27653.

Gurley, L. R., Walters, R. A., & Tobey, R. A. (1974). Cell cycle-specific changes in histone phosphorylation associated with cell proliferation and chromosome condensation. *The Journal of Cell Biology, 60*(2), 356-364.

Hackstadt, T., Baehr, W., & Ying, Y. (1991). *Chlamydia trachomatis* developmentally regulated protein is homologous to eukaryotic histone H1. *Proceedings of the National Academy of Sciences, 88*(9), 3937-3941.

Hagstrom, K. A., Holmes, V. F., Cozzarelli, N. R., & Meyer, B. J. (2002). *C. elegans* condensin promotes mitotic chromosome architecture, centromere organization, and sister chromatid segregation during mitosis and meiosis. *Genes and Development, 16*(6), 729-742.

Hale, T., Contreras, A., Morrison, A., & Herrera, R. (2006). Phosphorylation of the linker histone H1 by CDK regulates its binding to HP1α. *Molecular Cell, 22*(5), 693-699.

Halmer, L., & Gruss, C. (1996). Effects of cell cycle dependent histone H1 phosphorylation on chromatin structure and chromatin replication. *Nucleic Acids Research, 24*(8), 1420-1427.

Hanks, S. K., Rodriguez, L. V., & Rao, P. N. (1983). Relationship between histone phosphorylation and premature chromosome condensation. *Experimental Cell Research, 148*(2), 293-302.

Hannak, E., Kirkham, M., Hyman, A. A., & Oegema, K. (2001). Aurora-A kinase is required for centrosome maturation in *Caenorhabditis elegans*. *The Journal of Cell Biology, 155*(7), 1109-1116.

Hans, F., & Dimitrov, S. (2001). Histone H3 phosphorylation and cell division. *Oncogene, 20*(24), 3021-3027.

Happel, N., & Doenecke, D. (2009). Histone H1 and its isoforms: Contribution to chromatin structure and function. *Gene, 431*(1-2), 1-12.

Harshman, S. W., Hoover, M. E., Huang, C., Branson, O. E., Chaney, S. B., Cheney, C. M., Rosol, T. J., Shapiro, C. L., Wysocki, V. H., Huebner, K., & Freitas, M. A. (2014). Histone H1 phosphorylation in breast cancer. *Journal of Proteome Research, 13*(5), 2453-2467.

Harshman, S. W., Young, N. L., Parthun, M. R., & Freitas, M. A. (2013). H1 histones: Current perspectives and challenges. *Nucleic Acids Research, 41*(21), 9593-9609.

Hartman, P. G., Chapman, G. E., Moss, T., & Bradbury, E. M. (1977). Studies on the role and mode of operation of the very-lysine-rich histone H1 in eukaryote chromatin. *European Journal of Biochemistry, 77*(1), 45-51.

Hartwell, L. H. (1971). Genetic control of the cell division cycle in yeast: II. Genes controlling DNA replication and its initiation. *Journal of Molecular Biology, 59*(1), 183-194.

Hartwell, L. H., Culotti, J., & Reid, B. (1970). Genetic control of the cell-division cycle in yeast, I. Detection of mutants. *Proceedings of the National Academy of Sciences, 66*(2), 352-359.

Hayakawa, T., Haraguchi, T., Masumoto, H., & Hiraoka, Y. (2003). Cell cycle behavior of human HP1 subtypes: Distinct molecular domains of HP1 are required for their centromeric localization during interphase and metaphase. *Journal of Cell Science, 116*(16), 3327-3338.

Hayashi, T., Hayashi, H., & Koichi, I. (1987). *Tetrahymena* histone H1. Isolation and amino acid sequence lacking the central hydrophobic domain conserved in other H1 histones. *Journal of Biochemistry, 102*(2), 369-376.

Hellauer, K., Sirard, E., & Turcotte, B. (2001). Decreased expression of specific genes in yeast cells lacking histone H1. *Journal of Biological Chemistry, 276*(17), 13587-13592.

Hendzel, M. J., Lever, M. A., Crawford, E., & Th'ng, J. P. (2004). The C-terminal domain is the primary determinant of histone H1 binding to chromatin *in vivo*. *Journal of Biological Chemistry, 279*(19), 20028-20034.

Hendzel, M. J., Wei, Y., Mancini, M. A., Van Hooser, A., Ranalli, T., Brinkley, B., Bazett-Jones, D. P., & Allis, C. D. (1997). Mitosis-specific phosphorylation of histone H3 initiates primarily within pericentromeric heterochromatin during G2 and spreads in an ordered fashion coincident with mitotic chromosome condensation. *Chromosoma, 106*(6), 348-360.

Hergeth, S. P., Dundr, M., Tropberger, P., Zee, B. M., Garcia, B. A., Daujat, S., & Schneider, R. (2011). Isoform-specific phosphorylation of human linker histone H1.4 in mitosis by the kinase Aurora B. *Journal of Cell Science, 124*(10), 1623.

Hergeth, S. P., & Schneider, R. (2015). The H1 linker histones: Multifunctional proteins beyond the nucleosomal core particle. *EMBO Reports, 16*(11), 1439-1453.

Herrera, R. E., Chen, F., & Weinberg, R. A. (1996). Increased histone H1 phosphorylation and relaxed chromatin structure in Rb-deficient fibroblasts. *Proceedings of the National Academy of Sciences, 93*(21), 11510-11515.

Hirano, T., & Mitchison, T. J. (1994). A heterodimeric coiled-coil protein required for mitotic chromosome condensation *in vitro*. *Cell, 79*(3), 449-458.

Hirota, T., Gerlich, D., Koch, B., Ellenberg, J., & Peters, J. M. (2004). Distinct functions of condensin I and II in mitotic chromosome assembly. *Journal of Cell Science, 117*(26), 6435.

Hirota, T., Lipp, J. J., Toh, B.-H., & Peters, J.-M. (2005). Histone H3 serine 10 phosphorylation by Aurora B causes HP1 dissociation from heterochromatin. *Nature, 438*(7071), 1176-1180.

Horowitz-Scherer, R. A., & Woodcock, C. L. (2006). Organization of interphase chromatin. *Chromosoma, 115*(1), 1-14.

Hsu, J.-Y., Sun, Z.-W., Li, X., Reuben, M., Tatchell, K., Bishop, D. K., Grushcow, J. M., Brame, C. J., Caldwell, J. A., & Hunt, D. F. (2000). Mitotic phosphorylation of histone H3 is governed by Ipl1/Aurora kinase and Glc7/PP1 phosphatase in budding yeast and nematodes. *Cell, 102*(3), 279-291.

Inoue, A., Hyle, J., Lechner, M. S., & Lahti, J. M. (2008). Perturbation of HP1 localization and chromatin binding ability causes defects in sister-chromatid cohesion. *Mutation Research/Genetic Toxicology and Environmental Mutagenesis, 657*(1), 48-55.

Ishihara, H., Martin, B., Brautigan, D., Karaki, H., Ozaki, H., Kato, Y., Fusetani, N., Watabe, S., Hashimoto, K., & Uemura, D. (1989). Calyculin A and okadaic acid: Inhibitors of protein phosphatase activity. *Biochemical and Biophysical Research Communications, 159*(3), 871-877.

Izzo, A., Kamieniarz, K., & Schneider, R. (2008). The histone H1 family: Specific members, specific functions? *Biological Chemistry, 389*(4), 333-343.

Jacobs, S. A., Taverna, S. D., Zhang, Y., Briggs, S. D., Li, J., Eissenberg, J. C., Allis, C. D., & Khorasanizadeh, S. (2001). Specificity of the HP1 chromo domain for the methylated N-terminus of histone H3. *The EMBO Journal, 20*(18), 5232-5241.

Jeppesen, P. (2000). Immunofluorescence in cytogenetic analysis: Method and applications. *Genetics and Molecular Biology, 23*(4), 1003-1014.

Johansen, K., & Johansen, J. (2006). Regulation of chromatin structure by histone H3S10 phosphorylation. *Chromosome Research, 14*(4), 393-404.

Johns, E. W. (1964). Studies on histones. 7. Preparative methods for histone fractions from calf thymus. *Biochemical Journal, 92*(1), 55.

Kallio, M. J., McCleland, M. L., Stukenberg, P. T., & Gorbsky, G. J. (2002). Inhibition of Aurora B kinase blocks chromosome segregation, overrides the spindle checkpoint, and perturbs microtubule dynamics in mitosis. *Current Biology, 12*(11), 900-905.

Kamakaka, R. T., & Thomas, J. O. (1990). Chromatin structure of transcriptionally competent and repressed genes. *The EMBO Journal, 9*(12), 3997.

Kang, J., Chaudhary, J., Dong, H., Kim, S., Brautigam, C. A., & Yu, H. (2011). Mitotic centromeric targeting of HP1 and its binding to Sgo1 are dispensable for sister-chromatid cohesion in human cells. *Molecular Biology of the Cell, 22*(8), 1181-1190.

Kapoor, P., Lavoie, B. D., & Frappier, L. (2005). EBP2 plays a key role in Epstein-Barr virus mitotic segregation and is regulated by Aurora family kinases. *Molecular and Cellular Biology, 25*(12), 4934-4945.

Kasinsky, H. E., Lewis, J. D., Dacks, J. B., & Ausio, J. (2001). Origin of H1 linker histones. *The FASEB Journal, 15*(1), 34-42.

Kimura, H., & Cook, P. R. (2001). Kinetics of core histones in living human cells little exchange of H3 and H4 and some rapid exchange of H2B. *The Journal of Cell Biology, 153*(7), 1341-1354.

Kimura, K., Cuvier, O., & Hirano, T. (2001). Chromosome condensation by a human condensin complex in *Xenopus* egg extracts. *Journal of Biological Chemistry, 276*(8), 5417-5420.

Kimura, K., Hirano, M., Kobayashi, R., & Hirano, T. (1998). Phosphorylation and activation of 13S condensin by Cdc2 *in vitro*. *Science, 282*(5388), 487-490.

Kimura, K., & Hirano, T. (1997). ATP-dependent positive supercoiling of DNA by 13S condensin: A biochemical implication for chromosome condensation. *Cell, 90*(4), 625-634.

Kimura, K., Rybenkov, V. V., Crisona, N. J., Hirano, T., & Cozzarelli, N. R. (1999). 13S condensin actively reconfigures DNA by introducing global positive writhe: Implications for chromosome condensation. *Cell, 98*(2), 239-248.

Kirsch-Volders, M., Plas, G., Elhajouji, A., Lukamowicz, M., Gonzalez, L., Vande Loock, K., & Decordier, I. (2011). The *in vitro* MN assay in 2011: Origin and fate, biological significance, protocols, high throughput methodologies and toxicological relevance. *Archives of Toxicology, 85*(8), 873-899.

Koch, B., Kueng, S., Ruckenbauer, C., Wendt, K. S., & Peters, J.-M. (2008). The Suv39h–HP1 histone methylation pathway is dispensable for enrichment and protection of cohesin at centromeres in mammalian cells. *Chromosoma, 117*(2), 199-210.

Komitowski, D., & Janson, C. (1990). Quantitative features of chromatin structure in the prognosis of breast cancer. *Cancer, 65*(12), 2725-2730.

Konishi, A., Shimizu, S., Hirota, J., Takao, T., Fan, Y., Matsuoka, Y., Zhang, L., Yoneda, Y., Fujii, Y., & Skoultchi, A. I. (2003). Involvement of histone H1.2 in apoptosis induced by DNA double-strand breaks. *Cell, 114*(6), 673-688.

Koop, R., Di Croce, L., & Beato, M. (2003). Histone H1 enhances synergistic activation of the MMTV promoter in chromatin. *The EMBO Journal, 22*(3), 588-599.

Kops, G. J. P. L., Weaver, B. A. A., & Cleveland, D. W. (2005). On the road to cancer: Aneuploidy and the mitotic checkpoint. *Nature Reviews Cancer, 5*(10), 773-785.

Kornberg, R. D. (1974). Chromatin Structure: A Repeating Unit of Histones and DNA. *Science, 184*(4139), 868-871.

Kornberg, R. D. (1977). Structure of chromatin. *Annual Review of Biochemistry, 46*(1), 931-954.

Kouzarides, T. (2007). Chromatin modifications and their function. *Cell, 128*(4), 693-705.

Kratzmeier, M., Albig, W., Meergans, T., & Doenecke, D. (1999). Changes in the protein pattern of H1 histones associated with apoptotic DNA fragmentation. *Biochemical Journal, 337*(2), 319-327.

Kuzmichev, A., Jenuwein, T., Tempst, P., & Reinberg, D. (2004). Different EZH2-containing complexes target methylation of histone H1 or nucleosomal histone H3. *Molecular Cell, 14*(2), 183-193.

Kuzmichev, A., Margueron, R., Vaquero, A., Preissner, T. S., Scher, M., Kirmizis, A., Ouyang, X., Brockdorff, N., Abate-Shen, C., Farnham, P., & Reinberg, D. (2005). Composition and histone substrates of polycomb repressive group complexes change during cellular differentiation. *Proceedings of the National Acadamy of Sciences, 102*(6), 1859-1864.

Lachner, M., O'Carroll, D., Rea, S., Mechtler, K., & Jenuwein, T. (2001). Methylation of histone H3 lysine 9 creates a binding site for HP1 proteins. *Nature, 410*(6824), 116-120.

Laemmli, U. K. (1970). Cleavage of structural proteins during the assembly of the head of bacteriophage T4. *Nature, 227*, 680-685.

Landsman, D. (1996). Histone H1 in *Saccharomyces cerevisiae*: A double mystery solved? *Trends in Biochemical Sciences, 21*(8), 287-288.

Langan, T., Gautier, J., Lohka, M., Hollingsworth, R., Moreno, S., Nurse, P., Maller, J., & Sclafani, R. (1989). Mammalian growth-associated H1 histone kinase: A homolog of cdc2+/CDC28 protein kinases controlling mitotic entry in yeast and frog cells. *Molecular and Cellular Biology, 9*(9), 3860-3868.

Lee, H., Habas, R., & Abate-Shen, C. (2004). Msx1 cooperates with histone H1b for inhibition of transcription and myogenesis. *Science, 304*(5677), 1675-1678.

Lever, M. A., Th'ng, J. P. H., Sun, X., & Hendzel, M. J. (2000). Rapid exchange of histone H1.1 on chromatin in living human cells. *Nature, 408*(6814), 873-876.

Lewis, C. D., & Laemmli, U. K. (1982). Higher order metaphase chromosome structure: Evidence for metalloprotein interactions. *Cell, 29*(1), 171-181.

Lopez, R., Sarg, B., Lindner, H., Bartolomé, S., Ponte, I., Suau, P., & Roque, A. (2015). Linker histone partial phosphorylation: Effects on secondary structure and chromatin condensation. *Nucleic Acids Research, 43*(9), 4463-4476.

Lu, X., Wontakal, S. N., Emelyanov, A. V., Morcillo, P., Konev, A. Y., Fyodorov, D. V., & Skoultchi, A. I. (2009). Linker histone H1 is essential for Drosophila development, the establishment of pericentric heterochromatin, and a normal polytene chromosome structure. *Genes and Development, 23*(4), 452.

Luger, K., Mäder, A. W., Richmond, R. K., Sargent, D. F., & Richmond, T. J. (1997). Crystal structure of the nucleosome core particle at 2.8 Å resolution. *Nature, 389*(6648), 251-260.

Lutter, L. C. (1978). Kinetic analysis of deoxyribonuclease I cleavages in the nucleosome core: Evidence for a DNA superhelix. *Journal of Molecular Biology, 124*(2), 391-420.

Maeshima, K., Hihara, S., & Eltsov, M. (2010). Chromatin structure: Does the 30-nm fibre exist *in vivo*? *Current Opinion in Cell Biology, 22*(3), 291-297.

Maiato, H., & Logarinho, E. (2014). Mitotic spindle multipolarity without centrosome amplification. *Nature Cell Biology, 16*(5), 386-394.

Maison, C., & Almouzni, G. (2004). HP1 and the dynamics of heterochromatin maintenance. *Nature Reviews Molecular Cell Biology, 5*(4), 296-304.

Maison, C., Bailly, D., Peters, A. H. F. M., Quivy, J.-P., Roche, D., Taddei, A., Lachner, M., Jenuwein, T., & Almouzni, G. (2002). Higher-order structure in pericentric heterochromatin involves a distinct pattern of histone modification and an RNA component. *Nature Genetics, 30*(3), 329-334.

Maresca, T. J., Freedman, B. S., & Heald, R. (2005). Histone H1 is essential for mitotic chromosome architecture and segregation in *Xenopus laevis* egg extracts. *The Journal of Cell Biology, 169*(6), 859.

Maresca, T. J., & Heald, R. (2006). The long and the short of it: Linker histone H1 is required for metaphase chromosome compaction. *Cell Cycle, 5*(6), 589-591.

Marsden, M., & Laemmli, U. (1979). Metaphase chromosome structure: Evidence for a radial loop model. *Cell, 17*(4), 849-858.

Mateescu, B., England, P., Halgand, F., Yaniv, M., & Muchardt, C. (2004). Tethering of HP1 proteins to chromatin is relieved by phosphoacetylation of histone H3. *EMBO Reports, 5*(5), 490-496.

Matsumoto, Y.-I., Yasuda, H., Mita, S., Marunouchi, T., & Yamada, M.-a. (1980). Evidence for the involvement of H1 histone phosphorylation in chromosome condensation. *Nature, 284*(5752), 181-183.

Matsumoto, Y., Hayashi, K., & Nishida, E. (1999). Cyclin-dependent kinase 2 (Cdk2) is required for centrosome duplication in mammalian cells. *Current Biology, 9*(8), 429-432.

Meehan, R. R., Kao, C. F., & Pennings, S. (2003). HP1 binding to native chromatin *in vitro* is determined by the hinge region and not by the chromodomain. *The EMBO Journal, 22*(12), 3164-3174.

Meergans, T., Albig, W., & Doenecke, D. (1997). Varied expression patterns of human H1 histone genes in different cell lines. *DNA and Cell Biology, 16*(9), 1041-1049.

Mellone, B. G., Ball, L., Suka, N., Grunstein, M. R., Partridge, J. F., & Allshire, R. C. (2003). Centromere silencing and function in fission yeast is governed by the amino terminus of histone H3. *Current Biology, 13*(20), 1748-1757.

Méndez, J., & Stillman, B. (2000). Chromatin association of human origin recognition complex, Cdc6, and minichromosome maintenance proteins during the cell cycle: Assembly of prereplication complexes in late mitosis. *Molecular and Cellular Biology, 20*(22), 8602-8612.

Meng, Y., Yi, X., Li, X., Hu, C., Wang, J., Bai, L., Czajkowsky, D. M., & Shao, Z. (2016). The non-coding RNA composition of the mitotic chromosome by 5′-tag sequencing. *Nucleic Acids Research*, gkw195.

Millán-Ariño, L., Islam, A. B. M. M. K., Izquierdo-Bouldstridge, A., Mayor, R., Terme, J.-M., Luque, N., Sancho, M., López-Bigas, N., & Jordan, A. (2014). Mapping of six somatic linker histone H1 variants in human breast cancer cells uncovers specific features of H1.2. *Nucleic Acids Research, 42*(7), 4474-4493.

Minc, E., Allory, Y., Worman, H. J., Courvalin, J.-C., & Buendia, B. (1999). Localization and phosphorylation of HP1 proteins during the cell cycle in mammalian cells. *Chromosoma, 108*(4), 220-234.

Misteli, T. (2001). The concept of self-organization in cellular architecture. *The Journal of Cell Biology, 155*(2), 181-186.

Misteli, T., Gunjan, A., Hock, R., Bustin, M., & Brown, D. T. (2000). Dynamic binding of histone H1 to chromatin in living cells. *Nature, 408*(6814), 877-881.

Mora-Bermudez, F., Gerlich, D., & Ellenberg, J. (2007). Maximal chromosome compaction occurs by axial shortening in anaphase and depends on Aurora kinase. *Nature Cell Biology, 9*(7), 822-831.

Muchardt, C., Guillemé, M., Seeler, J. S., Trouche, D., Dejean, A., & Yaniv, M. (2002). Coordinated methyl and RNA binding is required for heterochromatin localization of mammalian HP1. *EMBO Reports, 3*(10), 975-981.

Murata-Hori, M., & Wang, Y.-l. (2002). Both midzone and astral microtubules are involved in the delivery of cytokinesis signals insights from the mobility of Aurora B. *The Journal of Cell Biology, 159*(1), 45-53.

Murzina, N., Verreault, A., Laue, E., & Stillman, B. (1999). Heterochromatin dynamics in mouse cells: interaction between chromatin assembly factor 1 and HP1 proteins. *Molecular Cell, 4*(4), 529-540.

Naumova, N., Imakaev, M., Fudenberg, G., Zhan, Y., Lajoie, B. R., Mirny, L. A., & Dekker, J. (2013). Organization of the mitotic chromosome. *Science, 342*(6161), 948-953.

Nielsen, A., Oulad-Abdelghani, M., Ortiz, J. A., Remboutsika, E., Chambon, P., & Losson, R. (2001). Heterochromatin formation in mammalian cells: Interaction between histones and HP1 proteins. *Molecular Cell, 7*(4), 729-739.

Nielsen, P., Nietlispach, D., Mott, H. R., Callaghan, J., Bannister, A., Kouzarides, T., Murzin, A. G., Murzina, N. V., & Laue, E. D. (2002). Structure of the HP1 chromodomain bound to histone H3 methylated at lysine 9. *Nature, 416*(6876), 103-107.

Noll, M., & Kornberg, R. D. (1977). Action of micrococcal nuclease on chromatin and the location of histone H1. *Journal of molecular biology, 109*(3), 393-404.

Nonaka, N., Kitajima, T., Yokobayashi, S., Xiao, G., Yamamoto, M., Grewal, S. I., & Watanabe, Y. (2002). Recruitment of cohesin to heterochromatic regions by Swi6/HP1 in fission yeast. *Nature Cell Biology, 4*(1), 89-93.

Norbury, C., & Nurse, P. (1992). Animal cell cycles and their control. *Annual Review of Biochemistry, 61*(1), 441-468.

Nurse, P., Thuriaux, P., & Nasmyth, K. (1976). Genetic control of the cell division cycle in the fission yeast *Schizosaccharomyces pombe*. *Molecular and General Genetics, 146*(2), 167-178.

Ohe, Y., Hayashi, H., & Iwai, K. (1986). Human spleen histone H1. Isolation and amino acid sequence of a main variant, H1b. *The Journal of Biochemistry, 100*(2), 359-368.

Ohsumi, K., Katagiri, C., & Kishimoto, T. (1993). Chromosome condensation in *Xenopus* mitotic extracts without histone H1. *Science, 262*(5142), 2033.

Olins, A. L., & Olins, D. E. (1974). Spheroid chromatin units (ν bodies). *Science, 183*(4122), 330-332.

Ono, T., Fang, Y., Spector, D. L., & Hirano, T. (2004). Spatial and temporal regulation of Condensins I and II in mitotic chromosome assembly in human cells. *Molecular Biology of the Cell, 15*(7), 3296-3308.

Ord, M. G., & Stocken, L. (1966). Metabolic properties of histones from rat liver and thymus gland. *Biochemical Journal, 98*(3), 888.

Ornstein, L. (1964). Disc electrophoresis-I: Background and theory*. *Annals of the New York Academy of Sciences, 121*(2), 321-349.

Orrego, M., Ponte, I., Roque, A., Buschati, N., Mora, X., & Suau, P. (2007). Differential affinity of mammalian histone H1 somatic subtypes for DNA and chromatin. *BMC Biology, 5*(1), 22.

Orthaus, S., Klement, K., Happel, N., Hoischen, C., & Diekmann, S. (2009). Linker histone H1 is present in centromeric chromatin of living human cells next to inner kinetochore proteins. *Nucleic Acids Research, 37*(10), 3391-3406.

Ota, T., Suto, S., Katayama, H., Han, Z. B., Suzuki, F., Maeda, M., Tanino, M., Terada, Y., & Tatsuka, M. (2002). Increased mitotic phosphorylation of histone H3 attributable to AIM-1/Aurora-B overexpression contributes to chromosome number instability. *Cancer Research, 62*(18), 5168.

Pan, C., & Fan, Y. (2016). Role of H1 linker histones in mammalian development and stem cell differentiation. *Biochimica et Biophysica Acta (BBA) - Gene Regulatory Mechanisms, 1859*(3), 496-509.

Paulson, J. R., & Laemmli, U. (1977). The structure of histone-depleted metaphase chromosomes. *Cell, 12*(3), 817-828.

Paulson, J. R., Patzlaff, J. S., & Vallis, A. J. (1996). Evidence that the endogenous histone H1 phosphatase in HeLa mitotic chromosomes is Protein phosphatase 1, not Protein phosphatase 2A. *Journal of Cell Science, 109*(6), 1437-1447.

Pederson, T., & Robbins, E. (1971). A method for improving synchrony in the G2 phase of the cell cycle. *The Journal of Cell Biology, 49*(3), 942-945.

Phair, R. D., Scaffidi, P., Elbi, C., Vecerová, J., Dey, A., Ozato, K., Brown, D. T., Hager, G., Bustin, M., & Misteli, T. (2004). Global nature of dynamic protein-chromatin interactions *in vivo*: Three-dimensional genome scanning and dynamic interaction networks of chromatin proteins. *Molecular and Cellular Biology, 24*(14), 6393-6402.

Prigent, C., & Dimitrov, S. (2003). Phosphorylation of serine 10 in histone H3, what for? *Journal of Cell Science, 116*(18), 3677-3685.

Ramakrishnan, V., Finch, J., Graziano, V., Lee, P., & Sweet, R. (1993). Crystal structure of globular domain of histone H5 and its implications for nucleosome binding. *Nature, 362*(6417), 219-223.

Ramón, A., Muro-Pastor, M. I., Scazzocchio, C., & Gonzalez, R. (2000). Deletion of the unique gene encoding a typical histone H1 has no apparent phenotype in *Aspergillus nidulans*. *Molecular Microbiology, 35*(1), 223-233.

Rea, S., Eisenhaber, F., O'Carroll, D., Strahl, B. D., Sun, Z.-W., Schmid, M., Opravil, S., Mechtler, K., Ponting, C. P., Allis, C. D., & Jenuwein, T. (2000). Regulation of chromatin structure by site-specific histone H3 methyltransferases. *Nature, 406*(6796), 593-599.

Reik, W. (2007). Stability and flexibility of epigenetic gene regulation in mammalian development. *Nature, 447*(7143), 425-432.

Roque, A., Iloro, I., Ponte, I., Arrondo, J. L. R., & Suau, P. (2005). DNA-induced secondary structure of the carboxyl-terminal domain of histone H1. *Journal of Biological Chemistry, 280*(37), 32141-32147.

Roque, A., Ponte, I., Arrondo, J. L. R., & Suau, P. (2008). Phosphorylation of the carboxy-terminal domain of histone H1: Effects on secondary structure and DNA condensation. *Nucleic Acids Research, 36*(14), 4719.

Rossetto, D., Avvakumov, N., & Côté, J. (2012). Histone phosphorylation: A chromatin modification involved in diverse nuclear events. *Epigenetics, 7*(10), 1098-1108.

Roth, S. Y., & Allis, C. D. (1992). Chromatin condensation: Does histone H1 dephosphorylation play a role? *Trends in Biochemical Sciences, 17*(3), 93.

Ruan, J., Ouyang, H., Amaya, M. F., Ravichandran, M., Loppnau, P., Min, J., & Zang, J. (2012). Structural basis of the chromodomain of Cbx3 bound to methylated peptides from histone H1 and G9a. *PloS One, 7*(4), e35376.

Sancho, M., Diani, E., Beato, M., & Jordan, A. (2008). Depletion of human histone H1 variants uncovers specific roles in gene expression and cell growth. *PloS Genetics, 4*(10), e1000227.

Sarg, B., Helliger, W., Talasz, H., Förg, B., & Lindner, H. H. (2006). Histone H1 phosphorylation occurs site-specifically during interphase and mitosis. *Journal of Biological Chemistry, 281*(10), 6573.

Schalch, T., Duda, S., Sargent, D. F., & Richmond, T. J. (2005). X-ray structure of a tetranucleosome and its implications for the chromatin fibre. *Nature, 436*(7047), 138-141.

Schmiesing, J. A., Gregson, H. C., Zhou, S., & Yokomori, K. (2000). A human condensin complex containing hCAP-C-hCAP-E and CNAP1, a homolog of Xenopus XCAP-D2, colocalizes with phosphorylated histone H3 during the early stage of mitotic chromosome condensation. *Molecular and Cellular Biology, 20*(18), 6996.

Schroeder, T. E. (1973). Actin in dividing cells: Contractile ring filaments bind heavy meromyosin. *Proceedings of the National Academy of Sciences, 70*(6), 1688-1692.

Shechter, D., Dormann, H. L., Allis, C. D., & Hake, S. B. (2007). Extraction, purification and analysis of histones. *Nature Protocols, 2*(6), 1445-1457.

Shelby, R. D., Vafa, O., & Sullivan, K. F. (1997). Assembly of CENP-A into centromeric chromatin requires a cooperative array of nucleosomal DNA contact sites. *The Journal of Cell Biology, 136*(3), 501-513.

Shen, X., & Gorovsky, M. A. (1996). Linker histone H1 regulates specific gene expression but not global transcription *in vivo*. *Cell, 86*(3), 475-483.

Shen, X., Yu, L., Weir, J. W., & Gorovsky, M. A. (1995). Linker histones are not essential and affect chromatin condensation *in vivo*. *Cell, 82*(1), 47-56.

Simpson, R. T. (1978). Structure of the chromatosome, a chromatin particle containing 160 base pairs of DNA and all the histones. *Biochemistry, 17*(25), 5524-5531.

Singh, P. B., Miller, J. R., Pearce, J., Kothary, R., Burton, R. D., Paro, R., James, T. C., & Gaunt, S. J. (1991). A sequence motif found in a *Drosophila* heterochromatin protein is conserved in animals and plants. *Nucleic Acids Research, 19*(4), 789-794.

Smothers, J. F., & Henikoff, S. (2000). The HP1 chromo shadow domain binds a consensus peptide pentamer. *Current Biology, 10*(1), 27-30.

Soloaga, A., Thomson, S., Wiggin, G. R., Rampersaud, N., Dyson, M. H., Hazzalin, C. A., Mahadevan, L. C., & Arthur, J. S. C. (2003). MSK2 and MSK1 mediate the mitogen- and stress-induced phosphorylation of histone H3 and HMG-14. *The EMBO Journal, 22*(11), 2788-2797.

Song, F., Chen, P., Sun, D., Wang, M., Dong, L., Liang, D., Xu, R.-M., Zhu, P., & Li, G. (2014). Cryo-EM study of the chromatin fiber reveals a double helix twisted by tetranucleosomal units. *Science, 344*(6182), 376-380.

Sun, L., Gao, J., Dong, X., Liu, M., Li, D., Shi, X., Dong, J.-T., Lu, X., Liu, C., & Zhou, J. (2008). EB1 promotes Aurora-B kinase activity through blocking its inactivation by protein phosphatase 2A. *Proceedings of the National Academy of Sciences, 105*(20), 7153-7158.

Swank, R. A., Th'ng, J. P. H., Guo, X. W., Valdez, J., Bradbury, E. M., & Gurley, L. R. (1997). Four distinct cyclin-dependent kinases phosphorylate histone H1 at all of its growth-related phosphorylation sites. *Biochemistry, 36*(45), 13761-13768.

Tachibana, M., Sugimoto, K., Fukushima, T., & Shinkai, Y. (2001). Set domain-containing protein, G9a, is a novel lysine-preferring mammalian histone methyltransferase with hyperactivity and specific selectivity to lysines 9 and 27 of histone H3. *Journal of Biological Chemistry, 276*(27), 25309-25317.

Tachibana, M., Sugimoto, K., Nozaki, M., Ueda, J., Ohta, T., Ohki, M., Fukuda, M., Takeda, N., Niida, H., & Kato, H. (2002). G9a histone methyltransferase plays a dominant role in euchromatic histone H3 lysine 9 methylation and is essential for early embryogenesis. *Genes and Development, 16*(14), 1779-1791.

Talasz, H., Helliger, W., Puschendorf, B., & Lindner, H. (1996). *In vivo* phosphorylation of histone H1 variants during the cell cycle. *Biochemistry, 35*(6), 1761-1767.

Telu, K. H., Abbaoui, B., Thomas-Ahner, J. M., Zynger, D. L., Clinton, S. K., Freitas, M. A., & Mortazavi, A. (2013). Alterations of histone H1 phosphorylation during bladder carcinogenesis. *Journal of Proteome Research, 12*(7), 3317-3326.

Terada, Y. (2006). Aurora-B/AIM-1 regulates the dynamic behavior of HP1α at the G2–M transition. *Molecular Biology of the Cell, 17*(7), 3232-3241.

Terada, Y., Tatsuka, M., Suzuki, F., Yasuda, Y., Fujita, S., & Otsu, M. (1998). AIM-1: A mammalian midbody-associated protein required for cytokinesis. *The EMBO Journal, 17*(3), 667-676.

Terasima, T., & Tolmach, L. J. (1963). Growth and nucleic acid synthesis in synchronously dividing populations of HeLa cells. *Experimental Cell Research, 30*(2), 344-362.

Terme, J.-M., Millán-Ariño, L., Mayor, R., Luque, N., Izquierdo-Bouldstridge, A., Bustillos, A., Sampaio, C., Canes, J., Font, I., & Sima, N. (2014). Dynamics and dispensability of variant-specific histone H1 Lys-26/Ser-27 and Thr-165 post-translational modifications. *FEBS Letters, 588*(14), 2353-2362.

Th'ng, J., Guo, X. W., Swank, R. A., Crissman, H. A., & Bradbury, E. (1994). Inhibition of histone phosphorylation by staurosporine leads to chromosome decondensation. *Journal of Biological Chemistry, 269*(13), 9568.

Th'ng, J., Sung, R., Ye, M., & Hendzel, M. J. (2005). H1 family histones in the nucleus: Control of binding and localization by the C-terminal domain. *Journal of Biological Chemistry, 280*(30), 27809-27814.

Thatcher, T. H., & Gorovsky, M. A. (1994). Phylogenetic analysis of the core histones H2A, H2B, H3, and H4. *Nucleic Acids Research, 22*(2), 174-179.

Thoma, F., Koller, T., & Klug, A. (1979). Involvement of histone H1 in the organization of the nucleosome and of the salt-dependent superstructures of chromatin. *The Journal of Cell Biology, 83*(2), 403.

Thomson, S., Clayton, A. L., Hazzalin, C. A., Rose, S., Barratt, M. J., & Mahadevan, L. C. (1999). The nucleosomal response associated with immediate-early gene induction is mediated via alternative MAP kinase cascades: MSK1 as a potential histone H3/HMG-14 kinase. *The EMBO Journal, 18*(17), 4779-4793.

Towbin, H., Staehelin, T., & Gordon, J. (1979). Electrophoretic transfer of proteins from polyacrylamide gels to nitrocellulose sheets: Procedure and some applications. *Proceedings of the National Academy of Sciences, 76*(9), 4350-4354.

Trojer, P., Zhang, J., Yonezawa, M., Schmidt, A., Zheng, H., Jenuwein, T., & Reinberg, D. (2009). Dynamic histone H1 isotype 4 methylation and demethylation by histone lysine methyltransferase G9a/KMT1C and the Jumonji domain-containing JMJD2/KDM4 proteins. *Journal of Biological Chemistry, 284*(13), 8395-8405.

Uemura, T., Ohkura, H., Adachi, Y., Morino, K., Shiozaki, K., & Yanagida, M. (1987). DNA topoisomerase II is required for condensation and separation of mitotic chromosomes in S. pombe. *Cell, 50*(6), 917-925.

Umbricht, C., Oberholzer, M., Gschwind, R., Christen, H., & Torhorst, J. (1989). Prognostic significance (relapse, non-relapse) of nuclear shape parameters in lymph node negative breast cancer. *Analytical Cellular Pathology, 1*(1), 11-23.

Urruticoechea, A., Smith, I. E., & Dowsett, M. (2005). Proliferation marker Ki-67 in early breast cancer. *Journal of Clinical Oncology, 23*(28), 7212-7220.

Vaquero, A., Scher, M., Lee, D., Erdjument-Bromage, H., Tempst, P., & Reinberg, D. (2004). Human SirT1 interacts with histone H1 and promotes formation of facultative heterochromatin. *Molecular Cell, 16*(1), 93-105.

Vermeulen, K., Van Bockstaele, D. R., & Berneman, Z. N. (2003). The cell cycle: A review of regulation, deregulation and therapeutic targets in cancer. *Cell Proliferation, 36*(3), 131-149.

Vicent, G. P., Koop, R., & Beato, M. (2002). Complex role of histone H1 in transactivation of MMTV promoter chromatin by progesterone receptor. *The Journal of steroid biochemistry and molecular biology, 83*(1), 15-23.

Vila, R., Ponte, I., Collado, M., Arrondo, J. R., & Suau, P. (2001). Induction of secondary structure in a COOH-terminal peptide of histone H1 by interaction with the DNA: An infrared spectroscopy study. *Journal of Biological Chemistry, 276*(33), 30898-30903.

Wei, Y., Yu, L., Bowen, J., Gorovsky, M. A., & Allis, C. D. (1999). Phosphorylation of histone H3 is required for proper chromosome condensation and segregation. *Cell, 97*(1), 99-109.

Weiss, T., Hergeth, S., Zeissler, U., Izzo, A., Tropberger, P., Zee, B. M., Dundr, M., Garcia, B. A., Daujat, S., & Schneider, R. (2010). Histone H1 variant-specific lysine methylation by G9a/KMT1C and Glp1/KMT1D. *Epigenetics & Chromatin, 3*(1), 1-13.

Widom, J., & Klug, A. (1985). Structure of the 300 Å chromatin filament: X-ray diffraction from oriented samples. *Cell, 43*(1), 207-213.

Winter, S., Simboeck, E., Fischle, W., Zupkovitz, G., Dohnal, I., Mechtler, K., Ammerer, G., & Seiser, C. (2008). 14-3-3 proteins recognize a histone code at histone H3 and are required for transcriptional activation. *The EMBO Journal, 27*(1), 88-99.

Wiśniewski, J. R., Zougman, A., Krüger, S., & Mann, M. (2007). Mass spectrometric mapping of linker histone H1 variants reveals multiple acetylations, methylations, and phosphorylation as well as differences between cell culture and tissue. *Molecular and Cellular Proteomics, 6*(1), 72-87.

Woodcock, C. L., & Dimitrov, S. (2001). Higher-order structure of chromatin and chromosomes. *Current Opinion in Genetics and Development, 11*(2), 130-135.

Woodcock, C. L., Frado, L.-L., & Rattner, J. (1984). The higher-order structure of chromatin: Evidence for a helical ribbon arrangement. *The Journal of Cell Biology, 99*(1), 42-52.

Woodcock, C. L., Skoultchi, A., & Fan, Y. (2006). Role of linker histone in chromatin structure and function: H1 stoichiometry and nucleosome repeat length. *Chromosome Research, 14*(1), 17-25.

Xu, N., Emelyanov, A. V., Fyodorov, D. V., & Skoultchi, A. I. (2014). Drosophila linker histone H1 coordinates STAT-dependent organization of heterochromatin and suppresses tumorigenesis caused by hyperactive JAK-STAT signaling. *Epigenetics and Chromatin, 7*(1), 1.

Yamagishi, Y., Sakuno, T., Shimura, M., & Watanabe, Y. (2008). Heterochromatin links to centromeric protection by recruiting shugoshin. *Nature, 455*(7210), 251-255.

Yang, G. G. (2011). Phosphohistone H3: New standard IHC marker for grading tumors via mitotic indexing. *Medical Laboratory Observer*.

Yellajoshyula, D., & Brown, D. T. (2006). Global modulation of chromatin dynamics mediated by dephosphorylation of linker histone H1 is necessary for erythroid differentiation. *Proceedings of the National Academy of Sciences, 103*(49), 18568-18573.

Zhang, L., Eugeni, E. E., Parthun, M. R., & Freitas, M. A. (2003). Identification of novel histone post-translational modifications by peptide mass fingerprinting. *Chromosoma, 112*(2), 77-86.

Zheng, Y., John, S., Pesavento, J. J., Schultz-Norton, J. R., Schiltz, R. L., Baek, S., Nardulli, A. M., Hager, G. L., Kelleher, N. L., & Mizzen, C. A. (2010). Histone H1 phosphorylation is associated with transcription by RNA polymerases I and II. *The Journal of Cell Biology, 189*(3), 407-415.

Appendix One
Full western blots

Figure 3.1

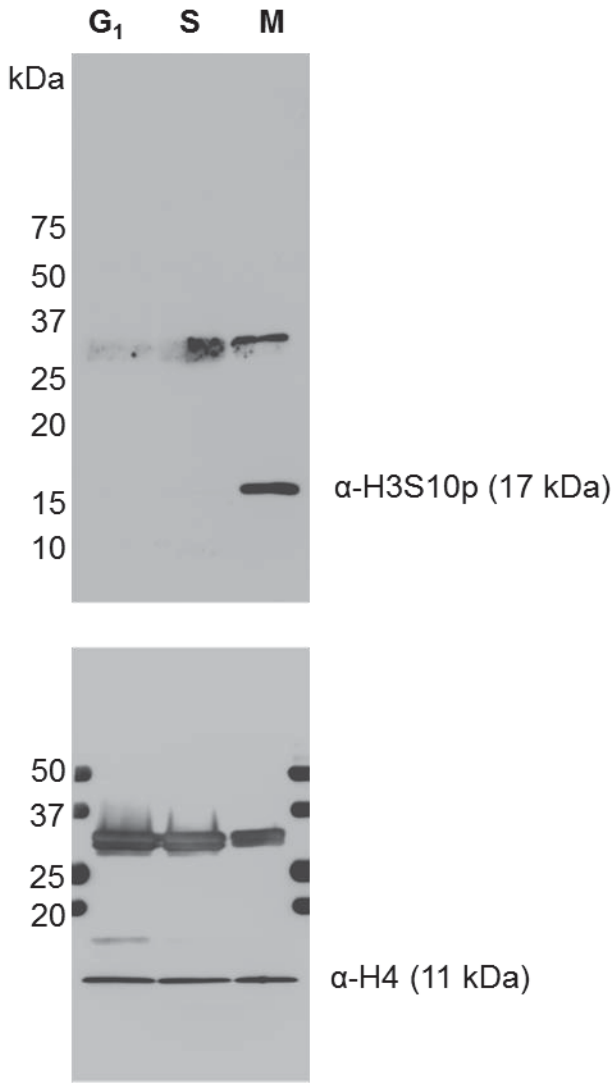

Figure 3.5 A

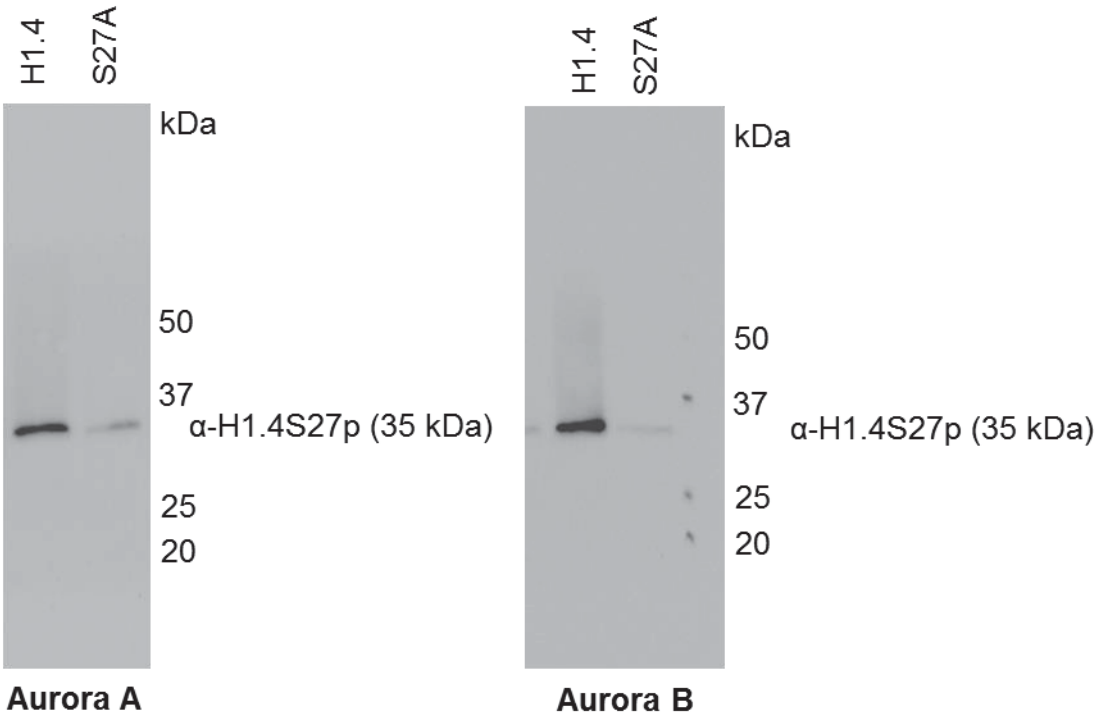
H1.4
S27A
kDa
50
37
α-H1.4S27p (35 kDa)
25
20
Aurora A
H1.4
S27A
kDa
50
37
α-H1.4S27p (35 kDa)
25
20
Aurora B

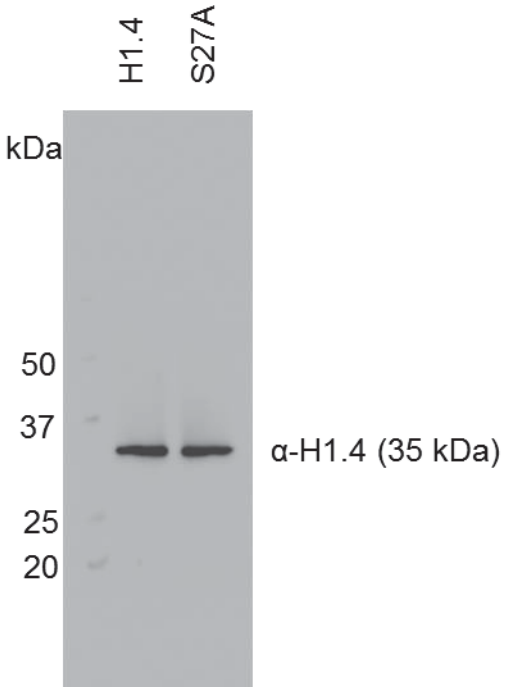
H1.4
S27A
kDa
50
37
α-H1.4 (35 kDa)
25
20

Figure 3.5 C

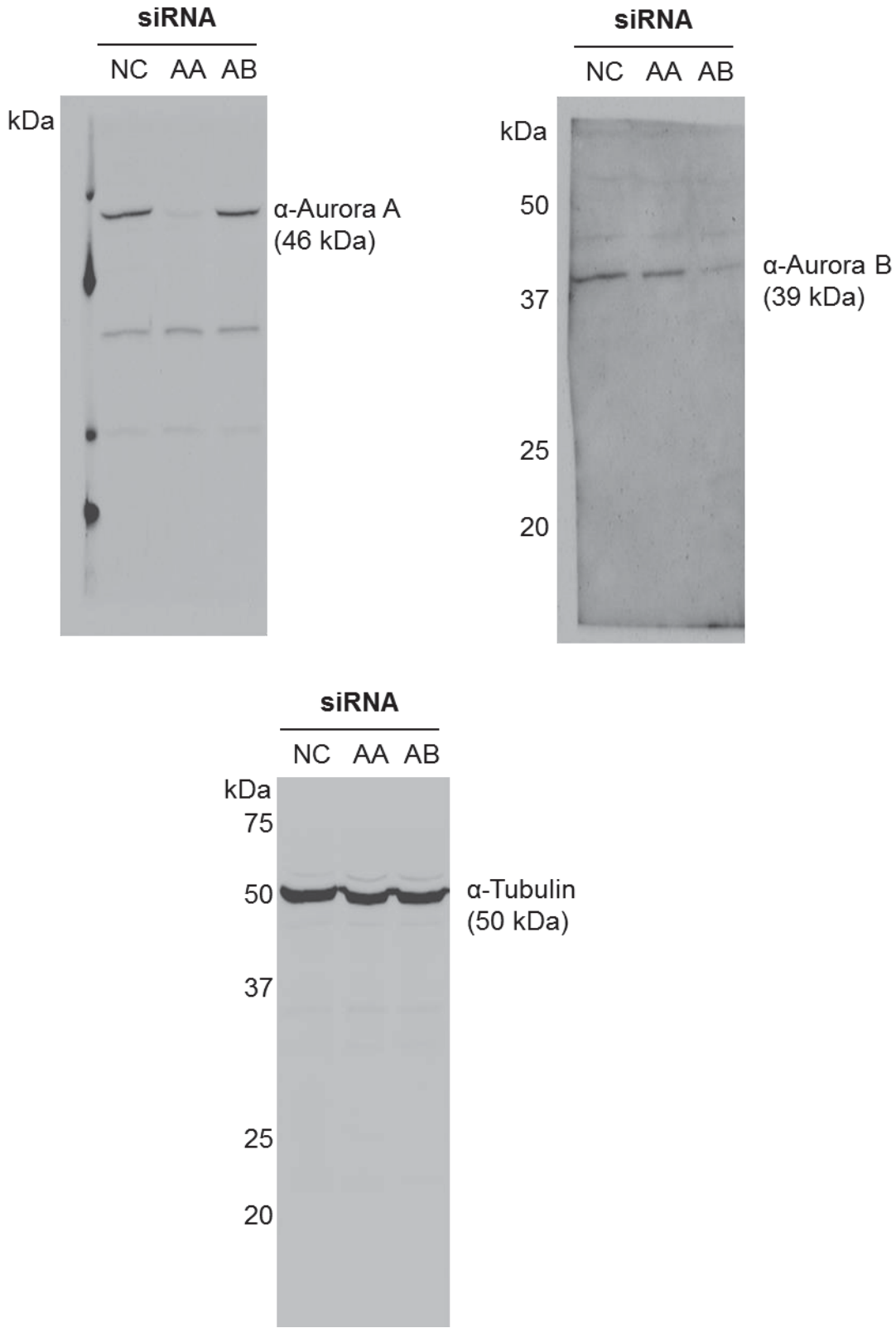
siRNA
NC AA AB
kDa
α-Aurora A
(46 kDa)
siRNA
NC AA AB
kDa
50
37
25
20
α-Aurora B
(39 kDa)
siRNA
NC AA AB
kDa
75
50
37
25
20
α-Tubulin
(50 kDa)

Figure 3.5 C

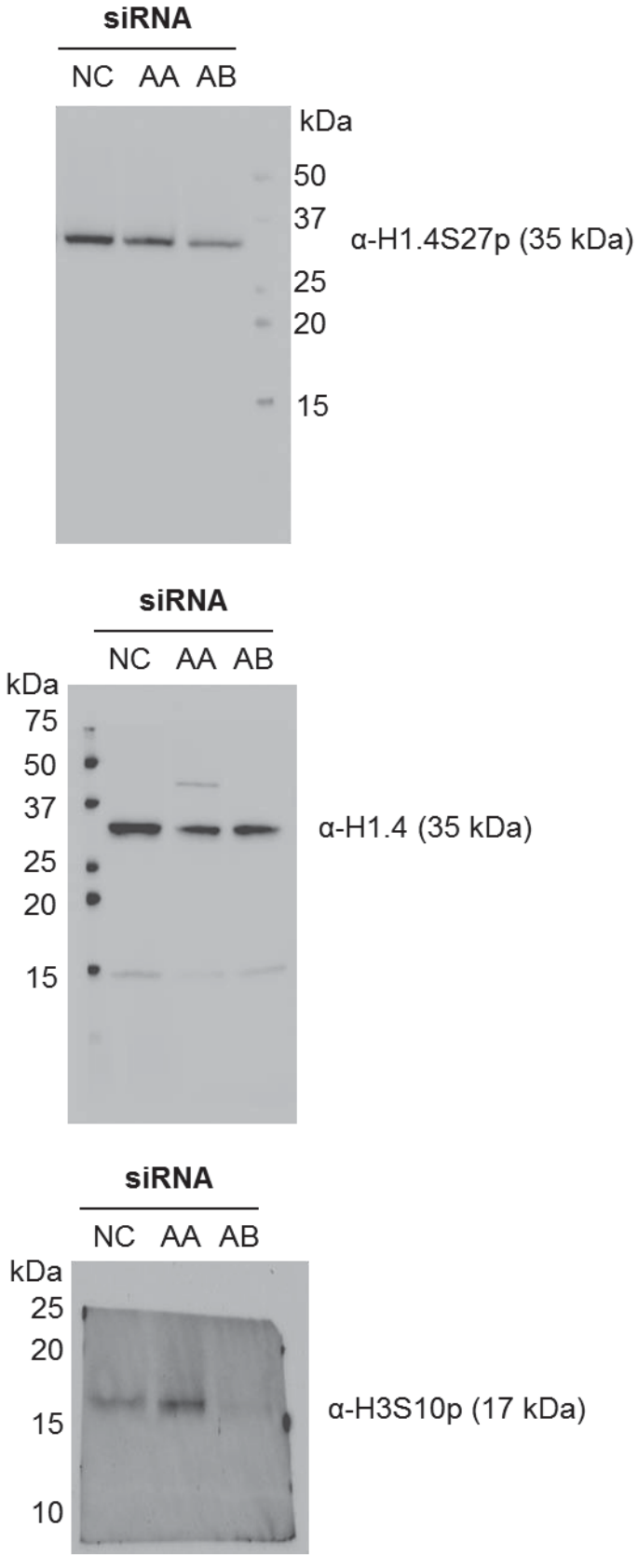
siRNA
NC AA AB
kDa
50
37
25
20
15
α-H1.4S27p (35 kDa)
siRNA
NC AA AB
kDa
75
50
37
25
20
15
α-H1.4 (35 kDa)
siRNA
NC AA AB
kDa
25
20
15
10
α-H3S10p (17 kDa)

Figure 3.9 A

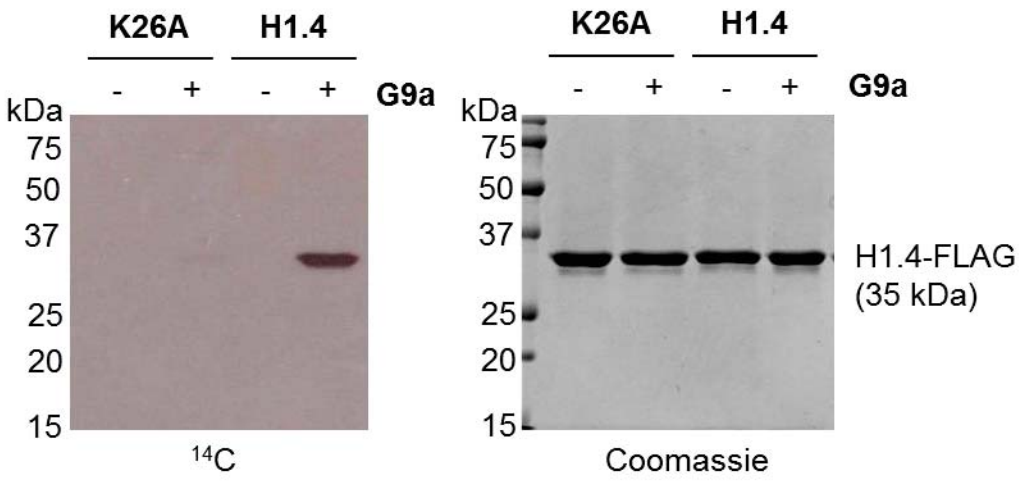
K26A
H1.4
- + - +
G9a
kDa
75
50
37
25
20
15
14C
K26A
H1.4
- + - +
G9a
kDa
75
50
37
25
20
15
H1.4-FLAG
(35 kDa)
Coomassie

Figure 3.9 B

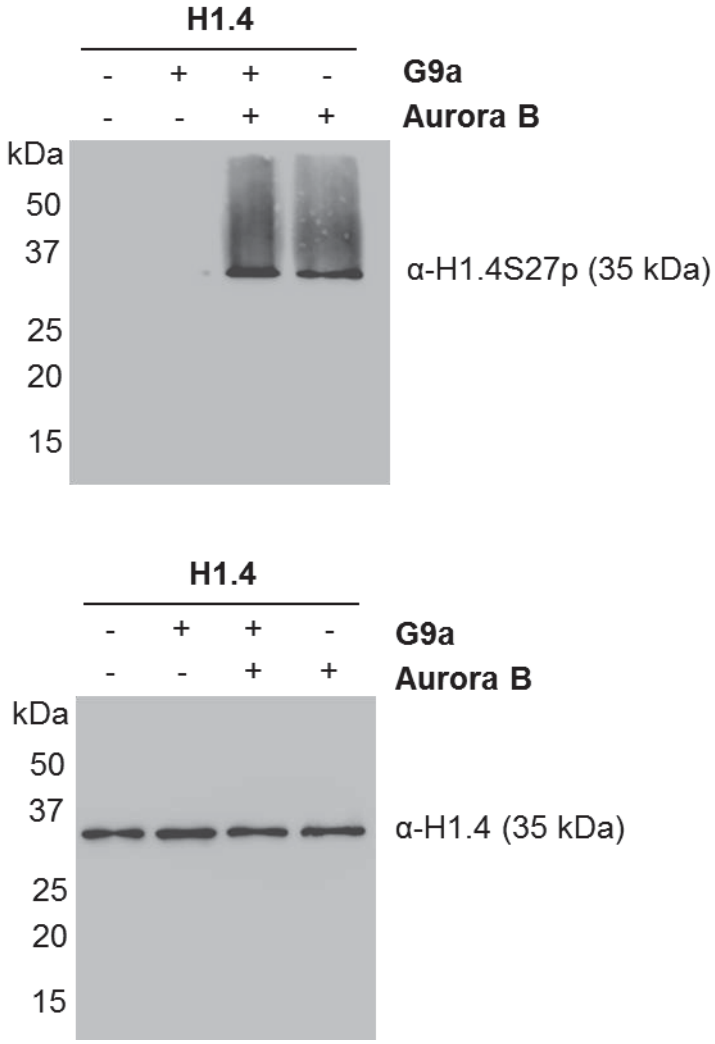
H1.4
- + + -
- - + +
G9a
Aurora B
kDa
50
37
25
20
15
α-H1.4S27p (35 kDa)
H1.4
- + + -
- - + +
G9a
Aurora B
kDa
50
37
25
20
15
α-H1.4 (35 kDa)

Figure 3.9 C

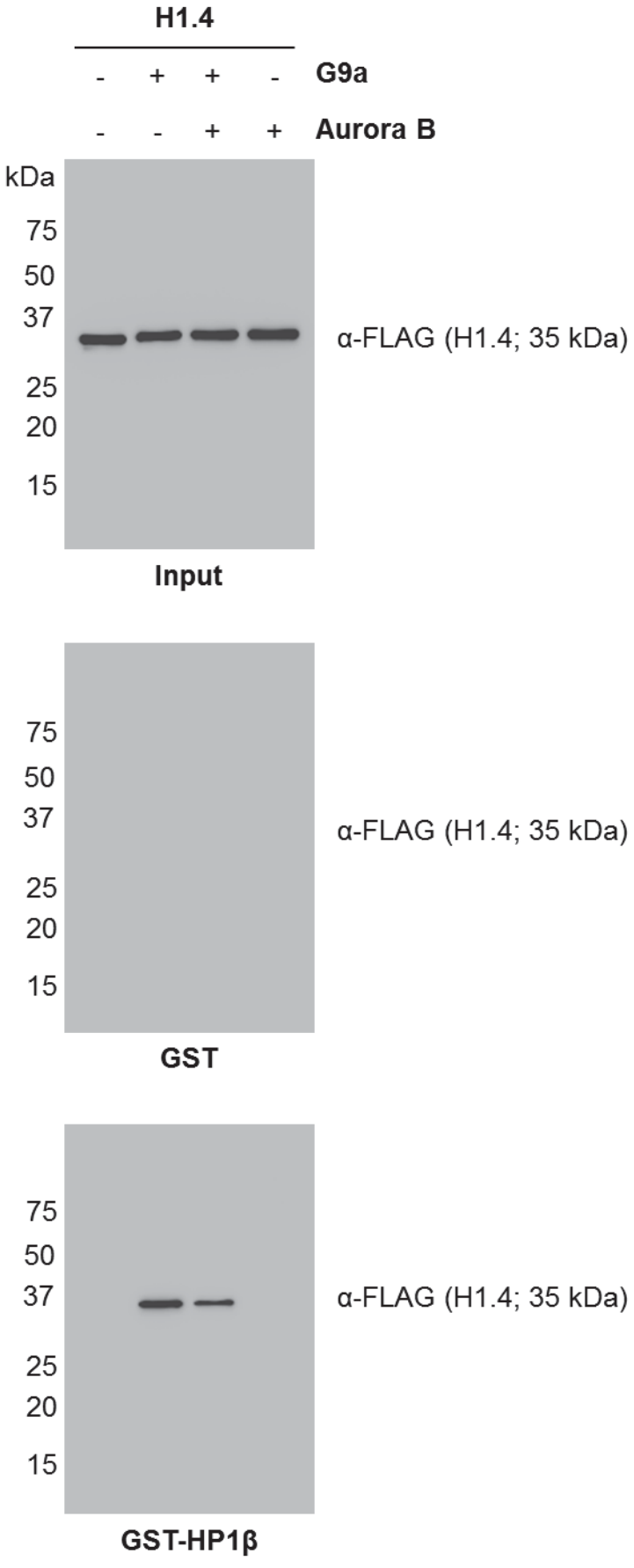
H1.4
- + + - G9a
- - + + Aurora B
kDa
75
50
37
25
20
15
α-FLAG (H1.4; 35 kDa)
Input
75
50
37
25
20
15
α-FLAG (H1.4; 35 kDa)
GST
75
50
37
25
20
15
α-FLAG (H1.4; 35 kDa)
GST-HP1β

Figure 4.9

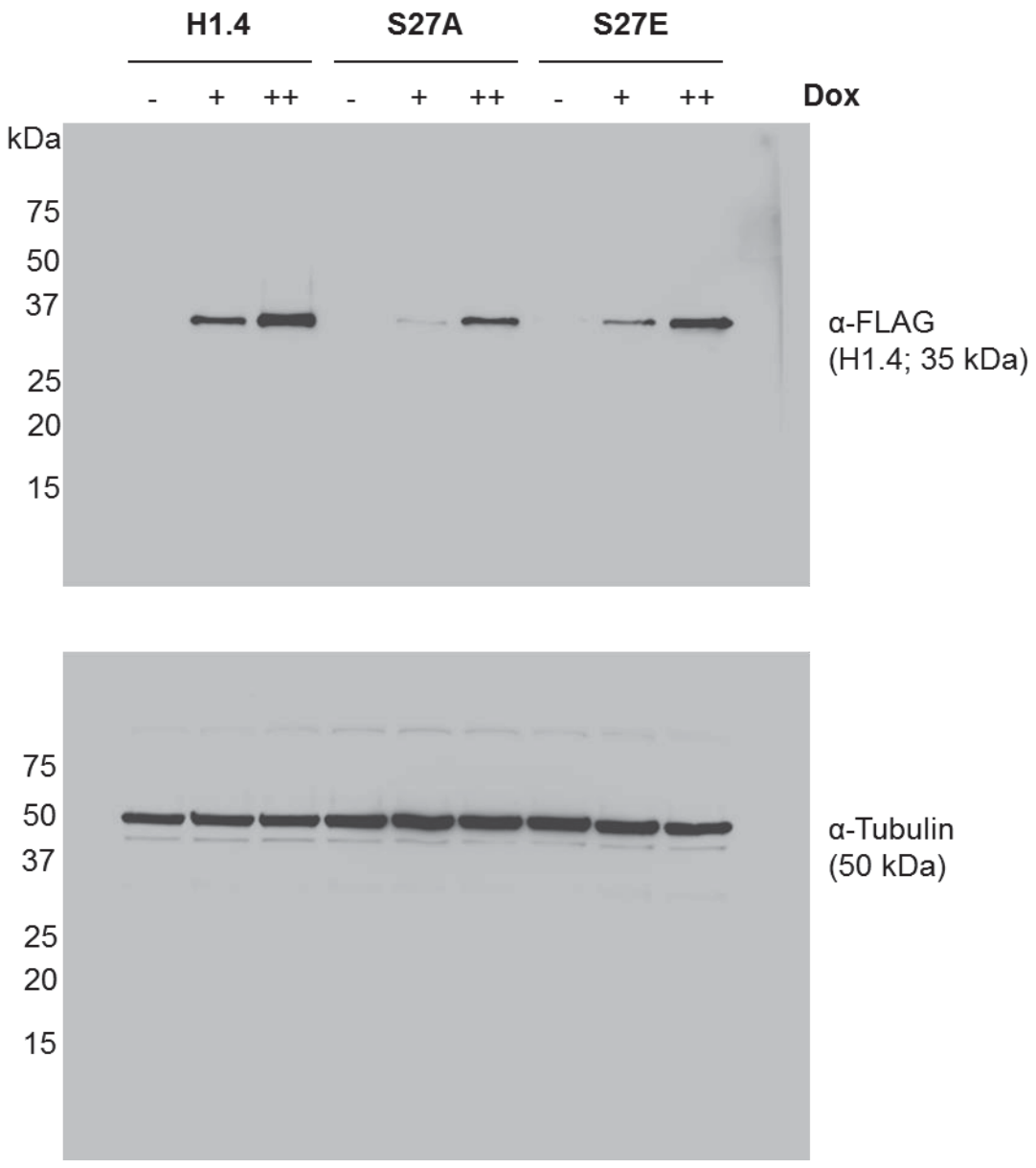
H1.4
S27A
S27E
- + ++ - + ++ - + ++
Dox
kDa
75
50
37
25
20
15
α-FLAG
(H1.4; 35 kDa)
75
50
37
25
20
15
α-Tubulin
(50 kDa)

Figure 4.9

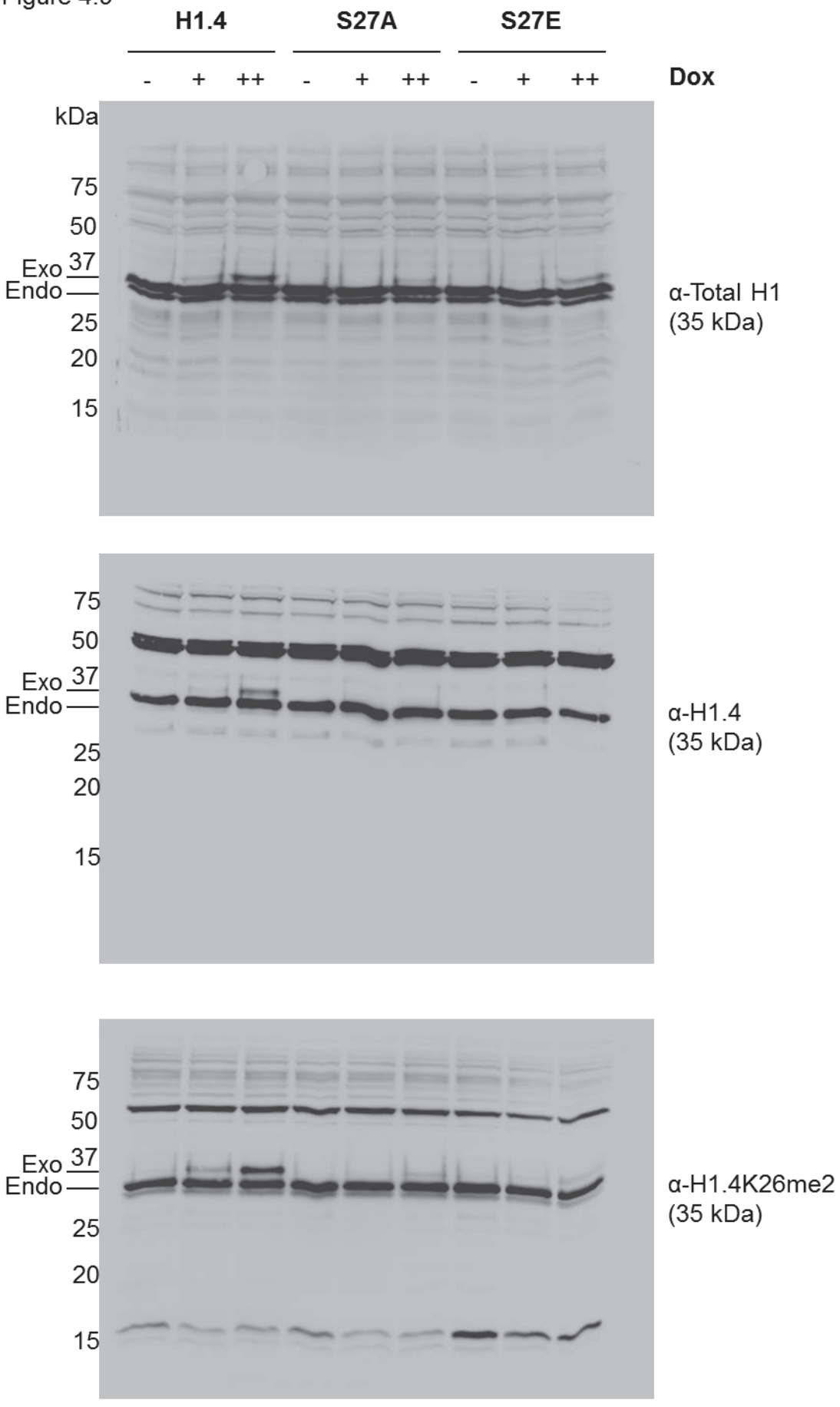
H1.4
S27A
S27E
- + ++ - + ++ - + ++
Dox
kDa
75
50
Exo 37
Endo
25
20
15
α-Total H1
(35 kDa)
75
50
Exo 37
Endo
25
20
15
α-H1.4
(35 kDa)
75
50
Exo 37
Endo
25
20
15
α-H1.4K26me2
(35 kDa)

Figure 4.10

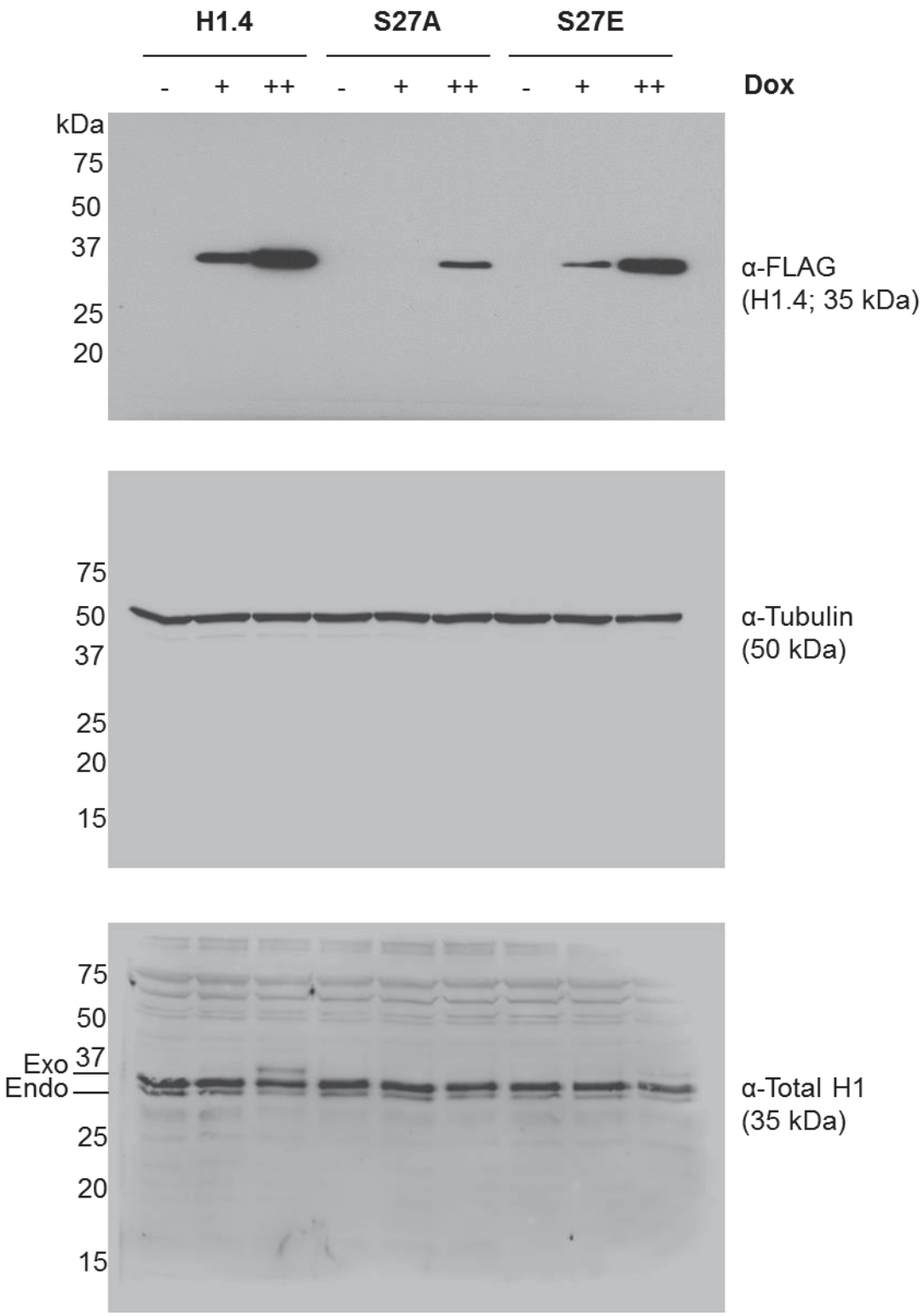
H1.4
S27A
S27E
- + ++ - + ++ - + ++
Dox
kDa
75
50
37
25
20
α-FLAG
(H1.4; 35 kDa)
75
50
37
25
20
15
α-Tubulin
(50 kDa)
75
50
Exo 37
Endo
25
20
15
α-Total H1
(35 kDa)

Figure 4.10

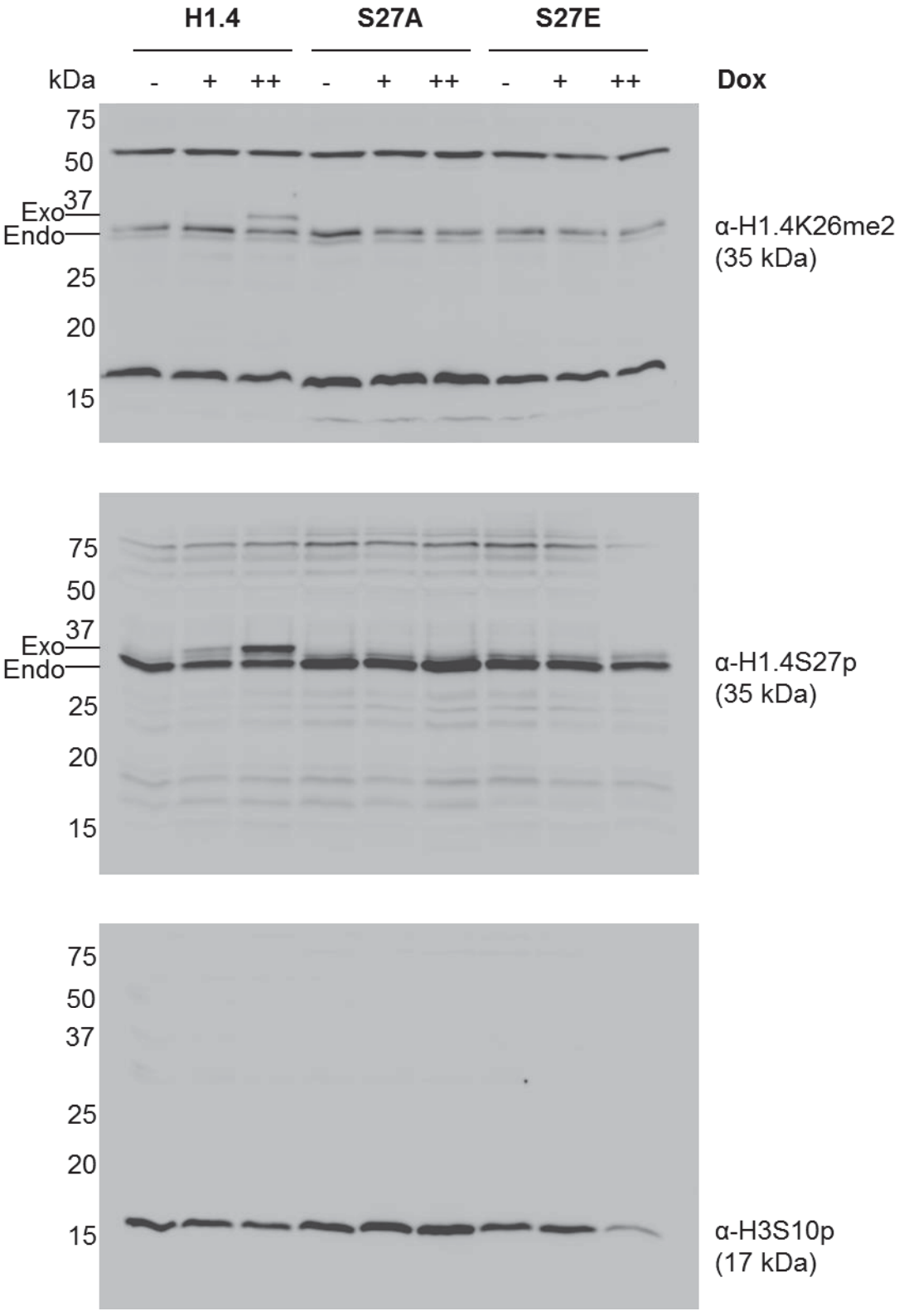
H1.4
S27A
S27E
kDa
- + ++ - + ++ - + ++
Dox
75
50
37
Exo
Endo
25
20
15
α-H1.4K26me2
(35 kDa)
75
50
37
Exo
Endo
25
20
15
α-H1.4S27p
(35 kDa)
75
50
37
25
20
15
α-H3S10p
(17 kDa)

Figure 4.12

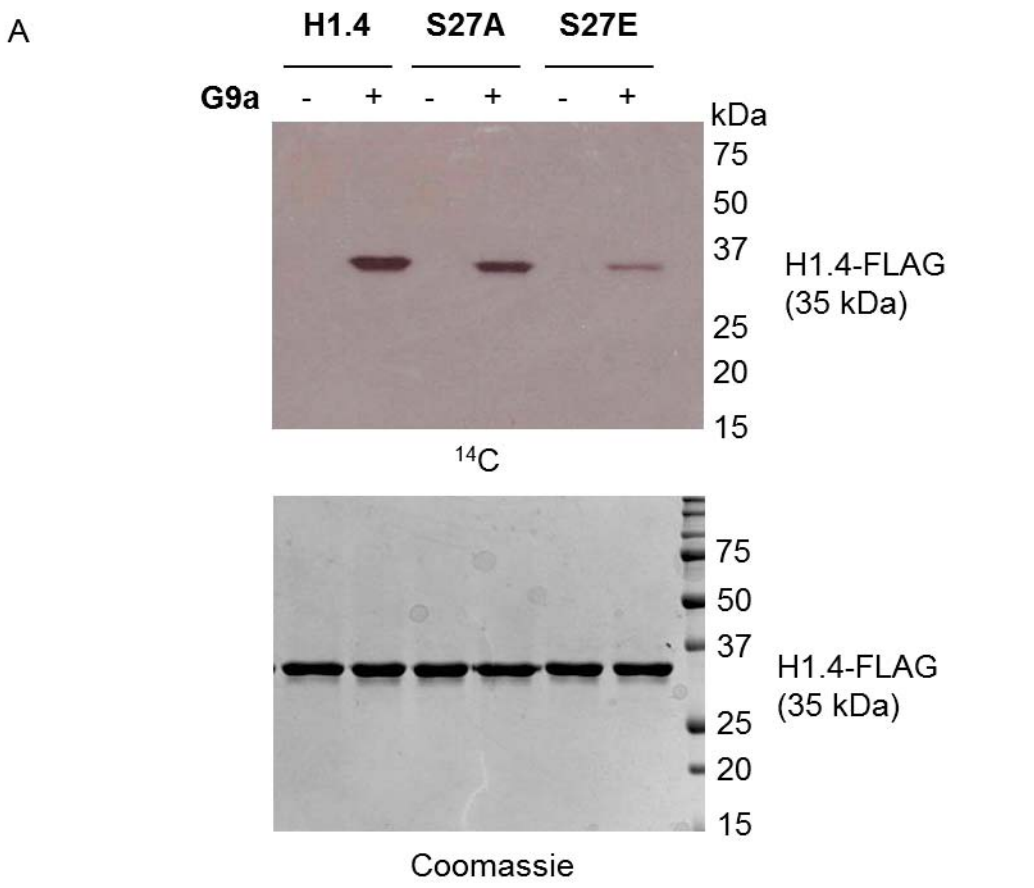
A
H1.4
S27A
S27E
G9a
- + - + - +
kDa
75
50
37
25
20
15
H1.4-FLAG
(35 kDa)
14C
75
50
37
25
20
15
H1.4-FLAG
(35 kDa)
Coomassie

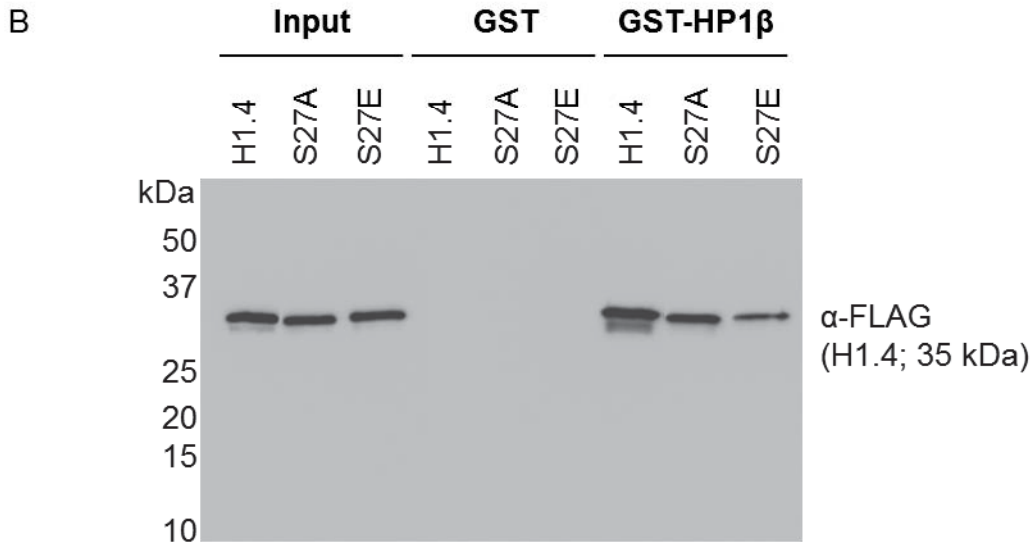
B
Input
GST
GST-HP1β
H1.4
S27A
S27E
H1.4
S27A
S27E
H1.4
S27A
S27E
kDa
50
37
25
20
15
10
α-FLAG
(H1.4; 35 kDa)

Figure 4.14

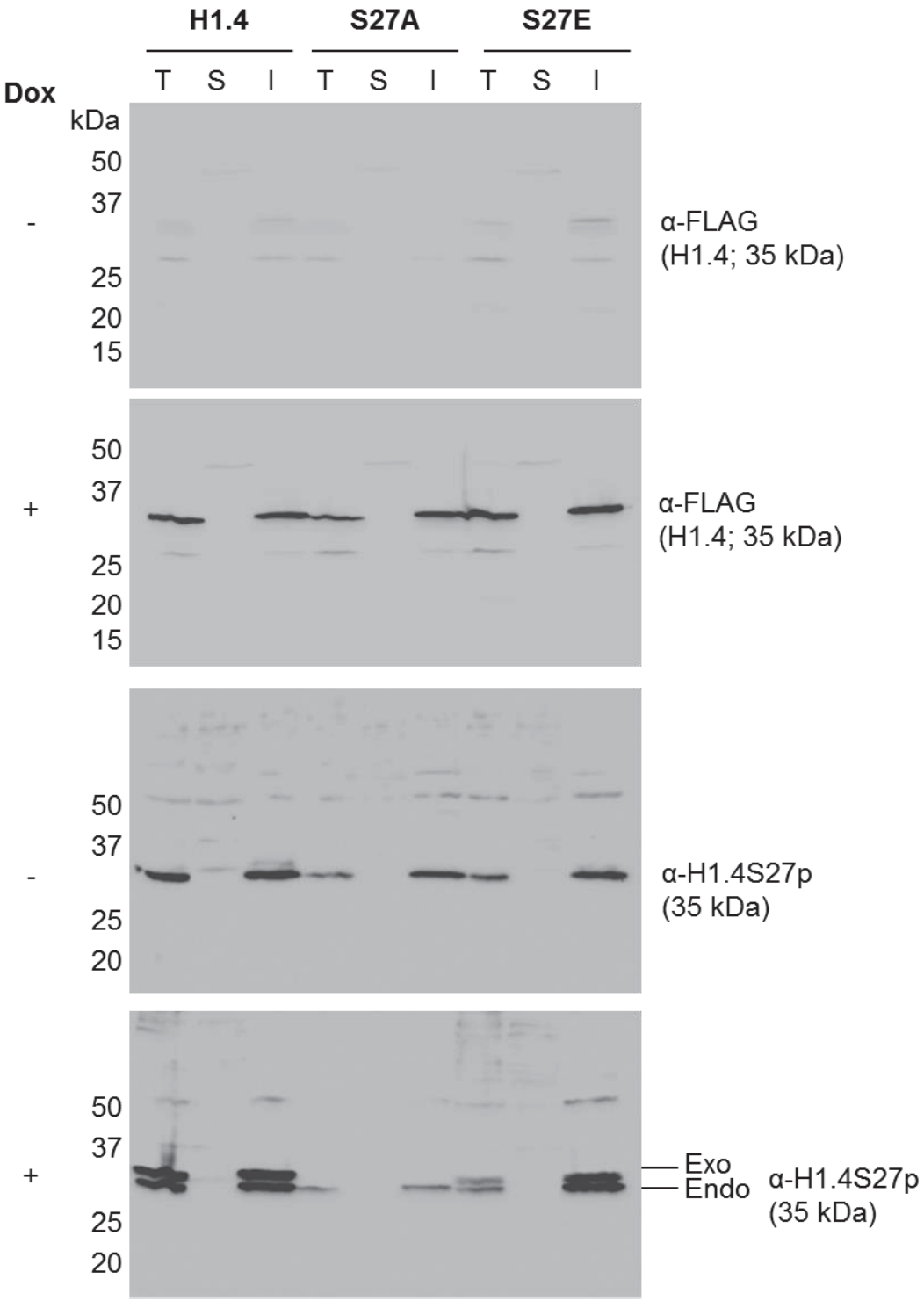
H1.4
S27A
S27E
T S I T S I T S I
Dox
kDa
50
37
25
20
15
-
+
α-FLAG
(H1.4; 35 kDa)
α-H1.4S27p
(35 kDa)
Exo
Endo

Figure 4.14

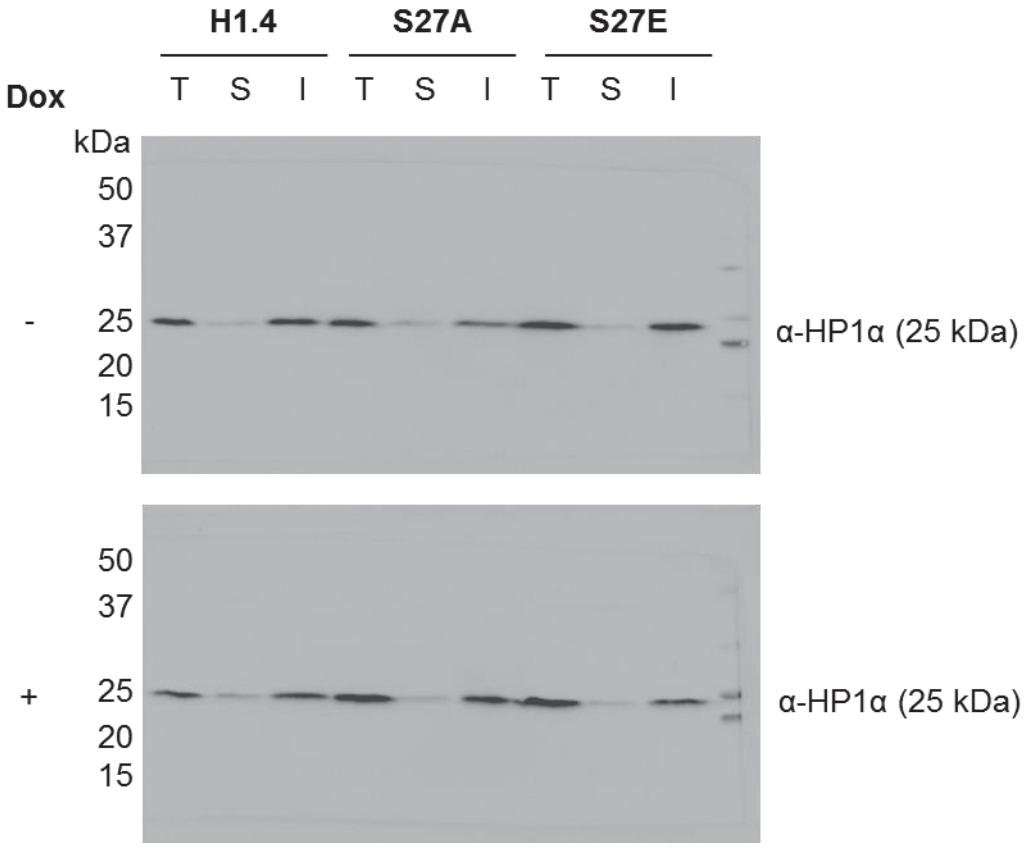
H1.4
S27A
S27E
T S I T S I T S I
Dox
kDa
50
37
-
25
20
15
α-HP1α (25 kDa)
50
37
+
25
20
15
α-HP1α (25 kDa)

Figure 4.15

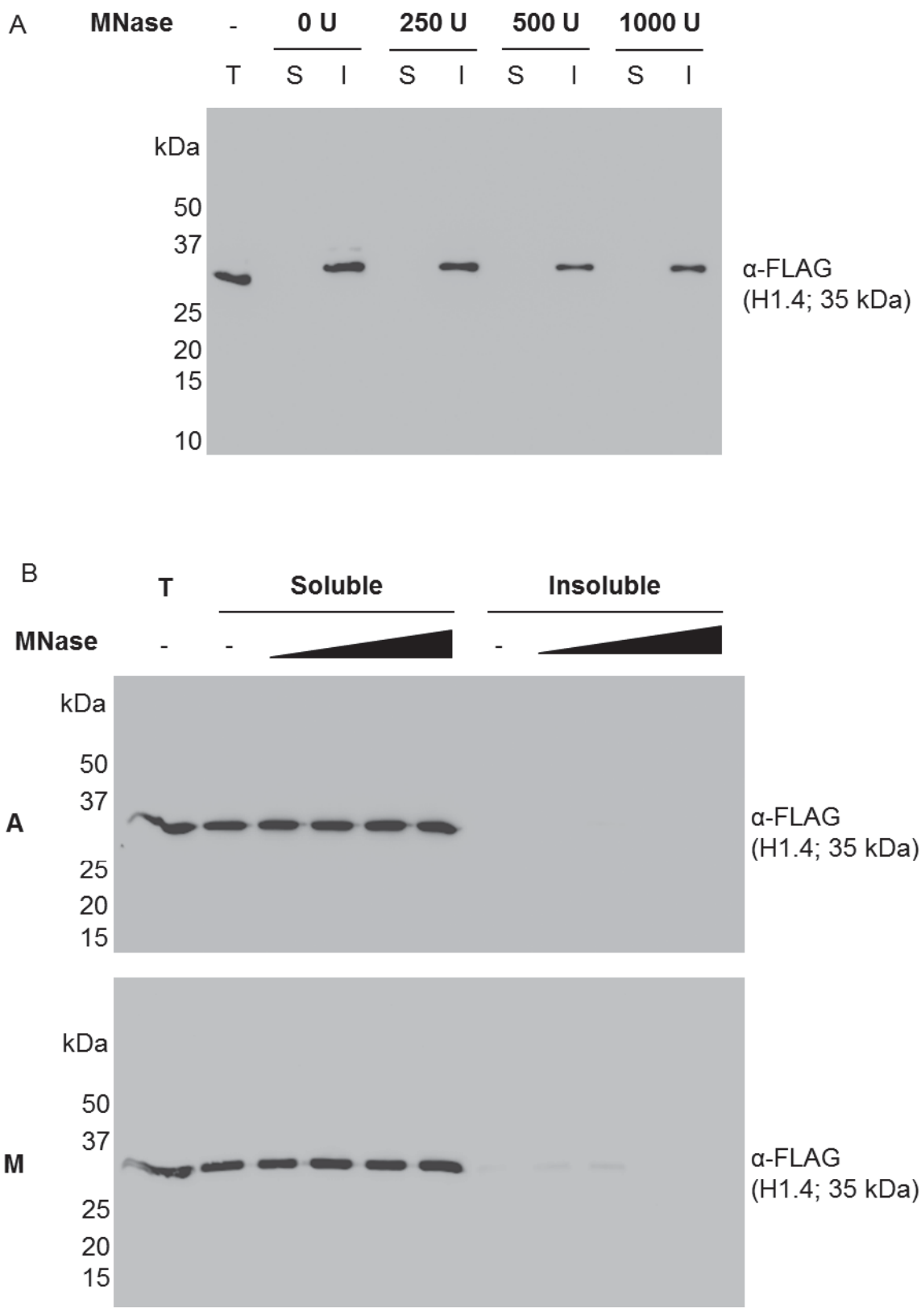
A
MNase
-
0 U
250 U
500 U
1000 U
T
S
I
S
I
S
I
S
I
kDa
50
37
25
20
15
10
α-FLAG
(H1.4; 35 kDa)
B
T
Soluble
Insoluble
MNase
-
-
-
A
kDa
50
37
25
20
15
α-FLAG
(H1.4; 35 kDa)
M
kDa
50
37
25
20
15
α-FLAG
(H1.4; 35 kDa)

Figure 4.17

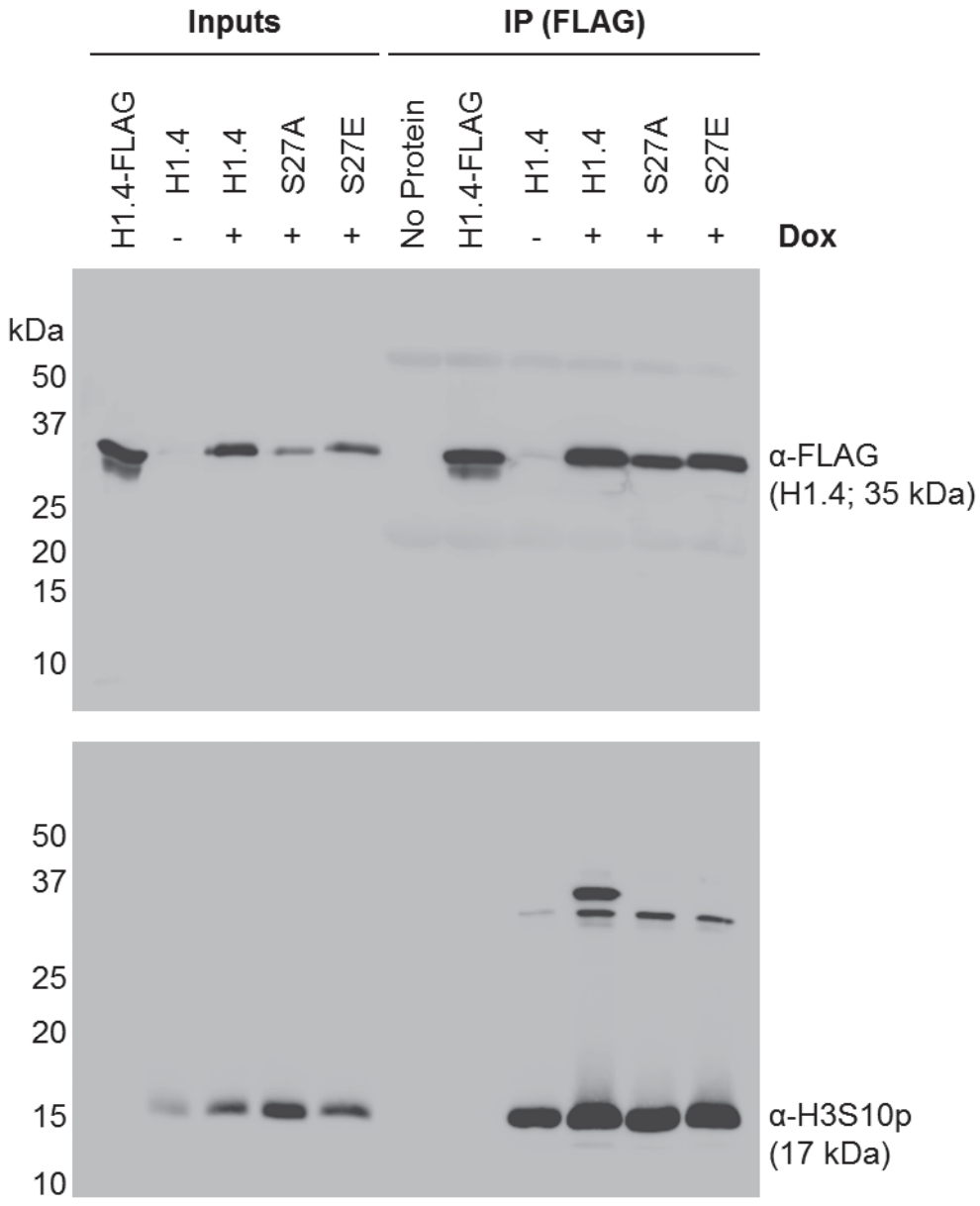
Inputs
IP (FLAG)
H1.4-FLAG
H1.4
H1.4
S27A
S27E
No Protein
H1.4-FLAG
H1.4
H1.4
S27A
S27E
- + + + - + + + +
Dox
kDa
50
37
25
20
15
10
α-FLAG
(H1.4; 35 kDa)
50
37
25
20
15
10
α-H3S10p
(17 kDa)

Figure 4.18

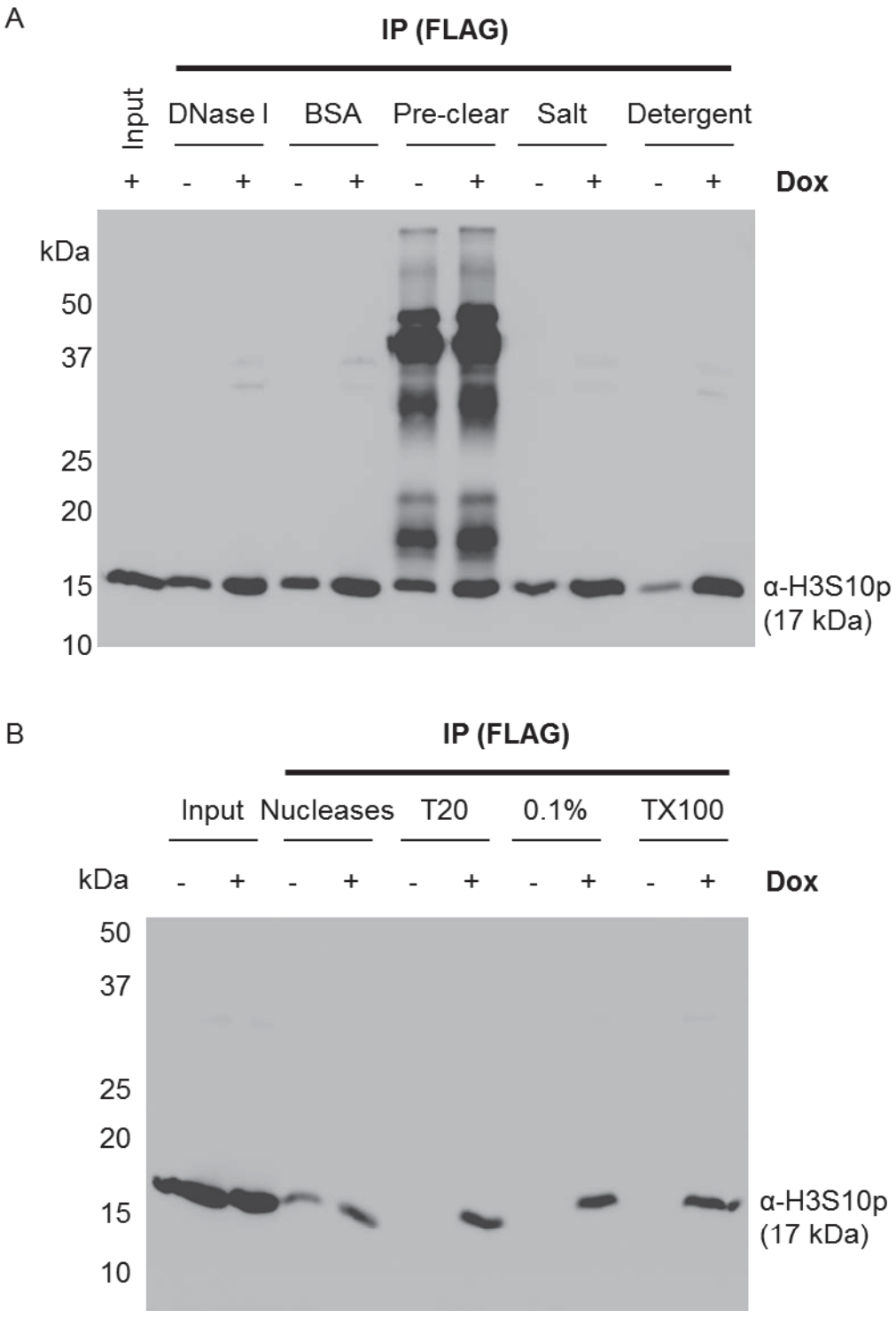
A
IP (FLAG)
Input
DNase I
BSA
Pre-clear
Salt
Detergent
+ - + - + - + - + - + Dox
kDa
50
37
25
20
15
10
α-H3S10p
(17 kDa)
B
IP (FLAG)
Input
Nucleases
T20
0.1%
TX100
kDa - + - + - + - + - + Dox
50
37
25
20
15
10
α-H3S10p
(17 kDa)

Figure 4.20

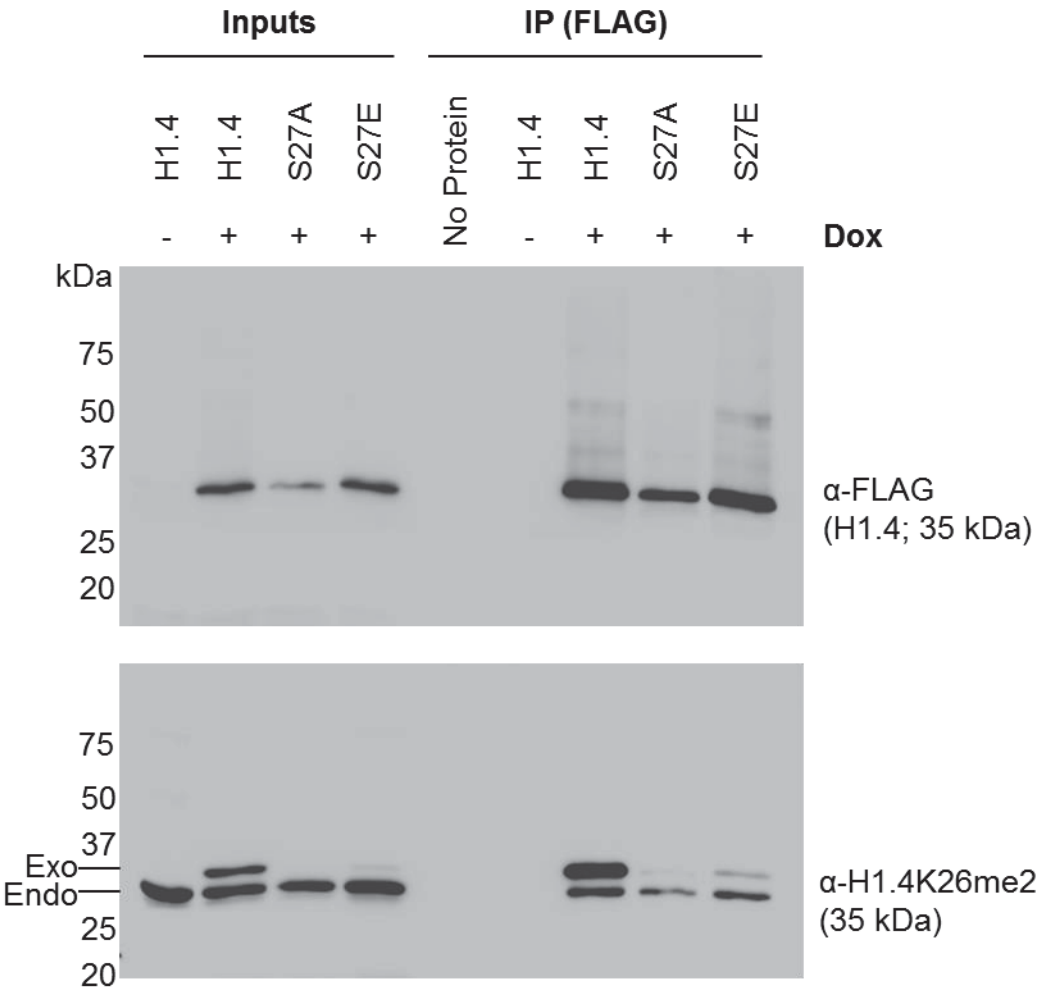
Inputs
IP (FLAG)
H1.4
H1.4
S27A
S27E
No Protein
H1.4
H1.4
S27A
S27E
-
+
+
+
-
+
+
+
Dox
kDa
75
50
37
25
20
α-FLAG
(H1.4; 35 kDa)
75
50
37
Exo
Endo
25
20
α-H1.4K26me2
(35 kDa)

Figure 4.20

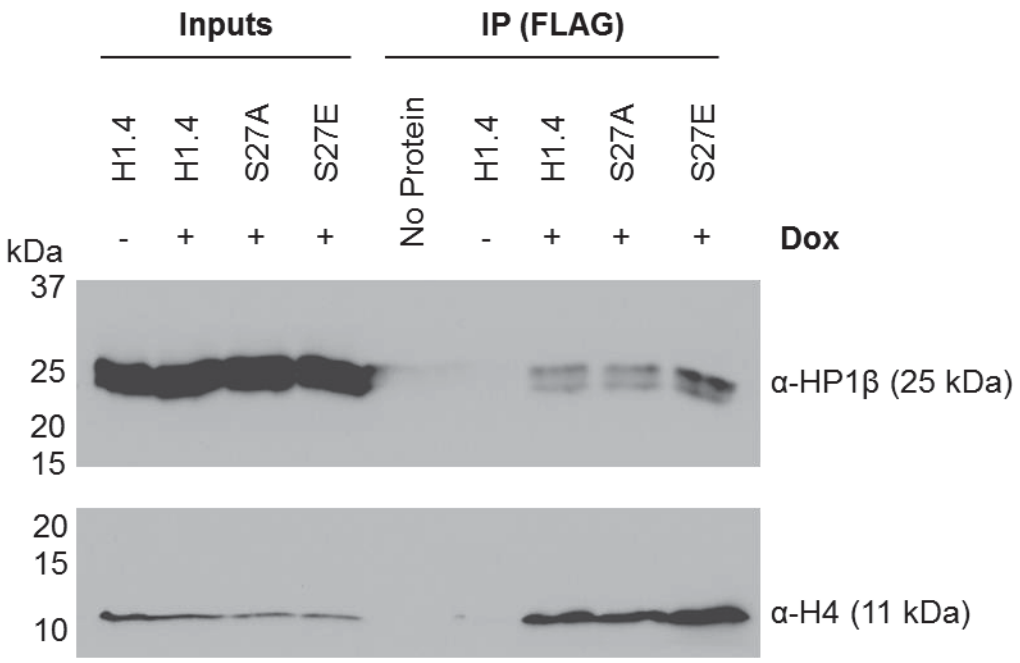
Inputs
IP (FLAG)
H1.4
H1.4
S27A
S27E
No Protein
H1.4
H1.4
S27A
S27E
kDa
- + + + - + + + Dox
37
25
20
15
α-HP1β (25 kDa)
20
15
10
α-H4 (11 kDa)

Figure 4.21

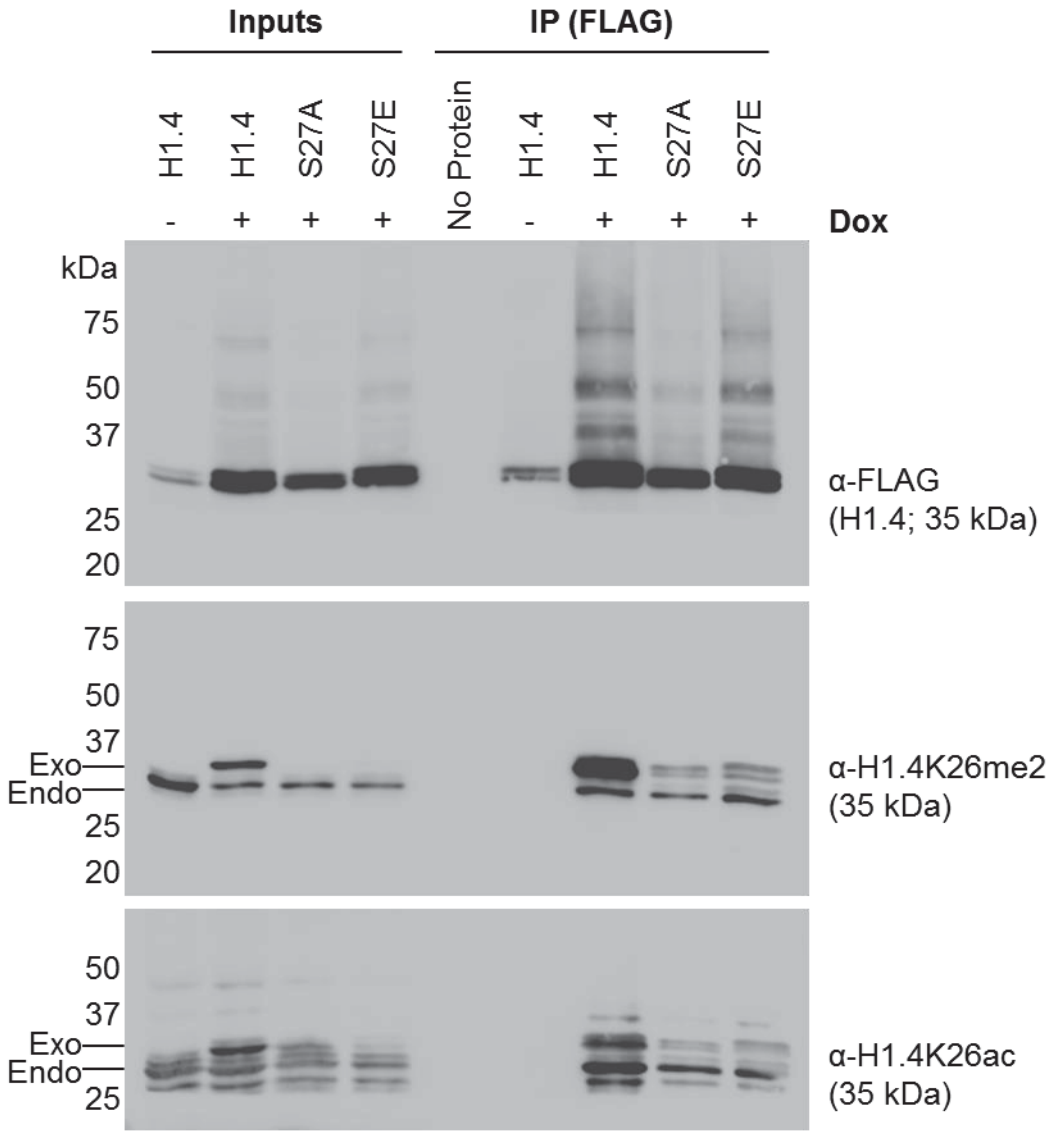
Inputs
IP (FLAG)
H1.4
H1.4
S27A
S27E
No Protein
H1.4
H1.4
S27A
S27E
-
+
+
+
-
+
+
+
Dox
kDa
75
50
37
25
20
α-FLAG
(H1.4; 35 kDa)
75
50
37
Exo
Endo
25
20
α-H1.4K26me2
(35 kDa)
50
37
Exo
Endo
25
α-H1.4K26ac
(35 kDa)

Figure 4.21

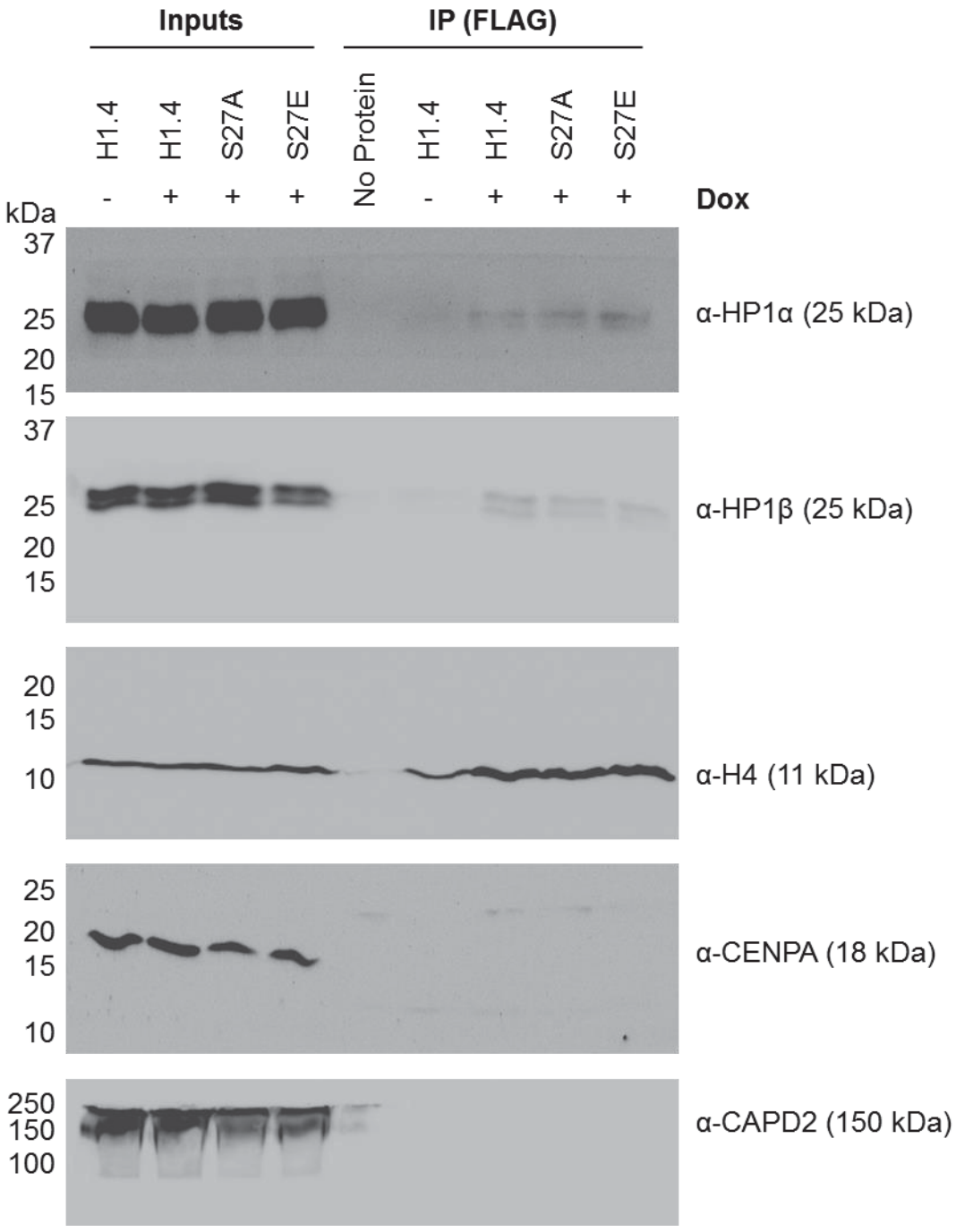
Inputs
IP (FLAG)
H1.4
H1.4
S27A
S27E
No Protein
H1.4
H1.4
S27A
S27E
- + + + - + + + +
Dox
kDa
37
25
20
15
α-HP1α (25 kDa)
37
25
20
15
α-HP1β (25 kDa)
20
15
10
α-H4 (11 kDa)
25
20
15
10
α-CENPA (18 kDa)
250
150
100
α-CAPD2 (150 kDa)

Figure 5.1 A

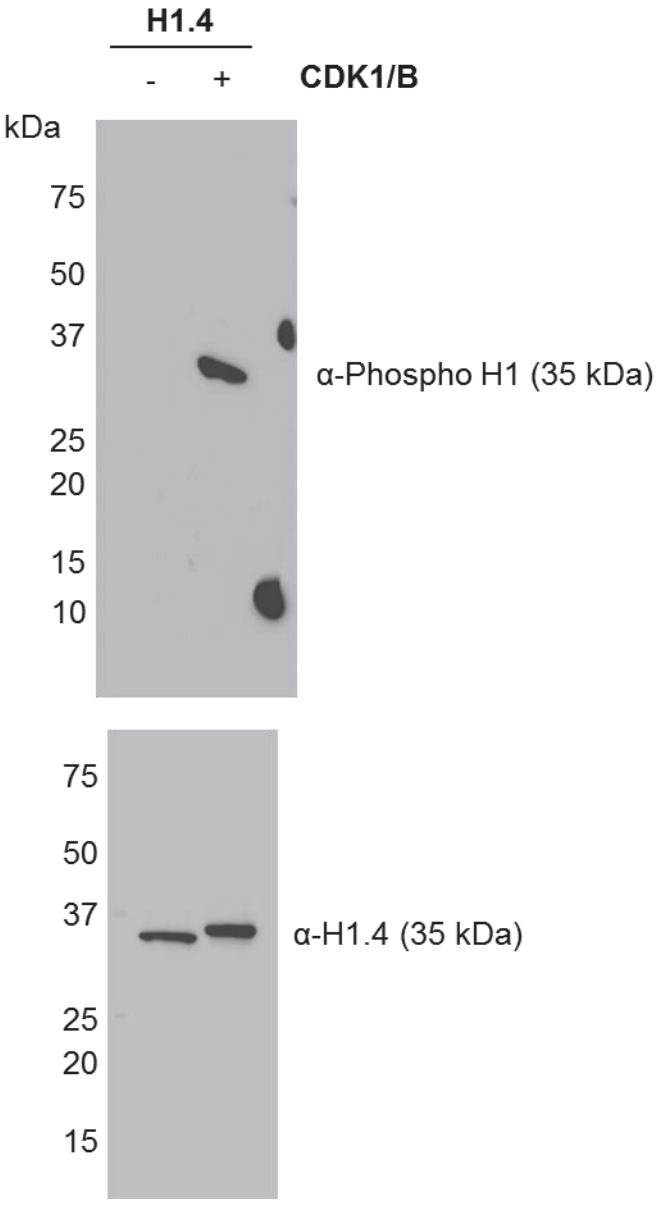
H1.4
-
+
CDK1/B
kDa
75
50
37
25
20
15
10
α-Phospho H1 (35 kDa)
75
50
37
25
20
15
α-H1.4 (35 kDa)

Figure 5.1 B

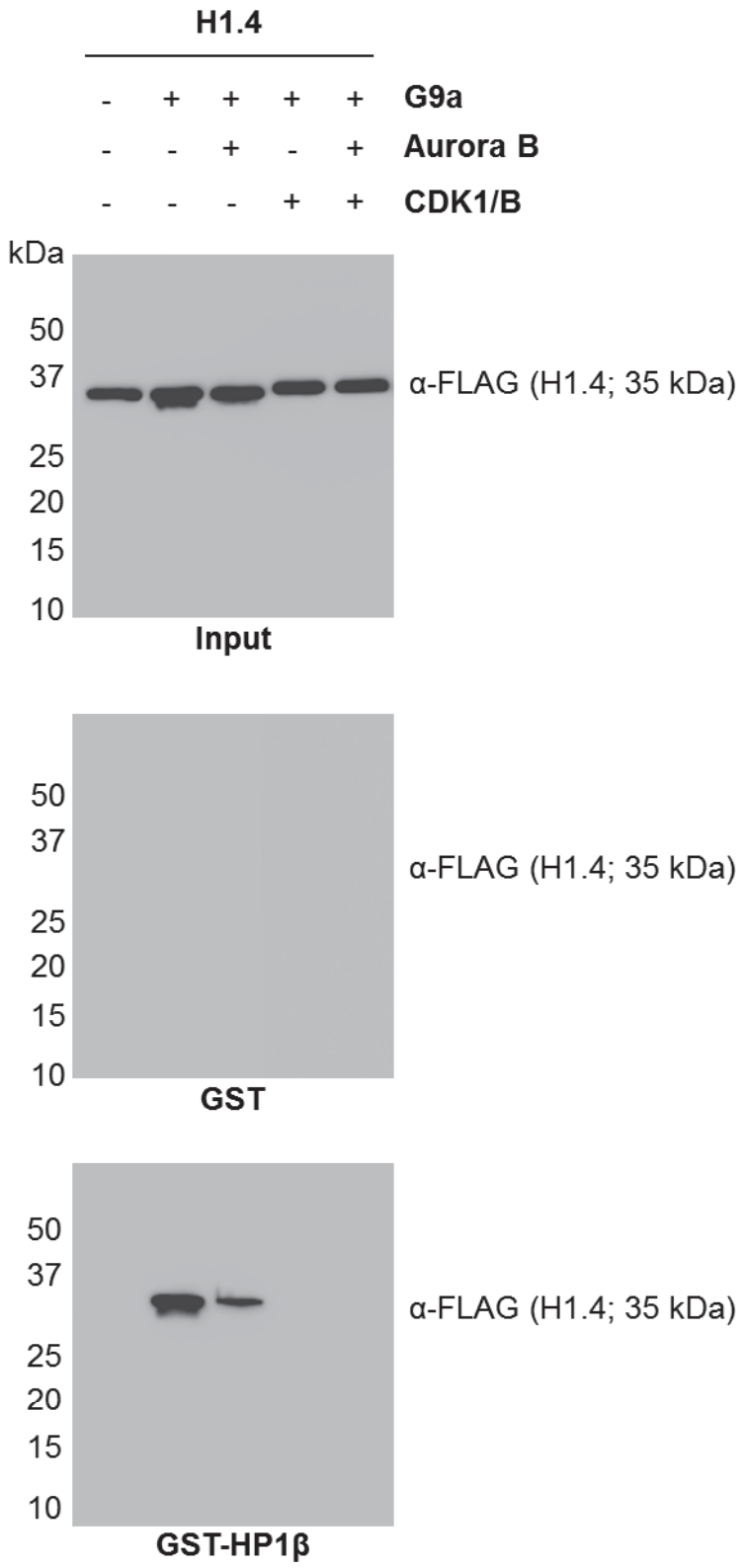
H1.4
- + + + + G9a
- - + - + Aurora B
- - - + + CDK1/B
kDa
50
37
25
20
15
10
α-FLAG (H1.4; 35 kDa)
Input
50
37
25
20
15
10
α-FLAG (H1.4; 35 kDa)
GST
50
37
25
20
15
10
α-FLAG (H1.4; 35 kDa)
GST-HP1β

Figure 5.2

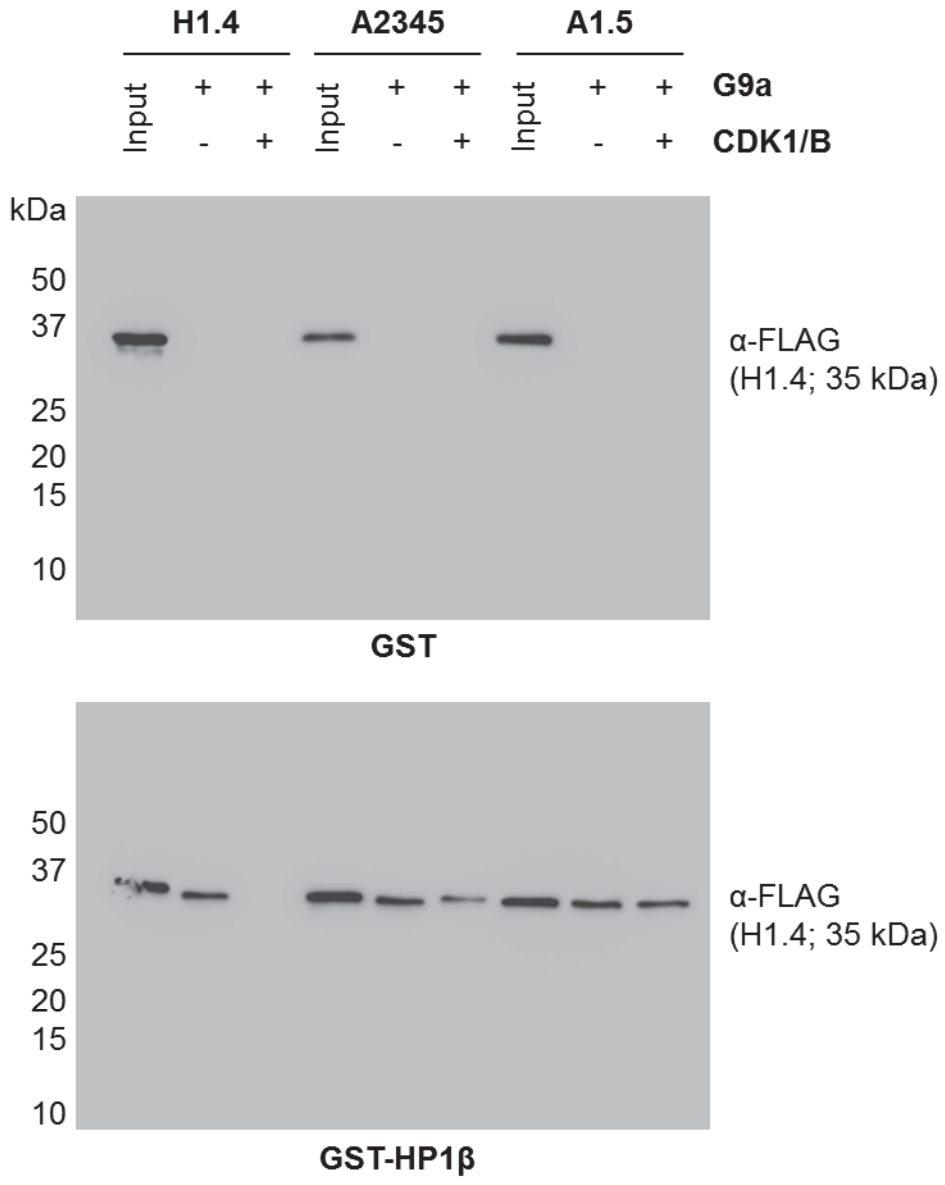
H1.4
A2345
A1.5
Input
+
+
-
G9a
CDK1/B
kDa
50
37
25
20
15
10
α-FLAG
(H1.4; 35 kDa)
GST
GST-HP1β

Figure 5.4

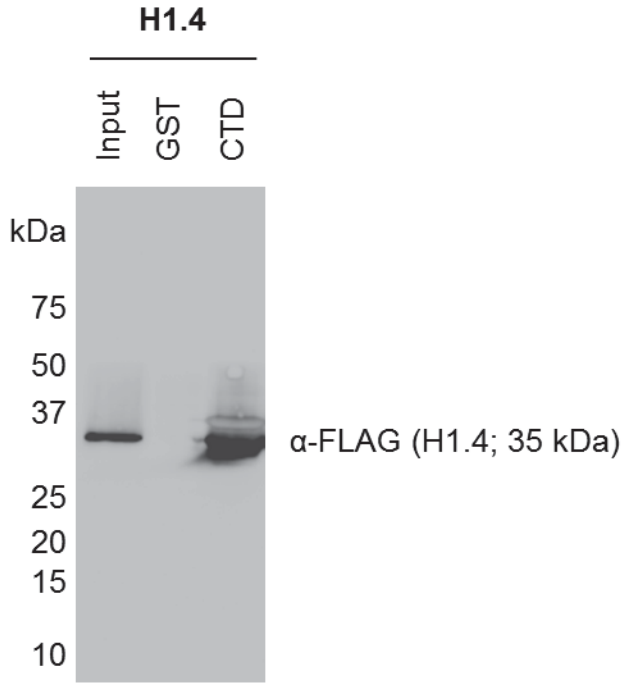

Figure 5.5

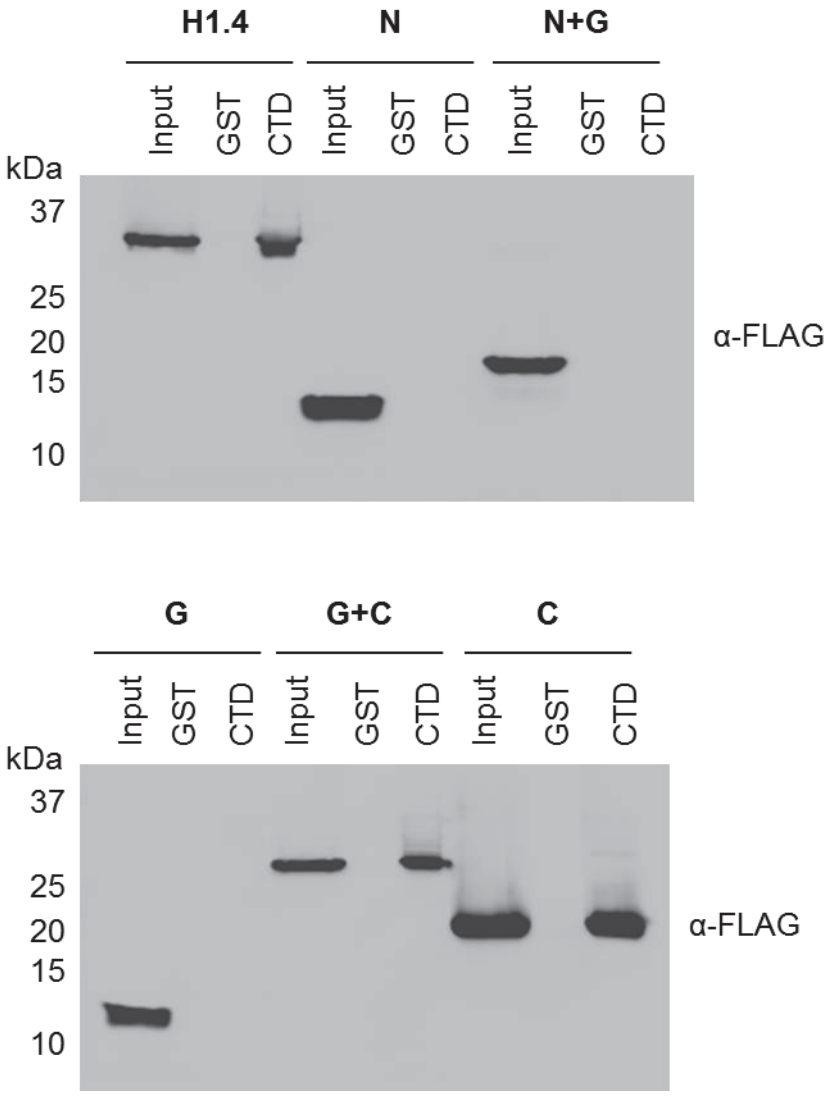
H1.4
N
N+G
Input
GST
CTD
kDa
37
25
20
15
10
α-FLAG
G
G+C
C
Input
GST
CTD
kDa
37
25
20
15
10
α-FLAG

Figure 5.6

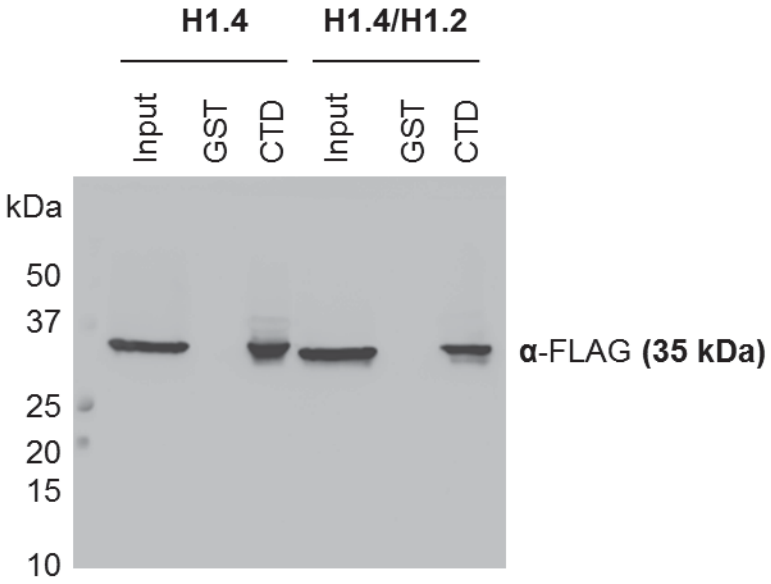
H1.4
H1.4/H1.2
Input
GST
CTD
Input
GST
CTD
kDa
50
37
25
20
15
10
α-FLAG (35 kDa)

Figure 5.7

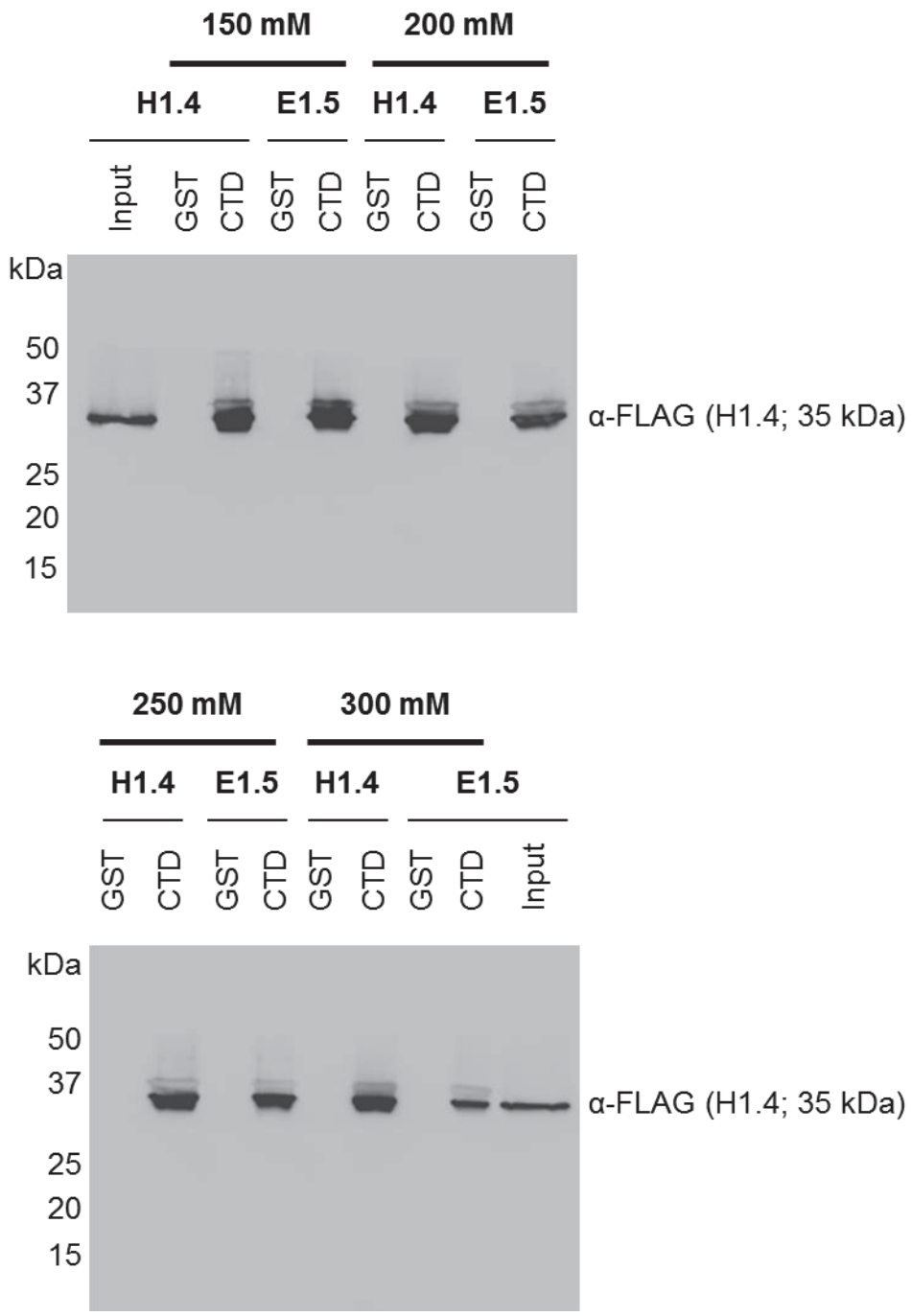
150 mM
200 mM
H1.4
E1.5
H1.4
E1.5
Input
GST
CTD
GST
CTD
GST
CTD
GST
CTD
kDa
50
37
25
20
15
α-FLAG (H1.4; 35 kDa)
250 mM
300 mM
H1.4
E1.5
H1.4
E1.5
GST
CTD
GST
CTD
GST
CTD
GST
CTD
Input
kDa
50
37
25
20
15
α-FLAG (H1.4; 35 kDa)

Figure 5.8

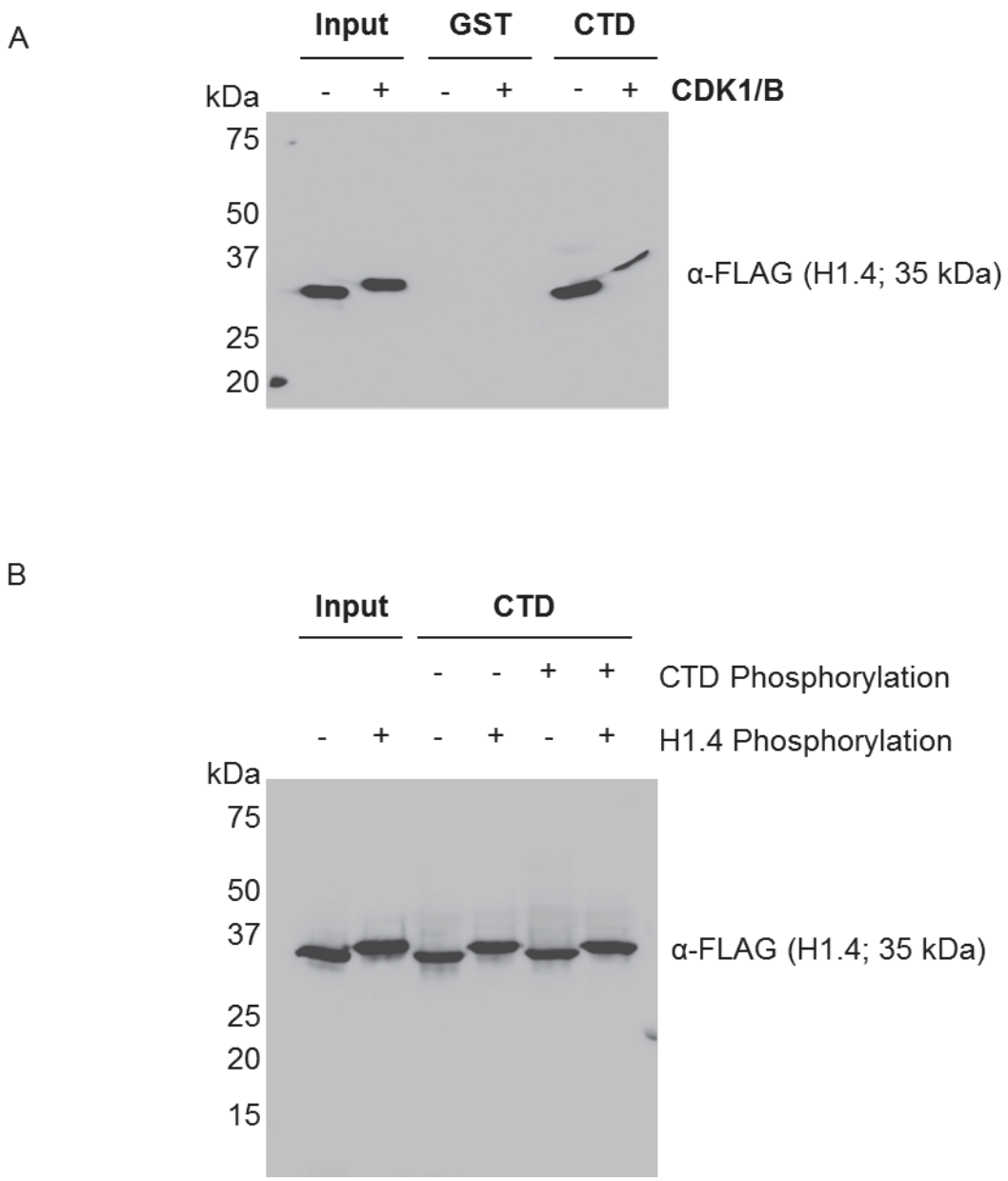
A
Input
GST
CTD
kDa
- + - + - +
CDK1/B
75
50
37
25
20
α-FLAG (H1.4; 35 kDa)
B
Input
CTD
- - + +
CTD Phosphorylation
- + - + - +
H1.4 Phosphorylation
kDa
75
50
37
25
20
15
α-FLAG (H1.4; 35 kDa)

Figure 5.9

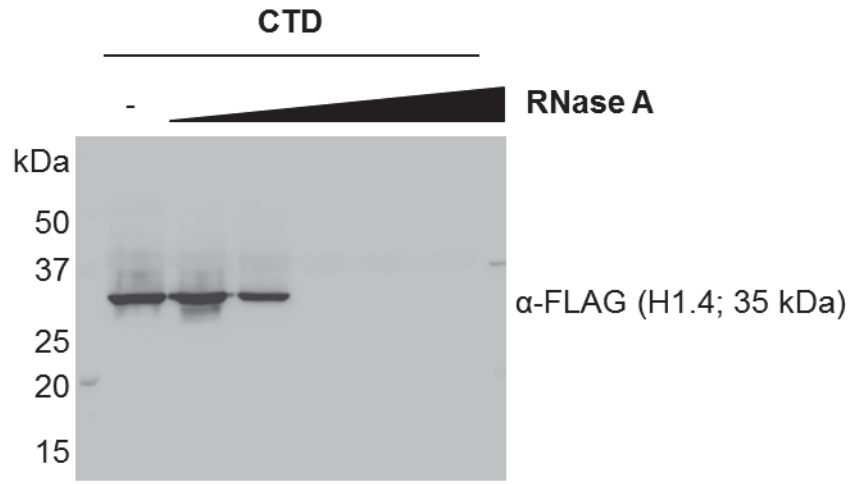

Appendix Two
Quantitation of selected western blots

Figure 3.5

C

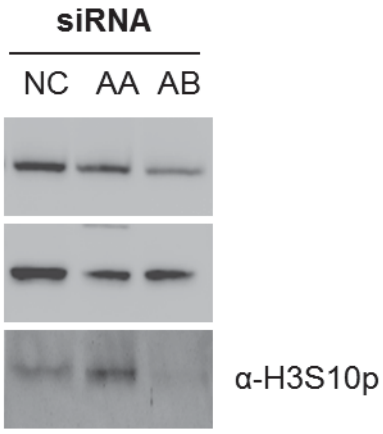
siRNA
NC AA AB
α-H3S10p

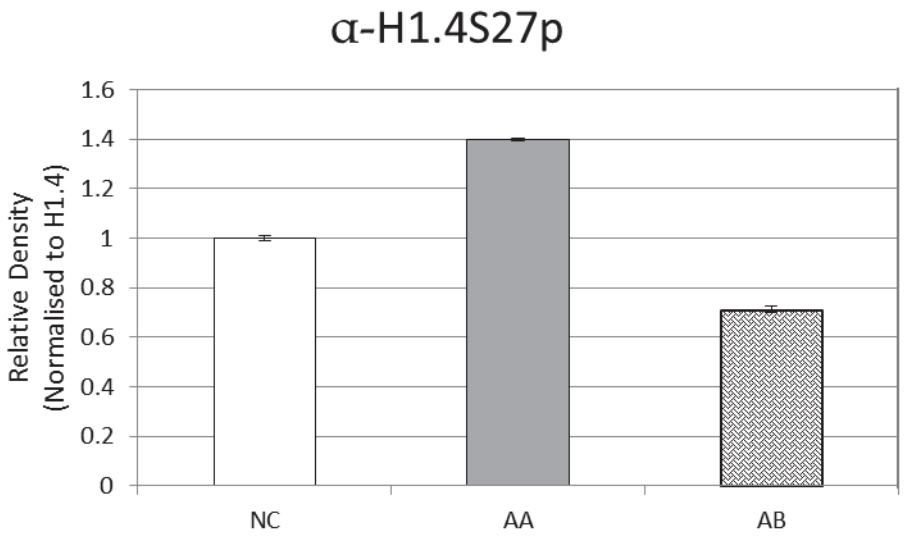
α-H1.4S27p
Relative Density (Normalised to H1.4)
1.6
1.4
1.2
1
0.8
0.6
0.4
0.2
0
NC
AA
AB

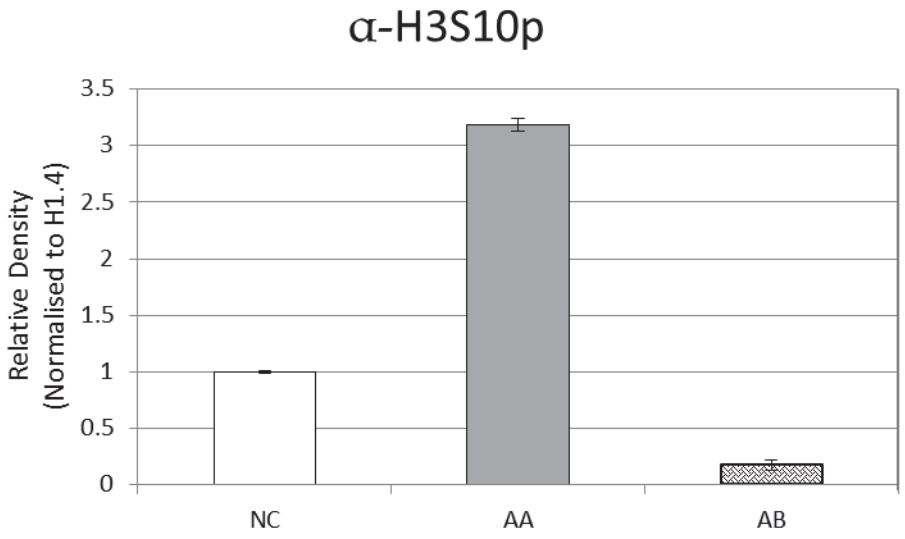
α-H3S10p
Relative Density (Normalised to H1.4)
3.5
3
2.5
2
1.5
1
0.5
0
NC
AA
AB

Figure 3.9

C

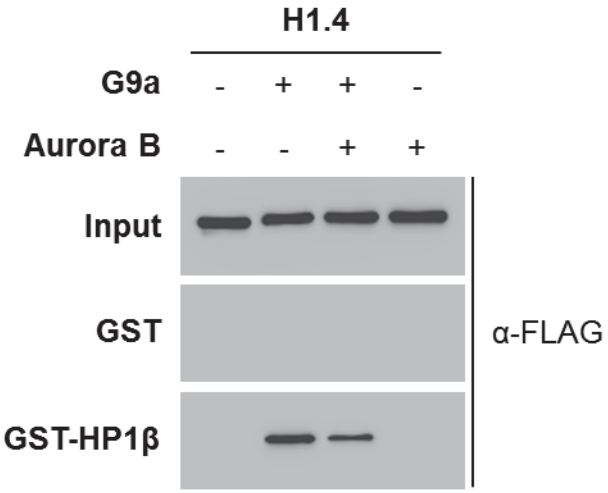
H1.4
G9a - + + -
Aurora B - - + +
Input
GST
GST-HP1β
α-FLAG

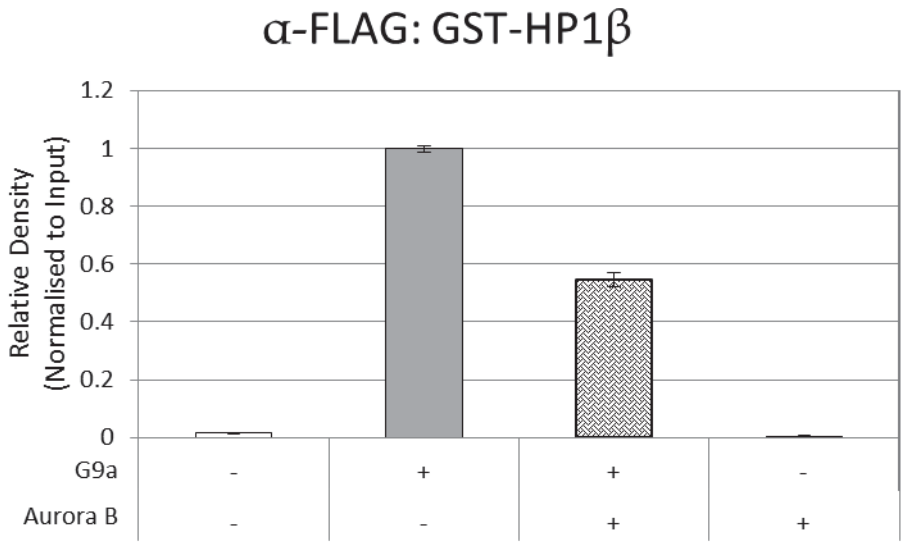
α-FLAG: GST-HP1β
Relative Density (Normalised to Input)
1.2
1
0.8
0.6
0.4
0.2
0
G9a - + + -
Aurora B - - + +

Figure 5.1

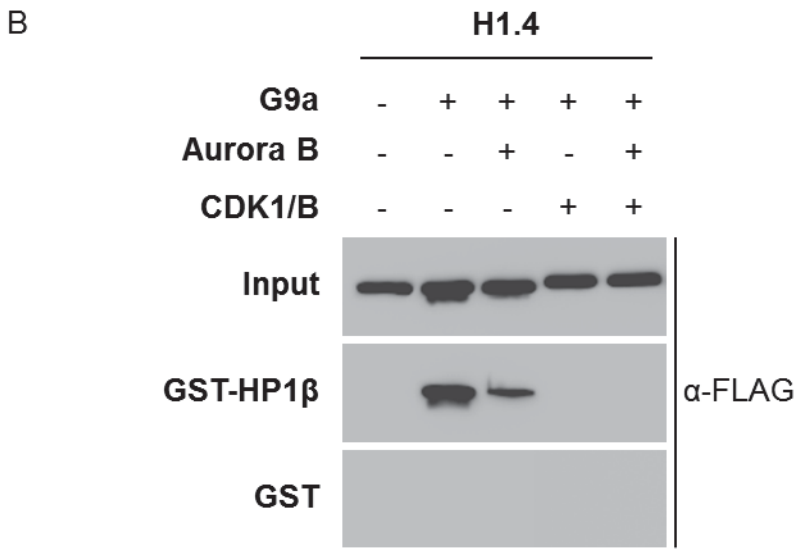
B
H1.4
G9a - + + + +
Aurora B - - + - +
CDK1/B - - - + +
Input
GST-HP1β
GST
α-FLAG

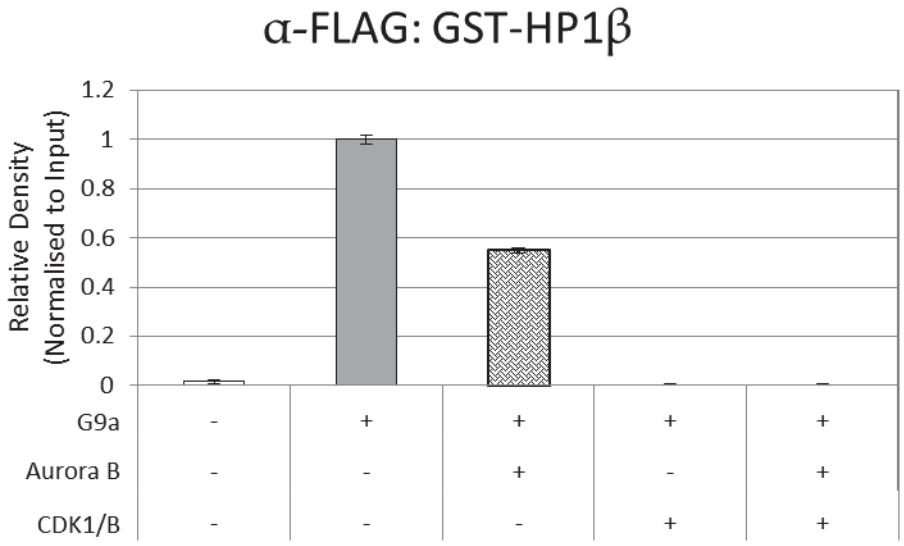
α-FLAG: GST-HP1β
Relative Density (Normalised to Input)
1.2
1
0.8
0.6
0.4
0.2
0
G9a - + + + +
Aurora B - - + - +
CDK1/B - - - + +

Figure 5.2

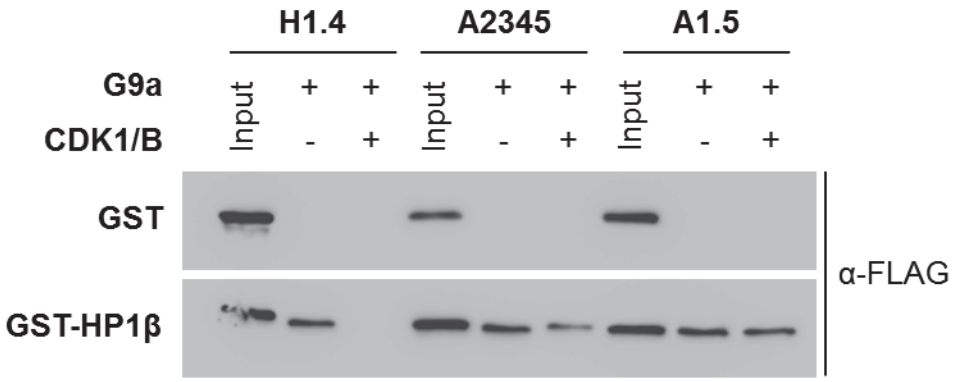
H1.4
A2345
A1.5
G9a
CDK1/B
Input
+
-
GST
GST-HP1β
α-FLAG

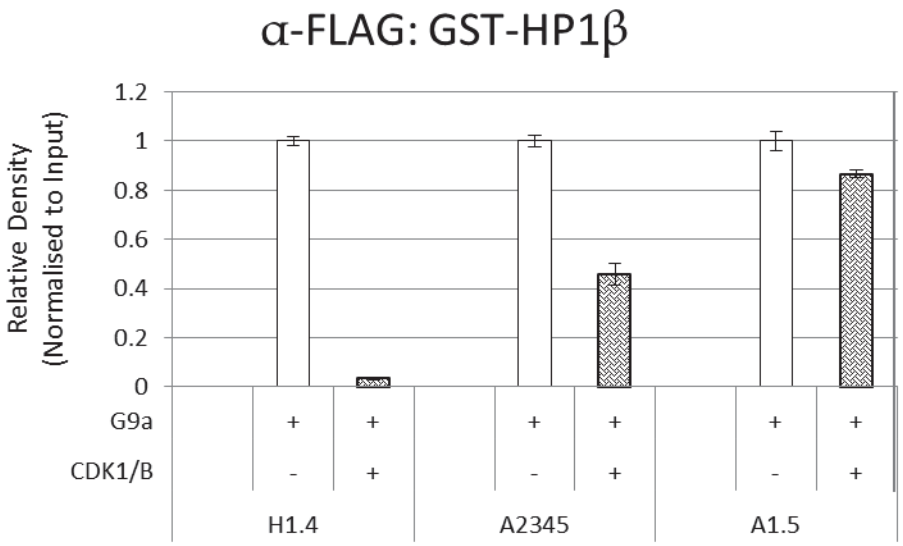
α-FLAG: GST-HP1β
Relative Density
(Normalised to Input)
1.2
1
0.8
0.6
0.4
0.2
0
G9a
CDK1/B
H1.4
A2345
A1.5